博士論文

THE STUDY ON HUMANS' THERMAL COMFORT AT A PEDESTRIAN LEVEL OF BLOCKS IN HOT AND HUMID AREA OF CHINA

The University of Kitakyushu

International Graduate School of Environmental Engineering

北九州市立大學國際環境工學研究科

2019 年 9 月

馬軒

MA XUAN

Acknowledgement

After finishing this thesis, I should thank for the help of tutors, family and my friends. Without their encouragement, I couldn't finish my job fluently.

First of all, the author wishes to express the deepest gratitude to my tutor professor Hiroatsu Fukuda. Under his guidance, I have learned too many interesting things. In addition, professor also gives me advice on finishing my research work. Meanwhile, I also need to express my kind gratitude to professor Weijun Gao, thanks for him giving the chance to study in Japan.

Above all, the author also should thank for professor Dian Zhou from Xi'an JiaoTong university. Professor provides me the research funding and simulated software, which helps me solve many difficult problems in my research work. This study is a sub-session of the Natural Science Foundation of China (No. 2013FY112500).

Finally, I am very grateful for thanking for my family and Miss Mengying Wang, under their encouragement, I can overcome problems in my difficult time.

Acknowledgement

After finishing this thesis, I should thank for the help of tutors, family and my friends. Without their encouragement, I couldn’t finish my job fluently.

First of all, the author wishes to express the deepest gratitude to my tutor professor Hiroatsu Fukuda. Under his guidance, I have learned too many interesting things. In addition, professor also gives me advice on finishing my research work. Meanwhile, I also need to express my kind gratitude to professor Weijun Gao, thanks for him giving the chance to study in Japan.

Above all, the author also should thank for professor Dian Zhou from Xi’an JiaoTong university. Professor provides me the research funding and simulated software, which helps me solve many difficult problems in my research work. This study is a sub-session of the Natural Science Foundation of China (No. 2013FY112500).

Finally, I am very grateful for thanking for my family and Miss Mengying Wang, under their encouragement, I can overcome problems in my difficult time.

Abstract

With the rapid development of urbanization, the global warming and urban heat island (UHI) effect have attracted our attention day by day. The extreme climate may lead to an increase in heat stress, causing not only financial damage but also threating to public health and safety. The pedestrian block plays an important role in humans' daily life which is not only a symbol of a city but also a significant factor affecting local tourism income. Therefore, the humans' requirement about the climate condition is of high importance for architects and urban planners.

In this study on-site measurement and numerical simulation are conducted to evaluate humans' thermal sensation in hot summer. Because of the complexity of China, the hot and humid area of China (hot-summer and cold-winter climate zone, hot-summer and warm-winter climate zone) is selected. Dao He Old Block and Tai Zhou Old Block are very famous scenic spot, located in hot-summer and cold-winter climate zone of China, attract tourists every year. In addition, Ling Nan Tian Di Block locates in Fo Shan city, which belongs to hot-summer and warm-winter climate zone. In this study, the three blocks are chosen for evaluation. In order to develop the local tourism, the local government has provided guidance for the appropriate directions and opportunities for future development of these regions. This study investigates the thermal comfort conditions in microclimate of different blocks and put forward some suggestion for the tourists determine the best time to visit, also help managers choose their business hours. In this region, humans' thermal acceptability and the thermal comfort sensation votes are assessed based on the Physiologically Equivalent Temperature (PET). About the new strategies of this block is shown in four cases: increasing the building height; increasing tree coverage ratio; increasing grass coverage ratio; changing the paving material with a higher albedo.

The thesis consists of eight chapters and the summary of each chapter is shown as following:

In the chapter-1, it's the introduction. This chapter mainly introduces the research background, objectives and methods of the thesis.

In the chapter-2, this chapter reviews the development status of outdoor microclimate in streets. From the four aspects (microclimate observations, thermal comfort indicators, outdoor thermal environment simulation model and simulation software development), author sums up and summarizes research results and main conclusions.

In the chapter-3, this chapter is a case study, and describes the cooling effect of different urban design parameter based on some examples including old city in Munich, old town of Leipzig and old town in LangZhong city.

In the chapter-4, this chapter shows on-site measurement during hot summer. Based on the site of Dao He Old Block,,Tai Zhou Old Block and Ling Nan Tian Di Block, researchers collect meteorological data including air temperature, relative humidity and wind speed, in addition, describe the relationship between urban morphology and microclimate.

In the chapter-5, this chapter introduces the software ENVI-met and describe the

verification and validation of this software.

In this chapter-6, this chapter describes the humans' thermal sensation in existing scenarios, thus helps to make a deep understand of thermal environment of all the blocks.

In this chapter-7, this chapter describes the relationship between humans' thermal sensation and different parameters, and finds out the best effective case to improve humans' thermal sensation.

In this chapter-8, the last chapter is summary and outlook, this section presents the conclusions of the paper and looks forward to future research work.

Table of Contents

Table of Figure

Table of Table

Chapter-1.

Introduction

1. Introduction

1.1 Background

1.1.1 Scale of climatic study

The very existence of a city has significant modifying effects on the local climate- both within the built-up area, and in the atmosphere above and beyond its boundaries. The nature of these modifications depends on a wide range of physical variables, which can be observed and evaluated at distinctly different spatial scales [1]. Relative to the Earth's diameter, the layer of atmosphere blanketing it is extremely thin. The portion of the atmosphere which is directly affected by the terrestrial surface, known as the 'troposphere', reaches a height of no more than 10Km, and on a short time scale of several days, this affected portion is limited to an even shallower layer known as planetary or atmospheric 'boundary-layer'. In an urbanized area, this lowest part of the atmosphere- known as the *urban boundary-layer* (UBL) - is decisively affected by the nature of the built-up terrain. The UBL may be further decided into a number of sub-layers, and the distinction between them is fundamental to urban climate [2-3].

The complete UBL is defined as the entire volume of air above the city that is influenced by its surface characteristics and by the activities within it. From the upwind edge of the city, the UBL grows in height as air passes over the built-up terrain (Figure.1-1).

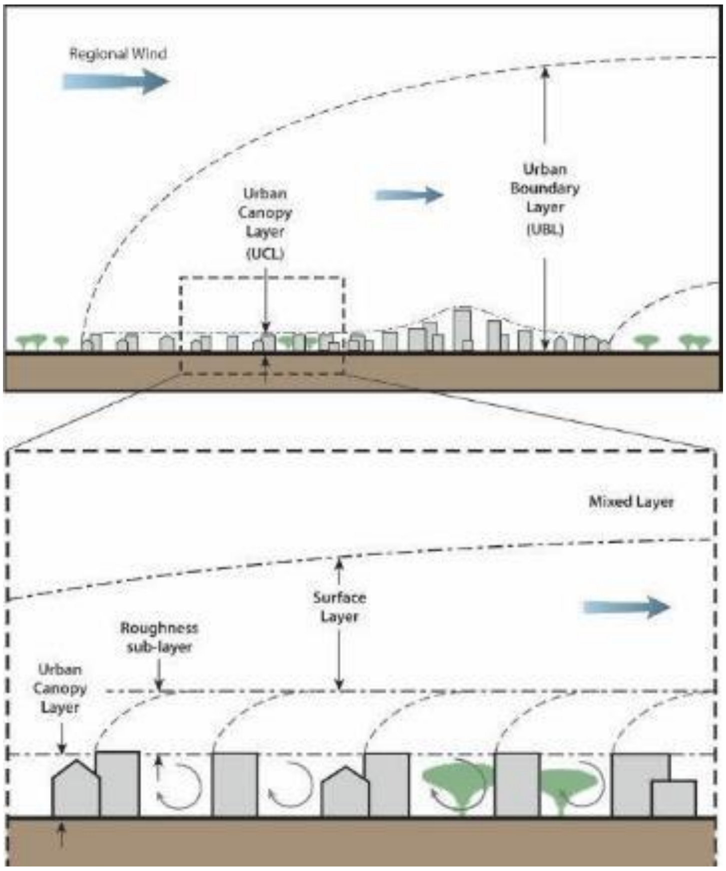

Figure.1-1 Schematic section of urban atmosphere, showing the development of the urban boundary-layer (UBL) relative to the urban canopy-layer (UCL), which reaches the average building (top), and the distinction between the homogeneous surface layer above the city and the

heterogeneous urban canopy (bottom) [3]

The UBL generally extends upward to about ten times the height of the buildings in the urban area, and it also extends beyond the urban area in the downwind direction, the upper part of the UBL, and the bulk of its volume, is considered a 'mixed layer' [4]. Within this layer the atmosphere is influenced by the presence of the urban surfaces, but is not fully adapted to it; in other words, the impact of non-urban upwind terrain is felt as well. The height of the mixed layer varies according to atmospheric stability and the magnitude of the urban effects [5]. Up to a height of about four to five times that of the average building, a *surface layer* may develop that is entirely conditioned by the 3D geometry and other attributes of the buildings and ground cover below. This surface layer forms when air has passed over a sufficient length of ground that has urban attributes, including the roughness created by sharp-edged structures and the heat that is generated within the city. Due to the turbulent mixing of air, however, the properties of this layer are not affected by individual urban elements such as single building and streets. Rather, they are conditioned by the texture of the urban surface as a whole. This blending of effects from individual surface features that characterizes the surface layer does not occur immediately above the roofs of buildings, and therefore tat layer's lower boundary is typically found at a height of at least twice the average building height. Below this level is a highly variable *roughness sub-layer,* in which the air-flow consists of interacting wakes and plumes introduced by individual roughness elements. This zone is also known as a layer of transition between the homogeneous surface layer above, and the highly variegated urban surface itself-which is typically comprised of buildings of different heights, vegetation and open spaces of various dimensions [6]. The very lowest part of the urban atmosphere is the *urban canopy-layer* (UCL), which extends from ground level to the height of buildings, trees and other objects. In a sharp distinction to the surface layer above, the UCL is characterized by a high level of heterogeneity, since conditioning vary widely from point to point within the canopy volume. Due to the inherent heterogeneity of the UCL [2-6,7], a unique microclimate is established within any given urban space, with air temperature, wind flow, radiation balance and other climatic indicators being determined by the physical nature of the immediate surroundings as well as by the urban and regional environment. The proportions of the space, the thermal and optical qualities of its finish materials and the use of landscape vegetation are all design parameters that modify climate at this scale. Because urban design may have localized impacts such as these on outdoor thermal comfort and building energy loads, the microclimate of urban spaces is rightfully considered an architectural issue [8].

The macro-scale is appropriate for describing air masses and pressure systems related to weather-phenomena which are viewed on a scale of hundreds of kilometers. While large urban areas may influence such weather patterns, this level of scale doesn't resolve detailed features of cities. However, at the meso-scale, which describes terrain on the order of magnitude of tens of kilometers, urban areas and their internal climatic effects are clearly identifiable. At the local scale, a resolution of single kilometers or less can clearly reflect man-made objects such as buildings, which - in the context of a city or town - make up the urban fabric. This scale, also known as the urban scale, is of primary interest in the study of urban climatology. The classification of these scenarios is shown in Figure.1-2.

	Scale	Approximate limits	Characteristic climatic phenomena
	Macro-scale	>100km	Jet stream, hurricanes
	Meso-scale	10km-200km	Thunderstorm
	Local scale	100m-50km	Tornados
	Micro-scale	1cm-1km	Scale turbulence

Figure.1-2 Differentiation of spatial scales for climatic study

In order to research the microclimate, distinguishing the difference between weather and climate is very necessary. The former refers to relatively rapid change or immediate change, the latter means the average or major weather conditions over a period of time, related to long-term behavior. Compared to weather conditions, climatic factors have more significant impacts on culture and society. So on-site measurement of weather conditions are the basis of determining climatic impacts [9-11]. Different from the landscape design researched by empiricism and qualitative methods, the used methods of urban climatology is positivism and quantitative methods [12]. For example, in the field of urban heat island, the model of energy balance based on the computer is widely used [13].

Therefore, the attention on correlation between microclimatic comfort and landscape design needs to complete two levels of work, firstly, architects and designers should make reasonable layout and proportion of different landscape elements and improve humans' comfort. Secondly, combining the landscape design with effective integration of urban climatology can deliberate and optimize the urban climatology research results in practice, thus improve the local climate.

1.1.2 Streets in cities

In traditional European cities, the relationship between streets and buildings is clear: the urban public space is consist of streets and squares. Buildings are continuous in their own plots, enclosing streets at the block scale [14-16]. B • Rudowski once comment on Italian streets: "Streets can't be existed in where there is nothing", that is, streets can't be separated from ambient environment. In current China, the new space (skyscraper and open space) has aroused a series of problems in our urban lives.

The concept "city of roads" means a new subsequent planning of transportation system under the circumstance of massive private cars [17]. From 1920 to 1950, all the America experienced this period, in addition, after 1980, this phenomenon also appears in Europe [18]. Nowadays, this trend of China is becoming obvious.

1.1.2.1 Road and street in city

In our daily lives, urban transportation system can be divided into two parts: road and street, which correspond to different users and functions. Table.1-1 represents the function of road and street. The street in modern world has both functions, in addition, which will also bring contradictions [19].

Table.1-1 Difference between road and street

	Road	Street
Concept	Connection of two distant places	Connection of two close places
Relationship with the site	No houses around road	Houses on both sides
If there are buildings	Office buildings and company	Residential building
Major users	Motor vehicles	Pedestrians
Street view	Roadside trees	Markets
Width	Four times wider than street	Width based on pedestrian walk

As a traffic link, the walkers need a continuous linear path to descend the interference during their trip, thus realizing the smooth connection between the starting point and the ending point. The purpose of this design is to make users pass this region quickly and conveniently and shorten the traveling time as possible [20]. The users of traffic link includes pedestrians, cyclists, small car drivers, passengers, bus passengers, truck drivers and so on. These people have different starting points and driving speed, they all competed for the limited resource of space when they appear on the road. As an urban space, the users need the reason about staying and appreciating. The reason is that street is the beginning or an end of a journey, but destination isn't just passengers. As an important role in humans' lives, street aims at providing a place for spending time and participating in activities. The representative users of urban space are "street-walkers", whose main activities are walking with characteristics of random, time-to-stop and low speed, is subject to noise and air pollution caused by motor vehicles [21-23]. Street is the main research object of this paper. In *The American Heritage*

Dictionary of the English language, the street is defined as "A public passenger of a city or a town, generally there are houses on both sides" [24]. This explanation does not emphasize the houses on both sides. In *Webster's Dictionary*, the explanation of *Street* is similar to the street in Chinese. The *street* in Chinese pays attention to meet the function the buildings and the paths on both sides [25].

Traditionally, the traffic regulations are based on road grade systems such as trunk roads, sub-trunk roads and branches, all of which emphasis on the capacity. The major *Traffic engineering* came into being in United States in 1930, after that, some journals have been published such as the *Handbook of Traffic Engineering* published in 1942, which firstly focus attention on the high-speed way and expanded to local residential work. In order to design and build different roads, governments have formulated technical specifications, but these standards only focus on the traffic function of streets and put them ahead of cities. With the emphasis on urban sustainability and livability, government departments are beginning to put more emphasis on it.

At present, in order to improve the speed of motor vehicles, many cities in our country continue to widen and rebuild existing urban roads. For example, the second ring road renovation project in Chengdu will construct continuous viaducts on the existing roads in dense urban areas to form a rapid construction. Even this way can improve urban efficiency of communication, but it neglects the space quality and walking comfort. With the development of the city and the population, adding more percentage of suitable space for pedestrian activities in the city is very necessary [26].

1.1.2.2 Composition of landscape of the street

Street-space is a basic element of the pedestrian space. Street Landscape Space includes five parts such as underground facilities, ground surface, plants, street furniture, buildings, all the five factors integrate into a special landscape [27].

1) Underground facilities: Underground condition is the basis of street landscape design, which includes power, communication, data cables, gas, water steam, cooling water, sewage and rainwater pipes. All the different factors are arranged underground to support the city. Soil condition, quality and depth can also affect plant health. Underground traffic such as metro, car tunnels and parking can affect the street landscape.

and support ventilation equipment.

2) Ground: The public landscape of the ground is divided into soft and rigid. Soft road is permeable vegetation and waterscape, hard region is road. Durability and Size of materials, hard and soft landscape. Proportion determines the characteristics and uses of the public sphere, and affects the microclimate of street space.

3) Vegetation: Including street trees and shrubs. The street trees in the city can largely improve the entertainment of a city, provide shading for urban spaces, improve air quality and promote energy efficiency. Lawn, ground cover and other low plants are suitable for low density areas. Because of the mechanical activities and garbage dump, the vegetation are not suitable for being planted in high dense area.

4) Furniture: Including facilities and shelters in all public spaces. Benches, bicycle frames, self-propelled Car shed, bus stops and waiting booths, newspaper booths and retail stalls, street lights, traffic lights, parking timers, etc. Considering different

functions of these, they all should be integrated to avoid hindering and affecting walking activities.

5) Buildings: The coordinated design with street landscape elements can strengthen the shape, material and characteristics of buildings along the street. The design of street landscape should follow some useful principles.

The reasonable design of the above five parts can ensure the equality of pedestrians and pedestrians on the street, and create satisfactory and good results. Ideal street landscape elements should form a condensation of local context, terrain and landscape. In the past, many traditional cities have succeeded in building a harmonious environment with the spirit of place. Landscape Design of Urban Streets Should Be Based on History and Present Cities, we should seek excellent cases and summarize its laws in space form, operation status and user activities [28].

1.1.3 The users in street

1.1.3.1 Urban planning and life of street

With the popularization of modernism and modern urban development, in 1933, after the publication of the *Charter of Athens*, it’s suggested that the division of cities should be advocated. Under this theory, the city has been transformed into a living, work, recreation and transportation service that meets the "basic needs of human beings", which is an abstract system of energy and not no longer an organic structure. The construction of modern pedestrian space should be designed by following the rules of road system planning and traffic planning, and neglect the development of streets. Streets are dominated by motor vehicles, non-motorized traffic is suppressed, and urban residents walk slowly. In our daily lives, streets are dominated by motor vehicles, non-motorized traffic is suppressed, and urban residents [29-32]. As a result, the links between streets and pedestrian activities in cities are becoming weaker and weaker. In order to provide enough sunshine and air circulation, the buildings such as residential buildings, public buildings and factories are scattered and sparse, in addition, the peoples’ activities are diluted. In these spaces, the walking activities are not time-cost-effective, the number of walkers and their activity time are reduced, compared to some traditional cities. Nobelschutz commented that "Tradition streets and squares in consciousness no longer exist, and the general result is an arbitrary combination of units, which means that a very clear picture shows a nonexistent relationship between the case and background. Moreover, the continuity of the landscape has been destroyed, and the buildings no longer form clusters or clusters. As a result of the decline of the traditional urban structure, landscapes lose their significance and become extensively expanded, the residue of the composite reticular organization formed by man-made elements called "summarizes the image of modern city". The disintegration of street landscape in planning has resulted in the lack of street life. But the symbolic relationship between culture and environment, the order of the world is more important than basic material function. In view of the lack of urban pedestrianism, urban planners in Europe began to transform the city, promote pedestrian activities, and then revitalize the urban center. In Copenhagen, Denmark, restoring the traditional street to pedestrian street since 1962, reconstructing the urban street network and restricting mobility. A series of studies conducted by Gail explored the impact of pedestrian system restoration on urban space and urban development. The impact of life in some parts of the city, designers are also promoting the use of streets, such as living in Berlin [33]. The streets and squares with good greening and developed pedestrian system are planned in the district, and human-scale space is designed.

1.1.3.2 Scale based on human

Urban sidewalks are part of the streets used by pedestrians, and are the most likely street space for leisure activities [34]. Jacobs believed that a successful block should include three important factors such as clear boundaries between public and private spaces, and street buildings. As a place where social life takes place, the main purpose is to satisfy people in society. In order to fulfil the needs of the needs of economic activities, cyclists, drivers, bus passengers and pedestrians on the streets are all needed to be protected under new design. In cities, providing pedestrian access and outdoor space is conducive to creating a sustainable city and promoting its livability [35]. According to the theory of green city, we need to take "people" as a role in street design and abandon the ideas of using motor vehicles. The Sociologist Herbert believed that the actual users' feeling is the central decision for deciding whether it is good or bad. People on the street are the measure of the criteria for success of street space design [36]. William H. White directly regards the number of people is an important factor. Therefore, observing the leisure activities of users. It is possible to improve the leisure activities of pedestrians and it is helpful to summarize the design principles of urban pedestrian street landscape. In our daily lives, the identity and attitudes of street users often changed, when the people driving or riding, residents expect the streets crowded and wide, with fewer traffic lights [37]. For different purposes, users have different needs for street space quality. The difference between routes and resting place determines the user's expectation of microclimate [38-40]. Users seldom choose paths based on thermal comfort, in their walking period, short-time discomfort will not cause significant harm. People will choose comfortable places when they are ready to sit down and rest, but uncomfortable environment will prompt them to leave quickly. Therefore, the purpose of the activity will affect the user's environmental comfort evaluation. With the development and transformation of society, leisure and tourism recreation, sports, performances, catering and other activities are increasingly taking place in outdoor space, under global warming and urban heat island effect [41-45]. With the intensification of outdoor thermal comfort, it is also of great economic value and has become an important factor to be considered, in this paper, based on the field microclimate test of walking space and the observation of space usage, the correlation between spatial form and thermal comfort are discussed.

1.1.3.3 The microclimatic expectation of human in pedestrian block

In our daily lives, the identity and attitudes of street users are often changed, when driving or riding, residents expect the street to be crowded, wide, pedestrian crossings and traffic lights are few, vision is open; when walking or riding a bicycle, they hate the impact brought by motor vehicles, noise, dust and safety hazards. For different purposes, users have different needs for street space quality. The difference between Routes and Resting Place determines the user's expectation of microclimate [46]. Users seldom choose paths based on thermal comfort, and short-term discomfort in the path will not cause significant harm. People will choose comfortable places when they are ready to sit down and rest, and uncomfortable environment will prompt them to leave quickly. Therefore, the purpose of the activity will affect the user's environmental comfort evaluation. With the development and transformation of society, leisure and tourism, recreation, sports, performances, catering and other activities are increasingly taking place in outdoor space, global warming and urban heat island effect. With the intensification of outdoor thermal comfort, it is also of great economic value and has become an important factor to be considered [47]. In this paper, based on the field microclimate test of walking space and the observation of space usage, the spatial form and are discussed.

1.2 Research methods

This study focuses on the usage and comfort of pedestrian streets under the influence of urban microclimate, and mainly investigates and analyses them. Urban leisure in pedestrian zone with the user's activities as an indicator, explores the design strategy of urban pedestrian zone. Through the present field survey and numerical simulation to study the urban pedestrian streets and talk about the different cooling effect under different strategies in hot summer and cold winter humid-hot areas. On the basis of summarizing the microclimate improvement strategies of urban pedestrian streets in hot and humid areas, the environment-friendly urban pedestrian streets are obtained. Sullivan believes that the great environmental design in history is metaphysical and passive design [48], the combination of the base and climate, aesthetic needs and social factors determine the form of houses and landscapes. This paper studies how to improve the room by optimizing the landscape greening design of residential groups in hot and humid climate. External thermal environment quality and the purpose of reducing energy consumption of single building. The main research objectives are as follows:

1. Through on-site measurement and numerical simulation of typical commercial pedestrian block in humid and hot climate, the existing thermal comfort evaluation index and its application are analyzed. The best outdoor thermal comfort evaluation index suitable for the climate characteristics is obtained in the comfort zone.
2. ENVI-met Software for Outdoor Thermal Environment Simulation Systematic verification (Verification & Validation) and Sensitivity analysis to determine the optimum convergent mesh size, time step and boundary conditions for the commercial zone.
3. Putting forward some suggestions for redesigning this commercial zone during the extreme summer.
4. The dynamic simulation method of outdoor thermal environment of pedestrian block is discussed, and the comprehensive performance simulation method of building is extended to residential group. Home group is used to realize the coupling simulation of thermal safety, thermal comfort and building energy consumption in small-scale areas.
5. Establish the standard process of optimum design of residential group Landscape Greening Based on thermal safety, thermal comfort and building energy saving, and summarize it. The weight of landscape greening design factors on thermal

environmental impact, such as the coverage rate of greening water body, the types and layout of landscape greening, etc. Coefficient is used to assist landscape greening designers in scheme design and optimization.

1.2.1. Research methods

In this paper, theoretical analysis, field measurement and computer simulation will be combined to study the method, and the method of comprehensive performance simulation of building units will be extended to commercial pedestrian block, to achieve the dynamic simulation of the thermal environment of residential areas throughout the hottest time, to evaluate the design scheme of landscape greening in residential areas at three levels of thermal safety, thermal comfort and energy consumption, and then to put forward the method suitable for the humid and hot climate region. There are six chapters in this paper, mainly discussing wetness under the requirements of different thermal safety, thermal comfort and energy saving of the commercial pedestrian block (Figure 1-3).

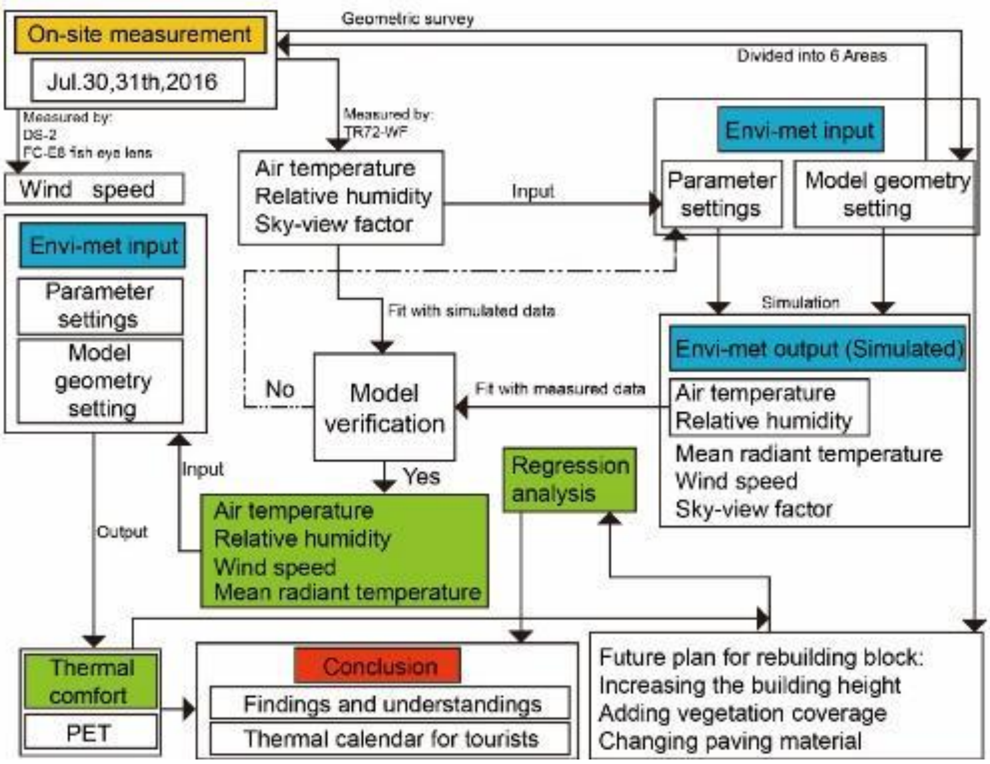

Figure.1-3 Research framework of this study

Chapter-2.

Summary of Research on Street Microclimate

2. Summary of Research on Street Microclimate

2.1. Introduction

The central topic of this paper is to explore the microclimate of urban pedestrian streets and its relationship with human subjective comfort, interrelationship and explore the use of different parameters on improving thermal sensation. The conclusion of this study can help designers to distinguish street landscape. The advantages and disadvantages of the design scheme are helpful to create outdoor space suitable for walking.

Under the influence of convergent urban construction and residents' production and lifestyle, the current urban climate in China tends to be as follows: Cities of different geographical regions have the similarity of climate increases (such as hot summer, cold winter, short spring and autumn), the urban-rural climate difference marked by urban heat island in a region increases. The climate similarity brought about by urbanization is increasing.

The above-mentioned reality reminds researchers: Firstly, comparing the locating in different cities, when dealing with street cases, special attention should be paid to the geographical location of the city, and to the urban style and features derived from regional climate characteristics. The characteristics of the Bureau and the traditional living habits of the local residents; the second is the impact of the lifestyle of the modern urban residents on the urban climate. With the increasing influence, the developed countries in Europe and the United States have maintained a pattern of urban life with high ecological footprint for many years, and at the same time, they have also made great progress. In actively exploring the road of sustainable urban development, we should choose to draw lessons from and absorb foreign urban street design.

2.2. Outdoor thermal comfort and microclimate

The natural factors involved in urban climate mainly includes sunshine, wind, rain and snow, which are shown as radiation intensity, wind speed and changes of meteorological parameters such as air temperature and humidity. With the development of climatology research in the twentieth century, such as street width, street width, etc. The design elements of building materials, building height and shape, paving materials and so on are all related to the study of urban climate. Combining with development of urban climatology, advances in science and technology and experimental equipment, taking into account the importance of outdoor activities in daily life. Importantly, architects and planners began to make use of the research results of urban climatology to build a better guide for urban space. In order to determine the distribution of outdoor microclimate and provide guidance and suggestions for urban outdoor space design, relevant studies are often carried out. After the change rule, the built environment is explained according to the difference of urban spatial form, plant disposition and underlying surface material.

Since 1883, Howard L firstly observed of Urban Heat Island (UHI), more and more scholars began to study urban climate. In recent years, these studies are no longer confined to temperature alone. Observations of conventional meteorological parameters such as degree, humidity, solar radiation and wind speed have also been extended to thermal comfort and pollutant diffusion. Thanks to the progress of science and technology, scientists can use satellite telemetry. Many new methods or high-tech devices, such as sensors, remote-controlled small airplanes, infrared cameras and self-recording devices, are used to observe a small house and the intensity of a district, a city, or even a country's heat island. After a long period of observation, scientists found many factors affect urban heat island [49-53]. Nevertheless, urban planning and commercial pedestrian block are under way. When designing residential areas, the consideration of climate factors is still insufficient. Observation Data Base Provided by Climate Scientists, this does not affect the specific plans of urban planning, and in most cases these data do not meet the needs of planners and planners. Ooka[54] summarized different types of microclimate and their corresponding scales, because of different types of microclimate, the testing methods are different, and the instruments and accuracy requirements are also different. In this paper, we will summarize the research results of the predecessors on microclimate from three aspects: field measurement, theoretical analysis and laboratory analysis.

2.3. Field measurement

2.3.1 Urban scale

In recent decades, with the rapid development of urban climatology and urban boundary layer theory.

Oke [55] summarized the development of urban heat island (UHI) of 20th century, especial in air temperature observation method of Near-Earth. Compared to his research result, even in past 20 years, Great progress has been made in means and instruments, but the method of testing urban heat island has not been changed significantly [56]. Moreover, Lowry [57, 58] summarized these methods have similar problems, these methods can’t accurately distinguish and define urban effect on urban heat island (UHI). These investigation methods includes: (1) The climate trend of urban meteorological station in near 20 years. (2) Comparing one or more urban meteorological stations with annual variation trends of Several Suburban Meteorological Stations [59, 60]. (3) The analysis of urban and suburban weather station [61, 62]. (4) Observation Network of Meteorological Stations in and around a City [63, 64]. (5) Horizontal comparison of urban areas [65, 66]. (6) A comparison of weekend and working day heat island conditions [67].

Although the research and observation about urban heat island (UHI) continues for a few decades, Oke [68] summarized the phenomena of urban heat island: 1. The intensity of heat island decreases with the increase of wind speed and cloud cover. 2. The phenomenon of heat island is more likely to occur in summer or in the warmer half year. 3. The intensity of heat island will increase with the expansion of urban scale and the increase of urban population. 4. The heat island phenomenon may disappear during the day, when the air temperature in the urban centre is lower than that in the surrounding areas.

At last, the conclusions of Oke has been tested for many times, but it did not represent the urban heat island after that. Many scientists have pointed out other ways to control the formation, size and change of heat island intensity. In tropical and subtropical regions, many scientists have tested the effect of urban heat islands during the dry season is more terrible than in winter. In fact, Adebayo [69] tested their research in Ibadan, Nigeria and Jauregui In Mexico City and found urban heat islands in the dry season is much greater than that in rainy season. Tereshchenko[70] tested the air temperature in different parts of Mexico from 1926-1944 and found the cold island effect is even obvious in the rainy season. Scientists from Singapore, Japan and China in Asia's hot and humid climate region began the research about urban heat island (UHI) in 1920s, Toshio [71] researched the annual population migration and land use through meteorological stations show urbanization is the fundamental cause of heat island phenomena. He divides the relationship between the environmental planning of Osaka County Town and the surface heat balance of the suburbs is analyzed, and the natural results of the region are obtained by regression. Based on the above results, he proposed that ground transportation, one of the best ways to solve the urban heat island is to transfer the activities with large heat excretion to the underground. Hironori [72] used the method of satellite remote sensing observation and provided a map of the Tokyo Metropolis. Mochida [73] used the macro-climate of Tokyo of 1930s and 1990s to check the heat island intensity applicable to the region. Tran Hung [74] utilize TERRA/MODIS and satellite data to draw the climate map of big cities in Asia and annual cloudless surface temperature color block map and the spatial distribution of typical days and quarterly heat island intensity in these cities are analyzed. The relationship between the intensity of heat island and the properties of urban underlying surface is obtained by heat flow on urban surface. Liangmei Huang [75] chose four kinds of large surfaces including cement ground, forest, lake and grassland were selected in Nanjing area.

From the literature collected at present, the observation of urban-scale microclimate in hot and humid areas is still concentrated on the macro-scale. At the level of analysis and comparison of meteorological test data in the past and present, it summarizes the process of urbanization and the whole process of urbanization. The relationship between anthropogenic factors, such as global climate change and population migration, has not yet been related to the situation of heat island and urban planning. Discussions on the field of international design and its specific methods. Satellite, remote sensing and meteorological stations are mostly used in research methods. Macroscopic observation is the main point; in the research goal, it still remains in qualitative discussion, but not for designers and government officials. Decision makers provide detailed quantitative indicators.

2.3.2 Residential area and blocks

As a small-scale urban building complex, the micro-environmental quality of residential areas and blocks has the closest relationship with the residents, but the quality of the micro-environment of residential areas and blocks has a close relationship with the residents.

Until 2000, there were successive reports on the observation and analysis of microclimate, mainly in the area of building density. Such as Thailand, Singapore, Japan, Paris, Sao Paulo, Taipei and other international metropolises with hot climate in high and summer.

Hong Chen [76] conducted field measurement of a determinant low-rise residential area in Shenzhen, Guangdong Province in summer, and use unsteady state CFD to simulate three kinds of outdoor thermal interactions, including conduction, convection and radiation. From the measured results, it can be concluded that it was found that in hot August, the total horizontal solar radiation intensity could reach as high as that of the high greening area, the outdoor maximum air temperature can reach 34℃ and relative humidity is 50%.

Katchai [77] investigated the citizens Thailand through questionnaire survey in different seasons. The survey found that because of Mann the Valley has been in the tropical climate of high temperature and humidity for a long time. Residents are more sensitive to the changes of weather temperature, so most of them hope to stay in rooms.

Bingfeng [78] researched the influence of reflectivity of building exterior wall materials on the outdoor thermal environment. At the same time, measuring the meteorological parameters of indoor and outdoor microenvironment in different seasons, it is found that if building exterior walls use materials with higher reflectivity. Material can reduce the temperature of the inner surface of the room about in summer.

Giridharan [79] researched effects of greening types on outdoor air temperature in high-density residential areas in Hong Kong. The test results show that the sky openness (SVF). The terrain is the cause of air temperature in the residential area. The main cause of the change is due to excessive building density and man-made heat exhaust. Through the analysis of simulation, if the coverage ratio is increased to 40%, the UHI will reduce 0.5℃.

Aspect ratio (H/W) is the most commonly used block design parameters to define different design schemes. Many scientists try to find high aspect ratio, air temperature and building energy consumption through field tests and the relationship between human thermal comfort level and so on. Height-to-width_Canyon_Ratio means height of buildings on both sides of the street. The ratio of street width (W) to street width (W) determines the amount of sunshine available in the valley. The study is often concluded Hejie Valley aspect ratio and street orientation discuss the thermal environment in the valley. Generally speaking, when H/W=l, it is called Standard Street. Valley is called shallow Street valley when H/W is 0.5, deep Street valley when H/W is 2, and equal height of buildings on both sides of the street. It is called Street Valley.

The theory about the aspect ratio has been conducted for many years. The critical value of the degree (H) ratio indicates that there exists a sense of symmetry when H/W=l; when H/W>l, there is a sense of symmetry on both sides of the street. Buildings are prone to interfere with each other, H/W increases further, streets will increase the sense of closure; when H/W < 1, it will increase the sense of closure. H/W = 0.5-0.67 is a reasonable proportional relationship, which can create a friendly space. Different from open space, the square is enclosed in four directions. The street is limited by the facades of buildings on both sides. People are in four different proportions. Visual perception is quite different in the streets of H/W=0.25. In the streets with a height-width ratio of 1:4 (H/W=0.25), the visual perception is very different. The sky in the domain is three times as large as the wall, and the feeling of enclosure is very weak. b) Streets with a height-width ratio of 1:2 (H/W=0.5) are visible. The sky is equal to the street wall, and the proportion of the surrounding sky in the visual range decreases. C)

The aspect ratio is 1:1(HAV=1) Streets of 1:1 height-to-width ratio provide comfortable urban streets because they restrict the horizon of the sky and create a strong sense of enclosure. d) The height of the surrounding buildings exceeds the width of the street (H/W>1), the sunlight penetration decreases, and the sense of claustrophobia increases.

Scholars use field measurements and computer simulations to establish the height-width ratio of street valleys, meteorological parameters and human comfort. Level relationship, for urban design reference. Studies generally show that higher H/W ratio is beneficial to improve urban pedestrian area. Outdoor microclimate. Ali-Toudert [80] selected symmetrical Valley Models with H/W values of 0.5, 1, 2 and 4 respectively, and used NVI-met software simulates the thermal comfort level of different orientations towards Street valleys in the subtropical region in summer, taking air temperature and physiology as the main factors. The impact on the thermal environment of street valleys. It is found that the air temperature decreases moderately with the increase of H/W value, and decreases at 3 p.m. The valleys at points H/W=4 and H/W=0.5 have a maximum temperature difference of 3 degrees C; wider streets (H/W<1) have a maximum temperature difference of 3 degrees C in all directions. It's more uncomfortable. Adding shade is the only way to improve the thermal environment. Wang [81] researched the thermal environment of the channel is simulated and calculated with ENVI-met software. The air temperature, relative humidity, wind speed and in street valleys with different aspect ratios perpendicular to and parallel to the direction of the incoming wind are studied. The difference between orientation and Physiological Equivalent Temperature indicates that in hot summer and cold winter areas, the East-West trend should be wide street and the North-South trend should be adopted. In order to obtain more summer sunshade and winter sunshine for the long street and short Lane block model of narrow lane. It should be noted that if the width of the street and the height of the building are infinitely enlarged, the ratio of height to width of the street is not ideal. Physiological scale determines that people will feel oppression under high buildings, and human horizon determines walking or sitting. Only a certain range of horizontal and vertical space can be concerned. Promoting the concept of modernist Super City and mega-structure. At present, the city esteems the combination of concrete forests and creates a large number of suitable automobiles and trees in the city.

Sky view factor, SVF or Sky Openness refers to sky visibility in a specific place. The area ratio of the region to the hemisphere sky is directly related to the outdoor thermal environment. SVF is also often used to describe street valleys. Unlike the simple calculation of the aspect ratio of street valleys, the measurement and calculation of SVF requires specific instruments and software. The height-width ratio of street Valley is only related to the shape of buildings on both sides, while SVF is affected by buildings, plants and structures at the same time. Classical SVF measurements use fisheye cameras to photograph the sky at Um altitudes (Figure. 9) and to take pictures. Input software (such as RayMan_model) calculates the percentage of space allocated to the site. This result is called single point SVF, the defect is that it can only calculate the occlusion condition of a certain location. The grid divides the site and takes five pictures of the southeast, northwest and top, which are synthesized into one picture and then counted by software.

Researchers often combine SVF with thermal comfort index to evaluate outdoor thermal environment. Lin [82l et al. from a university in Taiwan For example, two parameters, SVF and PET, are used to describe the effect of shading on long-term outdoor thermal comfort. The simulation with RayMan model shows that the site with low SVF value is more uncomfortable in summer and the site with low SVF value is less comfortable in summer. (High shading) venues are more uncomfortable in winter, and places with moderate shading level can provide the longest time of heat relief throughout the year. Hwang [83] et al. chose six streets from high shelter (SVF=0.236) to low shelter (SVF=0.616). Seasonal effects of shading on thermal environment in street valleys: air temperature, relative humidity and black rice at Um height. The spherical temperature was calculated to evaluate the thermal comfort level of the site by PET. It is found that the settings can be used in summer and removed in winter. The sunshade facilities and deciduous trees can improve the sunshine condition of streets; the demand for thermal comfort varies greatly in different seasons. It is impossible to provide definite shelter level or high aspect ratio advice for urban streets. Similar to urban climatology, the quantitative results of SVF research are less relevant to landscape design. Street high and Width ratio and sky visibility coefficient are more often used to evaluate the thermal environment of built sites than to guide street scenery in the early stage of design.

2.3.3. Urban park

Park is the most common urban public green space, mainly including large public parks, street park, green space of fitness zone in residential area, campus public green space and other forms of green space around the building. It can not only regulate the urban thermal environment but also reduce the outdoor environment [84]. The concentration of pollutants can also be used as a place for public recreation and social intercourse to improve the quality of urban life. The role of urban parks in the thermal environment is not only limited to the region itself, but also extends to the surrounding areas. Closer to the park, the lower the air temperature will be.

Chen Yu [85] measured Temperature and humidity of the air in and around the park Singapore Bukit Batok country home and Clementi Woods park. The results show that the ambient air temperature. Ca [86] found that a park can reduce 1.5℃ in Tokyo. Givoni [87] researched Benjamin Park in Israel Haifa city the weather conditions of four days in July, and he found that air temperature in the park at noon was warmer than that around it. Chi Ru Chang [87] surveyed ambient air temperature of total 61 parks in Taipei city, the results show that the temperatures in parks are generally lower than those in the surrounding environment, while parks with large areas are usually smaller. Parker [88,89] examined the differences in Miami, Florida, USA, the influence of the form of park greening on the temperature of the exterior wall of the surrounding buildings. Shade can be reduced in summer when solar radiation is intense. Al Hemiddi [90] measured the university of California, Los Angeles Annual Surface Temperature of Different Green Space in Campus. He found that on a clear summer day, the air temperature near the bushes in the park was comparable. In the hottest days, the surface temperature of an unshielded parking lot can reach 50℃, at the same time, the grassland in the park is 29℃, the tree-shaded sidewalks is 23℃. Cooling of Microclimate by Park

Greening is effective. Like public space of campus, N.H.Wong [91] Combined Satellite Infrared Observation with Field Measurement Methods The influence of green space on heat island in Singapore National University was studied. Through mobile observation, he found large areas of the city. Urban parks can significantly reduce the maximum daytime temperature, and the maximum air temperature difference within the park is as high as in other places. Even at night, the temperature difference can be reached 3℃.

Based on the above field measurement results, even if the park is greened in a small area, it can also play a role in the microclimate nearby. Certain improvement effect. However, its overall impact on the outdoor thermal environment has both advantages and disadvantages, especially for the new additions. For typical hot and humid climate such as slope and Taipei. On the one hand, the trees shade the strong summer solar radiation for pedestrians. It creates a cooler environment; on the other hand, if planted in the wrong place, trees may block or change. The direction of wind, and the transpiration of leaves will significantly increase air humidity, resulting in discomfort. Therefore, in hot and humid areas. The best way is to arrange trees with large trunks and broad branches and leaves along the exterior wall of the building so that their shade can be kept. Cover walls or roofs as much as possible; for street parks scattered between buildings, trees should not be planted.

2.3.4. Distract along the river

Due to the influence of geographic factors such as river direction, it is not common to study the thermal environment along the river at present. Some studies [92] have pointed out that rivers crossing the city can obviously improve the thermal environment of its surrounding areas in summer, but it has an impact on it. The range is limited to several hundred meters wide and tens of meters high. Tadahisa [93] tested the outdoor thermal environment of riverside and coastal residential areas in Fukuoka City, Japan in summer was compared and tested. They found that sea breeze blows to land, the wind speed on the river channel is obviously higher than that on the sea side, but the temperature is lower than that of the nearby shade. In the case of Fukuoka, the river serves as an effective opening for introducing sea breezes into inland residential areas. In summer, the natural ventilation in this area has been improved significantly. Saburo [94] tested results show that the improvement of outdoor thermal environment by rivers is influenced by building density, wind speed and wind direction in Hiroshima. In sunny days in hot seasons, the temperature over rivers is at least 5℃ lower than that around them. From the collected literature, the case study of thermal environment along the river and its surrounding areas is carried out by using the method of field measurement at the present stage. It is still relatively small, mainly concentrated in Japan and other Asian countries. However, how to determine its scope of action, and how to plan and design.Coupling to improve the thermal environment of more buildings around, how to make better use of the larger wind speed in the river to improve natural ventilation and so on.

2.3.5. Green roof

Green roofs and walls can be afforested by using the building's own enclosure structure without occupancy. The plot land outside belongs to the unconventional greening system. Most of the current planning and design standards and guidelines are not. These two areas will be counted. In this prescriptive index. However, in the construction of high density and public use in areas with insufficient land, such as Singapore and Hong Kong, these two unconventional greening systems can improve the local outdoor thermal environment. It still plays an important role.

Bass [95] researched the study points out that both forms of greening can effectively reduce surface temperatures if they are large-scale. The popularization and application of model land can also reduce the intensity of urban heat island. On the proposal, in American Green Building Commission (US Green Building Council, USGBC), green walls have been increased to LEED Certify one of the scoring points. Van [96] tested the effect of these two greening forms on reducing organic dust and deposition was emphasized from the perspective of Ecological Engineering. Greening roofs and walls can be planted through transpiration of plants, shelter of leaves from buildings, and planting. Covering soil to increase the insulation performance of the enclosure results is particularly important in hot wetland areas where the energy consumption of air conditioning and refrigeration is the main factor. Peck [97] found that wall green can decrease the air temperature range from 10-60℃ to 5-30℃. Alexandri [98] finished the measurements of greening walls in Hong Kong show that they can minimize surface temperature. A roof garden in Singapore was tested and different plant species were found. Surface temperatures vary, but they are much lower than bare cement floors; compared with green roofs and hard floors, maximum air Temperature, Black Sphere Temperature and MRT can reach 4.2℃, 4.05℃ and 4.5℃.

2.4. Microclimate in urban street

Microclimate in street valley includes air temperature, humidity, wind, solar radiation intensity, precipitation, shading and other conditions. Regional climatic conditions are related to the shape of street valleys. Comfortable microclimate means that the air temperature and temperature can support outdoor activities well. Sunshine and shade [99]. Brown believes that landscape design has a significant impact on sunshine and wind, while air temperature and wind are not be affected [100]. Bosselmami et al. studied urban open spaces and sidewalks in San Francisco. Choosing sunshine and wind as the main factors determining comfort [101].

2.4.1. Sunshine environment in urban street

Does the direction of the street determine the annual and daily sunshine in the valley? Patterns, landscape layout will also affect the sun's happiness. Shoot, change the comfort of street pedestrians. Landscape designers can create comfortable rooms by configuring the landscape with sunshine rules. External microclimate. The direct radiation in the human body is mainly affected by the time and the direction of the street valley. The excessive direct blitz results in. The discomfort is much greater than the discomfort caused by the increase of the average air temperature, and the comfort caused by the increase of temperature by 1℃. The change can be offset by about 70W/m2 of horizontal blister radiation, while the outdoor daylight illumination in hot summer and cold winter areas in summer is about l000W/m^2, which is equivalent to the temperature difference of 14℃ [102]. The direct heating of air by solar radiation is very small. Only 0.02 ℃ can be raised per hour. The main heating air is the surface heat dissipation Street produced by the sunshine on the ground. The color and material of the buildings and the pavement on both sides of the valley will affect the solar scattering and surface reflection, thus affecting the street and valley heat environment. The changing trend of sunshine and the situation of site use will affect the time of research. Thorsson [103] researched thermal comfort of Japanese parks and city squares was investigated from 11 to 15 o'clock, during which the air temperature and sunshine were measured. The radiation reaches the maximum daily value. Hwang et al. observed the thermal environment of the street valley from 8 to 18 o'clock every day. It was along the street. Business hours of shops. Chen Zhuolun's [104] Research on Outdoor Thermal Environment in Guangzhou Residential Area in summer. The test was consistent with the main outdoor activities of residents. The relationship between spatial sunshine and user behavior is the focus of research. Statistical analysis of the number of space users within the interval confirms that warm environment and sunshine have a great impact on space utilization, and air temperature is a positive correlation between the number of sitting users and the average sitting time in summer for places providing sunshine and shade was 50%. Montigny [105] et al. finished Statistical analysis of weather conditions (air temperature, sunshine and precipitation) and the number of walks showed that sunshine and temperature. The effect of walking is interestingly negatively correlated: the positive effect of temperature on walking decreases when there is sunshine, and vice versa. The effect of sunshine on walking is obvious at extreme temperatures, but not so obvious at moderate temperatures. Zacharias [106] et al. found that the attendance rate of public places continued to increase with the increase of temperature, but the temperature was over 20℃, users tend to move to shaded areas to avoid direct blitz, so the sun is strong. The relationship between light and attendance can be expressed as an inverted "U" curve, while the relationship between shadow and attendance is a "U" curve.

2.4.2. Wind environment in urban street

Wind is the manifestation of air flow and one of the most important factors affecting the comfort of pedestrians. By the global, it is difficult to predict and control the joint influence of regional and local factors. From high pressure to low pressure over the global scale. Flow forms wind, and regional and local landscape patterns can change the speed and direction of wind in a small range. Urban Design Significant influence on wind movement is shown by the lower wind speed in the area near the urban surface than in the open area of the countryside, and the boundary layer range. Large buildings with poor internal design are prone to air turbulence and deterioration of the wind environment. Ghiaus [107] found that the wind speed in urban street valleys is lower than that of uninterrupted wind, and when the speed of uninterrupted wind is greater than that of 2m/s-4m/s, there is correlation with the wind in the street valley, when 2m/s or stronger wind is perpendicular to the street valley, the street valley will fall. A catastrophic flow occurs; if the wind is parallel to the axis of the valley, the vertical wind speed in the valley is very small. The effects of ambient wind on human body can be divided into two categories: one is the direct "mechanical effect" of strong wind on human body, which focuses on the safety of the wind; the other is that the wind shares certain air temperature, relative humidity and sunshine. The Wind of Mechanical Effect speed over 4m/s- 5m/s can be perceived, more than l0m/s will cause discomfort on walking, and more than 15m/s may cause danger. Canary Wharf [108] London, UK, concluded that the wind speed values for the unsatisfactory rate of 20% were intolerable.

Comfort studies generally discuss the effects of wind below 5 m/s on different activities and the satisfaction of users in different areas. Level (Table 2-1) shows that the higher the environmental dependence and the longer the use time, the lower the acceptable value of wind speed. Incense sticks. The urban wind environment study conducted by the Chinese University of Hong Kong has proved that the summer wind environment in Hong Kong is 0.53m/s. 1.3 m/s breeze can bring thermal neutral PET at this time is 28.1 ℃[109].

Table 2-1 Characteristics of wind speed [109]

Activity	Region	Characteristics		
		Accepted	Unaccepted	Danger
Fast walking	Path	43%	50%	53%
Wandering	Park	23%	34%	53%
Short standing	Urban space	6%	15%	53%
Long standing	Restaurant	0.1%	3%	53%

With the increase of wind speed, the cooling effect of wind is gradually strengthened, and the influence on human thermal comfort is also different. The corresponding relationship is shown in Table 2-2. Steadrnan [110] points out that the cooling effect of wind is more obvious at low temperature, and that the cooling effect of wind is more obvious at low temperature. It is difficult for people to detect wind less than 2.5m/s. Therefore, a similar conclusion can be drawn from the study of wind speed below 2.5m/s. The relative wind speed of 2.7m/s displayed on the hand-held anemometer of the stationary person will be obtained when walking. Local climate conditions determine the role of ventilation design in cities. Preventing sunshine injury in hot and arid areas in summer. Hazards are more important than ventilation, so narrow streets that are not conducive to ventilation are widely used; ventilation in hot wetland areas is more important than other micro-ventilation. Climate design is more effective in improving comfort, so urban design in hot and humid areas should mainly avoid urban form on summer ventilation.

Table 2-2 Correlation between wind speed and cooling temperature

Wind speed (m/s)	0.1	0.5	1	2	2.3	4.5	10
Cooling temperature (℃)	0	2	3.5	5	6	7	9

2.5. Outdoor thermal comfort research

The human body is a comprehensive response system of physiological and psychological interaction. The comfort evaluation includes the human body's sense of heat and cold, and the visual acuity. The comprehensive response of sensation and hearing, and the thermal comfort related to urban physical space are the focus of this paper.

The Institute of Refrigeration and Air Conditioning Engineers (ASHRAE_Standard_55-2004) [111] defines thermal comfort as: judged by subjective evaluation. The disconnected state of consciousness of thermal environmental satisfaction is a commonly accepted definition at present.

Thermal comfort is simultaneous with physical comfort. Subjective sensation related to environment, physiological condition and psychological state. ASHRAE_Standard_55 Given Light Clothes.

The range of indoor thermal comfort parameters - air temperature 22.8℃ -25℃, relative humidity 20%-60%, wind speed 0.05m/s-0.23m/s, Mean Radiant Temperature. It's equal to the air temperature (Table 3).

Szolcolay [112] divides the factors affecting human thermal comfort into three categories: environmental factors, individual factors and other factors. Relevant factors (Table 2-3), including "health status", "adaptability and thermal experience", were also classified as "other Relevant factors".

The evaluation of outdoor human thermal comfort comes from the study of indoor thermal environment. Indoor thermal comfort mainly consists of laboratory test and real test. Two methods of geographic investigation: the former uses instruments to measure in laboratories (environmentally controllable rooms or artificial climate rooms).

Human physiological indicators, such as sweating, skin humidity or temperature; the latter are used in daily space through questionnaires and on-site research. Stepwise observation was used to obtain the thermal sensation of the respondents [113].

Field investigation and numerical simulation were often used in outdoor thermal environment research to Get comfort evaluation.

In the interior, climate factors first affect the building envelope structure, and then affect human comfort.

Outdoors, people who lack the protection of buildings are directly in contact with and affected by the natural environment, when the landscape is set up.

The thermal comfort of human body will be significantly affected by the design.

Table 2-3 Three kinds of factors affecting thermal comfort

Environmental factor	Individual factor	Other related factor
Air temperature	Metabolic Rate	Food and drink
Wind speed	Dress Conditions	Body type
Relative humidity	Health status	Subcutaneous fat
Radiant temperature	Subcutaneous fat	Age and gender

2.5.1. Thermal sensation in outdoor environment

The traditional comfort theory is based on the stable state model. The heat gain and heat loss of human body in the environment are equal and maintained. The body temperature at 37℃, and also is regarded as a state of thermal equilibrium. To achieve thermal comfort, besides achieving thermal balance, we also need to ensure human body and all kinds of heat transfer modes in the environment are limited to a certain range, that is, the total heat dissipation: convective heat transfer accounts for 25%-30% in Fukuoka [114]. Radiation and heat dissipation account for 45%- 50%. Psychological factors affect fever comfort, past experience, expectations and exposure time all affect thermal comfort satisfaction [115]. Hartz [116] considers thermal comfort to be an acceptable temperature range for 80% of local respondents. The upper limit of acceptable temperature calculated by PET is 31℃, differences in climate adaptability of the population, in outdoor thermal environment research includes detailed microclimate analysis, it's promoted by the development of urban climatology and biometeorology [117]. Analyzing and evaluating thermal comfort [118], the researchers revised the thermal comfort evaluation index derived from indoor research using field measured data. The research confirms that people's expectation of thermal comfort will be relaxed under the influence of various uncertainties in outdoor environment. Summer climate in Lisbon [119] surveys related to comfort showed that outdoor users directly exposed to sunlight and wind felt comfortable in a hot environment. The temperature is higher than that in the room. Nikolopoulou [120] found that in Cambridge's urban space, from 7.5℃ in winter and 27℃ in summer. In Europe and Asia, researchers used field tests and questionnaires. A large number of investigations were conducted by means of interviews [121]. There are two main types of applications of thermal comfort: 1) Selecting a criterion from a large number of thermal comfort indicators to evaluate c the thermal comfort in cities. 2) Field investigation and evaluation of the local residents' thermal comfort limit value. Envi-met or RayMan models are used to simulate and evaluate the urban thermal environment, or to test the microclimate on site. The testing sites are concentrated in Europe. In addition, relevant studies have been carried out in Malaysia, Brazil, the Middle East and Africa. The second kind of research is based on the thermal comfort criteria of local residents' adaptability assessment. The research objects and methods are different in different regions.

2.5.2. Comprehensive of thermal comfort

Thermal comfort is the user's comprehensive thermal feeling. Outdoor thermal comfort involves a variety of microclimatic factors, which need to be studied. Considering its impact on users. Nikolopoulou et al [121] competed against Cambridge City in the spring, summer and winter of 1997. Questionnaires and temperature measurements were conducted in four cities of the heart to correlate the outdoor thermal environment with the subjective evaluation of human beings. Lian [122] believes that simple physiological indicators are not enough to evaluate outdoor thermal comfort. It is suggested that psychological factors should be taken into account in evaluating outdoor thermal comfort. In follow-up studies, Nikolopoulou et al. [123] suggested that the effect of microclimate differences on thermal sensation could only be explained by 50% Actual Thermal Sensation Votes, ASVs difference, the rest need to use Thermal Sensation Votes, ASVs. Psychological adaptation explains thermal comfort at three levels: physical, physiological and psychological. Thorsson et al [124] survey of a Swedish urban park in 1997, the thermal environment, accessibility and design are important factors affecting the utilization of the park. Psychological factors such as exposure time, expectation value and experience will affect subjective heat assessment.

2.5.3. Regional characteristics of Thermal Comfort

Regional characteristics is the nature or characteristic associated with or related to a region [125], which manifests itself in the nature, climate and of the region. The unique features of culture and landscape. According to local characteristics, countries have recommended local thermal comfort standards (Table 4). It reflects the regionality of thermal comfort.

Table 2-4 Recommended air temperature in three countries

Space	Britain	Germany	America
Living room	18.3℃	20℃	22.8℃-23.9℃
Bedroom	16.5℃	20℃	22.8℃-23.9℃
Kitchen	15.5℃	20℃	22.8℃-23.9℃
Bathroom	15.5℃	22℃	22.8℃-23.9℃

Residents in different climatic zones have different heat requirements. Lin [126] survey of Taichung City in Taiwan proves that 90% of the local residents live in Taichung City. The temperature range of PET with acceptable thermal comfort is 21.3℃-28.5℃. It can be seen that Taiwan residents living in subtropical climate areas are more heat-resistant. Table2-5 shows the different fever of Taiwanese and Western/Central European residents. The comfort PET range, based on such criteria, is 50% of the year in Europe (from early April to mid-November). Comfort period (slightly cool to slightly warm), while the comfort period in Taiwan only accounts for 20% of the whole year.

Table 2-5 Recommended air temperature in three countries

Thermal sensation	Very cold	Cold	Cool	Slightly cool	Moderate	Slightly warm	Warm	Hot	Very hot
Taiwan	14	18	22	26	28	30	34	38	42
Europe	4	8	13	18	21	23	29	35	41

2.5.4. Thermal comfort index

There are many indices that evaluate outdoor thermal comfort, such as the Predicted Mean Vote (PMV) [126], Standard Effective Temperature (SET) [127], Effective Temperature (ET) [128], Outdoor Standard Effective Temperature (OUT-SET) [129], Universal Thermal Climate Index (UTCI) [130], and Physiological Equivalent Temperature (PET) [131].

PMV is an index based on the basic equation of human thermal balance and the level of the subjective thermal sensation in psychophysiology. It takes into account the comprehensive evaluation index of many related factors of human thermal sensation.

SET is an index which represents the dry bulb temperature of a hypothetical inner environment at 50 per cent relative humidity for subjects wearing clothing that would be standard for the given activity in a real environment.

ET is the temperature at which motionless saturated air can induce the same sensation of comfort as that induced by the real conditions of air temperature, humidity, and air movement.

OUT-SET is similar to the SET index, but it is widely used in outdoor environments.

UTCI is set as an isothermal air temperature and simulates dynamic physiological results by mixing advanced clothing models with a thermoregulatory model.

PET is an index which is based on the energy balance of the human body and is known to us as the air temperature that makes thermal conditions in an indoor space be in balance with the core and skin temperature in an outdoor environment. This index is defined for a 35-year-old man 75 kg in weight, 1.75 m tall, with clothing insulation of 0.08 m^2K/W, and a metabolic rate of 164.49 W/m^2 in summer [131]. Moreover, this index has been approved as an outdoor thermal comfort index by the VDI standard of

Germany.

According to the needs of scientific research, the researchers classified the indicators in order to explore the human behavior of thermal environment from different perspectives. For psychological impact, such as thermal safety index and thermal comfort index, equilibrium state index and non-equilibrium state index [132]. The validity of heat index varies in different climatic regions. It is necessary to select indicators that can represent the actual situation of the site according to the research objectives. Monteiro et al [133] in Brazil Paul's outdoor field research suggests that in subtropical climates, the equivalent perceived temperature (Temperature of Equivalent) Perception, TE) model parameters have the highest correlation with field measurements, and the best prediction rate can be obtained. Potential thermal storage coefficient (PSI) and PET. Based on previous research and research, the Wet Bulb Globe Black Sphere Temperature (Wet Bulb Globe) was selected in this study. Temperature, WBGT and physiological equivalent temperature (PET) were used as indicators to evaluate the summer microclimate of the base. It is a physical index that objectively describes the thermal environment of the measured site and is directly related to the climate and the site environment. It is used to evaluate the thermal environment of the site. Microclimate differences caused by landscape design prices users' subjective comfort.

2.6. Microclimatic regulation

Microclimate comfort is affected by climate conditions, and the key factors affecting comfort are different under different conditions. For example, in hot summer and cold winter areas, both summer ventilation and winter windbreak are advocated, so the site should be arranged in accordance with the local dominant wind direction. Buildings to create an open space with a good thermal environment. Giovanni [141] believes that in assessing the relative importance of climate conditions in winter and summer, the following factors need to be taken into account: individual cold proof is easy for personal heat proof; building heating equipment is simple and relatively economical, while air conditioning and refrigeration costs are expensive. The scheme design can effectively prevent the cold wind from intruding into the building; the wind speed is very small can also form a cross-hall wind; modern thermal insulation materials. It can greatly save heating energy consumption, but it is not suitable for adjusting room temperature in summer. It can be seen that winter is no matter personal outdoor cold protection. It's also easier to keep buildings warm, so it's more meaningful to use landscape design to adjust the urban environment in summer. In urban design, full consideration should be given to how to create summer comfort. Take Chengdu as an example, the summer and winter in this area. The outdoor environment is not very comfortable, considering the user's self-regulation ability, design difficulty and microclimate improvement. More attention should be paid to the improvement of thermal environment in summer. Business strategy can regulate people's environmental comfort from physical, physiological and psychological levels.

1) Physical adaptation: all artificial changes made to adapt to the environment or meet needs, including individual responses and cyclical changes. The former includes changing clothes, postures and positions, drinking hot and cold drinks, and the latter includes opening windows and shading umbrellas.

2) Physiological adaptation: The gradual adaptation of the human body to stimulation due to repeated exposure in extreme environments is called bio-adaptation.

3) Psychological adaptation: including people's tolerance of the natural characteristics of the environment, individual expectations, previous experiences, violence.

The effects of dew time, sensory control and other stimuli. This paper mainly studies the activities of the users in urban pedestrian street space, that is, the physical adaptation part.

2.6.1. Plant

Shading, transpiration and natural ventilation of plants can effectively improve the urban thermal environment. Density, density of trees, shape, size and location affect the distribution of sunlight and wind in the site, and control the air temperature and the surface temperature of the surrounding site. Increasing plant coverage at urban scale can significantly reduce air temperature.

Taha [142] research on the City of California, USA improved the environmental temperature by planting trees on a large scale, it was found that plants could reduce the air temperature by 2℃ at 2pm in summer. In extreme cases, it can reach 3.5℃. Dimoudi et al [143] supported by the European Union "PRECs" project to study urban plant pairs. he influence of microclimate proves that the increase of urban green space area can effectively reduce the urban air temperature and increase the built-up area. The 10% green space rate can reduce the temperature by 0.8K, and the design parameters which can be used in different climatic regions and urban texture are summarized. Plant species and morphology affect the ability to absorb and shield sunshine, resulting in differences in cooling effects. Zhao Jing [144] simulation calculates the cooling capacity of plants in the streets of Xi'an in summer, and considers that trees have the best cooling effect, followed by the WBGT value of 1.1 m below the crown at noon was 3.67℃, lower than that of non-greening. Lin Borong's research [145] shows that trees improve the outdoor thermal environment in summer in most cases. The effect is better. Trees are planted on the East and west side of the building, and the effect of improving the thermal environment is better than that of planting trees. In the follow-up study, Lin Borong et al [146] used numerical simulation experiments to explore the total green amount with the standard effective temperature as the index. If the average standard effective temperature is taken as the index, the thermal environment improvement effect of trees is better. Three Kinds of Planting Climate improvement of physical types is influenced by the layout and orientation of buildings. By adjusting the allocation of trees, a better result can be obtained.

2.6.2. Water body

The design of water body has both material and spiritual meanings. It has the functions of regulating microclimate, increasing symbolic meanings and pleasing senses. Water has a large heat capacity, which can absorb heat from the air to regulate the thermal environment above and around the water body. The evaporation of water will consume a lot of vaporization heat and increase air humidity, and excessive humidity may cause human body to fall. Sullivan [147] divides the design of water body in courtyard into static water, dynamic water and filling water according to the state of water movement. The jokes of air-water, water walkway and water are discussed. The water management form and climate adjustment facilities of traditional landscape are discussed. Li Donghua et al [148] used LancJsat5TM image data analysis, it is found that the cooling effect of rivers on urban land mainly concentrates on the two sides of rivers. Within the range of 200 m, the maximum temperature drop is 0.9 ℃, and the wider the river, the better the urban heat island effect can be alleviated. Introducing water system into urban streets is a common method of landscape design. The demarcation line between rail transit and pedestrian roads in the travel area. The cool water in summer attracts children to play in it. It is the street. In addition, street landscape also has powerful spiritual functions. David Irving Man-made Trees in Densely Populated Areas. The value is to make residents feel more happy in urban life. Therefore, we are discussing how landscape design affects micro-atmosphere. At that time, we should also think about the creation of the spirit of place by plants and water bodies, so as to put forward good strategies for street landscape design.

2.6.3. Clothing Adjustment

The thermal insulation property of clothing can adjust the heat loss of human body, and then affect the thermal comfort of human body. Adjustment of clothing. The degree depends on the style, quantity, texture and body area covered. The thermal resistance values of common garment combinations.

2.6.4. Activity regulation

Different levels of activity result in different energy metabolism and different thermal sensations. Clinical regulations are not in progress. Before breakfast, stay awake and lie still for half an hour, room temperature at 18℃, the metabolic rate measured between 25℃ is called Basal Metabolic Rate (BMR) as a criterion for measuring metabolism with age. Gradually, the number of young people is higher than that of old people, and that of women is lower than that of men. The metabolic rate unit lmet=58.2 W/m^2 is defined as the metabolic rate of a person during sitting down, corresponding to the average body size. The maximum metabolic rate of healthy people at 20 years old is 12 met, and it drops to 7 met at 70 years old. The increase in metabolic rate of Imet corresponds to the temperature change of 1.4℃, Table 6 are typical activities of the metabolic rate of walking (2met) is similar to that of sitting down (Imet). The metabolic rate of walking (2met) is similar to that of sitting down (Imet).

Table 2-6 Recommended air temperature in three countries

Activity type	met	W/m2	W(av)
Reclining	0.8	46	80
Sitting position(quiet)	1.0	58	100
Stand, sit and work	1.2	70	120
Light activities	1.6	93	160
Walking (0.9m/s)	2.0	116	200
Walking (1.2m/s)	2.6	150	260
Walking (1.8m/s)	3.8	220	380

This paper reviews the development of outdoor microclimate experiments and simulations from a functional perspective, and explores the evaluation index of street valleys. The characteristics of human outdoor thermal comfort and the evaluation index of thermal environment are summarized, and the influence factors of microclimate are discussed. The regulation of microclimate is discussed from three aspects of activities. From the above literature, we can see that the comfort degree of urban street environment is good.

1) The lack of knowledge exchange and interaction among disciplines, and the lack of quantitative research on design. Open space in City. In landscape design, abstract models and correlation formulas established by scientists based on quantitative analysis can not be used as landscape designers. The latter is more accustomed to spatial thinking and graphic expression. Chinese style

2) Research on the use of urban external environment related to thermal comfort mainly chooses urban parks or squares, but neglects Street space; the study of urban street valleys pays attention to the distribution of the thermal environment of the site, but pays insufficient attention to user behavior.

3) The study on the relationship between environmental comfort and user behavior should pay more attention to the ideal situation, and discuss the suitable outdoor activities.

In weather, the effect of small changes in physical environment on users' behavior is less discussed with users as the center. Psychological and psychological adaptation behavior in actual outdoor activities. Therefore, this paper will combine the current research situation and the key technical problems to be solved to launch the urban pedestrian street micro-ramming. Investigation and analysis of climate comfort and usage condition.

2.7. Simulated model of outdoor thermal environment

Using computer to simulate outdoor thermal environment can save the expensive cost of field experiments and is more convenient. The effect of different design schemes is predicted. At present, computer simulation technology has been applied to architecture, landscape and planning. The field of accounting is widely combined. John Arnfield [149] research directions of outdoor thermal environment simulation are summarized.

1) Turbulence in the urban atmosphere
2) Storage and anthropogenic heat in urban energy balance system (Fluxes in the urban energy balance)
3) Urban radiation balance in urban climate
4) Urban facet energy balance between urban underlying surfaces
5) Urban neighborhood water balance

Now we will introduce the mature computer simulation models of outdoor thermal environment one by one. Among them, "KLIMA- MICHEL-MODEL" [150] (KMM, Embedded UBLIMA Model) For European Standards VDI-3787 1998.

2.7.1. Surface thermal time constant (STTC) and Thermal time constants of buildings (CTTC)

Swaid and ME.Hoffman [151] are expanding the simulation of thermal inertia of materials in building energy consumption to urban micro-air. In the field of climate change, the surface thermal time constant is proposed. The concept STTC (Surface Thermal Time Constant, STTC) set the time when a homogeneous material changes its energy storage due to an increase or decrease in the absorption of heat radiation. The field measurements of impervious cement, asphalt and soil surface show that the values of STTC are different, as one of the thermal properties of underlying surface materials, it was then widely used in different outdoor meteorological conditions. The numerical simulation of the surface temperature of homogeneous materials:

$$\text{STTC} = \frac{1}{2}Lpc \times \frac{L}{K}\left(\frac{1/h}{1/h + 1/K}\right) \quad (1)$$

In formula, L is material thickness, p is material density, C is specific heat capacity, K is thermal conductivity, H is heat transfer coefficient.

In 1990s, H.Swaid and ME.Hoffman [152] take Consideration is given to man-made heat removal and building sunshade in cities. The thermal time constants of buildings are further proposed for the influence of surface radiation. (Cluster Thermal Time Constant, CTTC) [153] contains many design factors related to urban planning, such as construction. Building density, shading area and ratio of building height to street width can simulate the whole day under different underlying surface conditions.

$$\text{CTTC} = \sum_{i=1}^{n} L_i\, p_i c_i \left(\frac{1}{2}\frac{L_i}{K_i} + \sum_{j=k+1}^{n} \frac{L_i}{K_i}\right) \quad (2)$$

In formula, S is volume ratio, FA is the area of the roof in the block, WA is the area of the exterior wall of the building in the block.

CTTC is widely used to evaluate the ratio of block width to building height in mid-high latitudes and dry-hot climate zones [153]. There are many physical assumptions and constraints in the development process of the series model, which limit its application. Judging from the literature collected at present, STTC and CTTC are the application of series models is limited to middle and high latitudes and underground In the sea area, the application in the low latitude humid and hot climate area has not been reported yet.

2.7.2. MEMO-MIMO Model

MEMO is the Institute of Fluid Dynamics, University of Karlsruhe, Germany and the University of Aristotle, Greece [154]. A mesoscale hydrostatic model developed jointly with the heat transfer laboratory. It is used to describe air flow in complex terrain. Diffusion of dynamic and chemical dust. Based on MEMO, scientists at the Institute of Fluid Dynamics, University of Karlsruhe, Germany, developed a small scale. (Hydrodynamic model, MIMO). MIMO used three-dimensional staggered grid (Staggered grid arrangement) and coordinates transformation (Coordinate transformation). In order to achieve high-precision simulation of near-ground air boundary and surrounding buildings [155]. MEMO and MIMO have many similarities in control equation, mesh size and so on. They perform numerical calculations. In the simulation, the mass, momentum, energy and fluid kinetic energy equations need to be solved, and the dynamic viscosity in the governing equation needs to be solved. Hysteresis coefficients are expressed as pressure relations. Both models can use three-dimensional non-equidistant grids to increase spatial resolution. When calculating the turbulent diffusion coefficient, MIMO Adopt standard K- equation, and is used in small scale model. MIMO Point formulas used to simulate simple shapes and type building. The simulation results are further compared with the wind tunnel tests to verify the accuracy of the calculation results.

As mentioned earlier, large-scale models, MEMO in Small-scale model and MIMO Can accurately simulate different heights of large airflow condition. Moreover, the two models have many similarities in control equation and other aspects. All these provide conditions for coupling the two different scale simulation models. R.Kunz etc. [156] found three-dimensional interpolation, surface boundary modification and simplification of interpolation are used for model coupling simulation. The method of transverse boundary condition is introduced. The calculation of MEMO can calculate results of urban atmospheric flow simulation are transmitted to MIMO. The change of regional atmospheric circulation can directly affect the boundary conditions and initial conditions of small-scale wind environment simulation. The state is reflected in the simulation results. In MEMO-MIMO, coupling system has been used to simulate Mannheim Road in Germany. It is found that the wind speed simulation results are slightly larger, but the distribution is roughly the same as the measured results. (Figure. 2-6).

Although the preliminary coupling of different scale simulation models is realized, the coupling is from MEMO reach MIMO Unidirectional.

It is well known that large-scale air flow and pollutant diffusion are also affected by small-scale air flow and other factors. How to aggregate the simulation results of several small-scale models and output them to large-scale models It has not yet been reported that the model can modify its simulation accuracy and realize the interaction and coupling between multiple models of different scales.

2.7.3. Urban Bio-climatological Model

Urban Bio-climatological Model (Urbanes Bioklima Modell, UBIKLIM) meets the needs of urban planning and design. In the early formulation of the conceptual planning plan, the personnel can quickly evaluate the effects of the artificially modified microclimate environment on the biological climate and the biological climate.

The influence of human thermal comfort [157] can simulate the bio-meteorological parameters which have the strongest impact on human body in the block, and is designed for the purpose of design. Teachers and owners provide important reference for evaluating the health and comfort of different planning schemes.

The required input is the nature of land use in the simulated area (Such as water, forests, buildings, etc). After that, according to road orientation, building density, building height and green.

The simulation area is further subdivided by planning parameters such as conversion rate. In this case, one-dimensional boundary condition model met the underlying surface, which is called to calculate different porosity, and is off the ground. Thermal environmental parameters at meter. So far, all the microclimate parameters are only functions of land use properties. In the second step of simulation, terrain, altitude and self-occlusion gear and so on will be calculated by physical, statistical or empirical methods. In the synthesis of different horizontal networks. Finally, the bio-meteorological color block maps of sunny summer days are output. For further development of UBIKLIM. The scope of application of the model, Matthias etc. [158]. The model is extended is exhibited it with special simulation software for micro-environment ENVI-met Coupled to integrate wind, temperature and humidity in micro-environment. To evaluate the bioclimatic effects of different land types and landscape designs, combined with human thermal comfort indicators. UBIKLIM Sensory temperature was used in the model (Perceived Temperature, PT), As the main thermal comfort index, quilt Heat Island Strength for Simulating and Evaluating Urban Scale [159] Changes in thermal safety and comfort due to urban heat island [160]. And the impact of urban planning and design changes on the biological climate in Berlin, Karlsruhe and other large and medium-sized cities [161] and so on. His Applications are mainly concentrated in the cold regions of middle and high latitudes, such as Germany.

2.8. Computer simulation software for outdoor thermal environment and its application

On the basis of summing up the previous research results, scientists from all over the world make use of powerful computer cluster technology. Many easy-to-operate software have been developed to predict outdoor thermal environment and building. Some of them are soft. It also integrates other databases or analysis software, such as geographic information systems (Geographical Information System, GIS) and computational fluid dynamics (Computed Fluid Dynamic, CFD) applications of these software. It covers all stages of urban planning and architectural design, from the prediction of building energy consumption and outdoor environment to the evaluation of human body. Thermal comfort and health condition, etc. At the same time, by comparing the field measured data, wind tunnel experiments and other methods, the study does not. These tools are further checked to ensure the accuracy of their results, in line with climate conditions. Ooka [162] summary the field of building microenvironment, computer simulation SET.

2.8.1. Energy and Environment Prediction Software

Energy and Environment Prediction Software (EEP) is from Cardiff University in England (Cardiff University). It is mainly used for moderate quantitative simulation. Building energy, traffic pollutant diffusion and health conditions in urban area [163] Statistical analysis was used. Prediction of regional trends in energy consumption and carbon dioxide emissions [164]. In order to assist planners in choosing reasonable schemes, Effective control of ecological footprint. It passes with GIS. Connection of databases to obtain information about buildings and roads in cities Information, and from within high speed channel. In the energy consumption analysis model, the classification method of energy consumption for civil buildings issued by the British government is adopted. (Standard Assessment Procedure, SAP), According to the different building area, service life and type, it is divided into one hundred Planting Residential Buildings and Forty-eight. Each type of commercial building has its corresponding annual energy consumption cost and carbon dioxide. Emissions and SAP are in the traffic sub-model, the spatial analysis method is used. Determine the amount of traffic on each road and the total amount of pollutants it emits. After the simulation is finished, EEP Will be based on the corresponding color block maps are output according to the values of the same plot. EEP is the main results of the software

As an assistant decision-making software for urban planning, EEP should mainly be medium-sized cities in Commonwealth countries. It is recognized as official software, which is specially used to evaluate old city renovation and new city planning. In order to ensure the accuracy of the calculation results, EEP requires a large amount of actual data as support, such as building use years, area ratio of windows and walls, etc. The way to obtain these data is mainly archived construction documents and designs. At present, it only integrates British standards and is not suitable for global promotion. Although EEP Reasonable utilization and GIS resources, and can output the results as a more intuitive color block diagram, but by its huge demand for input data and the singleness of quoted evaluation index limit its further development. Besides this, it can not quantitatively evaluate the impact of meteorological parameters on regional energy consumption and carbon dioxide emissions.

2.8.2. ENVI-met

Institute of Geography, Bohong University, Germany Michael Bruse [165] by studying the exterior surface of buildings, vegetation and air, etc. Thermal stress relationship between them. Software for micro-environment simulation has been developed the ENVI-met. It uses three-dimensional non-fluid static model for simulating the surface of buildings in urban environments vegetation. The relationship between air. Its horizontal resolution by 0.5 to 10. In seconds, the order of time is between 24 and 48.Between hours, so it's especially suitable. It can be used to simulate small and medium-scale micro-environment. In addition to being able to deal with the thermal properties of natural and artificial structures, ENVI- met, there is also a water evaporation module, which can simulate the thermal effects of lakes on the environment. ENVI-met simplify set the plant into a one-dimensional rectangle according to the height of the plant, and assign these shapes according to the species standardized Leaf Area Index (LAD) and root area index (RAD). The interaction between leaves and surrounding air: three parameters can be expressed as direct heat transfer heat flow, evaporation intensity of surface water and transpiration intensity of plant itself. At present, ENVI-met is mainly applied to simulate greening roofs, walls, road materials and other different types of cities. The impact of mattress on micro-environment and the evaluation of landscape design schemes. The scope of its application is mainly at the level of large and medium-sized cities, and only for several typical underlying surface types. For smaller areas, such as building monoliths, residential districts and street parks, etc. No report has been reported. Therefore, it is necessary to further verify the accuracy of its application in small-scale simulation and to analyze the differences. Sensitivity between underlying surface form and material.

2.8.3. Architecture-Urban-Soil Simultaneous Simulation Model, AUSSSM

It was developed by the Urban and Architectural Environment Laboratory of Kyushu University, Japan (Urban and Architectural) Environment Laboratory, Kyushu University). The urban heat island simulation software has been checked and modified many times. Pieces. From the point of view of planning and design, it can predict the intensity of Heat Island based on urban meteorology principle (UHI) [166].

Strictly speaking, it is not only a mesoscale simulation software consisting of many

independent sub-models, but also a building tool. Single-computer software for simultaneous solution of building heat system, urban atmosphere and surface cover. It contains the following reciprocal elements influences sub-models: urban canopy sub-models for calculating one-dimensional momentum and heat and mass transfer in the atmosphere; building sub-models. The model is used to calculate the heating and air conditioning load, the soil sub-model is used to calculate the surface evaporation intensity, and the plant sub-model is used to calculate the surface evaporation intensity. It is used to calculate the heat transfer between vegetation and atmosphere on grassland and other surface. It should be pointed out that all these sub-models simplify the complex three-dimensional heat and mass transfer process into one-dimensional one. It has similar accuracy. Because of the lack of sub-models for large trees and their shadows. It can't be simulated yet. Other forms of greening besides grassland and their effects on the thermal environment were discussed. At present, it is mainly used to evaluate the interaction of building, man-made heat and outdoor thermal environment quality and the change of building energy consumption in urban scale
caused by the change of heat island intensity.

Yuemei Zhu etc [167] researched dynamic simulation and climate parameters, anthropogenic heat intensity and indoor and outdoor SET. Yinping Wang [168] researched outdoor thermal ring of a fictitious office complex in Shanghai circumstances and comforts.

2.8.4. Sustainable Urban Neighborhood Modeling

According to the Fifth EU Cooperation Framework Agreement Energy, Environment and Sustainable Development (Energy, Environment and) (Sustainable Development, NNE5-2001-00753) Britain, Czech Republic, Switzerland, France, Finland and Greece. Six other countries participated in the development of sustainable urban residential areas simulation program (Sustainable Urban Neighborhood) (Modeling tool, SUNtool) [169].

SUNtool was used in 2006, is a new generation of architectural design and Environmental Synthesis Simulate software. It helps users to optimize by simulating urban microclimate and the flow of energy, water and waste Sustainability of the master plan. The overall structure of the interface and the calculator of the software is shown in the figure 16. It includes microclimate, natural lighting, vegetation and equipment, random utilization and renewable energy.

The main application areas are: describing the factors affecting dynamic demand and supply of energy, water and waste. These substances are reflected by simulating the interaction between urban microclimate, residents' behavior, resources and buildings.

2.8.5. Radiation on the human body, Ray Man

Human thermal radiation assessment software (Ray Man) It's based on German norms. VDI is A Developed Biometeorology Model Domain simulation software [170]. It can simulate the total amount of solar radiation heat, as well as atmospheric cloudiness and other barriers. The effect on short wave radiation. The results of the final output include: the average necessary to study the energy balance of the human body Radiation temperature MRT. The duration of sunshine, the total amount of solar radiation and the solar balance under different sky visibility factors Mean and maximum values, shaded areas of trees, etc. For evaluating urban bio-meteorological indicators of thermal comfort, such as PMV, PET and SET. At present, it is mainly used to assess the impact of residential areas and other large-scale infrastructure projects on the environment, climate change. Analysis of outdoor environment with excessive thermal stress and calculation of complex residential environment. Solar radiation and prediction of natural processes from the perspective of landscape ecology

2.8.6. Mitigation Impact Screening Tool, MIST

To assess urban development strategies economically, rapidly and scientifically, the U.S. Environmental Protection Agency (Environment) (Protection Agency, EPA) Organization and development of urban heat island risk and impact assessment software (Mitigation Impact)(Screening Tool, MIST) It is an easy-to-use software that is summarized from long-term observations of cities. Based on the atmospheric model, the statistical models of the correlation between these meteorological parameters and ozone layer are summarized, and the energy is finally imported into the atmosphere. Preliminary Feasibility Analysis of Development Planning for American Cities The impact of urban development strategies on heat island intensity can be assessed quickly. However, due to the input parameters conditions have higher requirements and are limited. Further application. At present, it has not been found that the software is used in the United States [171].

2.8.7. Outdoor Human Comfort Expert System, OUTCOMES

Outdoor Human Thermal Comfort Professional System (OUTCOMES). It is a software for evaluating the thermal comfort of outdoor human body. Its operation is very simple and can be used to predict human thermal comfort or urban terrain in different urban structure systems. The impact on outdoor thermal comfort and urban landscape design based on thermal comfort demand. In order to facilitate the use of users, it also has a database with it [172].

All the software mentioned above are developed on the basis of rigorous scientific reasoning, and they are widely used in the field of computer science. Used in various fields of scientific research and engineering design. The emergence of these software effectively solves the problem in the field of construction technology. Prediction and evaluation of urban micro-environment and thermal comfort can be used for scientific research and engineering design. However, there are still several problems that can not be ignored. First, the calculation accuracy of these software needs to be further improved. Confirm it. In view of different climatic conditions, boundary layer and regional underlying surface, field measurements are carried out. In the wind tunnel experiment of scale model, more experimental data are needed to verify the software. Secondly, implement software. Cooperative computing between them. As far as the application of Urban Microclimate Simulation is concerned, there are various factors that influence each other in space. Su, the simulation of microclimate can not be limited to a small part of the analysis. Therefore, how to synthesize. It is very important to use different scales of evaluation software. From the development trend of sustainable architectural design, future construction. The object of architect's design is not the building group itself, but the comprehensive consideration of energy consumption, water resources, air pollution and so on. In many ways, this requires more than one software to simulate. How to make all kinds of software collaborative computing, integration. Combining the input conditions and output results of each other, it is a problem that needs to be solved to give several evaluation indexes at last. Question. Thirdly, these software can only evaluate the advantages and disadvantages of existing schemes, and architects can only do the best according to their own experience. Change. Finally, in terms of computing speed, there is still room for improvement. Architects need to be quick in their creative process Judge the advantages and disadvantages of several or even dozens of schemes. This requires the application software to get the simulation results in a short time. Of course, with the dramatic improvement of computer performance, this is no longer the main problem.

2.10. Impact of Urban Microclimate on Building Energy Consumption

Although the definitions of city size vary from country to country in the world, the number of inhabitants is basically used as the index. The impact of climate on building energy consumption mainly concentrates on large-scale or super-large-scale buildings with large population and high degree of commercialization and city types. The influence of urban climate on building energy consumption is mainly reflected in the increasingly serious urban heat island phenomenon in recent years. As a result, the energy consumption of air conditioning and refrigeration in summer increases significantly. As early as 1973, Watanabe [173] used satellite remote sensing, we observed the metropolitan area of Tokyo, Japan. The distribution of land surface temperature and thermal environment in the region were also studied. Based on the field investigation by the government, the distribution map of energy consumption was drawn. After analysis, they found that the energy consumption per unit area in the area was about higher than that in the surrounding area due to the excessive intensity of the heat island 10%. Ojima [174] studied from the annual meteorological data reveal the cooling load over the past ten years average increase 10%~20%. In 2000, the electricity load will be used increase 50%. M. Santamouris etc [175] researched urban and suburban areas of Athens and found a different block of gas. Like the data, it is found that the intensity of the urban heat island in Athens in summer exceeds that in Athens. By comparing the electricity consumption, it is found that urban housing, the cooling load of the house is almost double that of the suburbs, and the peak power consumption caused by refrigeration can reach three times. Because of outdoor air temperature is too high, resulting in the lowest energy efficiency of air conditioners 25%. At the same time, the winter heat load of downtown buildings is higher than that of suburbs lower than 30%. Akbari etc [176] studied of the overpopulation of the United States records of electricity use in 10,000 large cities show that every time the temperature rises. The meteorological data of the year can be found. Summer temperatures in these cities have risen on average.

Chapter-3.

Microclimate and Leisure Activities in street

3. Microclimate and Leisure Activities in street

Activities are free choices with people's willingness, designers should be good at observing the common behavior of places and summarizing the use. In order to anticipate site usage patterns in new projects and respond to them in design. The scheme is presented as the designer's concept of land use planning, project shuttle work and put into use, if the site is merged to promote user activities, proving the designer's vision of success, and vice versa. The above process is the design and use of in traditional environmental behavioral science. In real life, if the landscape resources are scarce and unevenly distributed, the free space may appear based on "rigid demand". And deviate from the user and usage method that the designer foresees. At this time, although there are many users and abundant activities, they are not. On the one hand, these behaviors may not be the most satisfactory choice for users, but not for users.

Shu Guozhi [177] depicted the envoy of Taipei's freshwater riverbank in the 1980s and 1990s in Shuicheng Taipei, uses status: "Riverbank, has been the meaning of the"people outside the culture" mixed trail. It is the place where people lean heavily in the past. When things get better, people go back inland. If you can listen to music in the concert hall, you don't have to go to the open air. Be able to play chess. When you play chess in the garden, you don't have to run to the River shed to find strangers and abandon them. If you can eat pure tea, of course you don't want to rent a straw mat [178]. It demonstrates the thinking mode of linking space use with social status in traditional Chinese concepts, as well as the public's attitude towards outdoor activities. The contempt of the environment. When encountering fully used sites, it is important to distinguish whether users are attracted by good site quality or not. Due to the lack of more suitable space for activities, we have to choose. On the other hand, the misuse of space environment presents design. Users are full of wisdom to develop new functions of the site. Designers should carefully observe and analyze the situation. Some "misuse" behavior, will find the design defects and shortcomings, and then put forward targeted improvements. The Geographic Working Group defines geography as: "Space research seeks to explore places and the use of human habitation. The relationship between the natural order and the type of activity in the place of work"[179]. Space and people's daily life exist in many ways, environmental science research should observe and analyze users' daily behavior in the context of activities. Only in this way can we abstract the laws that originate from reality rather than from the designer's imagination.

3.1. Environment and Activities

People choose outdoor activities because of their physiological and psychological needs. Many behaviorists have studied the needs of human beings and set up their own ideas. Maslow's hierarchy of needs theory, which divides human needs into "basic needs" Physiology, Safety, belonging and self-esteem are at various levels, and only one level is considered. Only when the second need is satisfied can we pursue the next level of need, to rank according to their preferences and willingness, this order is often fixed, it is difficult for designers to change. Designers can do what we need to do is to use users 'needs, priorities, feelings and satisfaction as materials, to establish the relationship between behavior and design. Design can encourage or hinder behavior. The designer's mission is to order and logic of user's behavior preferences are obtained to make the design satisfy user's se effectively. In practical design, it is very difficult to clearly link a certain environment with a certain need of human beings. It has the ability to stimulate people's behavior, but among the many factors that determine people's behavior, the material environment is probably the most important. The insignificant one is detailed description of user needs and analysis of behavior, and then get the design plan. It's not wise and goes beyond the designer's profession. The feasible research approach for designers is to combine specific design. Targeting simplifies the needs of users and summarizes the laws of environment and activities rather than thinking about the general needs of human beings users' satisfaction with the environment stems from the fact that the place can realize people's behavior tendency, while dissatisfaction is attributed to the inability of the environment to support it. Behavior that is customary to people. To build excellent urban pedestrian streets, we need to provide support for daily street life. The satisfaction of the public and attract its long-term use.

3.2. Leisure Behavior Characteristics of Users

User's personality and commonness should be distinguished in the study of user's behavior characteristics: personality refers to different users in the same category. Outdoor space shows a unique law of behavior. Statistical research will classify users according to a certain logic to obtain this. In contrast, commonality refers to the similarity of the behavior of different types of users in specific climatic zones to meet these categories. Similar to physiological or psychological needs, designers can design places that encourage most people to use.

User's behavior is related to many factors. Individual differences, i.e. who is the object, have been studied most extensively.

1) Cultural Background: Subcultural Groups including Ethnic, Regional, Religious and Ethnic Groups. Ethnic transmission from generation to generation. Customs shape specific patterns of behavior. Parisians, for example, like to sit in roadside cafes all the year round and relax in winter. Nordic countries with harsh climatic conditions do not have this tradition, that is, the impact of climate on living habits.

2) Social stratum: Sociologists believe that people are impartial about objective things under the same conditions of education, occupation and income. The understanding of animals will have the same view and motivation. Current or past social identities can make people behave similarly. Mode, such as the old people who live in Beijing Hutong all the year round, they are used to sitting in the cool at the door of their home in summer. Chinese style

3) Age: Age is closely related to family status, which determines users' psychological and psychological needs. Busy work Young white-collar workers often develop the habit of walking and playing with their children in parks or city squares after having children, while those before childbirth are not. Leisure behavior mainly occurs in urban consumption space, such as large shopping and entertainment centers.

4) Social roles: Occupational-related social roles influence people's behavior. Sometimes users need to be independent. Sexual expression and choice in social roles. 5) Gender: Some prejudices in traditional concepts, such as the belief that women are

subordinate to men, make gender influence people in the public. The behaviour of space has led to the feminist school in sociology. The above five features are commonly used user classification criteria in environmental behaviour. If the area considered is very small, the differences between social strata and social roles will narrow.

3.3. Climate-related commonalities

Research in environmental climatology has proved that regional climatic characteristics can form user behavior commonalities within a certain region.

3.3.1. Climate zone

Kevin Lynch describes in his General Design that any climate is complex and changeable, with temperature distribution and relative variation. Humidity, wind direction and wind power determine the effective temperature and its relationship with the comfort zone. Rainfall determines shelter and drainage. Demand, solar orbit and sunshine hours determine radiation and shading requirements. Except that the solar orbit depends on the degree of taboo, others should be considered. It varies from place to place. Lynch negated the method of describing the climatic characteristics of the site by means of meteorological work habits. He believed that regional climate is a range that varies according to the situation, especially considering the change of the relationship between various elements and the seasonal variation. Geographical location is the main determinant of climate. They are closely related. It is difficult to distinguish between geography and gas in practice. Waiting affects people's behavior. Climate determinism holds that climate inevitably leads to a kind of behavior, and that the environment is in a state of mind. Neo-Confucianists adopt a broader view that the interaction of many related variables determines human behavior. Research on when users act regularly, they should first divide reasonable climate zones according to their geographical location.

Golany [180] divides global climate into six main types, each representing a unique region that needs to be associated with regional climate-related urban design strategies to ensure that the city and its surrounding neighborhoods obtain the required thermal environment. Some designs the strategy applies to multiple climatic regions, such as dry-cold and dry-hot climates, which are typical stress climates. The thermal environment in each climatic region shows a specific diurnal and seasonal variation law, which is in the human production. Under the interference of construction activities, regional climate and base characteristics together form site microclimate.

3.3.2. Climate and outdoor activities

Discussing the Process of Physical Environmental Impact Behavior Based on the Equivalent Model in Environmental Psychology: Objective Physical Environment and Individual Causes. The mediation state is induced by factors, and then the coping strategies are stimulated. The objective physical environment includes temperature, elevation, and individual factors. Including people's level of adaptation to climate, comfort zone; coping strategies are to adapt to the environment or self-regulation (e.g. sweating). In practical research, this research method can be used for reference to explore the relationship between behavior the pedestrian street landscape design, microclimate conditions and users. High temperature and low temperature can affect social behavior, including interpersonal attraction, aggressive behavior and helping behavior. The results show that uncomfortable high temperature decreases interpersonal attraction and moderately uncomfortable high temperature increases aggressive, extremely uncomfortable high temperatures have complex effects on aggression, and extreme low temperatures have similar effects on aggression. Temperature increases helpful behavior in some cases and decreases in others. The Shadow of Low Temperature on Social Behavior. There are few studies on sound. Besides temperature, wind and air pressure also affect human behavior. In fact, weather changes first affect the user's mood, and the user's feelings get better or worse, resulting in a follow-up. Behavior, which involves many factors in the process, is difficult to express clearly with a simple model. It is necessary to clarify in the study. Firstly, compared with other factors, weather change has less impact on psychology and behavior; secondly, weather change has less impact on psychology and behavior. The effect of weather on behavior is mostly indirect and is an additional source of stress, just like the last straw on a road station, only in extreme cases, it has a greater impact. In the actual survey, it is difficult to observe and evaluate the user's emotional changes, even if they are users themselves can not accurately describe the process of emotional change, the more feasible way is to observe the user's behavior.

3.4. Lifestyle and Landscape

The progress of science and technology, the development of productivity and the expansion of urban space have greatly changed the living conditions and quality of human beings. In the era of industrial revolution, urban outdoor space was a good medicine for workers who worked in dirty and dark factories for a long time. Nowadays, most urban residents have long been away from the serious health problems associated with poor working environment and replaced by all kinds of sub-health. Under the impact of consumerism, "survival strategy" becomes "life strategy", and outdoor space shoulders the responsibility. From the mission of improving the quality of urban life, the improvement of the quality of life is closely related to the state of the landscape. As one of the important types of urban street space, traditional commercial pedestrian street takes purchasing activities as its ultimate appeal. The purpose of all design and activities is to consume and pursue the quality of space in order to generate greater commercial profits directly or indirectly. On the contrary, the urban street landscape design for leisure purposes should adhere to the design principle of "humanization" and use. It provides a place for physical and mental comfort and pleasure. Scholars and societies have long explored the relationship between environment and behavior. Critics try to understand the reasons for attracting citizens to public places and supporting social activities. Facts have proved that good things are good. Quality environment, successful activity planning and site management are the decisive factors of excellent sites.

3.4.1. Game Street

Streets used to be one of the main places for children's games. The increase of urban consumption space and the ensuing leisure model. Various interrelated reasons, such as the change of pattern and the insecurity caused by the rapid driving of motor vehicles, have jointly led to the failure of streets. Suitable for children's activities, Street vitality no longer. The playing day statistics for 2007 in the UK are very strong. According to the study, 71% of adults used to play alone near their families every day during their childhood, compared with 21% today. Parents' distrust of the urban environment is the main reason why children do so. Children's Social Studies 2006 According to society, research, 43% of parents believe that children under 14 should not go out alone. 22% of the parents thought that they should expand their age to 16-year-old residential development and local government's negligence would make their parents feel guilty. Children cannot be tolerated playing in the street. For these insecure parents, recreation in urban parks or residential areas as alternatives to sidewalks Places are good places for children to play, but parks can also have potential threats from adolescents, who are in the same boat. They left the street for lack of game facilities and venues. For children, it's hard to see the sewing needle in the street important social activities, lively sidewalks are to observe and learn adults to fulfill their social responsibilities and establish a sense of public responsibility. Places, these conveniences and educational functions can not be replaced by parks or indoor activity centers.

3.4.2. Streets for Recreation and Leisure

The traditional pedestrian mall only has shopping function. Since the late 1950s, the German planning field began to focus on pedestrian areas. Research and practice, and in Munich, Frankfurt, Stuttgart and other cities to build both commercial and cultural center integrated pedestrian areas with functions of culture, history and so on, which are different from Pedestrian Mall [181].

Domain pays more attention to people's life and walking freedom. Professor Rolf Monheim, German Urban Planning Specialist. Only store owners and suppliers are allowed to use motorized transportation (without time limit) to limit the speed of motor vehicles to the maximum range. To ensure the safety of pedestrians. At the same time, the type of pedestrian area has expanded from the early streets which simply restricted the traffic to Baozhang nowadays. Comprehensive public space including streets, squares, parks, inner courtyards, riverbanks and bridges. Some, but with rich activities: performance artists, musicians performing along the street; small kiosks selling local characteristics. A place for full appreciation. In festivals and holidays, streets will become Carnival places and small markets, shopping and entertainment will become the same. Mutually reinforcing symbiotic behavior. Recreation and leisure life made the city once in trouble because of crowded motor traffic. The downtown area has regained its vitality.

3.5. Case Study of Urban Pedestrian Street

Pedestrian areas are located in the centres of many big cities in Germany. These areas, which rely on old cities and historical buildings, have rebuilt the city. Firstly, this chapter chooses the old city pedestrian street of Munich, the old city of Leipzig, Germany, and the Christmas market of Fletching. Case study to explore the design experience of successful pedestrian streets. The organization and construction of traditional urban street space in China embodies the ancient times. Human wisdom, this paper then takes Langzhong Ancient City as an example to discuss the design of pedestrian streets related to regional culture. The renewal of urban streets generally comes from two reasons. One is the problem of the streets themselves, such as the lack of local characteristics and street dilemma. The relationship between waiting and user behavior, combined with diversified site use patterns, can create pleasant outdoor activities.

3.5.1. Pedestrian Street in Old Munich

As the most successful pedestrian area in Europe, the old city of Munich has developed public rail transit and good accessibility. Munich's old city was badly damaged during World War II, and the post-war redesign restored the old city's streets. The restoration of some historical buildings, so that the current urban center area maintained its original historical characteristics. The pedestrian block in downtown Munich was built in 1972 and gradually expanded to the present in the 1980s.

Apart from the towers of several churches, the heights of other buildings in the old city are basically the same, mainly 5-6 Layer. Two-storey attic with sloping roofs, there are also 6- 7-storey flat-roofed multi-storey building with a height of about 28m. In addition to the fixed walking area, Munich chooses a weekend in June and September each year to meet the old city. LudwigstraBe and Leopold Streets are connected by the Music Hall Square at the entrance of the northern pedestrian area. Leopoldstrafie holds Street Life Festival. From 11 a.m. on Saturday to 3 a.m. on Monday Close the streets, prohibit motor vehicle traffic, and show citizens the green life style of the city on the 1.5 km long street. In addition to the fixed walking area, Munich chooses a weekend in June and September each year to meet the old city. LudwigstraBe and Leopold Streets are connected by the Music Hall Square at the entrance of the northern pedestrian area. And the attraction of public space, and guide citizens to participate in social activities, provide play, sports and entertainment.

There are six thematic areas in the street festival:

1) The Green_City, the organizer of the event is in promoting information and suggestions on renewable energy, ecological investment, environmental protection, regional economy and energy use in the region
2) Display includes public transport, electric transport, car sharing, environmental tourism, etc. Continuous eco-transport information, promote urban green transport.
3) Creating attractive urban spaces is an important theme of street festivals. Organizers should promote diversified friendly cities at different scales. Provide explanatory services and construction materials in DIY area Material, let the public design their own balcony or courtyard Vanilla Garden and organic botanical garden.
4) Demonstrating a variety of sports types in the 2000m^2 area concepts of life style, including roller skating, rock climbing, hockey, skateboarding, basketball, fitness trails, etc. Professional staff are now in full swing. The exhibition encourages visitors to participate in it
5) Areas that provide activities for people of all ages in the family. Including children's playgrounds, parents and elderly leisure places. Publicity and promotion of products and information
6) Tourist companies provide information on leisure and holiday resorts; NGOs promote human rights, drug abuse, social well-being. Information on benefit and citizen participation; services provide health knowledge including spa, facial massage and meditation

The microclimate design of the pedestrian block in Munich's old city is mainly manifested in the control of the street form, and then formed streets. Open-air seat configuration. The north-south street has a larger height-width ratio, which can provide longer sunshade in summer, and is more suitable. As a space for outdoor stay. Munich has a comfortable climate and abundant sunshine; the streets in the city centre are linked by many historic buildings. The layout of buildings and streets is very attractive; the perfect public transport system ensures the accessibility and convenience of the city centre; Shops, restaurants and cafes blend well in the pedestrian area, and many public institutions in and around the city have expanded their use. They come from different sources and create activities at different times. Therefore, the success of Munich's central pedestrian district is climate and urban form. The product of coordination of state, transportation system and usage function [182], supported by a powerful alliance of business interest organizations Finally, a comfortable and attractive large-scale pedestrian area is formed.

3.5.2. The Old Town of Leipzig

Steineme Landschaft is located outside the University of Leipzig's new campus. The project attempts to build a business climate in the city centre. The enclosure creates an attractive comprehensive functional space for children, adolescents and the elderly. This Street landscape renovation projects originated from the Leipzig Municipal Government and the Deshao Urban Renewal Office. The traditional playground concept provides small-scale play and leisure opportunities for users of different age groups in inner city streets. This is the first time. Another project involved in the project is the labyrinth and running-bed facility on Reichsstra.

To investigate the use and subjective evaluation of new landscapes in Inner cities, a researcher from Deshao Urban Renewal Office, Yu Zhanzhao.In May and June 2010, we observed the difference of site usage on weekdays and weekends, and counted the users'age and age. Gender and form of activity; interviewing users and surrounding businesses with standardized questionnaires on their attitudes toward landscape renovation. Statistical results show that the average stay time of tourists in stone landscape is 6.1 minutes, less than 1 minute. 22% and 21% over 10 minutes. The average stay time on Saturday morning was the shortest, only 4.1 minutes; while the average stay time on Saturday morning was 4.1 minutes. The average length of stay on Saturdays (7.4 minutes) and Thursdays (7.2 minutes) was the longest, with some younger groups on the benches. Stay on for more than an hour. The proportion of female adults (56%) was slightly higher than that of male users, and the sex ratio of children was slightly higher than that of male users. This is the same. The number of children is 24% of adults. 37% of users come from abroad. More than 30% of users come to buy. Other reasons for visiting include playing (3%), hanging out and eating ice cream (23%), going to work, looking for a job, and going to work. University and travel with friends (42%). Landscape renovation of Leipzig Old Town improves summer microclimate by setting fountains to regulate environmental temperature and humidity. Sprout Springs not only increase the interest of space, but also provide evapotranspiration cooling. Fountain water mist can directly reduce the air. Temperature, and the overflowing water on the pavement also prolongs the cooling effect and absorbs the heat of the ground.

3.5.3. The LangZhong city

Langzhong is located in the central part of Sichuan Province, which is a subtropical monsoon wet. The moist climate has a history of more than two thousand years. Among the second batch of national historic and cultural cities in China, four Ancient Cities in the Best Preservation. Its urban street layout and spatial design are worth learning.

The present urban structure of Nine I Streets and Lanes in Langzhong Ancient City continues the road system of street system in Song Dynasty. The center is the middle skyscraper at the intersection of Shuangjianzi Street, North Street, West Street and Wumiao Street. High in the north and low in the South and high in the back. Limited by surface water, the city's chessboard roads are short and dense from south to north, and long and sparse from east to west. The location and construction of ancient cities in China were influenced by geomantic omen. The ancients introduced their ideas of astronomy, climate and earth. The plan of urban layout and architectural design is put forward in the advanced geotechnics. Meanwhile, the planning and design of the ancient city of Langzhong. It reflects the treatment method of urban microclimate design. The northern side of Langzhong ancient city is Panlong Mountains, which is combined with Fangshan and Longshan Mountains from Daba Mountains to form a barrier. Natural barrier against the northern cold wind [183].

At the same time, the south side of the ancient city is adjacent to the Jialing River, which makes the site well accepted to the south. The design of the skyscraper and the surrounding streets and alleys in the ancient city of Langzhong reflects the control of the ancient urban planning on the spatial order. Such spatial structure is conducive to the arrangement of urban public life, while promoting urban ventilation. Streets and lanes are mostly opposite to distant mountains, and can also form a good visual endpoint. The ancient city of Langzhong is surrounded by water on three sides, reflecting the pattern of "Jincheng embracing". Such a choice is conducive to site safety. The production and living are convenient, and the land and water breeze of the site can also be formed. Using the function of water heat storage to regulate and promote ventilation to improve. Langzhong ancient city is a typical case of microclimate design in urban planning. Including windward environment and sunshine in street layout.

According to the control of conditions, the introduction of land and water wind and the restriction of winter cold wind are selected. It can be seen that through rational planning and layout.

Chapter-4.

On-site Measurement in blocks at a pedestrian level

4. On-site Measurement in blocks at a pedestrian level

This chapter mainly introduces the fixed-point test of outdoor thermal environment of commercial pedestrian block in hot summer. Based on the Dao He Old Block in Tai Zhou city. The microclimate of this region was measured in the summer of 2016. Environmental indicators are used to explore the impact of street morphology and landscape design on microclimate.

4.1. Preface

In recent decades, due to the rapid development of urbanization, the change of underlying surface structure, transportation heat exhaust and building drainage Affected by heat and other factors, the urban thermal environment deteriorates gradually. Increasing population density and fast urban growth have increased the vulnerability of different cities to the global climate change [184]. With the urban heat island effect (UHI) and high-density development of cities, increasing heat issues have triggered a series of health problems for the human, moreover, outdoor thermal discomfort and extreme heat would be more fatal to the old man and the people who are with chronic disease [185]. Humans' outdoor thermal comfort is mainly about the thermo-physiology and outdoor heat energy balance of human [186]. In addition, the heat stress may lead to an excessive building energy consumption, high densely populated cities, particularly in Asian cities, the energy cost of buildings is nearly 40% of the total energy cost. A previous study of the trend of the energy consumption in hot-summer and warm-winter climate region during summer shows the energy cost of air conditioning occupies 50% of the building energy cost in each year [187]. Because air-conditioned buildings in built environment are also affected by outdoor microclimate, building a better outdoor environment can effectively decrease the inner energy consumption. This paper analyses the advantages and disadvantages of the design scheme of the pedestrian street and creates better outdoor space.

Today, with the improvement of urban life, urban environmental problems are becoming increasingly prominent. The urban climate in China tends to be similar in different geographical latitudes (hot summer, cold winter, short spring and autumn), and the urban heat island in the same region has great differences, and the climate similarity brought by urbanization is masking the climate differences in geographical location.

To sum up, researchers should also pay attention to: first, when comparing Street cases located in different city histories, they should pay more attention to the geographical location of the city, pay attention to the characteristics of urban features derived from regional climate and respect the living habits of local residents; second, the impact of modern urban residents' life on urban climate and regional microclimate is increasing day by day. I have made some research results in European and American cities. We can learn from it, but we can't copy it completely.

Streets have always played an important role in urban life. Pedestrian street system also has a great impact on urban life. Some pedestrian streets not only serve as a tourist destination in a region, but also as a symbol of a city. In the aspect of urban environment, urban design with climate adaptability in hot summer and cold winter districts has its own characteristics. Different from the other four thermal zones in China, hot summer and cold winter districts should take into account both summer and winter microclimate problems in accordance with the general principles of climate. However, through field research and development, it is found that the climate problems exposed in summer are more serious in this area.

4.2. The importance of the pedestrian street in daily lives

Urban pedestrianized-zones are known to us by its convenience, vitality and commercial value, which are not only symbols of cities or metropolis but also can increase local financial income. Unlike urban canyon space, the local design specification shows that the average building height won't exceed three story in order to keep the commercial value [188] (Figure 4-1).

Figure.4-1 The commercial pedestrian block [188]

4.3. The solar radiation in pedestrian block at daytime

Outdoor environment is different from the inner room, human stands in the street will experience fluctuations in the outdoor stimuli due to the two different forms of radiation which influence thermal sensation directly. The first form is called short-wave radiation, which is emitted from the sun. The second form is long-wave radiation, emitted by the terrestrial surfaces that surround human [189]. To extent that humans' body comes in direct contact with other surfaces, it will also gain and lose heat by conduction, in addition, humans' body in street dissipates heat through evaporation. The human energy balance can be expressed in terms of the rate at which energy is absorbed or emitted by a unit area of the surface of our body, and combined as a net exchange of solar radiation R_n between human and outdoor environment (Figure 22):

$$R_n = (K_{dir} + K_{dif} + K_h + K_v)(1 - a_s) + L_d + L_h + L_v - L_s \quad (1)$$

In this equation, K_{dir} means direct short-wave radiation incident on human. K_{dif} means diffuse short-wave radiation incident on human, K_h is the indirect radiation incident on human reflected by horizontal surfaces. K_v is the indirect radiation incident on human reflected by vertical surfaces. With a_s representing the albedo of humans' skin and clothes, $(1-a_s)$ means ratio of the short-wave radiation which is absorbed by human. L_d is the long-wave radiation incident on human which is emitted downwards by the sky. L_h is the long-wave radiation incident on human which is emitted downwards by the sky. L_v is the long-wave radiation incident on human emitted by vertical surface. L_S is the long-wave radiation emitted by human to outdoor environment [190,191].

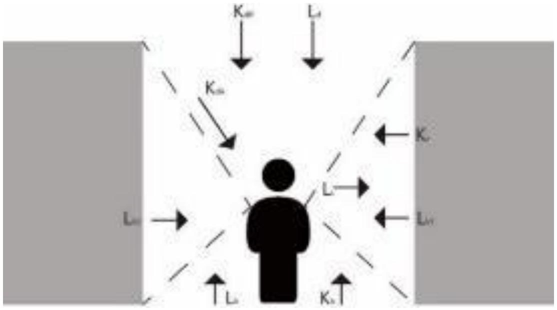

Figure 4-2 Outdoor energy exchange between block and surrounding urban environment

4.4. Case Selection and Base Survey (Hot-summer and cold-winter climate zone)

Taizhou (Figure 4-3) is a famous historical and cultural city in China. It is located in the north bank of the lower reaches of the Yangtze River. It has four distinct seasons. It has high temperature and rainy in summer, mild and little rain in winter. It has the characteristics of long frost-free period, abundant heat, abundant precipitation and the same period of rain and heat.

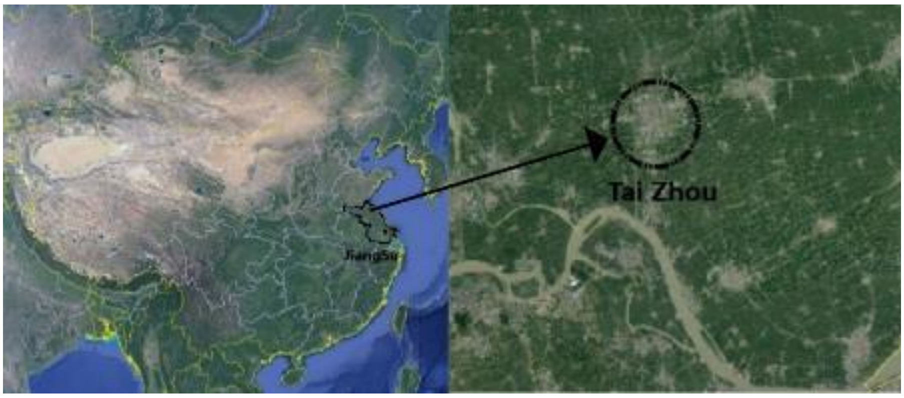

Figure 4-3 Location of Tai zhou

As shown in Table 4-1, the highest temperature in Tai zhou city is in July, the lowest is in January, the annual average temperature is between 14.4 and 15.1 ℃, the temperature zone in Tai zhou city belongs to subtropical zone, dry and wet zone belongs to wet zone. Meteorological data in recent years show that the highest temperature in Tai zhou can reach 38 ℃ in summer and - 11 ℃ in winter under extreme conditions, without central heating and poor comfort.

Table 4-1 Meteorological information（1981-2010）

Month	1	2	3	4	5	6	7	8	9	10	11	12
Average air temperature（℃）	2.4	4.4	8.4	14.4	20.1	24	27.5	27	22.9	17.4	10.9	4.9
Relative humidity（%）	74	74	74	74	74	75	79	83	81	76	75	73
Wind speed（m/s）	2.8	3	3.3	3.2	3.1	3	2.9	2.9	2.7	2.5	2.7	2.7

4.4.1. Dao He Old Block

In recent years, with the rapid development of Tai zhou City, the urban environment has also undergone tremendous changes. At the same time, the problems exposed are more obvious. Through the author's on-site investigation in Tai zhou, it is found that there are many pedestrian streets. After careful consideration, the author chose "Dao He Old Block" as an analysis case. The reasons for choosing this area are as follows. As a famous historical and cultural city in China, Tai zhou has many historic blocks with great protection value, among which Dao He Old Block is one of them. This region has both east-west street, north-south street and semi-open small square, which is conducive to the calculation, simulation and comparison of different forms of blocks (Figure 4-5).

Figure 4-4 The Dao He Old Block

In order to assure the accuracy of the measurement, the whole block is divided into six parts in accordance with different spatial morphology (Figure 4-5). The detailed information of the six measured points is shown in Table. 4-2and Table 4-3.

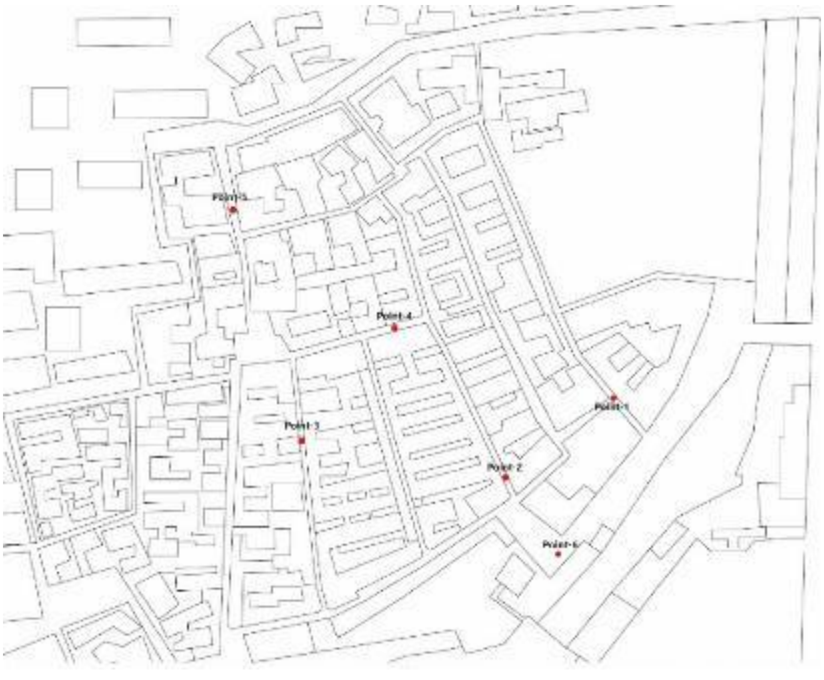

Figure 4-5 The selected points

Table. 4-2 Characteristics of the selected points

Point	Site Characteristic	Surface type	Shade	Aspect ratio(H/W)
1	NW- SE oriented street	Grey brick	√	4.6
2	NW- SE oriented street	Grey brick	√	1
3	N-S oriented street	Grey brick	-	2.3
4	NE-SW oriented street	Grey brick	√	2.3
5	N-S oriented street	Grey brick	√	2.75
6	Open space	Grey granite	√	0.33

4.4.2. Tai Zhou Old Block

Like Dao He Old Block, the Tai Zhou Old Block is also a very important scenic spot of Tai Zhou city (Figure 4-6). In order to assure the accuracy of the measurement, the whole block is divided into six parts in accordance with different spatial morphology (Figure. 4-7). The detailed information of the six selected points is shown in Table. 4-4 and Table. 4-5.

Figure 4-6 The Tai Zhou Old Block

Figure 4-7 The Tai Zhou Old Block

Table 4-3 The detailed information of the six points

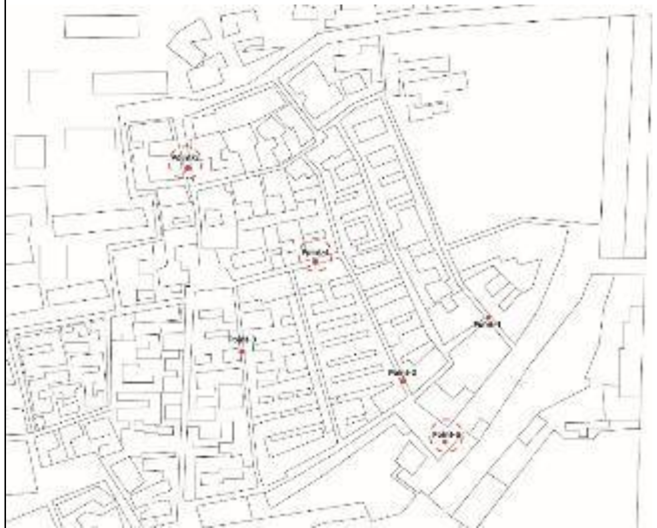	1			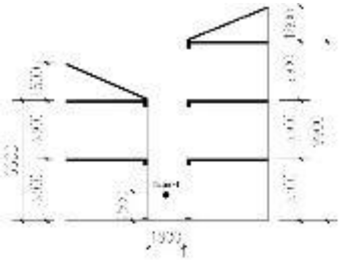
	2		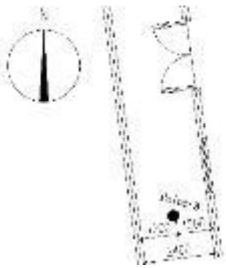	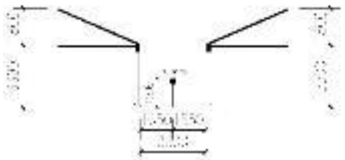
	3		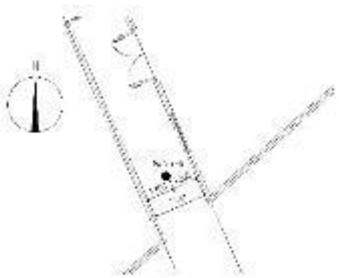	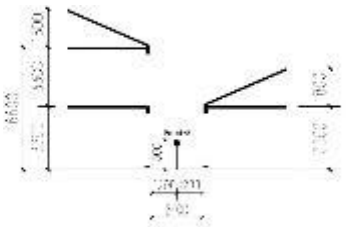

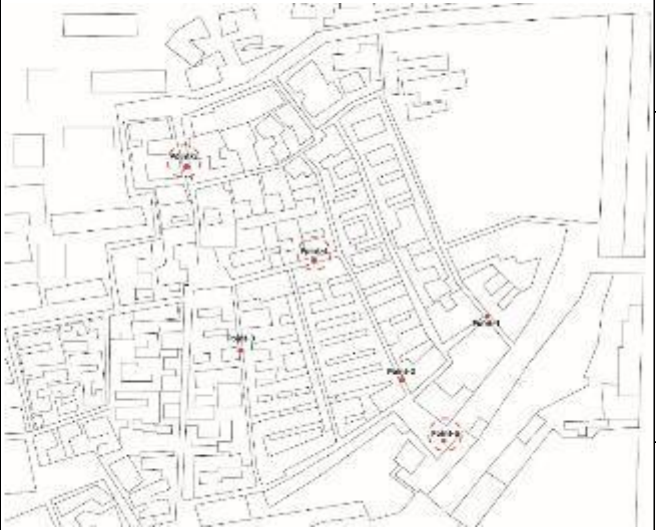	4		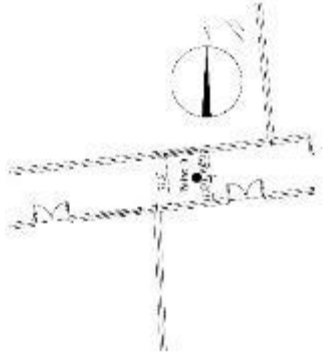	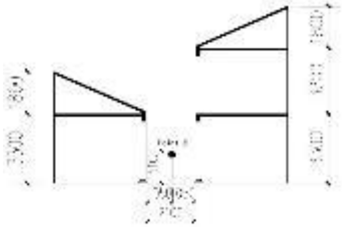
	5		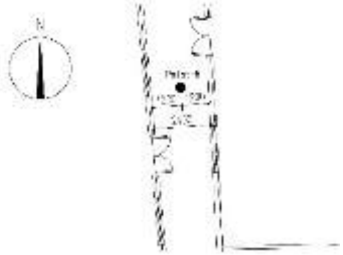	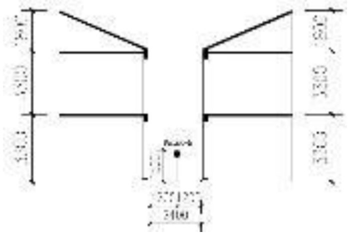
	6		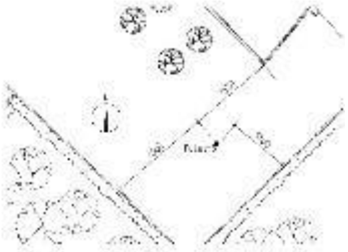	

Table 4-4 Characteristics of the selected points for the pedestrian block

Point	Site Characteristic	Surface type	Shade	Aspect ratio （H/W）
1	Open space	Paving granite	√	-
2	Open space	Paving granite	-	-
3	N-S- oriented street	Paving granite	√	0.75
4	E-W- oriented street	Asphalt	√	1
5	NE-SW- oriented street	Paving granite	√	1.5
6	NE-SW- oriented street	Paving granite	√	0.33

4.5. Case Selection and Base Survey (Hot-summer and warm-winter climate zone)

As mentioned above, China is very huge, and is covered with a very large territory with various climate zones, according to the national standard Thermal Design Code for Civil Building (GB50176-93), five climate zones are found as hot-summer and cold-winter area, hot-summer and warm-winter area cold area, severe cold area, and temperate area. Fo Shan (23 °02'W, 113 °06'E) locates in Guang Dong province (Figure. 4-9, 4-10) which is in hot-summer and warm-winter climate area.

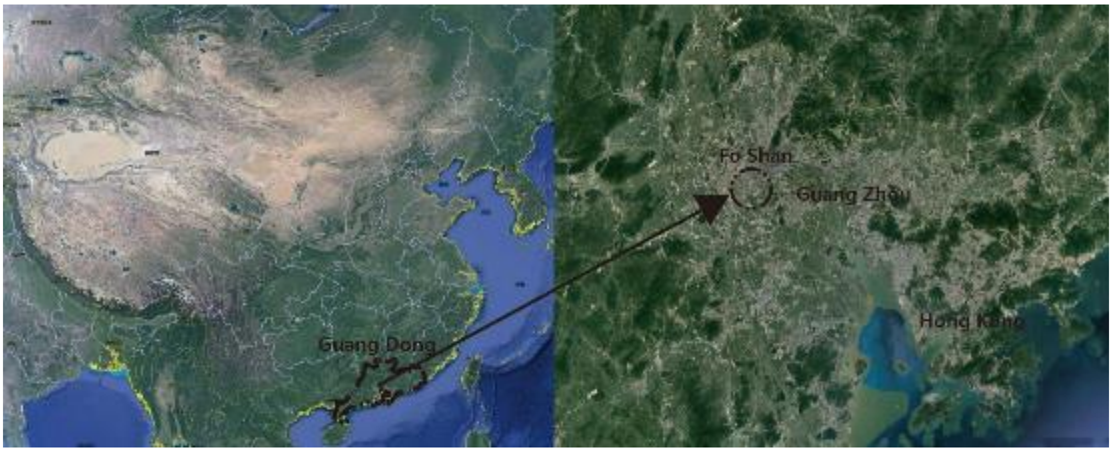

Figure 4-9 The Tai Zhou Old Block

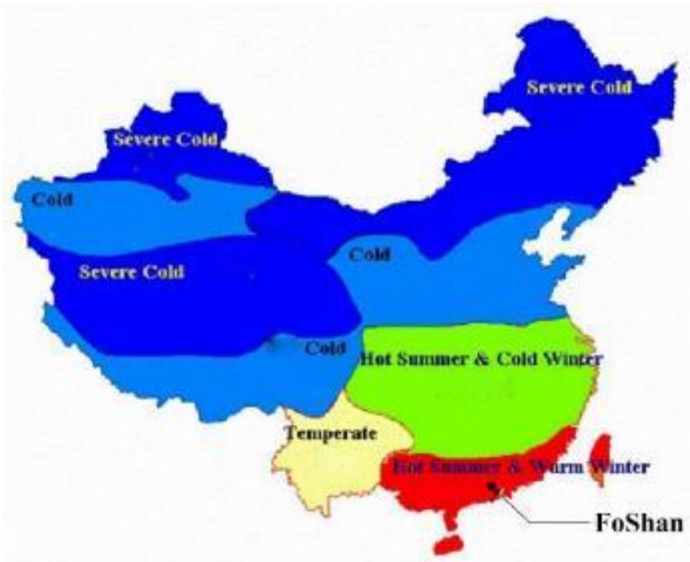

Figure4-10 The climate classification of Fo Shan

Table 4-5 The detailed information of the six points

Point	Model	Photo	Plan	Section
1			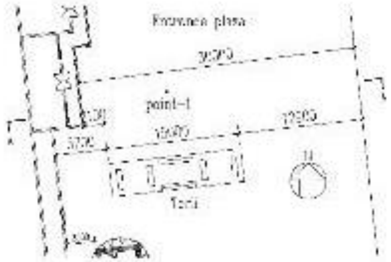	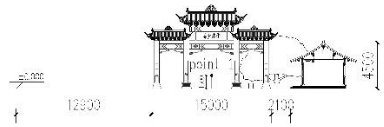
2				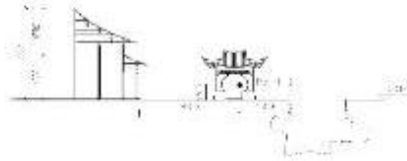
3	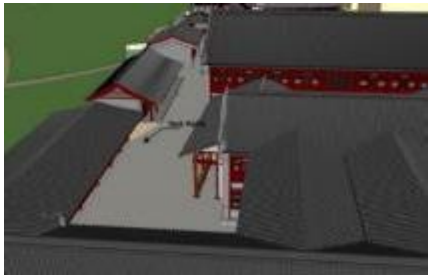		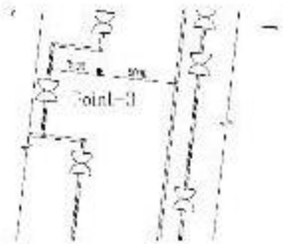	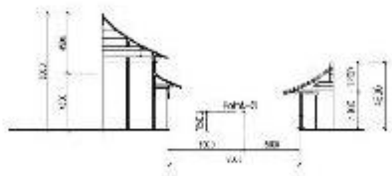

4				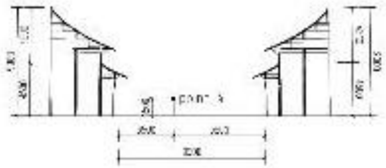
5			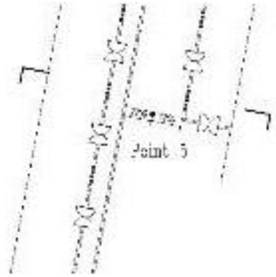	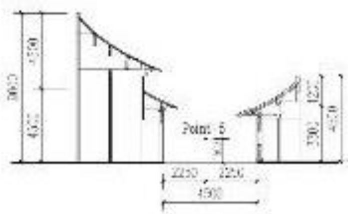
6			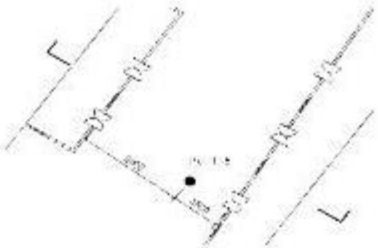	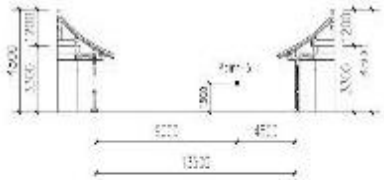

In this study, the Ling Nan Tian Di commercial pedestrianized-zone is selected to evaluate tourists' thermal sensation. The location of this region is shown in Figure 4-11. This commercial zone doesn't only play an important symbol of Fo Shan city but also a very important place increasing local financial income. Despite the uncomfortable thermal conditions in extreme summer, visiting pedestrianized-zone in this season has still got a high statistics.

Figure4-11 The location of the Ling Nan Tian Di pedestrianized-zone

Considering the published data of the weather stations, annual average air temperature of this city is 22.5℃ in summer and the prevailing wind is southeastern direction. The daily maximum air temperature in July (Figure. 4-12) can reach 37℃.

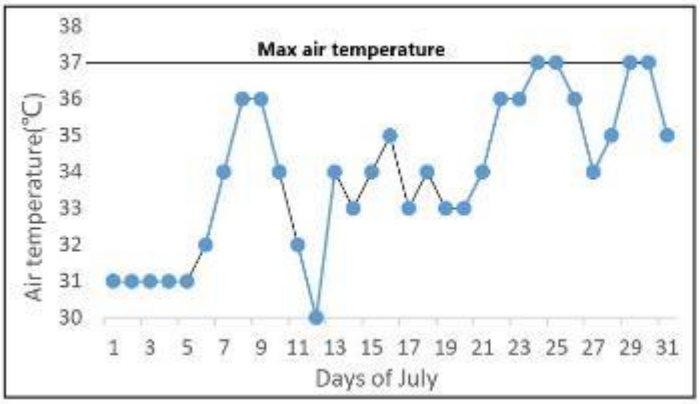

Figure 4-12 The location of the Ling Nan Tian Di pedestrianized-zone

According to the different spatial geometry of this region, it's divided into seven parts, Table. 4-6 and Table. 4-7 show the detailed information of the different points. These fisheye images at different measured sites are taken the fisheye lens and then input in ENVI-met to calculate the simulated SVF (Figure. 4-12).

Table. 4-6 Characteristics of the different sites of this pedestrianized-zone

Point	Characteristic	Surface	Shading	Aspect ratio（H/W）
1	WN-SE direction	Paving granite	√	1.25
2	N-S direction	Paving granite	-	1.25
3	WN-SE direction	Paving granite	√	1.5
4	Open space	Brick	-	0.2
5	WN-SE direction	Paving granite	√	0.5
6	NE-SW direction	Paving granite	√	1
7	Open space	Paving granite	√	0.25

Table. 4-7 Characteristics of different selected sites

	Point	Photo	Plane	Section
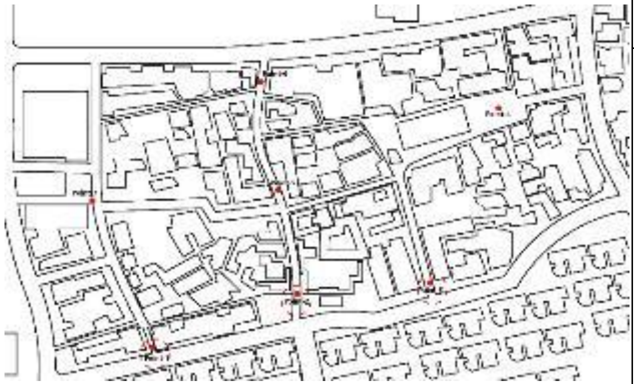	1		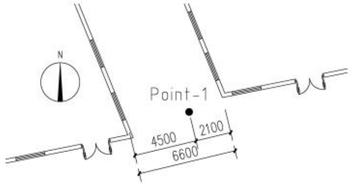	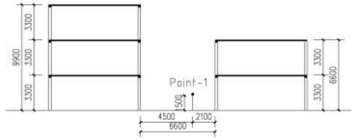
	2		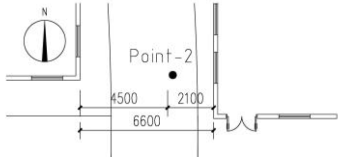	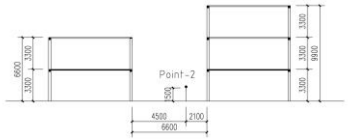
	3		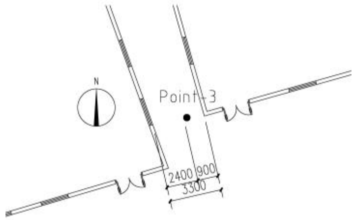	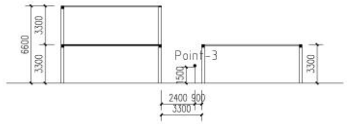

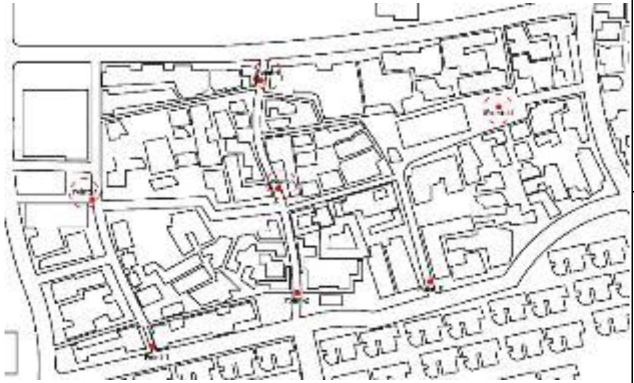	4		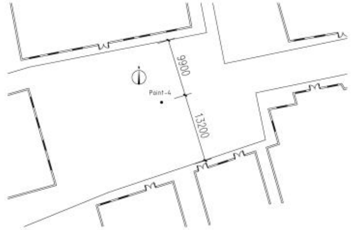9900 13200	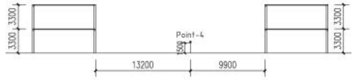Point-4 13200 9900
	5		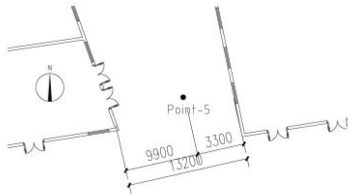Point-5 9900 3300 13200	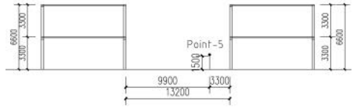Point-5 9900 3300 13200 6600 3300
	6		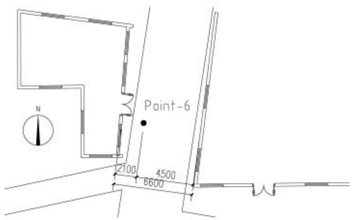Point-6 2100 4500 6600	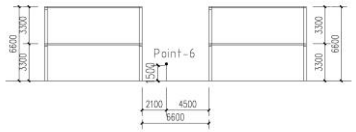Point-6 2100 4500 6600 3300
	7		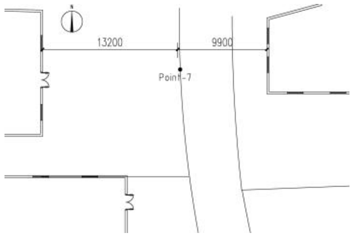13200 9900 Point-7	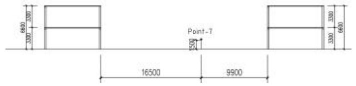16500 9900

4.6. On-site measurement

The test of summer temperature and climate of all mentioned sites are carried out on 24th (Fo Shan), 28th and 29th (Tai Zhou), 30th and 31th (Fo Shan). All the on-site measurement are conducted to record the air temperature, relative humidity and wind speed at daytime.

The measurement of outdoor microclimate conditions are made with mobile meteorological station (Figure 4-13) which can record the wind velocity (m/s), air temperature (℃) and relative humidity (%) and the instrument records the data every one minute. Each equipment is covered by a radiation shield and lifted up at a 1.5m height from ground. The detailed information of the station is in Table. 4-8.

(a) (b)

Figure. 4-13 The measured instrument (a) Anemoscope (b) Air temperature and humidity instrument

Table. 4-8 The detailed information of the instrument

Instrument	Measuring Instrument	Measuring Precision	Measuring Range	Recording Time	Recording Mode
Anemoscope	DS-2	±0.3m/s	0-70m/s	1min	Automatic
Air temperature	TR-72wf	±0.5℃	0-±55℃	1min	Automatic
Relative humidity	TR-72wf	±5%RH	10-95%RH	1min	Automatic

4.7. The measured result of Dao He Old Block

The observational data provided by the satellite ground station of meteorological bureau in the two cities during the test period are compared. According to the International Meteorological Organization (World Meteorological Organization, WMO). It is stipulated that urban meteorological stations must be built in flat and open areas. No building or other topographic changes shall affect the incoming wind; the air temperature and wind speed shall be separately off the ground. The height of the meter is measured. The measured values of urban meteorological stations satisfying the above conditions can be used to represent large-scale areas Macro meteorological conditions.

4.7.1. Air temperature of Dao He Old Block

As mentioned above, in data processing, the average an hour meaning of measured data is selected as an example to explore the trend of air temperature change at each selected points. During the measurement period, the weather on Jul, 30th is fine and Jul, 31th is cloudy. Figure 4-8shows the average air temperature of the two measured days, Because of the different spatial geometry, the selected points have different average air temperature at day time from 9:00 to 17:00. Because in canyon space and same urban geometry, the changing trend of the curves from point-1 to point-5 are same, in the two measured days, the average air temperature increases from 9:00 to 14:00, in which the data can reach maximum at 14:00. After 14:00, the air temperature will be down.

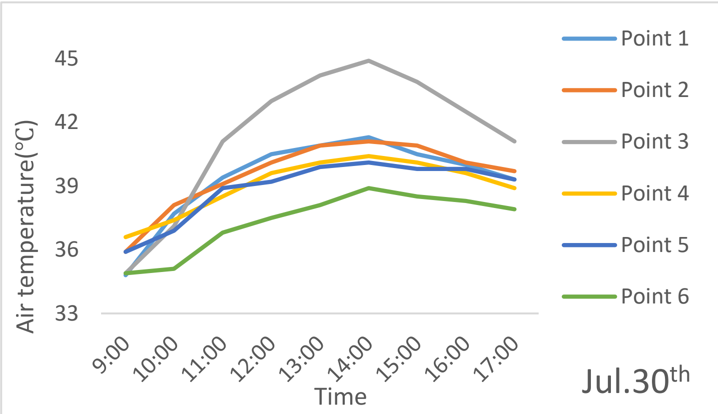

(a)

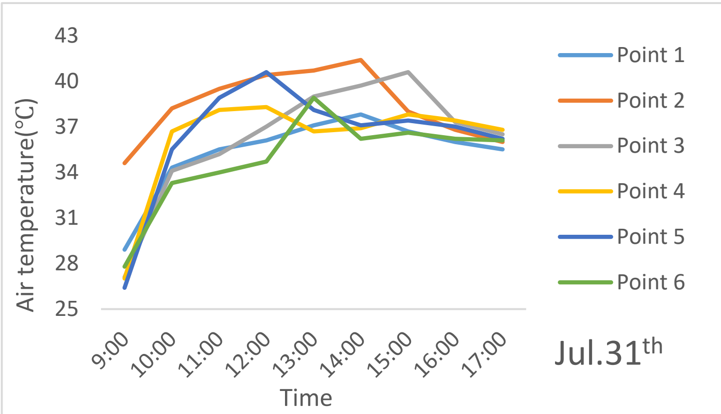

(b)

Figure. 4-8 The average air temperature (a) Jul 30th (b) Jul 31th

It can also be seen from the figure that since the 30th, point 6 is an open space, but the daytime air temperature is the lowest of all the selected points. Thereafter, the temperature value was always the lowest among all the measuring points, while the measuring point-1 was situated at the artificial lakeside, surrounded by trees and irrigation. In addition, wood and other green areas have been shaded by trees, and their air temperature is lower than other measuring points. Average of Point 5 and Point 1 the maximum temperature difference can be 3.5 C, while the maximum temperature difference can be up to 3.9 C all day. The average temperature of point 1 near the main entrance (without shade) can be found at different locations with different shelter conditions. Also, the air temperature of point 1 has a higher data at daytime. Compared with the measured point 9 (with tree shade), the temperature at the measured point 4 (without tree shade) at the pedestrian intersection is 40 C higher, respectively, and the average temperature at the measured point 4 (without tree shade) at the pedestrian intersection is 0.6 C and 1.4 C higher. It can be found that the extent of air temperature decrease varies greatly with the time of shading, which is also covered by shadows. There is a shadow at the measuring point 9 am, but the difference between the air temperature and the measuring point 2 is not significant, and the average temperature difference is less than 0.5 C. This shows that although greening, a landscape design factor, can effectively reduce the outdoor environment temperature, if the design position is incorrect, it will be counterproductive. Because of the lack of shade and trees. Point 3 has the highest air temperature at daytime. Further analysis of the temperature changes on July 30 and 31 reveals that the temperature at each measuring point during the day. The change law is similar, the minimum value appears at 10:00 in the morning, the maximum value appears slightly different, but basically all in the morning. Comparing with the corresponding test values of urban meteorological stations, the lake survey is carried out on sunny days, the latent heat has a significant cooling effect on the surrounding environment, while in cloudy shower days with severe weather changes. Compared with the corresponding test values of urban meteorological stations, no tree-shaded observation points are available throughout the day regardless of weather conditions. Shadow and transpiration of trees are limited by solar radiation intensity and relative humidity, and their cooling effects on the environment. All the above phenomena show that landscape design factors such as greening and artificial lakes can be evaporated through their own transpiration. It can delay the occurrence time of the highest ambient temperature and reduce the frequency of the occurrence of the highest ambient temperature, thus weakening summer. The influence of seasonal urban heat island on the thermal environment in residential quarters.

4.7.2. Relative humidity of Dao He Old Block

Relative humidity measurements at different points are shown in Figure 4-9. From diagram, it can be seen that the hourly average, maximum and minimum relative humidity of the two measuring points are not very different, basically. At 13:00 to 14:00 in the afternoon, the minimum of the whole day appeared. This indicates that although these two areas are far and near to artificial lakes. But the change of relative humidity of air caused by evaporation of grass and tree is not reflected. The change of relative

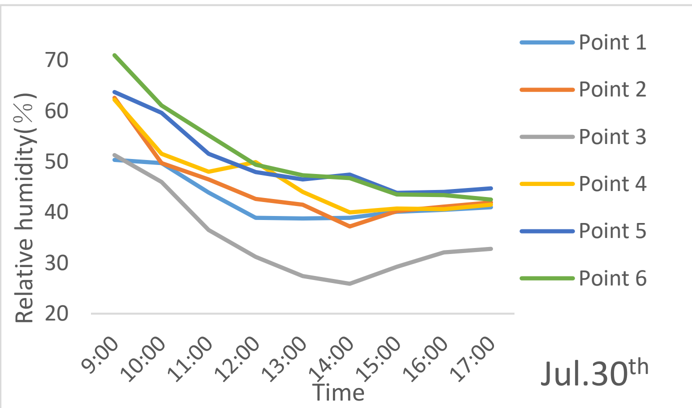

(a)

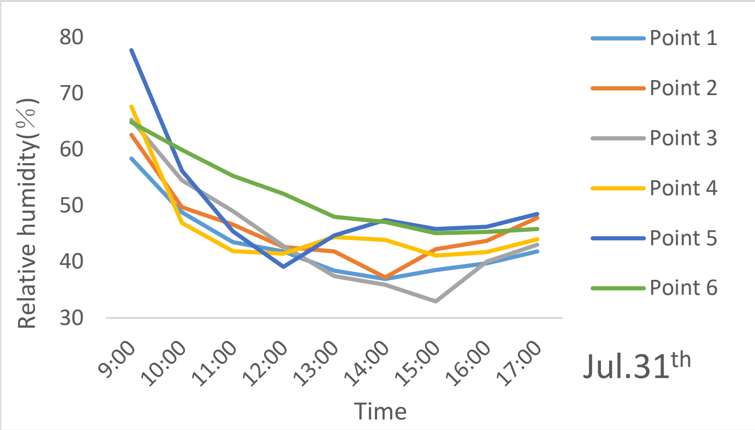

(b)

Figure. 4-9 The average relative humidity (a) Jul 30th (b) Jul 31th

humidity of two measuring points is not reflected. The trend is also roughly the same. On sunny days, the relative humidity of point 2 is 3%-5% lower than that all the points, while on cloudy showery days (July 31), it is affected by the influence of rainfall and strong gust, the relative humidity of the two measuring points changed dramatically, especially in the afternoon level of the measuring point 2. The difference of mean value is 30%, and the range of humidity fluctuation is more than 35%. This shows that gusts with variable wind speed and direction and gust energy. It can quickly change the distribution of relative humidity in the pedestrian block.

4.7.3. Wind speed of Dao He Old Block

When measuring the wind speed at each measuring point, the hotline anemometer is used to test continuously for 1 minute, and the arrays during this period are obtained respectively. Short dashes and hollow data markers are used to represent group external measurements. The wind speed of points is indicated by solid lines and solid data marks. As can be seen from the picture, the wind speed distribution has strong randomness and is not directly affected by other meteorological parameters such as temperature and humidity. Speed of 30th to 31th is higher than that of other measuring points inside the cluster; wind speed of outside measuring points is common (Table 4-9).

Table. 4-9 The wind velocity of the selected points (m/s)

Point	1	2	3	4	5	6
Jul.30th	0.62	0.51	0.47	0.41	0.54	0.66
Jul.31th	0.66	0.64	0.46	0.55	0.56	0.78

The average wind speed in the first measured day of different points is same, all the sites are locating in a calm wind region. In the second measured day, the final result is same. Pedestrian and traffic main roads can play a good role in guiding the wind, while the other main roads are subject to the dominant wind. The blockade of the wind direction of the residential complex prevents the outside wind from entering, which leads to the increase of the time of the breeze or the windless state, and the wind environment.

4.8. The measured result of Tai Zhou Old Block

Like the case in Dao He Old Block, the measured data of Tai Zhou Old Block is following.

4.8.1. Air temperature of Tai Zhou Old Block

According to the field measurement, the first measured day is sunny, and the second day is cloudy. Figure. 4-10 shows the average air temperature.

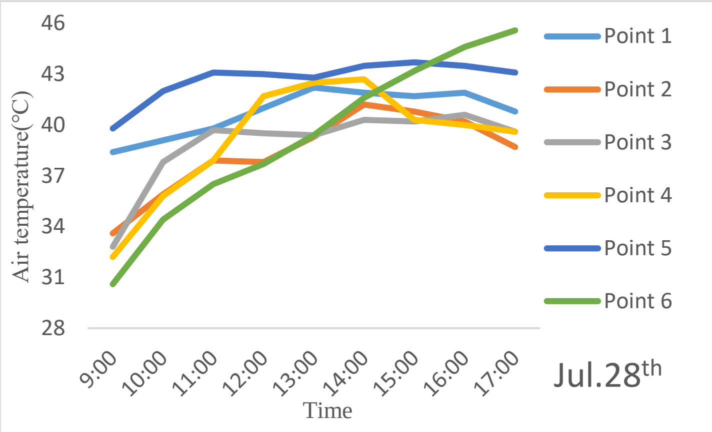

(a)

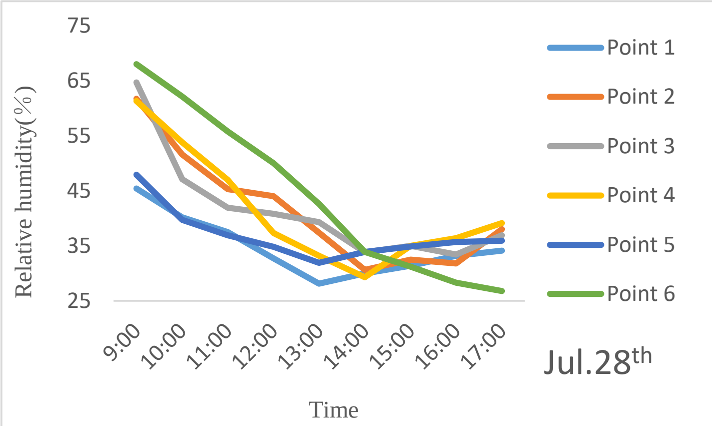

(b)

Figure. 4-10 The air temperature on (a) Jul 30th (b) Jul 31th

During the measurement period, the weather on Jul, 28th is fine and Jul, 29th is cloudy. The discrepancy of the curve shows that on Jul, 28th the air temperature of the point-6 is growing all the daytime which can reach 45.7℃, other five points increase from 9:00am and after 2:00pm the air temperature decreases. On Jul, 29th, the air temperature of all the points increase from morning and decrease after 2:00pm. Like the first day, point-6 has the highest air temperature in the daytime.

4.8.2. Relative humidity of Tai Zhou Old Block

Like the on-site measurement in Dao He Old Block, the curve of relative humidity is opposite to air temperature at daytime. The detailed information is shown in Figure 4-11.

4.8.3. Wind speed of Tai Zhou Old Block

The collected data of wind velocity is in Table. 4-10. The table shows the average data of the six measured points.

Table 4-10 The wind velocity of the selected points (m/s)

Point	1	2	3	4	5	6
Jul.28th	0.65	0.63	0.49	0.45	0.5	0.62
Jul.29th	0.66	0.51	0.5	0.39	0.49	0.33

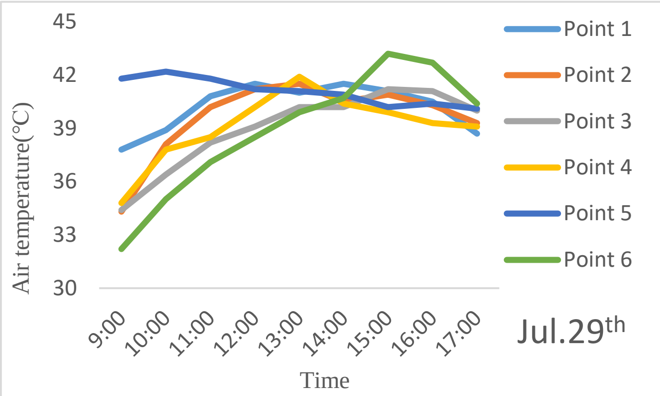

(a)

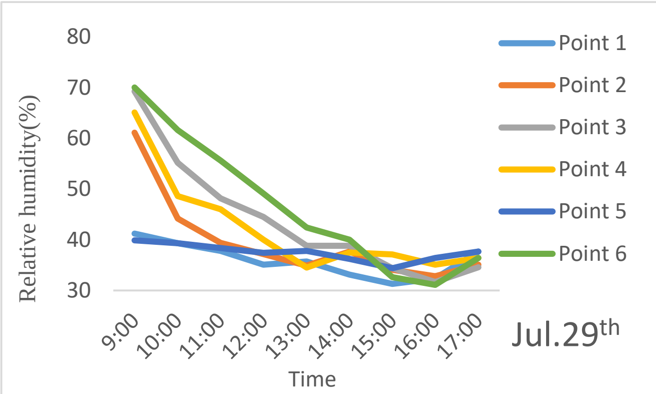

(b)

Figure. 4-11 The average relative humidity (a) Jul 28th (b) Jul 29th

4.9. The measured result of Ling Nan Tian Di Block

Like mentioned two cases, the measured data of air temperature, relative humidity are shown in Figure. 4-12, 4-13. The average wind speed is shown in Table. 4-11.

4.9.1. Air temperature and relative humidity of Ling Nan Tian Di Block

The final measured data of air temperature is shown in Figure. 4-12. The average data shows that the point-4 has the highest air temperature at daytime. The reason is that point-4 is an open space, and this space is lack of shading. All the other points are canyon space, except of point-2, other points have a same range. Because of the lower aspect ratio (H/W) and higher SVF, no shading area for human can impede solar radiation at daytime.

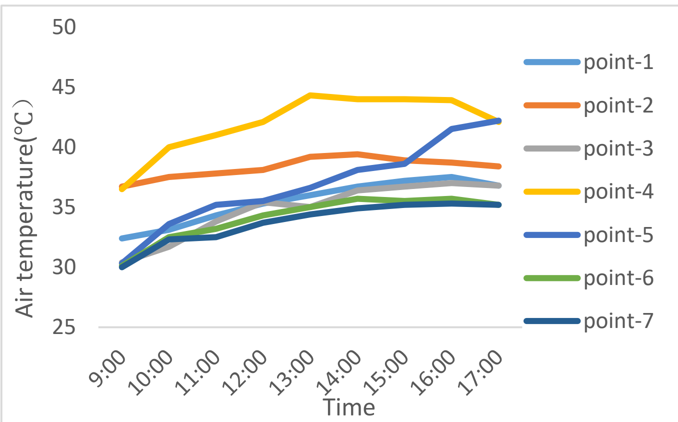

(a)

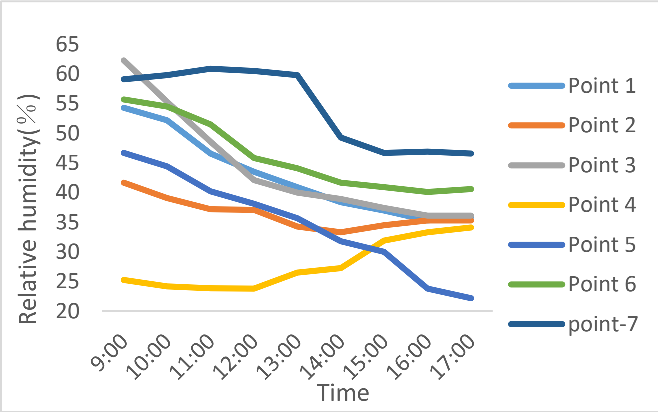

(b)

Figure. 4-12 The measured data (a) Air temperature (b) Relative humidity

In Figure 4-12 (b), the curve of relative humidity is opposite to the change of air temperature. The point-4 has the lowest relative humidity at daytime.

4.9.2. Wind speed of Ling Nan Tian Di Block

The collected wind velocity is displayed in Table. 4-11, which shows average data of these seven sites. All the data shows that the commercial zone stays in a calm wind area, which explains the tourists' thermal sensation in this zone won't be influenced by the wind velocity obviously.

Table.4-11 The collected data of wind velocity of the seven points (m/s)

Point	1	2	3	4	5	6	7
Jul.24th	0.43	0.54	0.35	0.32	0.27	0.32	0.35

4.10. Conclusions

4.10.1. Summary of Dao He Old Block

1) Air temperature: Single peak in clear and cloudy days, distribution shows that the maximum temperature of the whole day occurs between 13:00 and 14:00 p.m., while in cloudy shower days, the distribution is approximately sinusoidal. The maximum appears at 12:00 and the minimum appears at 15:00.

2) Relative humidity: It is maintained between 30% and 60%, with little change over time.

3) Wind speed: The distribution of wind speed is very random, and it is not directly affected by other meteorological parameters such as temperature and humidity. The average wind speed of the measured points in the cluster is less than 1.0 m/s.

4.10.2. Summary of Tai Zhou Old Block

1) Air temperature: Single peak in sunny and cloudy days and distribution of final result shows that the maximum temperature of the whole day occurs between 13:00 and 15:00 p.m., while in cloudy shower days, the distribution is approximately sinusoidal. The maximum appears at 12:00 and the minimum appears at 15:00.

2) Relative humidity: It is maintained between 30% and 50%, with little change over time.

3) Wind speed: The distribution of wind speed is low, which describes the whole region stays in a calm wind region.

4.10.3. Summary of Tai Zhou Old Block

1） Air temperature: Single peak in sunny and cloudy days and distribution of final result shows that the maximum temperature of the whole day occurs between 13:00 and 15:00 p.m., while in cloudy shower days, the distribution is approximately sinusoidal. The maximum appears at 12:00 and the minimum appears at 15:00.

2）Relative humidity: It is maintained between 30% and 50%, with little change over time.

3）Wind speed: The distribution of wind speed is low, which describes the whole region stays in a calm wind region.

Chapter-5.

ENVI-met Analysis

5. ENVI-met Analysis

Although the research on urban heat island and microclimate environment is increasing day by day, it is aimed at these two phenomena. There are few specially developed numerical simulation software, especially those that can accurately simulate landscape greening and outdoor thermal environment and software for relationships with buildings. Generally speaking, because of things, the results of microclimate simulation of these softwares will vary greatly with different physical basis, spatial or temporal iteration equations. In view of the high temporal resolution micro-scale model currently used, a detailed criterion for judging is proposed and pointed out. ENVI-met can simulate and analyze outdoor environmental and climatic parameters with fine grids (up to 0.5 m x 0.5 m at the minimum) and the distribution of thermal comfort may be the best special hydrodynamic simulation software for micro-environment at present. Therefore, the article will use ENVI-met to analyze the layout and greening forms of different landscape designs in the residential group with hot and humid climate. Microenvironment and outdoor thermal comfort changes caused by distribution. The literature review also points out that the development objects of ENVI-met and current applications are limited to the cold climate of middle and high latitudes, so it is necessary to systematically verify whether the software is available or not [192-193].

In order to get a deeper understanding of the application of the software in hot and humid climate Sex, Section IV of the software contains part of the database, as follows: mattress materials and structure, types of greening, water depth Sensitivity analysis was carried out. Based on the simulation results of the previous sections, the application of ENVI-met in hot and humid climate is summarized. The optimum convergence time, simulated grid size, boundary condition type and greening type are the following landscape greening. Variable simulation analysis of chemical design factors determines the corresponding software settings and database.

5.1. Introduction of ENVI-met

ENVI-met consists of three independent sub-models and nested grids. The sub-models include three-dimensional master model and soil. Soil model and one-dimensional boundary model, the structure of which is shown in Figure 30. The three-dimensional main model is divided into three parts: horizontal X and Y coordinates and vertical Z coordinates. With most other fluid forces. Like CFD simulation software, it mainly studies the characteristic parameters such as building, greening, water body and underlying surface structure in the region. And so on, they should be set in the three-dimensional main model. The main model can analyze the governing equation by calling meteorological prediction subroutine. The atmospheric variations and all surface-plant-air interactions are calculated. In order to ensure the accuracy of simulation, one-dimensional boundary model will scale the boundary of three-dimensional main model to 2500. The initial conditions of the atmospheric boundary layer are transferred to the boundary of the main model. In addition, the boundary model According to user input conditions, the vertical distribution characteristics, such as gradient, are also set for all variables in the boundary of the three-dimensional master model. Wind and so on. The soil model is also a one-dimensional model, which consists of 14 layers from the surface of the underlying surface to 1.75 meters deep.

From top to bottom, the mesh width of different layers also changes from narrow to wide. This model calculates heat transfer processes and plants from the surface to the interior of the land. The moisture transfer process of root system in soil and the underlying surface temperature and humidity caused by heat and humidity transfer in soil caused by transpiration change [194] (Figure 5-1).

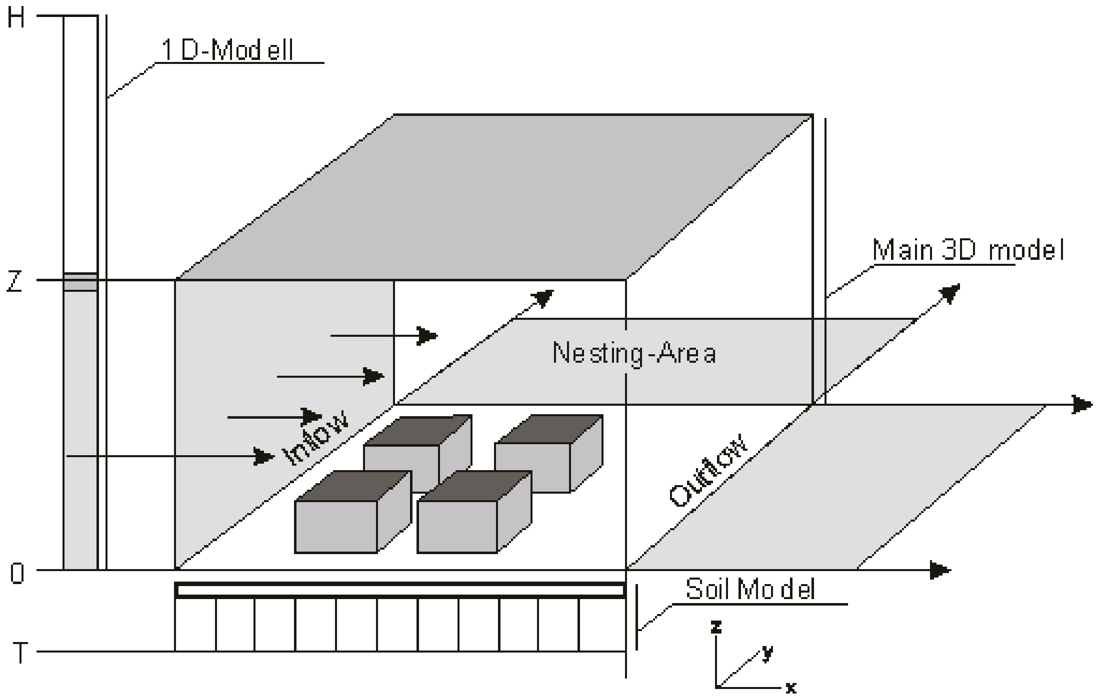

Figure. 5-1 The introduction of ENVI-met [194]

5.2. Grid structure

The three-dimensional model is mainly divided into three parts: horizontal x-axis and Y-axis and vertical Z-axis coordinates. In order to simulate accurately, like other software for analysis and simulation, the main research areas of buildings, streets, water bodies and greening should be established in the analysis model. The horizontal boundary at the upper part of the model and the boundary layer at the upwind and downwind should be the interface of the model. In order to ensure the accuracy of the simulation, the one-dimensional model will proportionally extend the boundary of the three-dimensional model to the atmospheric boundary layer of 2500m and convert all initial values into the boundary of the analysis model. The core area of the model to be simulated is three-dimensional cells. In the trial version, fewer cells can be set. The maximum height (Z) set in the model is twice the height of the highest building. Each small unit (Delta x, Delta y, Delta z) is not only used to define the length and height of the building, but also to define the height and width of vegetation and other elements. In addition, ENVI-met software also provides an equal scale enlarged mesh structure, so that the same number of meshes can cover the building as much as possible. It is worth mentioning that besides this mesh, there are nested meshes, which are equivalent to a buffer zone. As a boundary area, the boundary area of the analysis model is to avoid the analysis error caused by the boundary effect. ENVI-met also provides an equally scaled-up grid structure to allow the same number of grids to cover more high buildings, in figure 5-2, Use in Type B2 Users can customize an equal scale zoom in the starting height zT, and all grids below this height will follow the set value Delta Z. Equal division. These scaled-up grids are very helpful in simulating extremely high building heights, but due to the top of the grid. The mesh size is much larger than that of the bottom layer, which leads to the decrease of simulation accuracy, and only the simulation results near the ground at the bottom layer can be used. Therefore, it is not suitable for the study of high-rise full-scale cases.

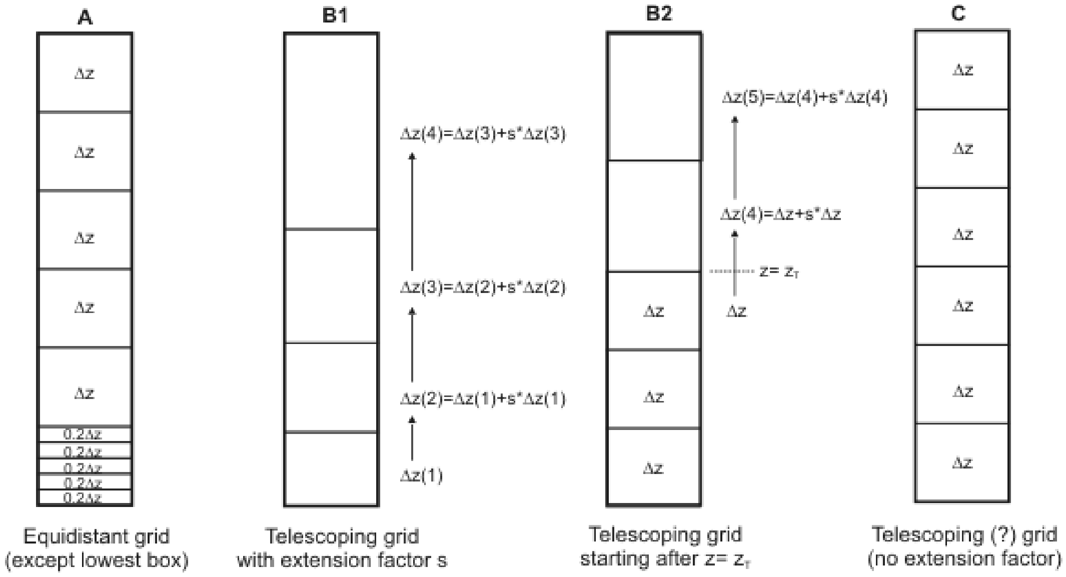

Figure. 5-2 The vertical configuration of ENVI-met

Type C is a combination of types A and B. It has no magnification factor and will not be used on vertical grids. Scale up, and the underlying mesh will not be divided into 5 smaller meshes. This type of mesh is suitable for use in simulated areas, especially in near-Earth areas, where there is no intense heat and moisture transfer. Since this type bisects all meshes, meaning that the materials in the vertical direction have the same properties, the accuracy of the simulation results is the same. In ENVI-met, there is also a special kind of grid structure - nested grid. They are strip-shaped grids distributed around the 3D simulation area. The larger the size, the farther the center area is from the boundary. The purpose is to keep the model boundary away from the simulation center to ensure that the initial conditions such as one-dimensional wind speed can fully develop before entering the central area, forming a three-dimensional gradient wind.

5.3. Related Computational Equations and Numerical Models

When ENVI-met couples various factors, it adopts five types of models: building surface, atmosphere, soil, greening and biological meteorology. Each item has a calculation formula. Here is how the ENVI-met software is simulated, as follows:

i. Atmospheric sub-model

This sub-model is mainly used to simulate the coupling between wind speed, temperature and humidity, eddy current and long and short wave radiation. According to the relevant mechanics theory, four control equations of mass, momentum, heat transfer and mass transfer are adopted. This sub-model is mainly used to simulate the coupling between wind speed, temperature and humidity, eddy current and long and short wave radiation. According to the relevant mechanics theory, four control equations of mass, momentum, heat transfer and mass transfer are adopted.

1) Wind farm

The equation of three-dimensional vortex air flow is non-hydrostatic Navier-Stokes equation to describe the evolution of air flow field turbulence in space and time. The calculation formula is as follows:

$$\frac{\partial u}{\partial t}+u_i\frac{\partial u}{\partial x_i}=-\frac{\partial p}{\partial x}+K_m\left(\frac{\partial^2 v}{\partial x_i^2}\right)-f\left(v-v_g\right)-S_v \qquad (5\text{-}1)$$

$$\frac{\partial v}{\partial t}+u_i\frac{\partial v}{\partial x_i}=-\frac{\partial p}{\partial x}+K_m\left(\frac{\partial^2 v}{\partial x_i^2}\right)-f\left(u-u_g\right)-S_v \qquad (5\text{-}2)$$

$$\frac{\partial w}{\partial t}+u_i\frac{\partial w}{\partial x_i}=-\frac{\partial p}{\partial x}+K_m\left(\frac{\partial^2 w}{\partial x_i^2}\right)+g\frac{\theta(z)}{\theta_{ref}(z)}-S_w \qquad (5\text{-}3)$$

$$\frac{\partial u}{\partial x}+\frac{\partial v}{\partial y}+\frac{\partial w}{\partial z}=0 \qquad (5\text{-}4)$$

Where: f(=104s-1) is the Lie constant, p is the local disturbance pressure, θ is the air temperature at the z-height, Km is the rate of change of the motion viscous coefficient, and g is the gravitational acceleration. The reference temperature θref break represents the meteorological conditions of the macro-climate and is obtained by averaging all the grids except the building. Ui and xi represent the speeds u, v, w and the coordinate axes x, y, z, and are denoted by i = 1, 2, 3, respectively, and the Posniske buoyancy hypothesis approximation is used to eliminate the self-compressible Navier-Stokes equations. The air density, in the w direction (5-3) will add additional source terms to describe the role of thermal buoyancy in the vertical direction. In order to maintain mass conservation in the formula, each iteration calculation should satisfy the formula (5-4). The source term in the formula at the same time, Su, Sy, Sz as the calculation of resistance caused by local possible vegetation, resulting in wind speed loss, calculated according to the following equation:

$$S_{u(i)}=\frac{\overline{\partial p}}{\partial x_i}=c_{d,f}LAD(z)\cdot W\cdot u_i \qquad (5\text{-}5)$$

Where: W is the average wind speed of height z, LAD is the leaf area density of the plant, and cd, f is the mechanical drag coefficient, usually set to 0.2.

2) Air temperature and relative humidity

The calculation of air temperature and humidity is calculated by solving the heat convection and diffusion equations. The calculation equations are as follows:

$$\frac{\partial \theta}{\partial t}+u_i\frac{\partial \theta}{\partial x_i}=K_h\left(\frac{\partial^2 \theta}{\partial x_i^2}\right)+\frac{1}{c_p\rho}\cdot\frac{\partial R_{n,lw}}{\partial z}+Q_h \qquad (5\text{-}6)$$

$$\frac{\partial q}{\partial t}+u_i\frac{\partial q}{\partial x_i}=K_q\left(\frac{\partial^2 q}{\partial x_i^2}\right)+Q_q \qquad (5\text{-}7)$$

Where: Qh and Qq represent the heat and moisture transfer between the plant surface and the surrounding environment, which is calculated by the greening submodel. Kh and Kq are the heat and humidity diffusion coefficients respectively, and the long-wave radiation in the vertical direction is Rn, lw/∂z Indicates the effect of radiation on the cooling and warming of the environment.

3) Atmospheric turbulence

The first-order closure (K-theoretical) is based on the exchange coefficient K and the gradient change of each quantity in all directions, and this method is also the simplest method, but since this method does not take into account the obstacles existing in the urban environment, such as The influence of buildings or structures and vegetation, so it only applies to the homogeneous environment. If the calculation of more complex closed turbulence (second order or above) is quite complicated, in order to save computation time, the scholars summed up a compromise method, namely the 1.5-level closed equation (E-ε equation), which can simulate The horizontal flow process takes into account the effects of horizontal non-uniformity, making it suitable for simulating urban environments, so this calculation formula is adopted by the ENVI-met design team, in which two variables are written into the calculation equation In order to determine the exchange coefficient, that is, the turbulent flow energy E and the consumed dissipation rate ε, the specific formula for the calculation equation is as follows:

$$\frac{\partial E}{\partial t} + u_i \frac{\partial E}{\partial x_i} = K_E \left(\frac{\partial^2 \theta}{\partial x_i^2} \right) + Pr + Th + Q_E - \varepsilon \qquad (4\text{-}8)$$

$$\frac{\partial \varepsilon}{\partial t} + u_i \frac{\partial \varepsilon}{\partial x_i} = K_\varepsilon \left(\frac{\partial^2 \varepsilon}{\partial x_i^2} \right) + c_1 \frac{\varepsilon}{E} Pr + c_3 \frac{\varepsilon}{E} Th + Q_E - c_2 \frac{\varepsilon^2}{E} \qquad (4\text{-}9)$$

$$Pr = K_m \left(\frac{\partial u_i}{\partial x_j} + \frac{\partial u_j}{\partial x_i} \right) \frac{\partial u_i}{\partial x_j} \qquad (4\text{-}10)$$

$$Th = \frac{g}{\theta_{ref\,(z)}} K_h \frac{\partial \theta}{\partial z} \qquad (4\text{-}11)$$

Where: Pr and Th respectively represent the turbulent energy and its dissipation caused by wind shear and temperature stratification, which can be calculated by formulas (4-10) and (4-11). In the above formula, c1, c2 and c3 are related to the turbulence state. According to the reading of historical data, the existing standard values have been used, but different values may be used under different conditions. The standard values generally take 1.44, 1.92, 1.44. Where: QE represents turbulence caused by plants, while Qε represents plants the acceleration level of the turbulent flow energy near the blade, which can be calculated by the following formula:

$$Q_E = c_{d,f} LAD\,(z) \cdot W^3 - 4 c_{d,f} LAD\,(z) \cdot |W| \cdot E \qquad (5\text{-}12)$$

$$Q_E = 1.5c_{d,f}LAD\ (z)\ \cdot W^3 - 6c_{d,f}LAD\ (z)\ \cdot |W| \cdot \varepsilon \qquad (5\text{-}13)$$

Where: take ε=0.163/2/l, cd,f is the wind resistance coefficient of the plant leaf, W is the wind speed at the reference height, and when the coupled equation is solved, a more ideal state is assumed to determine the turbulent flow. The exchange coefficient, the relevant parameters in its calculation formula are the relevant data obtained by the experiment, and the calculation equation is as follows:

$$\begin{aligned} K_m &= c_\mu \frac{E^2}{\varepsilon} \\ K_h &= 1.35K_m \\ K_E &= \frac{K_m}{\sigma_E} \\ K_\varepsilon &= \frac{K_m}{\sigma_E} \end{aligned} \qquad (5\text{-}14)$$

Where: cu=0.09, σE=1 and σε=1.3. However, the E-ε turbulence model also has its own big problem. Therefore, Envi-met uses the first-order closed mode in the homogeneous model region. The wind field and thermal stress are solved by the turbulence model, that is, the free convection molecular energy exchange, calculation the formula goes as follows:

$$Ri_b = \frac{g}{\theta}\frac{\Delta\theta\cdot\Delta w}{(\Delta u)^2} \qquad (5\text{-}15)$$

Where: Δw is the distance between the first grid of surface air, u is the horizontal wind speed, the turbulent flow momentum at the surface, and heat and water vapor are calculated according to the Moo similarity theory.

4) Radiant flux

Ignoring the influence of vegetation factors, the long-wave radiation of air at height Z is synthesized by synthesizing n single layers. The specific formula is as follows:

$$R_{lw}^{\downarrow}\ (z)\ = \sum_{n=1}^{n} \sigma_B T^4\ (n)\ [\varepsilon_n\ (l + \triangle l)\ - \varepsilon_n\ (l)\ ] \qquad (5\text{-}16)$$

Where: l is the moisture content between the height Z and the lower layer n, and εn is the emissivity of the n layer. The short-wave radiation R_SW^* can be estimated by the wavelength radiation I_0 from λ=0.29 up to λ=0.40.

$$R_{sw}^{*}\ (z)\ = \int_{0.29}^{4.0} I_0\ (\lambda)\ exp\{-\alpha_R\ (\lambda)\ m + \alpha_M\ (\lambda)\ m\} d\lambda \qquad (5\text{-}17)$$

Where: I_0 by querying the existing data, the optical quantity m is a function of Ray's Rayleigh scattering (α_R=0.00816λ^(-4)) and Mies scattering (α_m=λ^(-1.3) β_tr).

$$R_{sw,dir}^{0*} = R_{sw}^{*} - R_{sw,abs} = R_{sw}^{*} - \ (70 + 2.8VP_{2m} \cdot m) \qquad (5\text{-}18)$$

Where: R_(sw, dir)^0 is the absolute amount of short-wave radiation of the model, and R_(sw, abs) is the energy value of the water content in the atmosphere. The former is obtained by subtracting the value of the latter. At the same time, the short-wave radiation depends on the direct solar radiation and the solar elevation angle. The corresponding formula is as follows:

$$R^0_{sw,dif} = f\ (R^0_{sw,dir},\ \emptyset) \tag{5-19}$$

In the formula: ∅ is the solar elevation angle. According to the research of relevant personnel, the direct radiation R_(sw, dir)^0 of the sun is reduced under cloudy conditions. For a given grid point in the simulated area, if a building obstructs direct solar radiation, then when R_(sw, dir)^0 is set to 0, for other radiation quantities, there is a ratio of influence on the sky, which can be The SVF proposed above is expressed as follows:

$$\sigma_{svf} = \frac{1}{360}\sum_{\pi=0}^{360} cos\,\omega\ (\pi) \tag{5-20}$$

Where: ω refers to the angle formed by the obstruction at azimuth π, direct radiation and diffuse reflection (R_(sw, dir), R_(sw, dif)) and long-wave radiation (σ _lw^↑, σ _lw^↓) ,Calculated as follows:

$$\sigma_{sw,dir\ (z)} = exp\left[-F \cdot LAI^*\ (z)\right] \tag{5-21}$$

$$\sigma_{sw,dif\ (z)} = exp\left[-F \cdot LAI\ (z, z_p)\right] \tag{5-22}$$

$$\sigma^{\downarrow}_{lw\ (z)} = exp\left[-F \cdot LAI\ (z, z_p)\right] \tag{5-23}$$

$$\sigma^{\uparrow}_{lw\ (z)} = exp\left[-F \cdot LAI\ (0, z)\right] \tag{5-24}$$

Where: F is the extinction coefficient, and LAI is the coefficient calculated by the integration of plants at different heights. For short waves, the LAI is replaced by the more suitable three-dimensional direction LAI*.

Then the short-wave radiation R_(sw, dir(z)) at the height z is calculated as:

$$R_{sw,dir\ (z)} = \sigma_{sw,dir\ (z)} R^0_{sw,dir} \tag{5-25}$$

The diffuse total radiation R_(sw, dif(z)) is calculated as:

$$R_{sw,dif(z)} = \sigma_{sw,dif(z)} R^0_{sw,dir} \sigma_{svf(z)} + \left[1 - \sigma_{svf\ (z)}\right] R^0_{sw,dir} \cdot \langle\alpha\rangle \tag{5-26}$$

Where: the first part corresponds to diffuse radiation, and the second part is the diffuse reflection associated with the average reflectivity of all walls and ground in the simulated area.

For the vegetation in the simulated area, the upward long-wave radiation σ _lw^↓ and the downward radiation σ _lw^↑ are expressed as:

$$R^{\downarrow}_{lw(z)} = \sigma^{\downarrow}_{lw(z)} R^{\downarrow,0}_{lw(z)} + (1 - \sigma^{\downarrow}_{lw(z)}) \varepsilon_f \sigma_B \langle T_{f+} \rangle^4 \qquad (5\text{-}27)$$

$$R^{\uparrow}_{lw(z)} = \sigma^{\uparrow}_{lw(z)} \varepsilon_s \sigma_B T_0^4 + (1 - \sigma^{\uparrow}_{lw(z)}) \varepsilon_f \sigma_B \langle T_{f-} \rangle^4 \qquad (5\text{-}28)$$

Where: <T_(f+)> and <T_(f-)> are the average temperatures of the upper and lower layers of the leaves, T_0 is the surface temperature, <T_w> is the average temperature of the building facade, and σ_B is the Stephen-Boltz The MANN constants, ε_f, ε_s, and ε_w are the reflectances of the foliage, the ground, and the wall, respectively.

ii. Soil model

The power of Envi-met software is not only in the analysis of the building and the surrounding environment, but also the soil mentioned in the front is one of the shared elements, from the ground 0 to the underground 20 cm, the underground 20 cm to 45 cm and the underground 45 cm to It consists of three layers of 175 cm. Each layer has its own independent properties. The soil type needs to calculate its thermal conductivity and albedo.

iii. Vegetation model

The vegetation in the software is simplified into a one-dimensional model, and the growth height zp and root depth zr are set respectively. The leaf area index (LAD) and the root area index (RAD) are used to indicate the distribution of leaves and plant roots at different heights or depths. The plant model uses sensible heat flow (Jf, h), leaf surface evaporation (Jf, evap) and leaf surface transpiration heat dissipation (Jf, trans) to describe the heat and moisture transfer between plants and the surrounding air. The formula is as follows:

$$J_{f,h} = 1.1 r_a^{-1} (T_f - T_a) \qquad (5\text{-}29)$$

$$J_{f,evap} = r_a^{-1} \triangle q \vartheta_c f_w + r_a^{-1} \triangle q (1 - \vartheta_c) \qquad (5\text{-}30)$$

$$J_{f,trans} = \vartheta_c (r_a + r_s)^{-1} (1 - f_w) \triangle q \qquad (5\text{-}31)$$

$$\triangle q = q^* \cdot T_f - q_a$$

Where: Ta is the air temperature around the blade, Tf is the blade surface temperature, and ra is the air damping coefficient of the blade. At the same time, according to the definition of Equation 4-21 above, Δq is the heat dissipation of the air to the blade, q* is the blade surface qa The saturation value, when the plant shows transpiration during the day, ie ⩽q ⩽ 0, δ _c = 1,; when the nighttime shows condensation, the value is zero. F_w is the ratio of wet leaves. For a normal plant, rs is the stomatal resistance of the soil moisture content in the root system under real-time and maximum short-wave radiation, which can be calculated by the formula:

$$r_s = r_{s,min} \left[\frac{R_{sw,max}}{0.03 R_{sw,max} + R_{sw}} \right] + \left(\frac{\eta_{wilt}}{\eta} \right)^2 \qquad (5\text{-}32)$$

In order to calculate the surface temperature of the blade, the steady-state heat balance equation of the blade surface is established, as shown in the formula (5-32), which assumes that the energy stored inside the leaf can be ignored. The short-wave radiation R_(sw,net) and the long-wave radiation R_(lw,net) absorbed by the surface of the leaf can be calculated by formulas (5-33) and (5-34):

$$R_{sw,net}(z) = \left(F \cdot R_{sw,dir}(z) + R_{sw,dif}(z)\right) \cdot (1 - a_f - tr_f) \tag{5-33}$$

$$R_{lw,net}(z, T_f) = \varepsilon_f R_{lw}^{\downarrow}(z) + R_{lw}^{\leftrightarrow}(z) + \varepsilon_f R_{lw}^{\uparrow}(z) - 2\varepsilon_f \sigma_B T_f^4 - (1 - \sigma_{svf}(z))\, \sigma_B T_f^4 \tag{5-34}$$

Where: cp is the specific heat of the air, and L is the latent heat of vaporization. F is a dimensionless constant, which is used to indicate the relative positional relationship between the blade and the sun. At the same time, for a randomly extracted blade, F=0.5, af is the emission coefficient of the blade, and trf is the transmission coefficient. In the plant model, in the ideal state, each leaf leaves only the upper surface and the surrounding air to transfer heat and absorb short-wave radiation, while the upper and lower sides have long-wave radiation. According to the assumptions, the source term and absorption in the atmospheric submodel Items can be calculated according to the following formula:

$$Q_h(z) = LAD(z) \cdot J_{f,h} \tag{5-35}$$

$$Q_q(z) = LAD(z) \cdot (J_{f,evapo} + J_{f,trans}) \tag{5-36}$$

iv. Building (structure) surface sub-model

ENVI-met can simulate the long- and short-wave radiation on the surface of the sky and different buildings. The main control equations for the energy balance of the long-short-wave radiation on the outer surface of the structure are as follows:

$$0 = R_{sw,net} + R_{lw,net} - c_p p J_h^0 - pL \cdot J_v^0 - G \tag{5-37}$$

Where: R_(sw,net), R_(lw,net) are short-wave radiation and long-wave radiation, J_h^0 and J_v^0 are heat flow and water flow, and G is the underlying surface of soil or building envelope Surface heat flow. At the same time, the long-wave radiation from the building is approximately expressed as R_lw^↔, which is also calculated based on the average surface temperature <T_w> of all walls:

$$R_{lw(z)}^{\leftrightarrow} = (1 - \sigma_{svf(z)})\, \varepsilon_w \sigma_B \langle T_w \rangle^4 \tag{5-38}$$

The turbulent fluxes H0 and LE0 are the air temperature and humidity at the ground (z = 0) and the first grid point (z = 1) in the vertical direction. Ground surface fluxes and turbulence and molecular energy fluxes are expressed as follows:

$$G_0 = \lambda_s \frac{\partial T}{\partial z} = \lambda_{s(k=-1)} \frac{T_0 - T_{k=-1}}{0.5 \triangle z_{k=-1}} \tag{5-39}$$

$$H_0 = pc_p \left[-K_h^0 \frac{\partial T}{\partial z}\bigg|_{z=0}\right] = pc_p \left[-K_h^0 \frac{T_0 - \theta_{k=1}}{0.5 \triangle z_{k=1}}\right] \tag{5-40}$$

$$LE_0 = pL_0 \left[-K_q^0 \frac{\partial q}{\partial z}\right] = pL_0 \left[K_q^0 \frac{q_0 - \theta_{k=1}}{0.5 \triangle z_{k=1}}\right] \tag{5-41}$$

Where: λs is the thermal conductivity of the soil, k=±1 corresponds to the grid point above or below the surface, and K_h^0 and K_q^0 are the exchange coefficients of heat and water vapor between air and water.

The energy balance of a wall or roof surface is expressed as follows:

$$R_{sw,net} + R_{tw,net}^{w,r} - H_{w,r} - G_{w,r} = 0 \qquad (5\text{-}42)$$

Where: Hw, r and Gw, r are the heat flux and heat flux through the roof. The net short-wave radiant flux R_(sw,net) is expressed as follows:

$$R_{sw,net} = \{cos\,\beta^* \cdot R_{kw,dir}(z_{w,r})\}\ (1 - a_{\delta}) \qquad (5\text{-}43)$$

Where: z_wr is the height, as is the reflectivity of the roof and the wall, and β* is the angle between the incident ray R_(kw, dir) of the direct sunlight and the surface normal. However, because the roof and the wall have different orientations, there is a difference in the long-wave radiation of the surface. The net long-wave radiation flux of the roof is expressed as follows:

$$R_{lw,net}^{r} = \sigma_{svf} R_{lw}^{\downarrow,0} + (1 - \sigma_{svf})\varepsilon_w \sigma_B \langle T_r \rangle^4 - \varepsilon_r \sigma_B \langle T_r \rangle^4 \qquad (5\text{-}44)$$

The vertical building wall not only receives solar radiation but also radiation from other surrounding environments. The net long-wave radiant flux of the wall is expressed as follows:

$$R_{lw,net}^{w} = \sigma_{svf}\ (0.5\varepsilon_s \sigma_B \langle T_r \rangle^4 + 0.5 R_{lw}^{\downarrow,0} + (1 - \sigma_{svf})\ (0.33\varepsilon_w \sigma_B \langle T_r \rangle^4 + 0.67\varepsilon_w \sigma_B \langle T_r \rangle^4)\ - \varepsilon_r \sigma_B \langle T_r \rangle^4 \qquad (4\text{-}45)$$

The sensible heat flux Hw of the building facade near the surface of the wall is expressed as follows:

$$H_w = pc_p K_h^w \frac{\partial T}{\partial z}\bigg|_w = pc_p K_h^w \frac{T_0 - T_{w-1}}{\triangle w} \qquad (5\text{-}46)$$

The heat flow Qw,r through the wall can be calculated directly from the surface temperature of the wall or roof and the indoor air temperature:

$$Q_{w,r} = U\,(T_w - T_{a,i}) \qquad (5\text{-}47)$$

Where: U refers to the thermal conductivity. The thermal conductivity of different materials can be found in the existing data.

v. Biological meteorological sub-model

There have been many studies on Tmrt so far, and its accuracy has been confirmed. Envi-met software has provided a good reference in this regard.

$$T_{mrt} = \left[\frac{1}{\sigma_B}\left(E_t\ (z)\ + \frac{a_k}{\varepsilon_p}\ (D_t\ (z)\ + I_t\ (z))\right)\right]^{0.25} \qquad (5\text{-}48)$$

$$E_t(z) = 0.5\left[\left(1 - \sigma_{svf}(z)\right) R_{lw}^{\leftrightarrow} + \sigma_{svf}(z) R_{lw}^{\downarrow 0}\right] + 0.5\varepsilon_w \sigma_B T_0^4 \qquad (5\text{-}49)$$

$$R_{lw}^{\leftrightarrow}\ (z)\ = \left(1 - \sigma_{svf}(z)\right) \varepsilon_w \sigma_B \overline{T_w^4} \qquad (5\text{-}50)$$

$$D_t\text{（}z\text{）}=\sigma_{svf}(z)R_{sw,dif}^{\downarrow,0}+\left(1-\sigma_{svf}(z)\right)\bar{a}R_{sw,dir}^{\downarrow,0} \quad (5\text{-}51)$$

$$I_t\text{（}z\text{）}=f_p(z)R_{sw,dif}^{\downarrow,0} \quad (5\text{-}52)$$

$$f_p=0.42\cos\emptyset+0.043\sin\emptyset \quad (5\text{-}53)$$

As shown in the formula (4-49), Tmrt is calculated using the point z long-wave radiation total intensity Et(z), the direct irradiation amount It(z), and the solar scattered radiation Dt(z). The calculation formula is as shown in (5-50) to (5-54). In addition, Envi-met can also calculate evaluation coefficients such as PMV-PPD and PET.

5.4. Software boundary condition types and input and output

The horizontal boundary condition (LBC) in Envi-met software determines how the software handles model boundaries. Envi-met provides three LBC types:

1) Open: The iterative operation of the model assigns a grid value close to the boundary to the boundary. This boundary condition has little effect on the internal mesh, and the result will result in inaccurate simulation results.

2) Closed: The calculation result of the independent one-dimensional model is used as the boundary of the overall three-dimensional model. This format is relatively stable.

3) Cyclic: The boundary value of the downwind direction is given to the boundary of the upwind direction, where the average value of the wind direction is similar to the environment of the whole model. Since the value of the outflow boundary will be iteratively flowing into the boundary, the value is not to some extent.

i. Input quantity

Before using ENVI-met for numerical simulation calculation, you need to input the initial values of macroscopic meteorological parameters and analog control. Parameters that define the underlying surface and the thermal properties of the building, as shown in Table 5-1.

Table 5-1 Input quantity in ENVI-met

Category	Input
Macroscopic meteorological parameters	Geographical location, 10 m high wind speed, wind direction, initial air temperature, 2500 m height moisture content, 2 m high relative humidity, daily cloud amount, solar radiation intensity adjustment factor
Underlying surface and building properties	Initial temperature and relative humidity of different depths of soil, building room temperature, heat transfer system of envelope structure
Number and reflectivity	Simulation start and end times, simulation duration, time steps at different sun elevation angles, edges Boundary condition type, turbulence model, number of embedded meshes

In addition, if the user wants to customize the material, the type of tree or the underlying surface structure, the number of software needed According to the library, the relevant physical parameters are input.

ii. Output quantity

The calculation results of ENVI-met can be divided into two categories: ASCII binary code and color block diagram. Detailed output column in Table 5-2. By setting the "monitor" in different positions, you can get all the calculation results in the vertical direction of the point. Binary code. If the calculation result of ENVI-met is imported into the own processing software LEONARDO, then obtain a two-dimensional vector map and a patch map of certain parameters.

Table 5-2 Output quantity in ENVI-met

Category	Output
Macroscopic meteorological parameters	Wind speed and direction, air temperature, moisture content, blade surface temperature, direct and short scattering
Micro-environment air quality (contaminants)	Contaminant concentration, CO2 distribution
Structure parameters LAD distribution	Biological meteorological parameters PMV, average radiant temperature

5.5. Limitation of ENVI-met

As stated at the beginning of this chapter, although ENVI-met is considered to be the best microclimate fluid dynamics simulation at present. Software, with a very solid physical foundation, but due to its control equations to simplify the calculation process, a lot of fake. Designed to limit its application. The limitations of the software are summarized as follows:

1) As an ENVI-met developed for the mid-high latitude cold climate, the area can be accurately simulated outdoor thermal conditions. But is it equally applicable to tropical and subtropical regions with completely different climate types. Systematic verification of theory and experiment is required.

2) Some studies have pointed out, when the software simulates a hot and humid climate, it will underestimate the daily temperature change value, resulting in the temperature is generally high at night. Although this is good for evaluating the thermal comfort during the day, it is impossible to evaluate the outdoor night pass.

3) Dynamic wind environment assessment is not possible. Since the software only allows input of fixed wind speed and direction, it cannot be dynamic. It is impossible to evaluate the quality of the wind environment at different times by inputting the winds on time.

4) Exaggerate or underestimate the intensity of solar radiation. Time-varying solar radiation cannot be manually defined when entering simulation conditions. Intensity can only be adjusted simply by adjusting the coefficient in the range of 0.5 to 1.5 times, resulting in the input of solar radiation. The total amount of radiation and the maximum value cannot be consistent with the actual situation, thus exaggerating or underestimating solar radiation.

5) The impact of cloud volume changes on the thermal environment is not yet clear. Due to the input conditions, the cloud amount is only high. The simple definition of the

three levels of low and medium, there is no specific proportion, and there is no corresponding time period, which makes it impossible to evaluate the cloud amount. The impact on the thermal environment.

6) There are too few plant species and related physical parameters. In the database that comes with the software, there are only a few plant species. Classes, and most of these plants grow in cold regions at mid-high latitudes.

5.6. Verification and Validation

The long-term development of computational fluid dynamics software (CFD) over the past four decades is beyond expectations. In recent years, the speed of numerical simulations brought about by the replacement of computer hardware has also increased rapidly. Accelerate the application of CFD software in engineering design, industrial manufacturing and scientific research. Although more and more designers and researchers are using CFD simulation software, they have passed certain evaluation processes. The work of systematically determining the reliability and accuracy of the calculation results has not stopped. Most scholars is recommended to compare the experimental data to determine its accuracy, but this method is firstly subject to the accuracy of the experimental instrument. The limitations, especially in the field of microclimate simulation, the accuracy range of temperature test instruments are mostly between ±0.3~1 ℃. This article refers to the American Institute of Aeronautics and Astronautics (AIAA) issued a fluid mechanics simulation software calibration specification, taking the typical representative city of hot and humid climate Tai zhou as an example. The microclimate simulation software ENVI-met conducts theoretical verification and verification (Verification and Validation, V & V).

The word simulation software development process is a dynamic reciprocating process of "discovering problems, solving problems, checking accuracy, and modifying models". Process, which involves two important models - conceptual mathematical model and numerical simulation computerized model. Conceptual mathematical models are abstracted from the corresponding physical processes, including describe all relevant information about the main features of the phenomenon, the data of the mathematical model, and the governing equations. In CFD simulation soft. In the piece, the conceptual mathematical model is dominated by three partial differential equations of mass, momentum and energy. Numerical simulation a model, or simulation software, is a computer program that can be run to solve conceptual mathematical models.

Verification: Determine whether a conceptual mathematical model can fully reflect objective engineering techniques and the mathematical nature of the problem, the precise analysis of the test process of the governing equation.

Validation: A school that determines the accuracy of numerical simulation software to simulate actual engineering problems. Conceptually, Verification is to verify that the CFD software program correctly reflects the control. Whether the computational core, conceptual mathematical model, etc., has correctly solved these two problems in the program.

Whether the abstract process that does not involve the mathematical model is consistent with the actual engineering and technical issues, so it is linked with the actual situation. The system is not tight. The Validation focuses on confirming the consistency of the simulation results with the actual situation, and compared with the calculation accuracy of the calculation software, it is more necessary to provide the corresponding evidence to prove the calculation model in the software. The corresponding practical problem can be solved correctly and with high precision.

From the above definitions, we can find two common points of theoretical test and experimental check:

1) The two names correspond to a cyclical process with no clear end points. People are true Continuous understanding of the problem and objective phenomenon, improvement of experimental testing and development of computer performance, it will lead to the improvement of conceptual mathematical models, simulation calculation software, and higher requirements for simulation accuracy. In addition, there are many practical problems in engineering, and CFD simulation software cannot guarantee the same when solving each type of problem. The result of precision, and any software or mathematical model will have a certain calculation error. This makes V&V a process that keeps going.

2) The importance of Accuracy is emphasized in the definition. Mathematical model in the process of theoretical testing. The accuracy of the calculation is often determined by simulation of the simplified benchmark model and case; during the experimental calibration process, the software. The accuracy is obtained by comparing with the actual test results. The disadvantage of doing this is that the benchmark model and case pass often limited by fluid properties and geometric dimensions, it is impossible to judge complex situations; the actual measurement results are saved. In instrumentation and observation errors, this often makes the accuracy of the measurement results even lower than the software simulation progress. In the subsequent discussion of this chapter, two simplified cluster models will be used for the ENVI-met microclimate simulation software. Verification of applications in Guangzhou, including boundary conditions (BLC) and turbulence models (TKE) analysis type, vertical grid size, and iteration time step impact on software convergence, simulation time is 8. In the middle of the month, the test time was uniformly set to 240 hours. In the course of the experimental check, the third chapter is used. Cases of typical residential quarters in Guangzhou tested by thermal environment, comparing horizontal and vertical heights and relative humidity

The measured and simulated values of the quantity and distribution law, and the relationship between the various measuring points. Tested by V&V. After that, I got the best setting in the numerical analysis process when ENVI-met software was used in hot and humid climate areas such as Taizhou. The value lays the foundation for the subsequent six-phase landscape design factor quantitative change simulation analysis.

5.7. Method of validation

According to the relevant information, although Envi-met software is considered to be the most accurate microclimate simulation software, many scholars have done accurate software so far because of many additions in the calculation equations and many assumptions. Sexual research proves that the software has errors in the following aspects:

(1) Enqui-met software is suitable for cold regions in the middle and high latitudes

by querying data. Whether it can be applied to hot areas remains to be verified.

(2) Regarding the section of the wind speed fluid, since the initial wind speed value and the wind direction can only be input, the parameters cannot be input dynamically and time-wise, which makes the accuracy of the evaluation wind greatly reduced.

(3) The influence of solar radiation also has a certain deviation. When inputting the simulation conditions, the time-dependent solar radiation intensity cannot be manually defined, which causes a certain error, thereby exaggerating or reducing the actual solar radiation.

(4) Some researchers have suggested that Envi-met ignores the daily temperature change when simulating temperature and humidity, which causes the temperature to be too high at night.

(5) The amount of cloud changes per day Envi-met has not been considered too much. In the initial input of data, only the cloud quantity has been defined by three levels of high, medium and low, and there is a large error.

(6) There are few types of plants and various vegetations, and the vegetation that comes with the software belongs to the vegetation in the cold regions of high latitudes. Therefore, there is a big error in the microclimate analysis of the tropical regions.

The six errors mentioned above are inevitable and can only be used by error evaluation after the simulation. The current error-based evaluation index criteria include mean absolute error (MAE), mean deviation (MBE), and average absolute percentage error (MAPE), Root Mean Square Error (RMSE) and Hill Inequality Coefficient, error component analysis mainly consists of deviation rate, variance rate and co-variation rate. The commonly used evaluation coefficient of the model has complex correlation coefficient (R), the coefficient of determination (R^2), the coefficient of determination of the correction (R^2), etc., the model evaluation coefficient of this paper and the comparison of the measured data and the simulated data select R^2. By consulting the literature, it can be seen that R^2 is 0.3 to 0.7, indicating that there is correlation. When the range is 0.7 to 0.9, there is a strong correlation, and above 0.9 is an absolute correlation.

5.8. Method of verification

In order to test the simulation accuracy and convergence time of ENVI-met software in hot and humid climate, take Taizhou area as an example. Two simplified building unit models and the same initial values were used for different evaluation objects. Keep it under the premise of constant parameters, change the boundary condition (BLC) type and vertical grid size to observe ENVI- met the change in simulation results, convergence, etc. The theoretical test model is set in ENVI-met as shown in Figure 32. The parameters of each model are shown in Table 5-3. The showing model in this session is a 20-meter-tall (6 m × 3 m) north-south direction with no greening around. This model is mainly used for inspection ENVI-met three different boundary condition (LBC) types, three "surveillances" are set before and after the building receptor is used to record the simulation results of temperature, wind speed, etc. at different locations. Model 2 is a 15 meter wide, 20 meters long north-south street, 20 meters high on both sides, 4 meters wide road in the street and 3 meters wide on both sides of the road this model is mainly used to test the different types of vertical grid sizes for the final simulation results and convergence time.

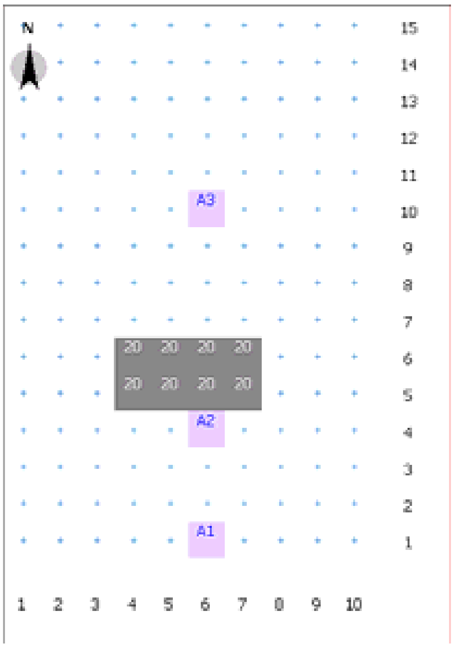

Figure. 5-2 The tested model of ENVI-met

Table 5-3 Theoretical test model ENVI-met set value

Model	Grid size	Time	Region	Air temperature	Relative humidity	Wind speed	Wind direction
a	3 ×3×3	48	50×50	37℃	45%	2.0m/s	145
b	3 ×3×3	48	50×50	37℃	45%	2.0m/s	145

According to understand software structure and control equations of ENVI-met, there are three types when setting simulation conditions. The boundary conditions are available to the user: open, closed, and cyclic LBC. Each of these three types of boundary conditions has advantages and Disadvantages, which boundary to use for simulation needs to be determined by specific cases. This article takes model 1 as an example, testing. The simulation results obtained by setting different boundary condition types are shown in Figure 33. As can be seen from the figure, although different boundary condition types were chosen, but the simulation results of ENVI-met are not obvious.

Figure 33-a shows the simulation results for the open boundary conditions. The direction of the wind in the simulated area, the number of down-winds. The value (below the plan view, the right side of the profile) is copied to the upwind direction (above the plan view, to the left of the profile), until the border. Therefore, the influence of the boundary conditions on the simulated area is weakened and becomes very small. This type of boundary condition is suitable for use in external conditions such as temperature and humidity that are susceptible to solar radiation and underlying surface properties. The simulation of meteorological parameters, their changes in the microclimate are very small by the surrounding area.

Figure 33-b shows the simulation results for closed boundary conditions. The value in the inner boundary of the simulation area along the direction of the wind is given the grid next to it. Therefore, the microenvironment around the building is

significantly affected by the boundary conditions. The type is more suitable for simulating meteorological parameters such as ambient wind that are more affected by changes in boundary conditions.

Figure33-c shows the simulation results for the cyclic boundary conditions. Simulation of the flow from the downwind to the boundary along the direction of the wind. The regional environmental wind meteorological parameters are used as new boundary conditions and are used to replace the original boundary conditions. Such boundary strip. The initial value of the piece is relatively high. When the initial value of the input is close to the final result, it can make the control equation close, which reduces calculation time. However, if the initial value is not chosen properly, or the simulated area is too complex Miscellaneous, the calculation results are not easy to control, but will consume more computing time.

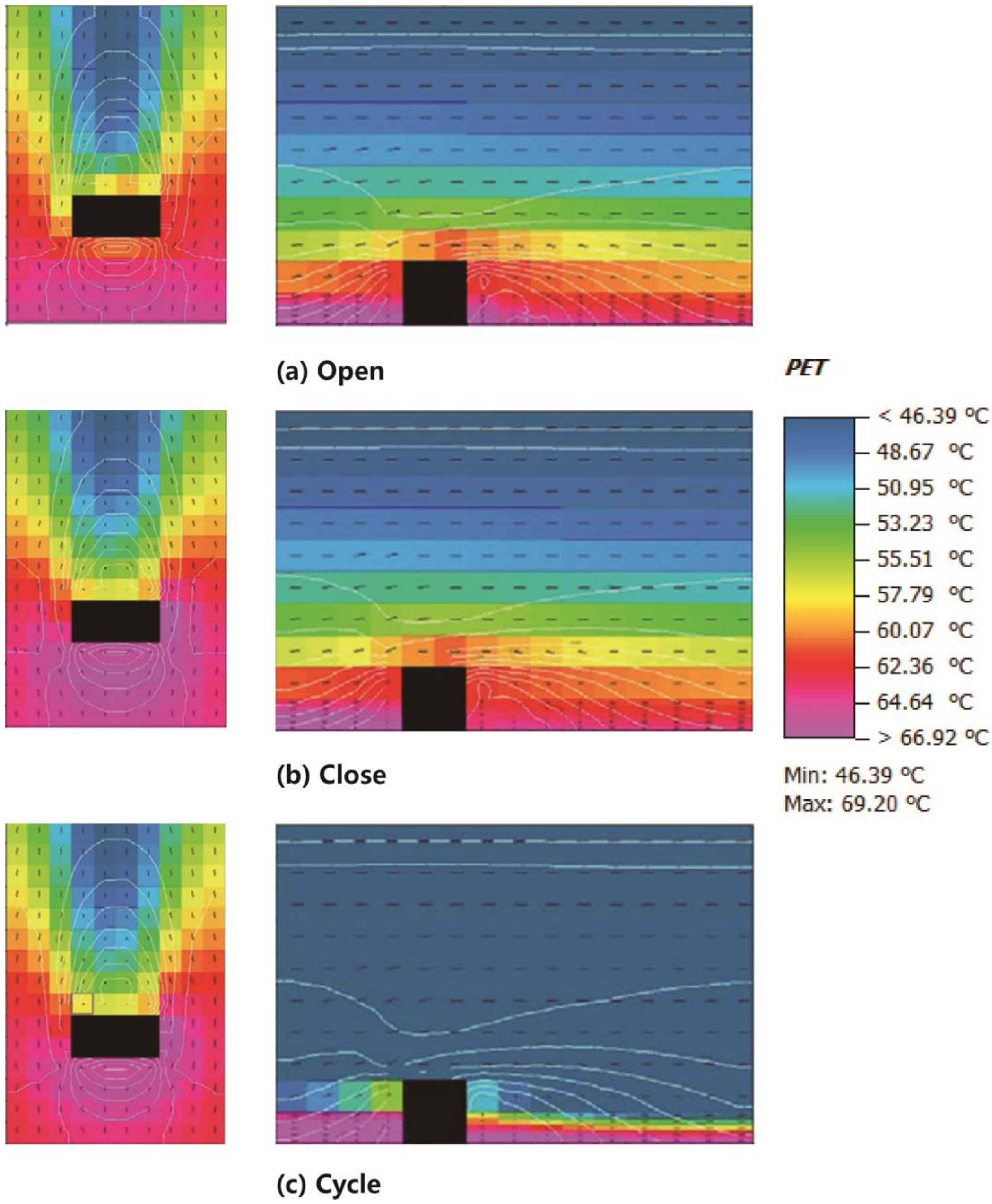

Figure. 5-3 The configuration of boundary of ENVI-met

In general, the three sides are used regardless of the numerical value of the test case simulation results or the distribution law. The calculation results of the boundary condition types are similar. Open LBC controls temperature and relative humidity better, while closed LBC is good for simulating ambient winds, and circular LBC is able to reduce the number of iterations of specific case control equations, saving calculating time. In the ENVI-met simulation analysis of the subsequent chapters, the open LBC will be used as the boundary bar for temperature and humidity. The closed LBC is used as the boundary condition for the ambient wind turbulence. In addition, during the boundary condition test, it was found that ENVI-met requires a certain warm-up time to receive Convergent simulation results, this time interval is related to the set iteration time step.

By comparing the three types of boundary conditions (BLC), it is found that the climate of hot and humid regions is hot and humid. At the time of microclimate simulation, open LBC should be used because of the change in the hourly value of temperature and humidity. The closed LBC is beneficial to control the convergence characteristics of the turbulence model and to facilitate the simulation of the ambient wind. The test results show that if the case is high enough to meet the simulated area, it is twice as large as the highest building in the area. Simulation of the two vertical grid types of equidistant grids and telescopic grids with different scaling ratios As a result, the distribution law of both numerical and vertical heights is similar.

5.9. Numerical simulation

According to AIAA's recommendation, a complete Complete System should include CFD software. Subsystem Cases, Benchmark Cases, and Unit Conversion Issues (Unit Problem) three steps. And each of these steps has fluid flow conditions and geometry with different characteristics. The size is complex. As in the literature review in Chapter 2, the authors of ENVI-met software and other researchers have already Many cases of bit conversion have been checked, which proves to some extent the calculation results of the software. The actual situation has a good agreement. About the 3D micro-climate modelling system, ENVI-met was selected as the preferred modelling tool, mainly due to its capability in the model foundation on the principles of computational fluid dynamics for modelling plant-surface-atmosphere interaction in complex environment with buildings of different shapes, height, the material of the street and the vegetation of different configuration [195]. It can simulate with a high spatial and temporal resolution which supplies near-accurate modelling of microclimate parameter.

In this model, the buildings including shading devices and artificial structures are approximated to a normal cube, their sizes are configured in accordance with the Google maps and the field survey. ENVI-met has been widely applied in several studies and the accuracy of results had been accepted by researchers [196-199]. These results have shown the acceptable accuracy in different climate model [200].The initial input data of the various meteorological elements used in the ENVI-met simulation is shown in the Table. 5-4. The initial data is in accordance with the calculation of the average measured data of the first measured day.

5.9.1. The introduction of Dao He Old block

Table. 5-4 Initial simulated data for ENVI-met input

Data	Initial input value for ENVI-met simulation
Temperature	37℃
Humidity	45％
Wind velocity	2.0m/s
Wind direction	145°
Main model area (x-grids, y-grids, z-grids)	200×100×20
Size of grid cells (meter) (x, y, z)	3×3×3

In this study, the whole simulation is 48 hours, starting from midnight 00:00, 30th, 2016 with a calculation of one minute. The simulation results are output in an hour basis. We obtain the data at a 1.5m high level. The three-dimensional model is shown in Figure. 5-4.

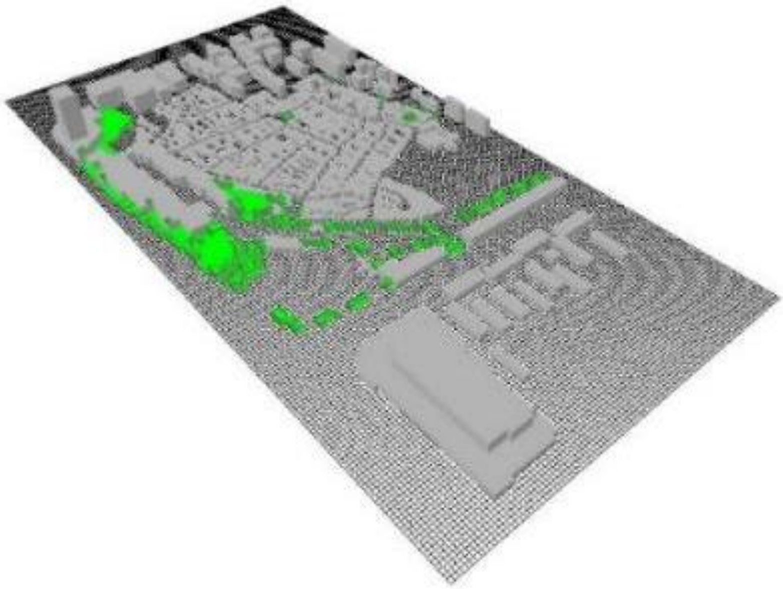

(a)

(b)

Figure. 5-4 The simulated model in ENVI-met (a) Perspective (b) Plan

About the vegetation, plant is not only symbolized as a porous media to solar insolation and wind, but are treated as a biological body which can be influenced by the evapotranspiration in the surrounding environment. As ENVI-met analyzes vegetation based on leaf area density (LAD) and leaf area index (LAI), Eq. 5-54 shows relationship between the two parameters [201]:

$$\mathrm{LAI} = \int_{0}^{h} \mathrm{LAD.z} \qquad (5-54)$$

h is height of the tree (m)
z is vertical grid size
LAI is the leaf area index
LAD is the leaf area density (m^2/m^3)

About the border tree in this block, a self-developed leaf area density folder was set for the measured tree [202], based on the field survey includes the fisheye image and the vertical configuration of the tree. According to the field survey, the local border tree is called the camphor tree (Figure. 5-5). The detailed data of the tree is added to ENVI-met plant database to fulfil the work (Figure. 5-6).

(a) (b)

Figure 5-5 (a) A typical image of *camphor tree* (b) Fisheye image of *camphor tree*

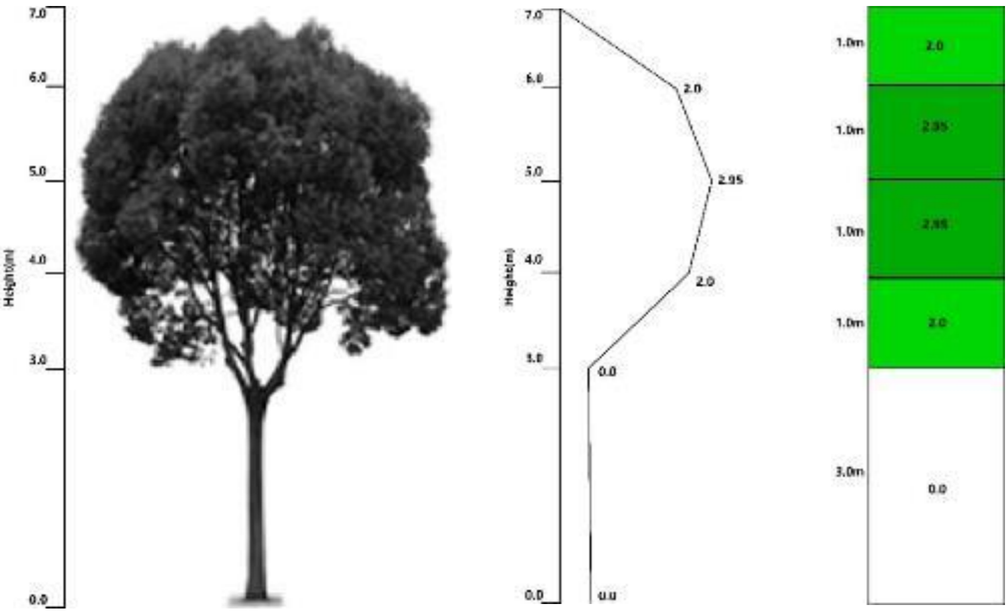

Figure 5-6 Schematic of the *camphor tree* database model for simulation

In addition, the measured SVF of different selected points was calculated by Rayman through fisheye images; meanwhile, using Google maps and on-site survey, we built a simulated model including artificial structure and shading devices in ENVI-met to calculate the simulated SVF. A comparison between the measured and simulated SVF was used to assure the accuracy of the built model and the final simulated results (Figure 37).

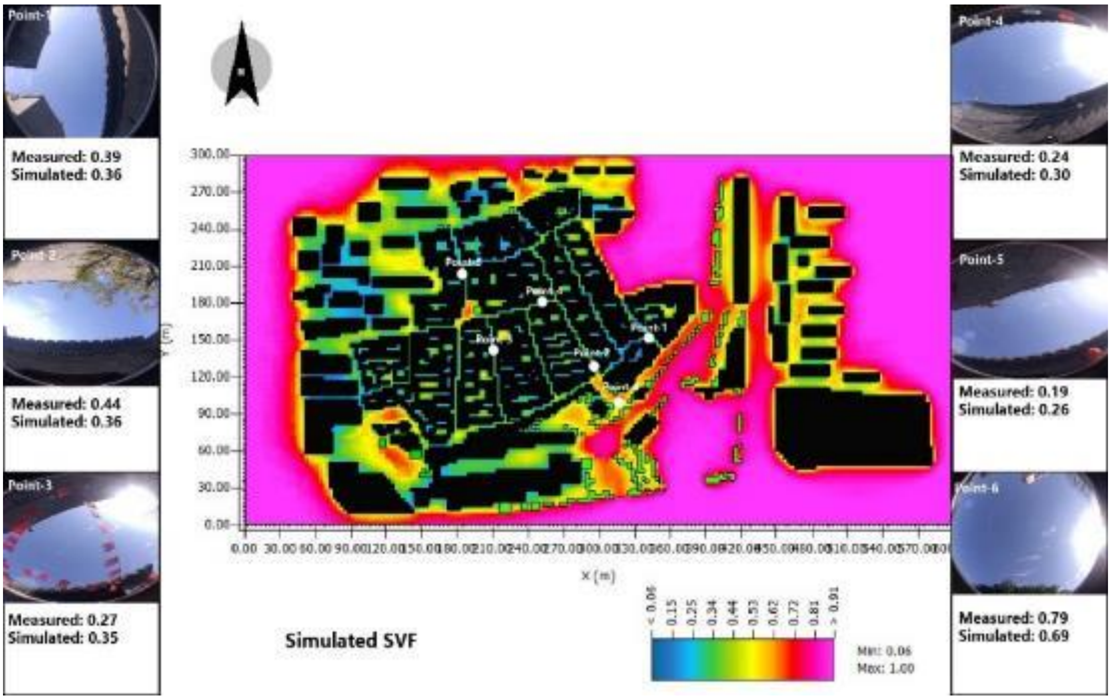

Figure 5-7 The correlation between the measured SVF and simulated SVF

5.9.2. The introduction of Tai Zhou Old block

About the 3D microclimate modelling system, Envi-met was selected as the preferred modelling tool, mainly due to its capability in the model foundation on the principles of computational fluid dynamics for modelling plant-surface-atmosphere interaction in complex environment with buildings of different shapes, height, the material of the street and the vegetation of different configuration. It can simulate with a high spatial and temporal resolution which supplies near-accurate modelling of micro-climatic parameter.

In this model, the buildings including shading devices and artificial structures are approximated to normal cubic, their sizes are configured according to the Google maps and the measurement survey. Envi-met has been widely applied in several studies. The accuracy of Envi-met results accepted by researchers. These results have shown the acceptable accuracy in different climatic model. The initial input data of the various meteorological elements used in the Envi-met simulation is shown in the Table. 5-5.

In this study, the whole simulation is 48 hours, starting from midnight 00:00, 28th, 2016 with a calculation of 1 min. The simulation results are output into an hour basis. We obtain the data at 1.5m high level. The detailed information of all the paving material is shown in Table. 6. The three-dimensional model is shown in Figure. 5-8.

The material of the buildings in the block is brick, and the material's color, emissivity and albedo is dark, 0.9 and 0.3. About the vegetation in the model, plant and

Table 5-5 Initial simulated data for Envi-met input

Data	Initial input value for Envi-met simulation
Temperature	38℃
Humidity	45％
Wind velocity	2.0m/s
Wind direction	145°
Main model area (x-grids, y-grids, z-grids)	110×180×20
Size of grid cells (meter) (x, y, z)	3×3×2

Table 5-6 Initial information for each selected point

Point	Color	Emissivity	Albedo
1,2,3,5,6	grey	0.92	0.40
4	dark	0.90	0.20

vegetation are not only symbolized as a porous media to solar insolation and wind, but are treated as a biological body which can be influenced by the evapotranspiration in the surrounding environment. As Envi-met analyzes vegetation based on leaf area density (LAD) and not leaf area identity (LAI), equation which shows relationship between the two parameters :

$$LAI = \int_{0}^{h} LAD.\,z \quad (1)$$

h is the height of the tree (m)
z is vertical grid size
LAI is the leaf area index

LAD is the leaf area density (m^2/m^3).The tree models are provided by Envi-met database. However, all modelling systems must be validated against field measurement to determine their ability in producing accurate outputs within the urban environment. Therefore field measurements were conducted in this study to validate the simulated results with the recorded data.

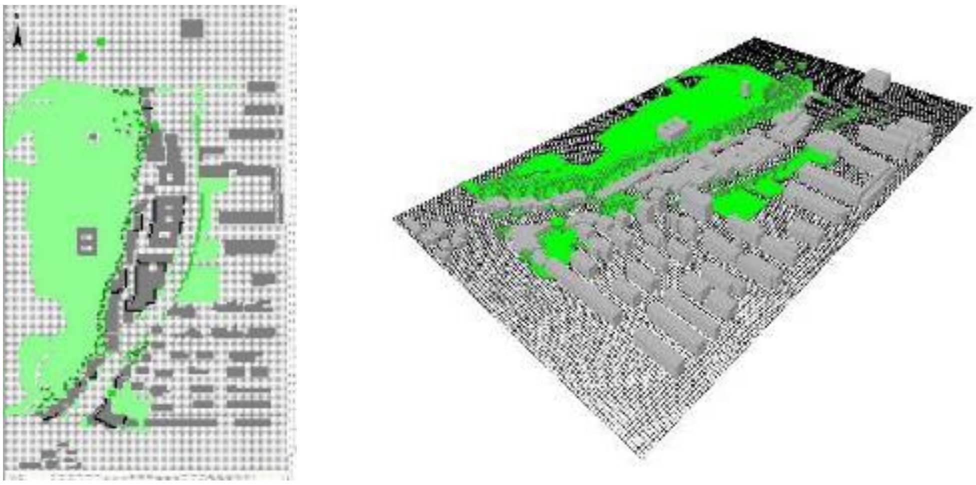

(a) (b)

Figure. 5-8 The simulated model in Envi-met (a) Plan (b) Perspective

The fisheye image at each selected sites are taken using a fisheye lens and then input into the software (Envi-met) to calculate the simulated SVF (Figure. 5-9).

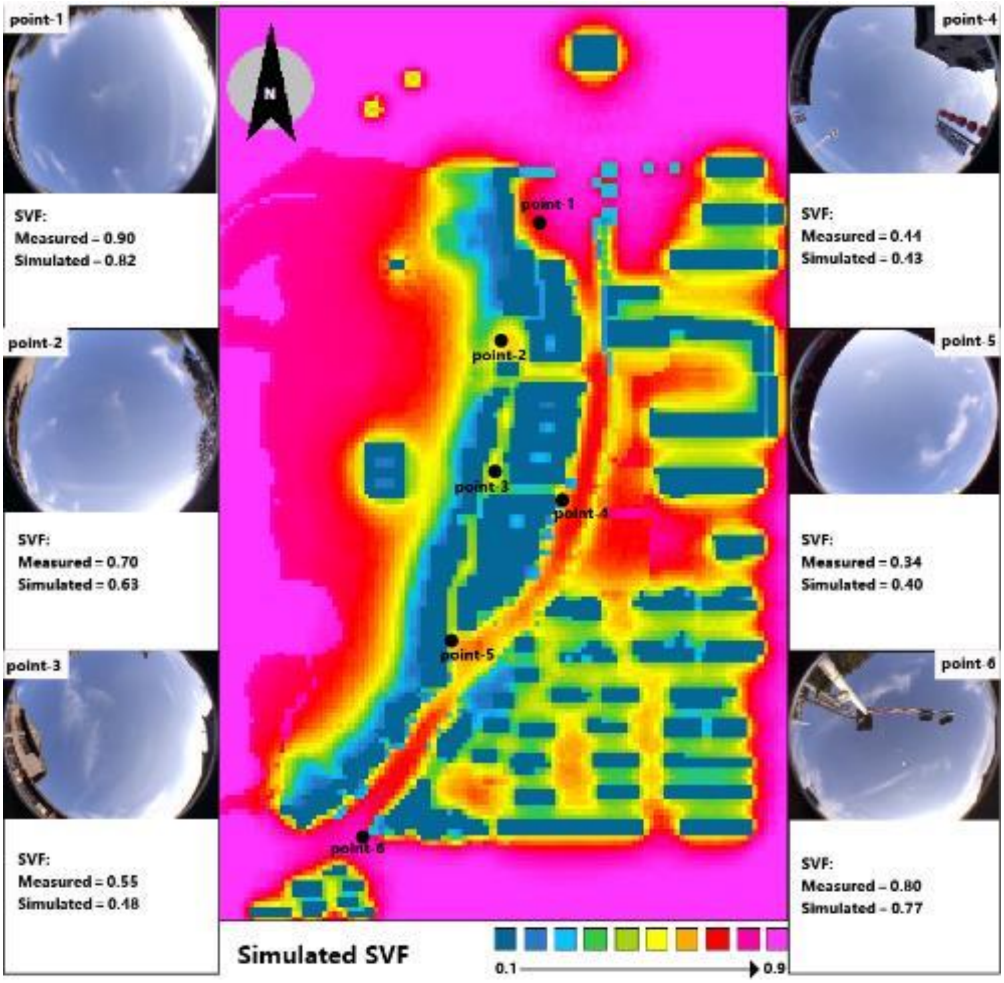

Figure 5-9 The correlation between the measured SVF and simulated SVF

5.9.3. The introduction of Ling Nan Tian Di block

As mentioned above, the microclimatic model was used in the software ENVI-met, mainly because the capability in the foundation of model on the theory of the computational fluid dynamics (CFD) for building plant-surface-atmosphere interaction about outdoor environment with different building, various pavement material and various vegetation with different configurations. The accuracy of ENVI-met has been assessed in many previous studies by comparing the simulated result to measured result [41-44, 52], these have proved that ENVI-met can be able to simulate outdoor microclimate in different climates. The vegetation in ENVI-met can't only be designed as a porous media to solar radiation and incoming wind, but also is symbolized as a biological body which interacts with outdoor microclimate through evapotranspiration.

As we all know, ENVI-met builds the vegetation based on the leaf area density (LAD) and the leaf area index (LAI), following equation explains relationship between the two factors:

$$\mathrm{LAI} = \int_0^h \mathrm{LAD.\,z} \qquad (2)$$

h means the height of the tree (m)
z means the vertical grid size

In the aspect of energy absorption, the distribution of leaf density and the height of the plant are estimated in the simulation to illustrate the two different kinds of solar radiation. A folder about leaf area density of this planted border tree in this zone is set for the measured tree, based on the on-site measurement including the fish eye images and the vertical configurations. The images were then put into software Hemisfer for calculating the LAD and LAI. According to the on-site measurement, the total simulation time is 24 hours, starting from 0:00am, Jul.24th, 2016 with a calculation of each one minute. Also, the simulated results are output into each one hour basis.

Figure. 5-10 Vertical configuration of the tree (Bischofia Javanica)

Table. 5-7 Initial simulated data for simulation

Input for simulation	Value
Starting time	0:00, July 24th, 2016
Total simulation time	24h
Wind speed in 10m (m/s)	1.8
Wind direction	145
Initial air temperature (℃)	37
Relative humidity (%)	55
Roughness length	0.1
No. of x grid	200
No. of y grid	100
No. of z grid	30
Dimension of the grid in dx (m)	3
Dimension of the grid in dy (m)	3
Dimension of the grid in dz (m)	3
Albedo ground	0.4
Albedo roof	0.2
Albedo wall	0.3

Total	Single-story building	Two-story building	Three-story building	Tree	Grass	Pavement Material
100%	11%	20.3%	35%	12.5%	3.0%	21.2%

Figure. 5-11 various types of different coverage ratio of base case

5.10. Summary

This chapter focuses on the applicability of the microclimate simulation software ENVI-met in hot and humid climates:

1) Inductive analysis software basic structure, boundary conditions, input and output, and when performing microclimate simulation limitation. Influenced by the development background, the current use of ENVI-met is concentrated in the mid-high latitudes of the cold climate. District, but less used in hot low latitudes, and no use of ENVI-met in hot and humid climates System verification report. In addition, due to limitations in input conditions and control equations, the software cannot be input. At the time of solar radiation, it is also impossible to dynamically simulate the wind environment.

2) Theoretical verification and experimental calibration (V&V) of ENVI-met in hot and humid climates. Combining the actual conditions of the hot and humid climate, some software features of ENVI-met, such as boundary condition type, vertical. The grid form, etc. were verified, and the simulation results were checked by examples.

3) The results of theoretical verification show that the optimal ENVI-met boundary conditions are affected by the characteristics of hot and humid climate. Types for temperature and humidity simulations with open boundaries, turbulent simulations with closed boundaries; as simulated cases at height. Equidistant grid and different scaling ratios when the simulated area is greater than twice the highest building in the area.The simulation results obtained by the two vertical mesh types of the telescopic mesh, regardless of the numerical or vertical height distribution.The rules are similar.

4) Using the third chapter of the experimental calibration table for the summer outdoor thermal environment test results of a typical residential community in Taizhou. Using macroscopic meteorological observation data as a boundary condition, ENVI-met can simulate the micro-study of residential areas in hot and humid climates. The environmental condition, within the instrument error range, the numerical value, spatial distribution law and time distribution law of the simulation results. The measured

values are basically consistent: when the simulation is full sunny, the calculation results of the software agree well with the measured values, and the temperature and humidity are high. The temporal variation of the degree and the horizontal distribution are similar; the weather changes dramatically with cloudy or showery days, and the simulation results. It is quite different from the measured value.

This chapter takes Tai Zhou and Fo Shan, typical representative cities of hot and humid climate, as an example, combined with the outdoor thermal environment on-site analysis of Chapter 3. Therefore, the systematic theoretical test and experimental check and sensitivity analysis of ENVI-met software were obtained. The best boundary condition type, vertical mesh shape for the software when performing microenvironment simulation in a hot and humid climate zone Types, as well as greening types and underlying surface structures that can be used for landscape design quantitative analysis.

Chapter-6.

Thermal environment of all the blocks

6. Thermal environment of all the blocks

This chapter focuses on how to implement a pedestrian block by coupling computer numerical simulation programs with different functions. Simulation and evaluation of external thermal environment safety, comfort and building energy consumption. First, introduce the hot ring of residential groups. The overall idea of coupling simulation of environment and building energy, and put forward requirements for extreme day and typical daily meteorological data; The hot climate represents the city of Guangzhou as an example, which summarizes and summarizes the selection of simulated meteorological data according to different simulation targets. Process; in addition, combined with the microclimate simulation software ENVI-met output and energy simulation software EQUEST. The input requirements were confirmed and analyzed for typical meteorological days and typical meteorological years of microclimate. The coupled dynamic simulation method proposed in this chapter will be used as the basic analysis of the quantitative analysis of the landscape design factor in Chapter VI. Method for qualitative and quantitative evaluation of landscape design from three aspects: thermal safety, thermal comfort and group building energy consumption and its combination [203-205].

6.1. Dynamic Simulation and Evaluation of Thermal Environment

As summarized in the second chapter of the literature review and the third chapter of the experimental analysis, the current hot ring for pedestrian block. The environmental assessment system is too singular, mostly limited to one aspect of thermal comfort and thermal safety. The organic link between the methods. In the simulation of the impact of landscape design on the thermal environment of residential groups, too much emphasis. The relationship between greening environmental effects and outdoor thermal comfort, neglecting the landscape greening system for building energy consumption and outdoor thermal safety.

This paper draws on the method of building comprehensive performance simulation and extends it to residential groups to achieve outdoor bundled simulation of thermal safety, thermal comfort and building energy consumption.

This coupled simulation system requires the integration of values for different functions. Analyze software for different simulation purposes, the most important of which is to couple the input and output of these software so that the output of one kind of software is used by another software, for example, the hydrodynamic simulation software is applied to the microclimate temperature and humidity. The results of the field simulation are used as input conditions for the energy simulation software. In order to be soft in fluid mechanics. In the case of simulating the simulation of hot moisture, long and short wave radiation and air flow for different residential groups, it is necessary to input the topographical data such as the layout of the building and the layout of the landscape structure, and define the surface type and roughness of the underlying surface. Nature and coverage, solar elevation, azimuth and geographical factors such as sunshine and sun, as well as external macro boundary conditions such as wind speed, temperature and humidity, and solar radiation. Among them, the macro weather conditions are mainly from urban gas observations from the station, or typical meteorological year (TMY/TRY) data developed specifically for architectural

simulation. According to the World Meteorological Organization (WMO), the National Ocean and the United States
National Oceanic and Atmospheric Administration (NOAA), National Meteorological Administration [206-210].

Uniform provisions of the meteorological observation authority, all urban meteorological stations must be in the same observation site environment, instrument layout. Meteorological elements are observed and recorded in terms of accuracy, accuracy and level. The requirement for the level is: wind speed 10 meters above the ground, the temperature and relative humidity are 1.5 meters above the ground; in addition, solar radiation, wind speed, wind direction observation. There must be no obstruction around the instrument. In order to facilitate the acquisition of meteorological elements in various places, the boundary conditions of fluid mechanics software are unified. One uses observations that meet the above requirements. Since the typical meteorological year data is based on suburban or airport city weather stations Long-term observations of historical regressions, usually used to represent large-scale ranges (such as a city or a number of cities). The climatic environment of the administrative districts will be collectively referred to as the macro-climate typical weather year (Macro TMY), the macro-meteorological data is the boundary condition, and the microclimate calculation results obtained by simulating different residential groups through CFD software.

Through the simulation calculation of the fluid mechanics simulation software, the weather elements of the microclimate of the residential group are output (wind, temperature and humidity) time, spatial distribution of the degree, radiation, etc., and based on the prediction results combined with human clothing, activity status [211-213]. In the specific case, the thermal safety and thermal comfort indicators are calculated separately. At this point, the outdoor thermal environment of the residential group was simulated. Cheng, enter the simulation stage of building energy consumption. When building energy simulation, you need to enter in the corresponding simulation software: the phase of each building in the pedestrian block. And select the appropriate typical weather year (TMY). An important goal of this coupled simulation system is to evaluate. The internal microclimate of the group and the corresponding building energy consumption caused by different landscape design factors and layout methods Chemical. Therefore, the meteorological data used by the energy simulation software should not be the Macro TMY. It should be the output of Micro TMY, the fluid dynamics simulation software. After the whole year Energy consumption simulation can get the hourly heating and air conditioning load of the building group and the monthly electricity consumption. These two values can be used as micro Climate evaluation indicators for building energy efficiency [214].

This article will couple the special software for microclimate simulation ENVI-met according to the heat. Three aspects of total, thermal comfort and energy saving, qualitative evaluation of the landscape design factors in the hot and humid climate area Body influence. Among them, according to the theoretical verification of Chapter 4, the comparative analysis of experimental data and the conclusion of sensitivity analysis, ENVI-met's best convergence grid size, simulation time step, etc. are used for subsequent simulation calculations to ensure all cases the results of the simulations all have the same or similar convergence accuracy. According to the purpose of the simulation, the weather types in the map can be divided into two categories: one is the coldest and the hottest. Extreme Condition, by analyzing the measured data of the obsolete weather station, according to the wind speed is not satisfied 20%, other meteorological elements do not meet 1% for selection, used as meteorological boundary conditions for the thermal climate within the group microclimate. Full-scale evaluation; the other is typical meteorological data, which represents the overall characteristics of a region's ageing climate, used for the group. The internal thermal comfort evaluation of the group and the simulation analysis of building energy consumption [215]. In order to simulate the annual building energy consumption of residential groups, it is necessary to obtain micro-climate hourly weather data. Ideal and accurate the exact method is through Microclimatic Computational Fluid Dynamic, Micro CFD) 8760 hours a year to simulate different landscape design plans, and combine the results of the simulation into the required gas. Like the data format. However, this method takes a long time to get all the simulation results, which is set in the landscape. The metering phase cannot be achieved, and there is no guarantee that each result will achieve the same convergence accuracy. Therefore, it needs to be the macroscopic typical meteorological data as a boundary condition is appropriately simplified by examining the distribution rules of meteorological elements. Law, choose a typical meteorological day from each of the Typical Meteorological Month (TMM) (Macro TMD). Distribution frequency and standard of meteorological elements such as solar radiation, temperature and humidity, and wind speed on a typical meteorological day continuity and associated similarities are similar to typical meteorological months. After obtaining the Macro TMD, the meteorological elements are used as the boundary conditions of ENVI-met. The simulation was performed 24 hours a day, and the simulation results at this time were Micro TMD.

Due to only meteorological data, energy simulation software can not simulate the annual building energy consumption, so the interpolation method is needed. Method and appropriate treatment of micro-climate typical weather day (Micro TMD) to generate microclimate typical meteorological year (Micro TMY). So far, microclimate fluid force has been achieved through statistical calculations of meteorological data and CFD simulation results. Learning simulation software ENVI-met for simulation.

6.2. Typical weather day

The process and calculation steps for developing a typical meteorological day in typical meteorological data; the longest observation time and the latest data source. The China Standard Meteorological Data (CSWD) is an example of a typical meteorological day in Guangzhou, where the hot and humid climate represents the city. Input values in the microclimate simulation software ENVI-met; finally analyzed the limits of the solar radiation input values due to software System, which causes the difference between the boundary conditions of the simulated area and the actual TMD.

The main role of the typical weather day (Macro TMD) is two, one is through TMD. The typical meteorological year is divided into several days to reduce the calculation time of microclimate simulation; the second is to simulate by TMD and

CFD. The software is combined to obtain a typical weather day for microclimates, which is used for outdoor thermal comfort evaluation and group energy consumption simulation.

At present, many organizations around the world have developed meteorological data for energy simulation, such as the national sea of the United States National Oceanic and Atmospheric Administration (NOAA), the state can re National Renewable Energy Laboratory (NREL) and Lawrence Berkeley Lawrence Berkeley National Laboratory (LBNL), etc. These meteorological data are widely used. In the simulation of building energy consumption, the thermal performance of the building envelope is evaluated according to the requirements of different domestic standards. Evaluation of performance indicators.

1) Chinese Standard Weather Data (CSWD) [216]

CSWD was jointly developed by the Department of Building Technology of Tsinghua University and the National Meteorological Administration of China, and analyzed domestically. Timely weather data for 270 cities from 1971 to 2003. The generated database can provide design outdoor air

Like parameters, typical meteorological year, year-round meteorological parameters, high devaluation design, typical annual meteorological parameters, etc., as well as wet and dry. The maximum and minimum values of the ball temperature and solar radiation from month to month.

2) Chinese Typical Year Weather (CTYW) [217]

The CTYW database is taught by Professor Zhang Qingyuan of the University of Tsukuba, Japan and Joe of the Lawrence Berkeley National Laboratory.

Huang cooperated in development. The main source of data for this database is the observations provided by the National Meteorological Data Center.

A total of 57 cities in China from 1982 to 1997 were analyzed.

3) Energy consumption calculations (International Weather for Energy Calculations, IWEC) [218]

IWEC was developed based on the DATSAV3 database of the National Weather Data Center of the United States. This database

Contains 18 years of hourly weather observations, but does not include solar radiation data. Therefore, it needs to be based on the sun and the earth.

Estimate other geometric parameters such as geometric positional relationship and cloudiness.

4) Chinese Typical Meteorological Year version 2 (Chinese Typical Meteorological Year version 2, China-TMY2) [219]

China-TMY2 is funded by the China-Architecture Science and Technology.The Institute hosted the development. This data provides meteorological data for 30 major cities and can be applied to both TRANSYS and DOE-2.

5) USA Typical Meteorological Year (US-TMY) [220]

US-TMY is funded by the US Department of Energy and is supported by the National Oceanic and Atmospheric Commission (NOAA) and the State Co-hosted by the Key Laboratory of Renewable Energy (NREL) for DOE2.1e and above. The database mentions. The typical meteorological year provided includes not only major cities in the United States but also some Chinese cities. In order to reflect the impact of urbanization on urban meteorology, the analysis of this paper uses the longest observation time and data source of the latest China Standard Weather Data (CSWD).

New construction by computer energy consumption simulation software. The building will conduct a year-by-year simulation to determine that the heating and air conditioning load can meet the corresponding performance index requirements. But this These typical meteorological data are located in cities over the past three decades (mainly from the 1970s to the beginning of the 21st century).

Based on the hourly value observed by airports and weather stations in the outer suburbs, calculated by data analysis and statistical methods. It can only represent the long-term stable climate change level of the city, but it cannot reflect the microclimate status and day within the city. A serious urban heat island phenomenon. Using these typical meteorological years data for energy simulation, the results may deviate. In reality, it is impossible to accurately evaluate the energy saving effect caused by the improvement of microclimate.

China covers a very large territory with various climate zones. According to the national standard Thermal Design Code for Civil Building (GB50176-93) [221], five climate zones are found: hot-summer and cold-winter areas, hot-summer and warm-winter areas, cold areas, severe cold areas, and temperate areas (Figure 6-1).

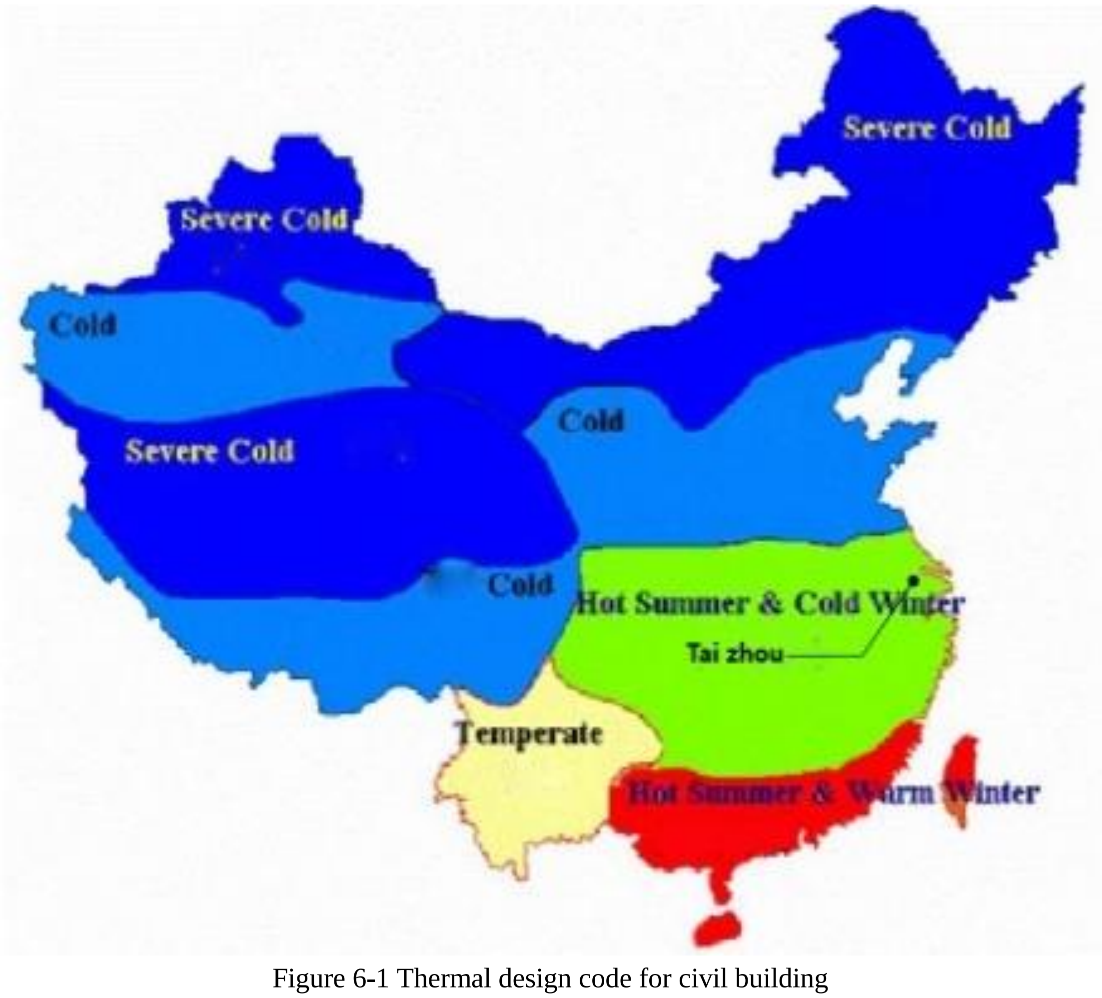

Figure 6-1 Thermal design code for civil building

6.3. The simulated result

6.3.1. The simulated result of Dao He Old block

According to the characteristics of the numerical simulation of ENVI-met software, the curve of air temperature is shown in Figure. 6-2. In these two figures, the change of simulated data is similar to the measured data.

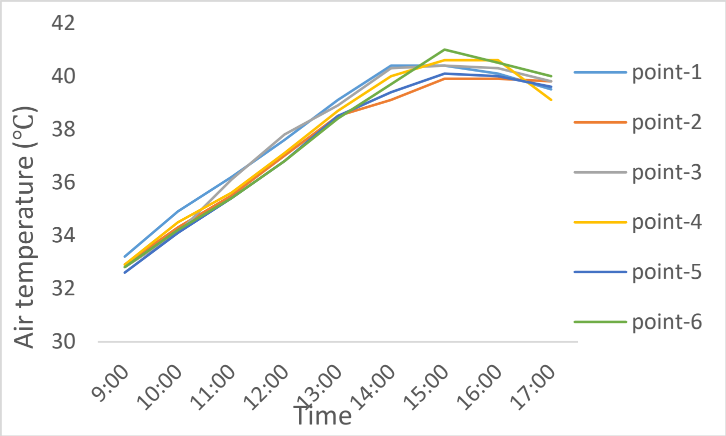

(a)

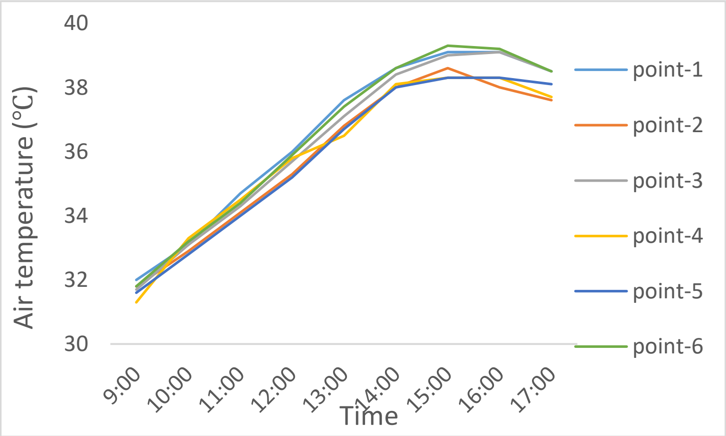

(b)

Figure 6-2 The simulated air temperature in two measured days

The simulated relative humidity is shown in Figure. 6-3.

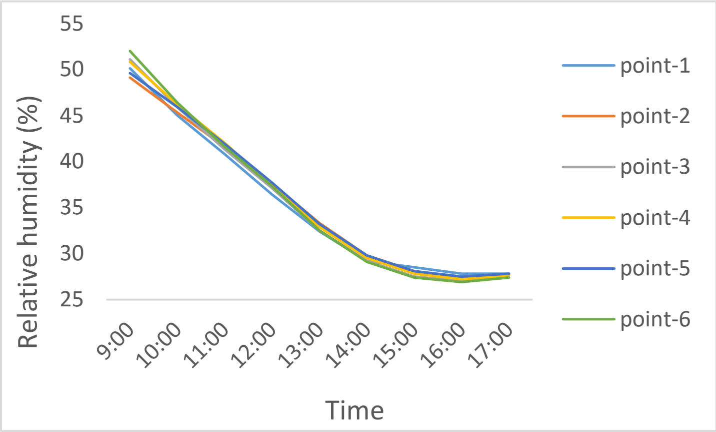

(a)

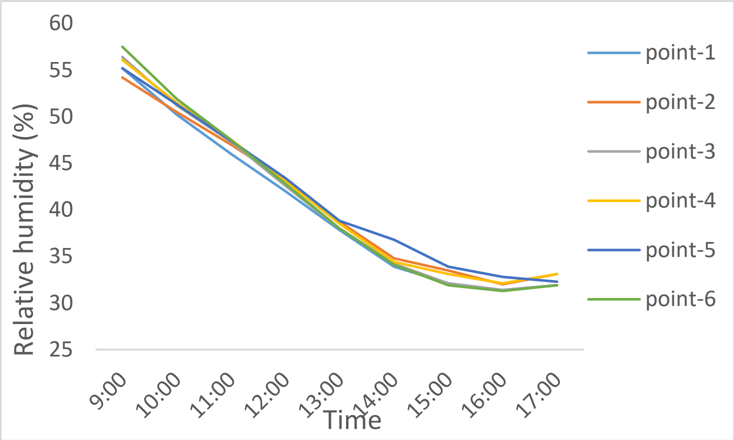

(b)

Figure 6-3 The simulated relative humidity in two measured days

The final result of simulated relative humidity also has a high similarity with the measured data.

6.3.2. The simulated result of Tai Zhou Old Block

Like the measured data of The Tai Zhou Old Block, the simulated is very similar to the measured data at daytime. Figure 6-4 shows the detailed information about the simulated data of air temperature.

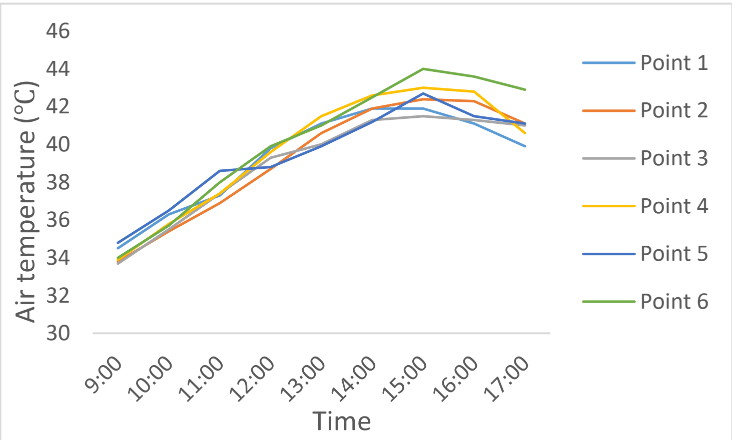

(a)

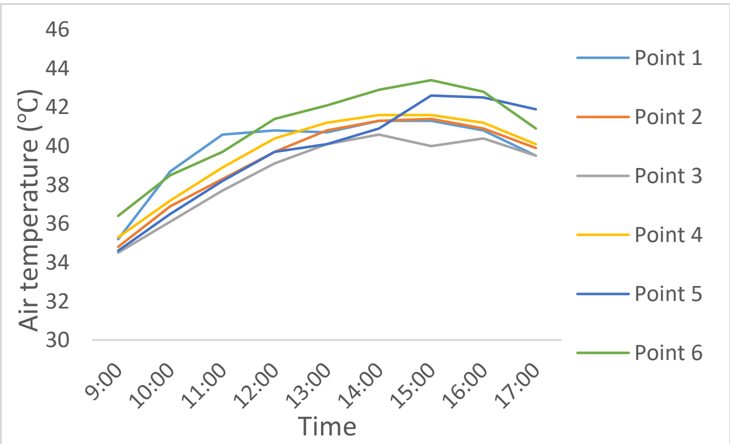

(b)

Figure 6-4 The simulated air temperature in two measured days

The simulated relative humidity is shown in Figure 6-5. The final result show that the simulated result has a high accuracy in simulating result.

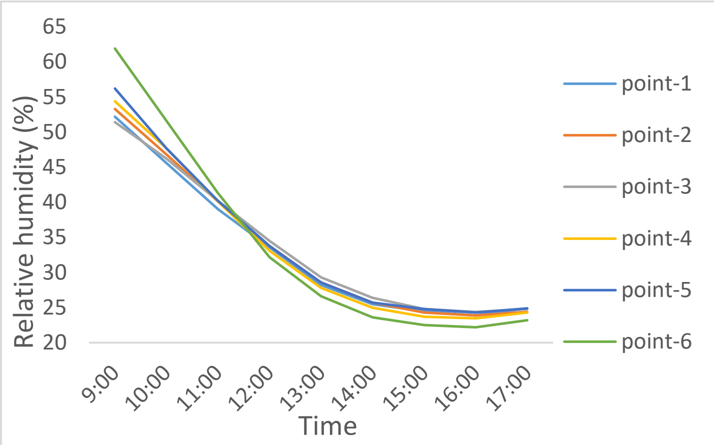

(a)

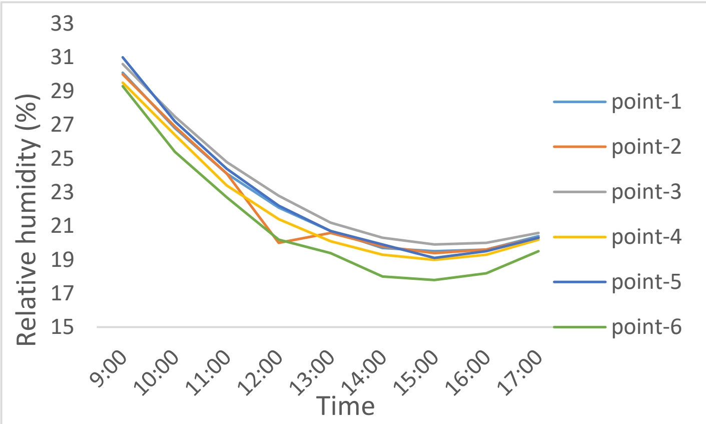

(b)

Figure 6-5 The simulated relative humidity in two measured days

6.3.3 The simulated result of Ling Nan Tian Di Block

Different from the above mentioned two cases, the measurement in Ling Nan Tian Di Block is the single day (Figure 6-6). The final result is shown in Figure. 6-6 and Figure. 6-7.

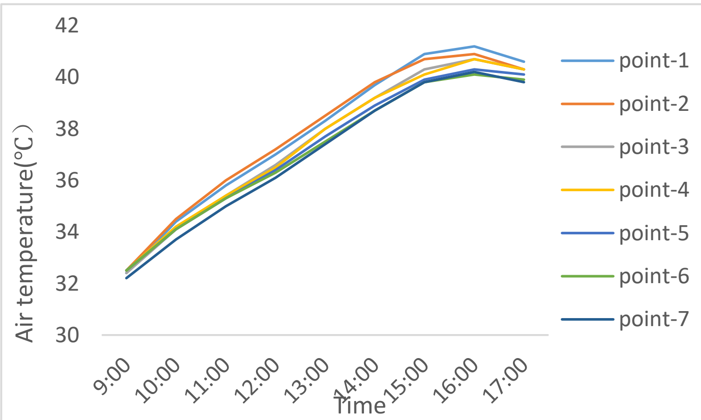

Figure 6-6 The air temperature in measured day

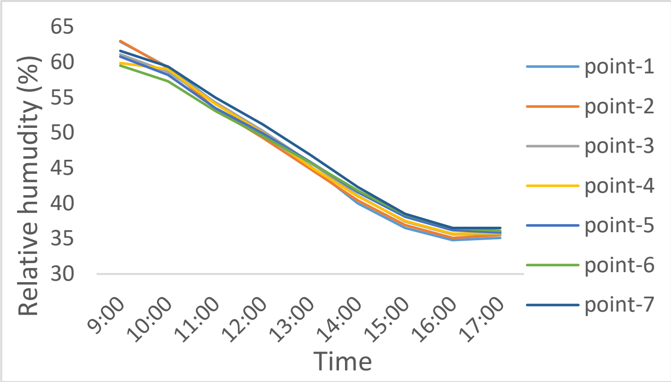

Figure 6-7 The relative humidity in measured day

6.4. The validation between measured and simulated data

To evaluate the deviation between the measured result and the simulated result, the root-mean-square error (RMSE) was used in this study. The index RMSE is a frequently used measure of the differences between values predicted by a model or an estimator and the values observed, representing the square root of the second sample moment of the differences between the predicted values and the observed values, which is a significant factor for the calculation of error [222, 223]. If the RMSE reaches or approaches zero, the most accurate model is achieved. Lower RMSE values mean that the simulated results are within the measured value. In our study, each RMSE is calculated through nine sets of data from 9:00am to 5:00pm.

6.4.1. The validation of Dao He Old block

As is shown in Figure.6-8, point-3 has the highest error in the daytime, which can reach 2.85℃. This error can be attributed to the position of the record machine, due to the tourists' safety, the data machine isn't fixed at the middle of the street and instead fixed along the sidewalk. In addition, the accuracy of the relative humidity is better than air temperature. Except of the index RMSE, analyzing correlation between simulated and measured data is another step to evaluate the numerical simulation. To test the validity of the simulated model, the measured data are fitted with the simulated by liner regression. A good liner regression obtained is shown in Figure. 6-9 and Figure. 6-10, where R2 value for air temperature of this region ranges from 0.75 to 0.9578, while these for relative humidity are within 0.7518 and 0.9813. The deviation between simulated and measured data may cause by anthropogenic heat from humans in reality. These results are similar or even smaller than previous studies, the final liner regression values proves that the ENVI-met is a valuable software to fulfil future research in this study.

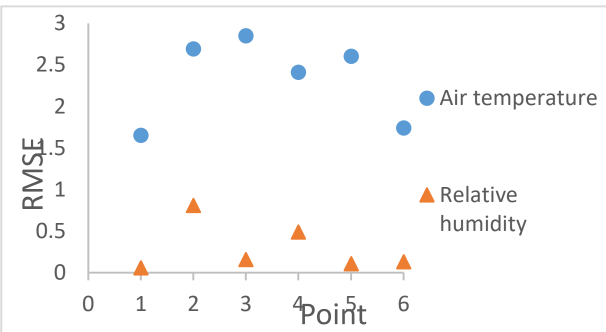

Figure 6-8 The RMSE between measured data

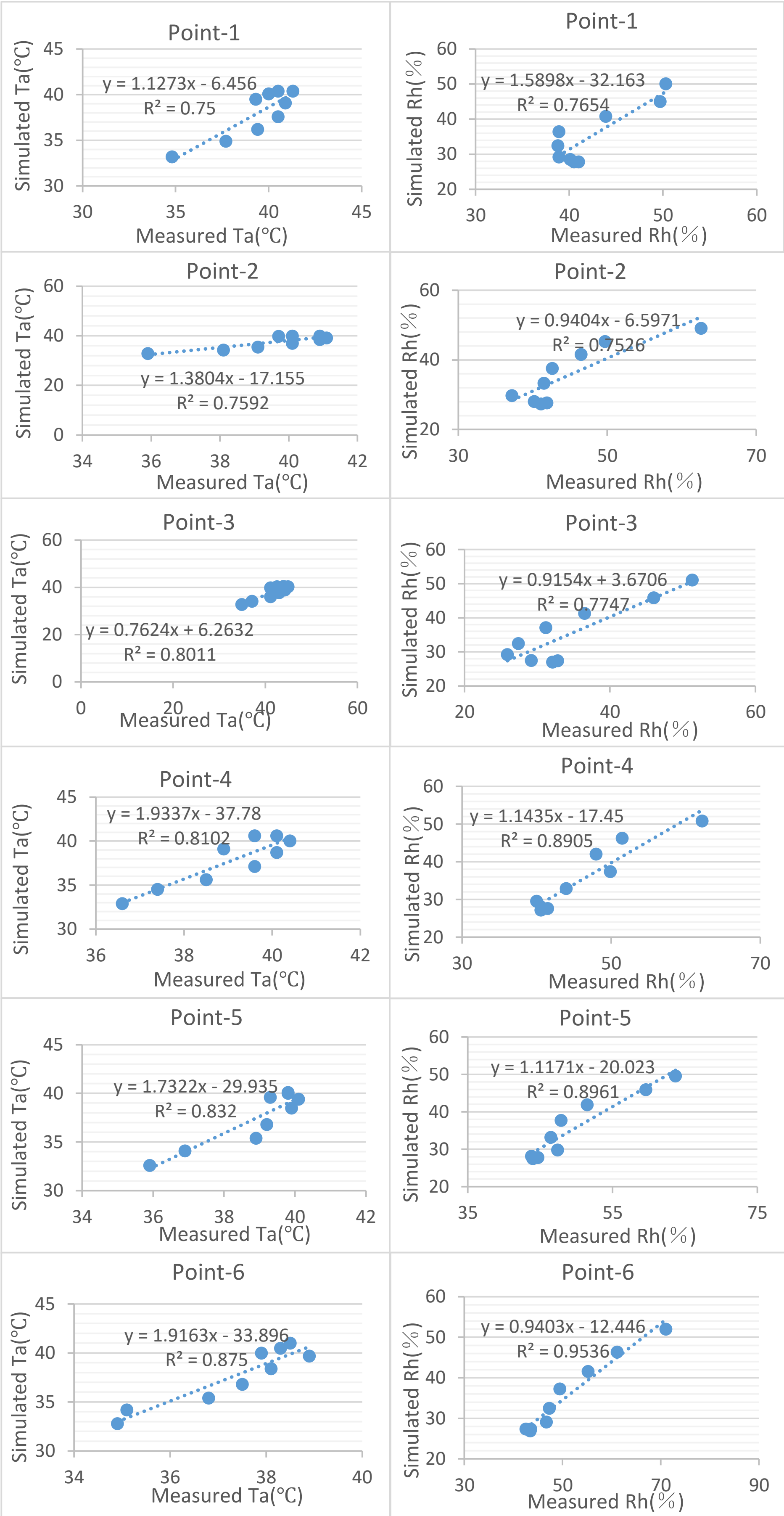

Figure 6-9 The correlation between the simulated data and measured data on Jul. 30th

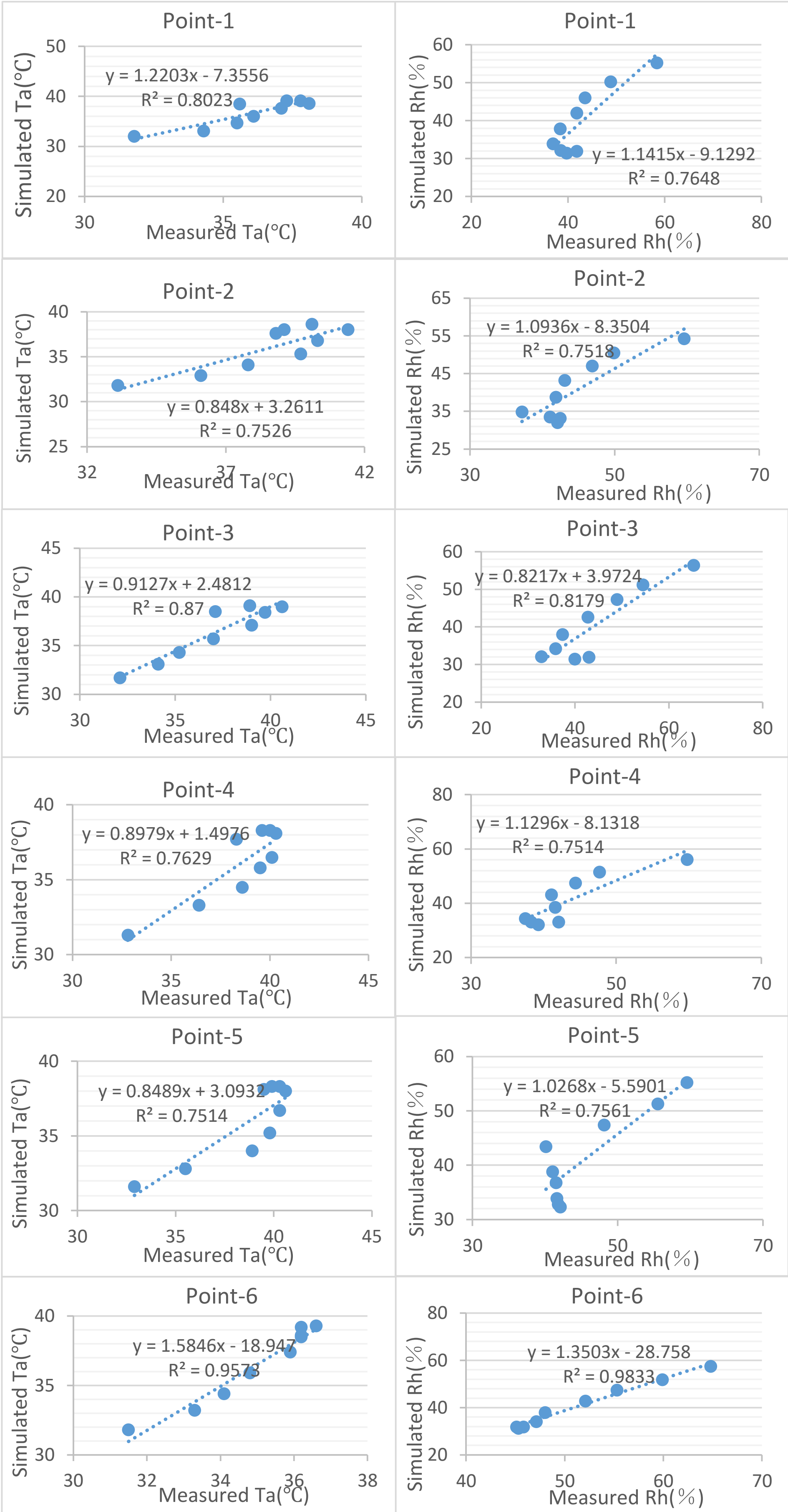

Figure 6-10 The correlation between the simulated data and measured data on Jul. 31th

6.4.2. The validation of Tai Zhou Old block

In order to quantify the gap between measured data and simulated data, the RMSE is calculated in each point, which is a significant factor for calculating the error and also has been widely used in previous studies. The most accurate model can be achieved when RMSE approaches zero, in addition, lower RMSE value shows that most of the variations are all under the observed value. Figure. 6-11 summarizes that the RMSE values for the two factors between simulated data and measured data. Point-5 has the highest error in Ta , which can be attributed to the location of the data logger, due to the safety reasons, the loggers can't be fixed in the middle of the street and instead are fixed at the roadside. Other small deviations for the three factors are probably caused by anthropogenic heating from human and other machines, which are similar or even less significant than the previous studies. The result of liner regression values shows that the ENVI-met is a reliable tool to simulate outdoor environment for this pedestrian block. To evaluate the accuracy of the simulating model, the measured u_a , T_a and R_h in this site are fitted with the simulated data by liner regression (Figure.6-12 and 6-13). Where R^2 values between the measured u_a and simulated u_a ranges from 0.7724 to 0.9424, T_a ranges from 0.741 to 0.9582, R_h are within 0.7469 and 0.9693.

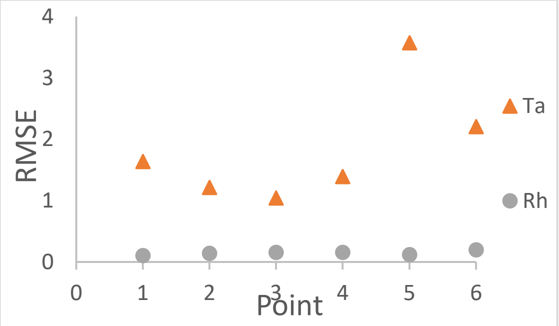

Figure 6-11 The RMSE between measured data

6.4.3. The validation of Ling Nan Tian Di block

Figure. 6-14 shows that the RMSE values between the measured and simulated air temperature, relative humidity. Point-4 has the highest error in the daytime, which can reach 4.6℃ at daytime. In addition, the accuracy of the relative humidity is better than air temperature. Except of index RMSE, analyzing the regression between measured and simulated data is another step to evaluate the simulated model. A good liner regression obtained is shown in Figure. 6-15, where R2 value for air temperature of this region ranges from 0.7544 to 0.9847, these for relative humidity are within 0.7664 and 0.9813.

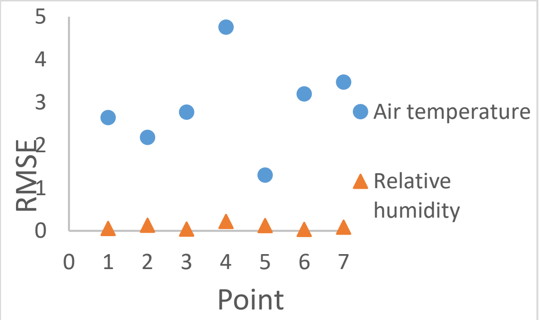

Figure 6-14 The RMSE between measured data

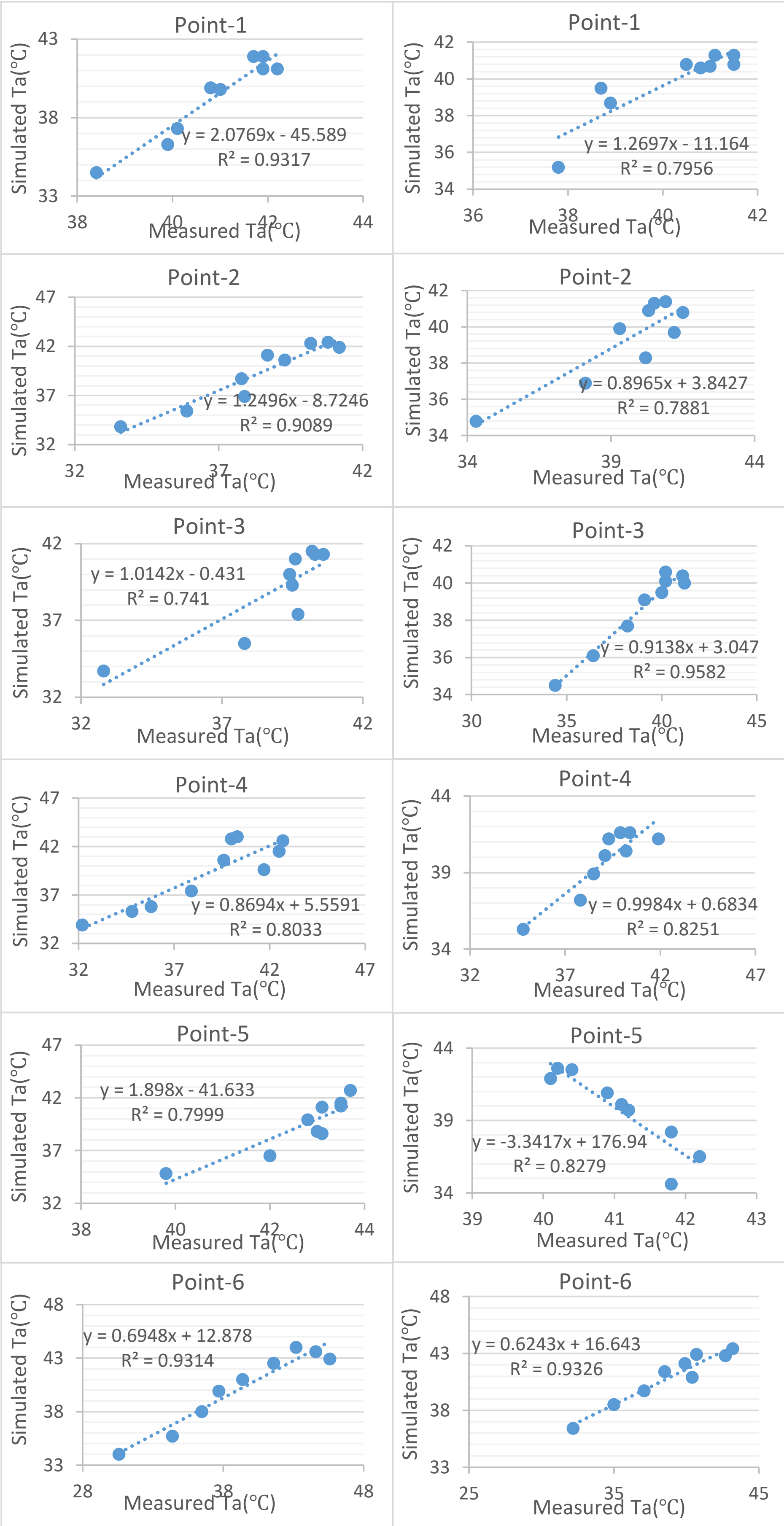

Figure. 6-12 The correlation between the simulated and measured data in two measured days

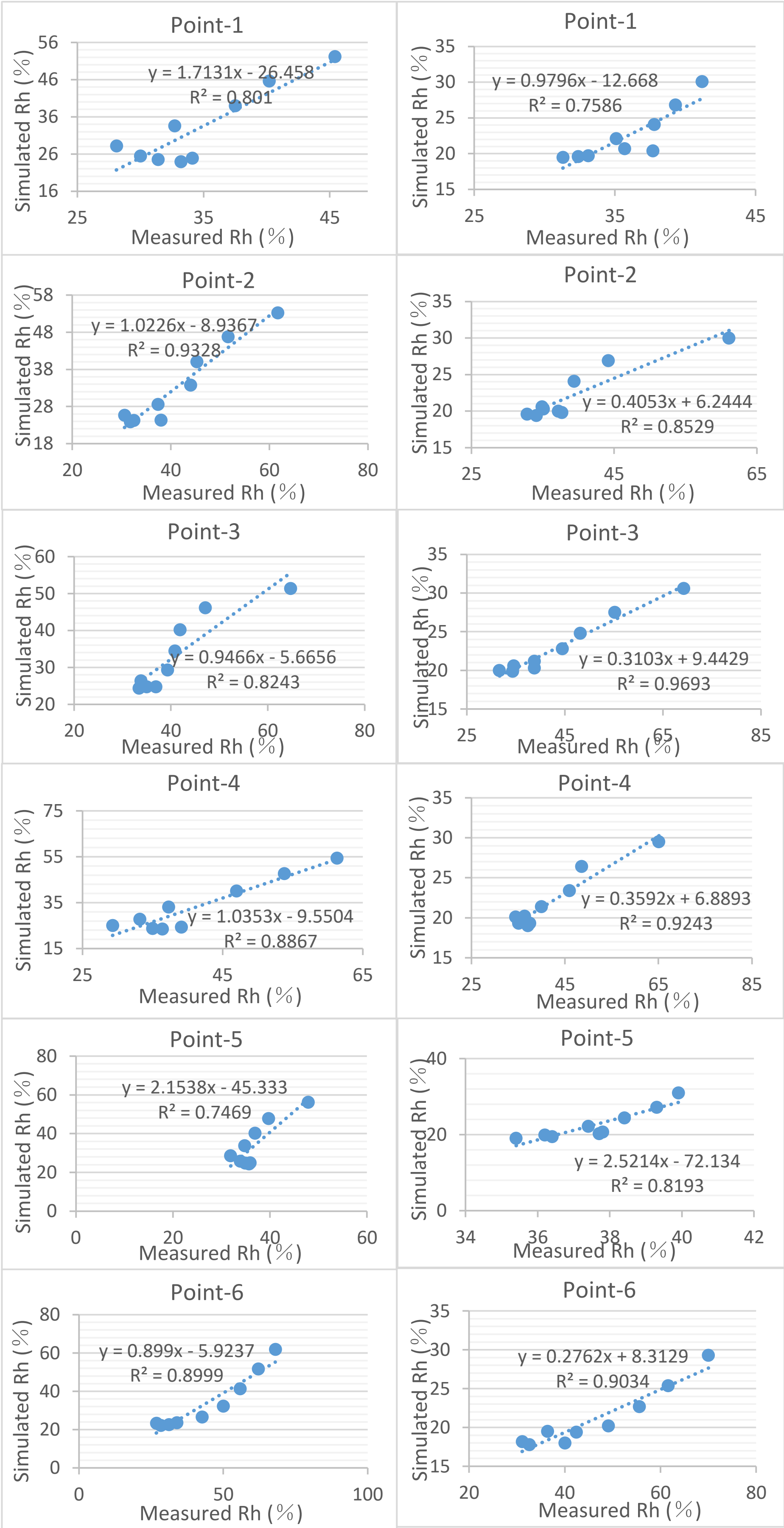

Figure. 6-13 The correlation between the simulated and measured data in measured days

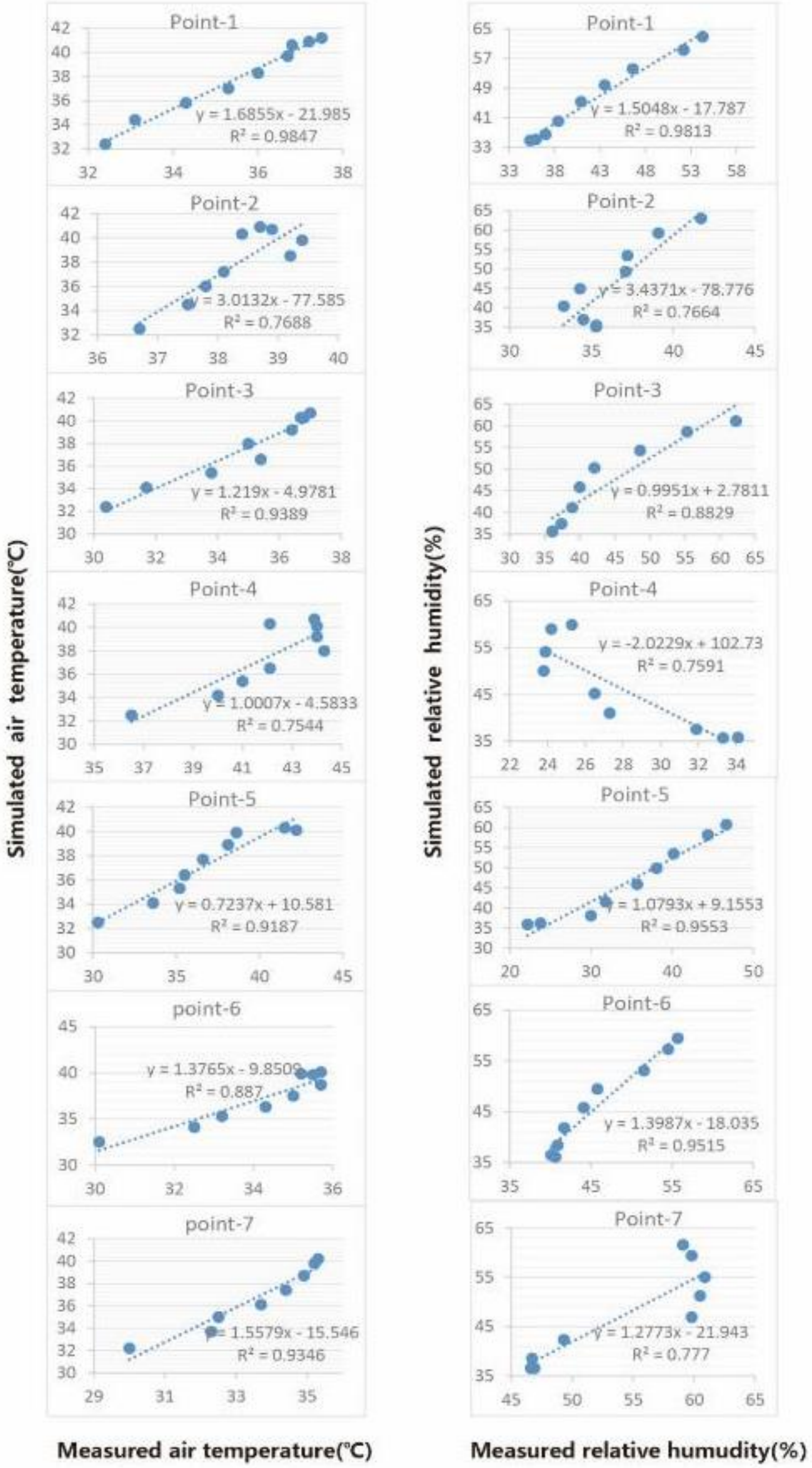

Figure. 6-15 The correlation between the simulated and measured data in the measured day

6.5. The humans' thermal sensation

The necessary parameters for calculation is wind speed, air temperature, relative humidity, mean radiant temperature, humans' clothing and activity. Simulation can supplement measurement on occasions when instrumentation is lacking, many studies have used this method to finish research [228-230]. As mentioned above, there are two climatic zones in our study. Weiwei Liu provides the humans' thermal sensation classification for the people who live in hot-summer and cold-winter region by collecting microclimatic data and questionnaire survey upon local habitants [231] (Table. 6-1). Also, the thermal sensation in hot-summer and warm-winter area is shown in Table 6-2.

Table. 6-1 The distribution of humans' thermal sensation in hot-summer and cold-winter area [231]

Thermal sensation	PET(℃)
Very Cold	-4＜
Cold	-4 ~ 3
Cool	3 ~ 11
Slightly Cool	11 ~ 19
Neutral	19 ~ 26
Slightly Warm	26 ~ 34
Warm	34 ~ 42
Hot	42 ~ 49
Very Hot	＞49

Table. 6-2 Thermal sensation of hot-summer and warm-winter climate region [232]

Thermal sensation	PET(℃)
Very Cold	13＜
Cold	13 ~ 17
Cool	17 ~ 21
Slightly Cool	21 ~ 25
Neutral	25 ~ 29
Slightly Warm	29 ~ 33
Warm	33 ~ 37
Hot	37 ~ 41
Very Hot	＞41

6.5.1. The PET of Dao He Old block

In this study, we choose the hottest day (30th) for the calculation of PET values, according to the simulated results of ENVI-met, the PET values of whole region in the two measured days are shown from Figure 6-16. All the simulated results are shown in appendix-1.

6.5.2. The PET of Tai Zhou Old block

Similar to the PET in Dao He Old block, the PET of existing scenario of Tai Zhou Old block is shown in Figure 6-12. Nearly, after 9:00am, all the region stands in uncomfortable region. The simulated result is shown in appendix-2.

6.5.3. The PET of Ling Nan Tian Di block

In order to compare the thermal conditions in this whole region, the PET during the daytime (for the measured day) is shown in Figure. 6-18. According to the final results of thermal sensation during daytime, the minor gap in thermal conditions at each of the different points occurred at 1:00 p.m. (4.6 ℃ PET) and the major one was at 8:00 a.m. (13.1 ℃ PET). The simulated result is shown in appendix-3.

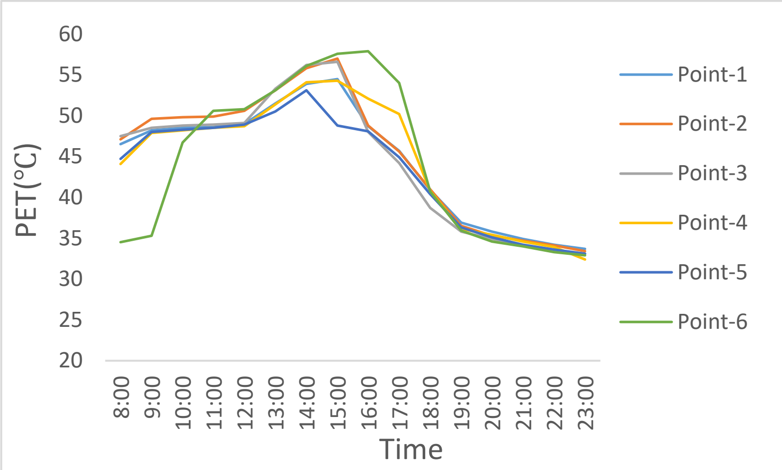

Figure. 6-16 The PET of the existing scenario

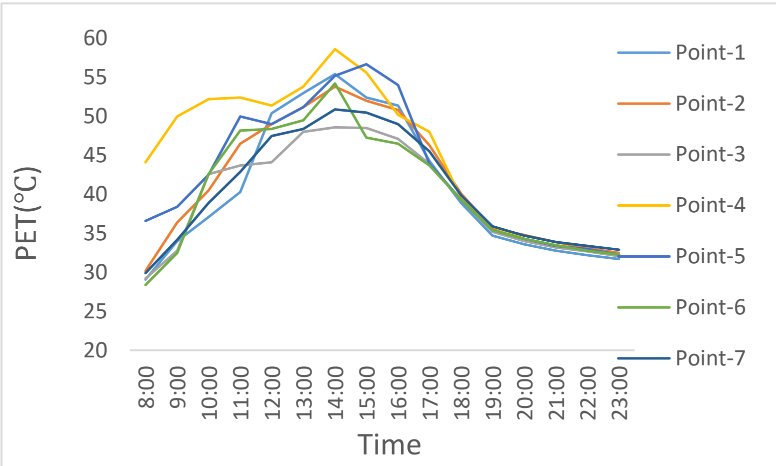

Figure. 6-17 The PET of the existing scenario

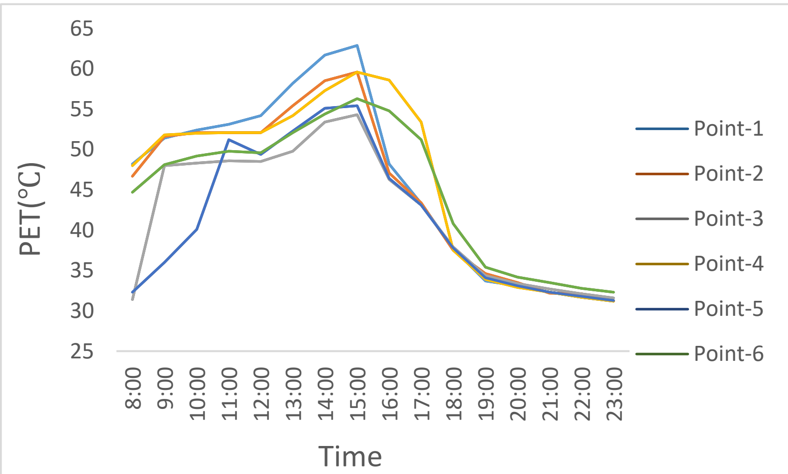

Figure. 6-18 The PET of the existing scenario

6.6. The box plot of humans' thermal sensation of existing scenario

According to the final results of the simulated software, in the hottest day of each one year, the thermal environment in this commercial pedestrian block is very serious. Based on previous studies, the box plot is the data variance to clearly express the statistics is a view. Used to visually summarize and compare distributions that consist primarily of many levels. It is used in various fields, but it is used especially in quality control. Based on the thermal sensation in hot-summer and cold-winter climate zone of China, the whole region is located in 'Hot' and 'Very hot' stages.

6.6.1. The box plot of Dao He Old block

Based on the simulated result of the simulation, the boxplot of all the selected points are shown in Figure 6-19. Because of the urban morphology, point-6 has the highest average air temperature at daytime, due to the higher SVF.

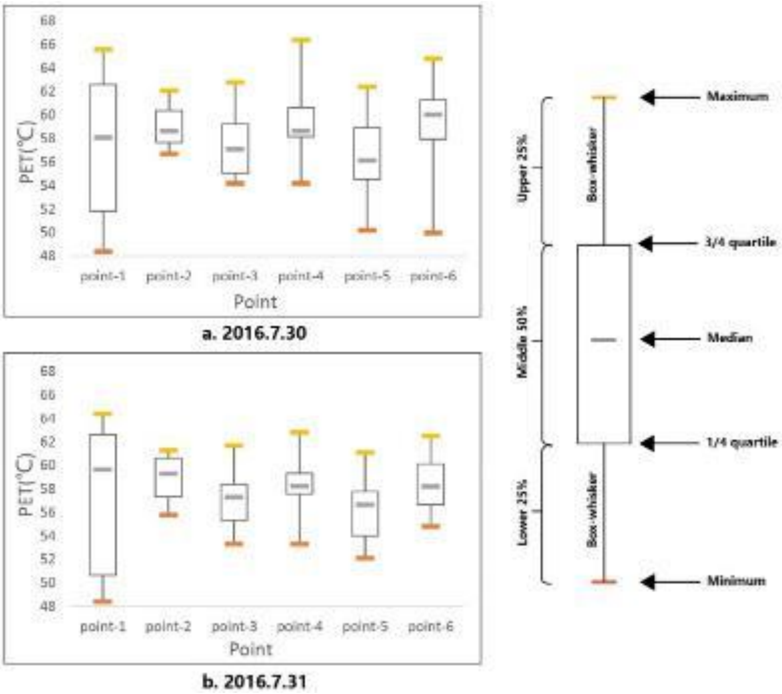

Figure. 6-19 The box plot of the existing scenario

6.6.2. The box plot of Dao He Old block

In accordance with outdoor thermal sensation in hot-summer and cold-winter climate zone of southern China , almost all the commercial region are within the "Hot" and "Very hot" two stages. Moreover, in order to the detailed thermal sensation of the different selected sites, Figure 6-20 was established to display thermal sensation of the existing scenario, where the extreme PET can reach between 48.2 and 62.1℃.

6.6.3. The box plot of Ling Nan Tian Di block

In accordance with humans' thermal sensation in the hot-summer and warm-winter climate region of China [54], almost all the selected points are located within the "hot" and "very hot" stages. In addition, in order to obtain a deep understanding of the thermal sensation of the different selected points, Figure 6-21 was established to show the existing scenario, in which the extreme summer PET of different points can reach up to between 45.7 and 65.6℃

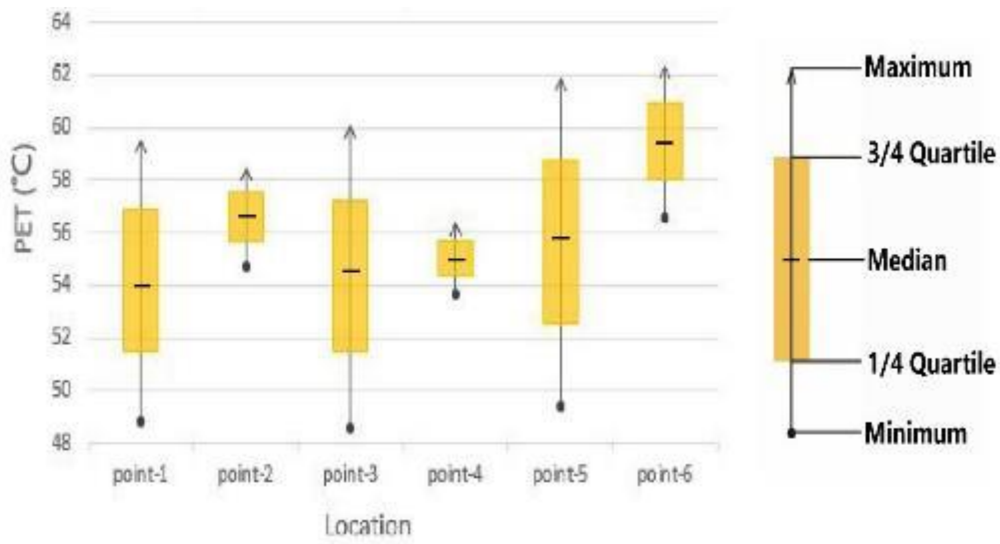

Figure. 6-20 The box plot of the existing scenario

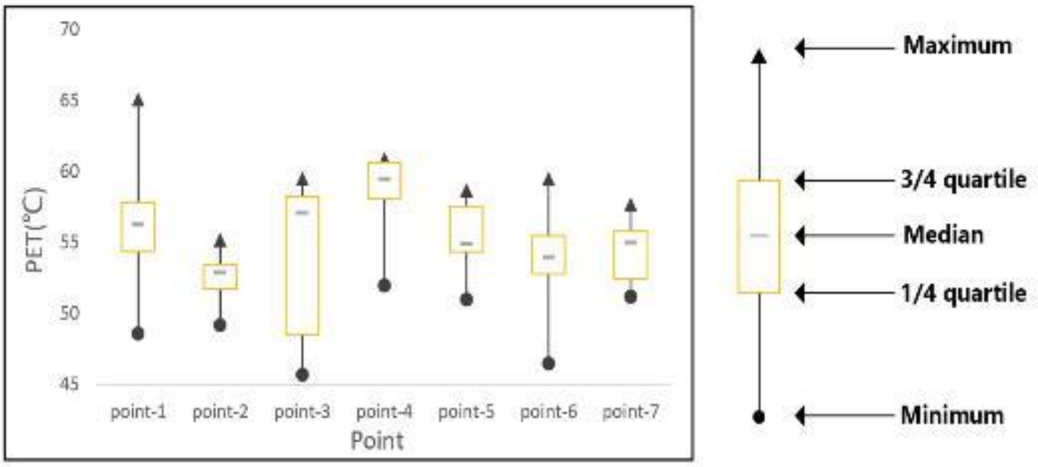

Figure. 6-21 The box plot of the existing scenario

6.7. The thermal calendar for tourists of existing scenario

In this study, the new thermal calendar for tourists is put forward. Thermal comfort calendar can help the tourists to choose a most suitable time to visit the commercial block a during the hottest time in summer, the scenario thermal conditions of this block are determined into one-hour intervals from 8:00am to 12:00pm, each color in calendar represents 3℃ range of the index PET. In order to get the most suitable time for tourists, it is convenient to define "Slightly warm" as "Suitable", "Warm" as "Fairly suitable", "Hot" and "Very hot" as "Unsuitable".

6.7.1. The thermal calendar of Dao He Old block

The Figure. 6-22 shows the existing scenario of the thermal comfort calendar. The microclimatic condition is very bad, in which point-5 has a suitable time for visiting from 8:00am to 11:00am and point-3 can be visited from 8:00am to 9:00am, other points are all not suitable for visiting from 8:00am to 6:00pm.After 6:00pm, all the points have a good visiting time.

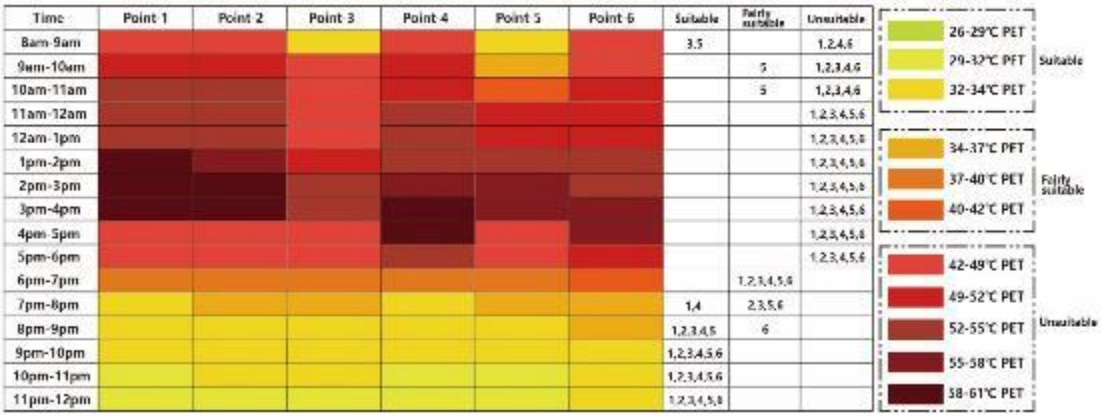

Figure. 6-22 Thermal comfort calendar of existing scenario

6.7.2. The box plot of Tai Zhou Old block

The thermal comfort calendar can help the tourists to choose a most suitable time to visit the commercial block during the hottest time in summer, the thermal conditions of this block are determined into one-hour intervals from 8:00am to 24:00pm, each color in calendar represents a 3℃ range of the PET's index. In order to get the most suitable time for tourists, it is convenient to define "Slightly warm" as "Suitable", "Warm" as "Fairly suitable", "Hot" and "Very hot" as "Unsuitable". The Figure 6-23 shows the existing scenario of the thermal comfort calendar. From 8:00am to 18:00pm, except point-6 has a suitable time for visiting from 8:00am to 10am, all the other points are all not suitable for visiting. After 18:00pm, all the points have a better visiting time.

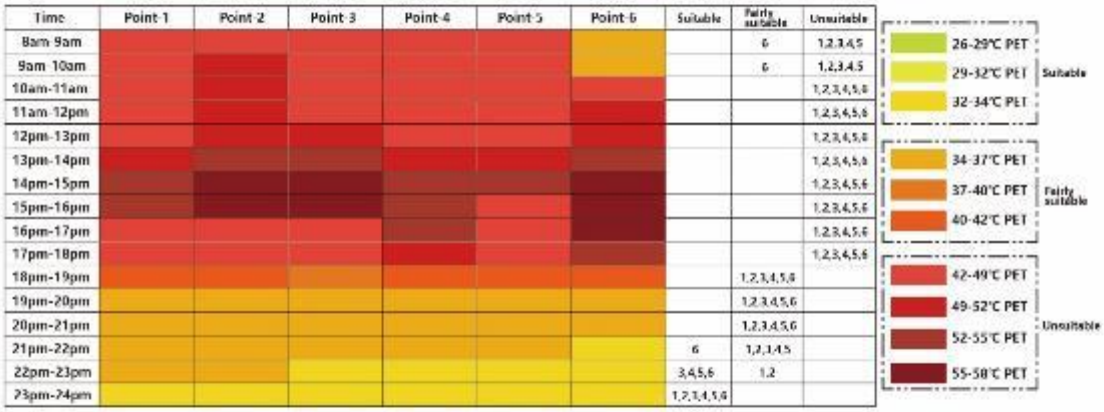

Figure. 6-23 Thermal comfort calendar of existing scenario

6.7.3. The box plot of Ling Nan Tian Di block

The thermal calendars can help tourists to select a comfortable time to visit this commercial pedestrianized zone during the hot summer. The outdoor thermal sensation of this zone is defined at each one-hour interval from 8:00 a.m. to 12:00 p.m., and each color in this thermal calendar represents a nearly 2 ℃ interval of the PET. It is necessary to provide a most suitable period for tourists, and it is easy for us to define "Very hot" and "Hot" as "Unsuitable", "Warm" as "Fairly suitable", and "Slightly warm" as "Suitable". Figure. 6-24 shows the thermal comfort calendar of the base case. At 8:00 a.m. and 9:00 a.m., except for point 4 being "unsuitable", all other points are "suitable" or "fairly suitable"; point 3 and point 6 are "suitable" and points 1, 2, 5, and 7 are all "fairly suitable". From 10:00 a.m. to 7:00 p.m., all the sites are not comfortable for visiting, and point 4 has the worst thermal comfort. After 7:00 p.m., all the points can be visited comfortably.

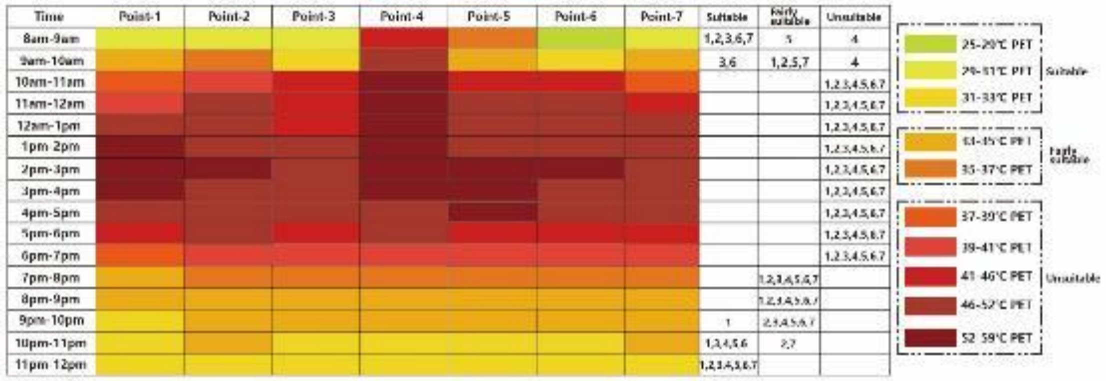

Figure. 6-24 Thermal comfort calendar of existing scenario

6.8. Summary

In this chapter, the final humans' thermal sensation are evaluated by the index PET, all the studies are assessed in southern China. According to the thermal sensation of hot-summer and cold-winter region and hot-summer and warm-winter zones, all the three blocks all stand in the 'Hot' and 'Very hot' stages.

Chapter-7.

Different design parameter on designing pedestrian block

7. Different design parameter on designing pedestrian block

7.1. The introductions of different cases

In fact, many previous studies have focused on reducing the demand for saving energy and enhancing human life [232, 233]. The alteration of urban morphology is an effective method to attenuate solar radiation in the daytime. Increasing building height can decrease the sky view factor (SVF) and increase the aspect ratio (H/W). Several studies have shown that there is a strong correlation between humans' thermal comfort and H/W; a street with a high H/W will produce a large shading region, which can mitigate heat stress effectively [234]. SVF is a number ranging from 0 to 1 that controls the incoming of solar radiation. Studies have investigated whether a street with a low SVF has a lower daytime air temperature [235]. In addition, a study on the effect of street canyons explained that street orientation has the largest influence on improving humans' thermal comfort at a pedestrian level in southern China. Additionally, trees and other vegetation can provide shading for canyon space and reduce ambient air temperature [236]. Vegetation's evaporation and transpiration can effectively alleviate heat stress. Previous studies have shown that the cooling effect of shading is better than evapotranspiration, thus contributing to energy saving [237]. A microclimatic study on the block scale showed that a 10% increase in the coverage ratio of green plants would produce a 0.8℃cooling effect [238]. The modification of paving material is also another method to alleviate heat stress in extreme summer temperatures [239]. Regression analyses are conducted to consider the characteristics of each different parameter in this zone. The final findings of this research will provide a comparative assessment that considers the effect of multiple parameters on reducing PET and improving humans' thermal comfort during business hours, thus helping local managers and policymakers to enhance outdoor energy efficiency and improve environmental sustainability. Moreover, this study will fill a gap in the literature on thermal studies of commercial pedestrianized zones.

7.2. The effect of different cases in the new scenarios

7.2.1. The new cases of Dao He Old block

As explained above, the new models were simulated under the same microclimate conditions as the existing scenario. In case-1, the building height was increased in accordance with the local design specification, which restricts buildings in the pedestrianized zone from exceeding three floors to protect the commercial value of this region [240]. In case-2, the total numbers of trees were increased to supply extra canopy coverage for this zone in accordance with local design specifications (increasing the green coverage ratio to 25%) [240]. In case-3, the grass coverage ratio was increased to alleviate heat stress, and the green coverage ratio was the same as in the second case. Case-4 aimed to research the cooling effect of the pavement material with higher albedo. Table 5 shows the cases modeling the future scenarios (Figure 7-1). The detailed information is in appendix-4.

Table. 7-1 The new scenarios

Scenario	Selection strategies
Base-case	Existing parameters in this study domain
Case-1	The average building height is increased

Case-2	The number of trees increased in the block
Case-3	The grass is increased in the block
Case-4	The pavement material is changed to the one with higher albedo

As mentioned above, increasing average building height can effectively impede solar radiation at daytime, the evaporation and transpiration of vegetation can cool ambient air temperature, in addition, paving material with higher albedo can also improve thermal sensation at daytime.

According to the final results, under case-1, after increasing average building height (Figure 7-10), in all canyon space, the PET values are improved obviously. This function can be attributed to the higher aspect ratio (H/W) can impede solar radiation at daytime, in addition, it can provide shading area for human. Except of point-6, the PET values doesn't change too much.

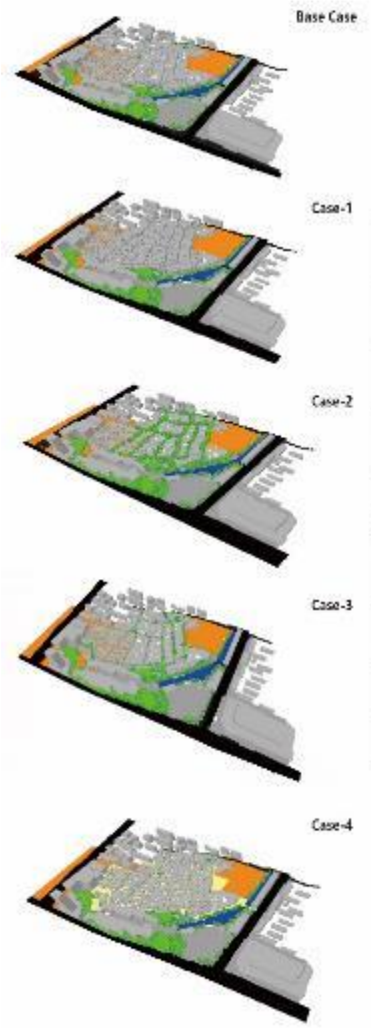

Model Area, %	Base case	Case-1	Case-2	Case-3	Case-4
Single story building	50.3	0	50.3	50.3	50.3
Double story building	17	0	17	17	17
Three story building	0	67.3	0	0	0
Total Building coverage	67.3	67.3	67.3	67.3	67.3
Tree coverage	3.5	3.5	18.2	3.5	3.5
Grass coverage	6.8	6.8	6.8	21.5	6.8
Ground surface	22.4	22.4	7.7	7.7	22.4
Total Area	100	100	100	100	100

Figure.7-1 Various types of parameter in new configuration

The cooling effect of case-2 is through providing shading area and transpiration for human, the final results also proved that the effect of trees can make a contribution to canyon space and open space. The thermal environment of all the selected sites can be improved obviously. The cooling effect of case-2 isn't better than case-1 in canyon space (Figure 7-3).

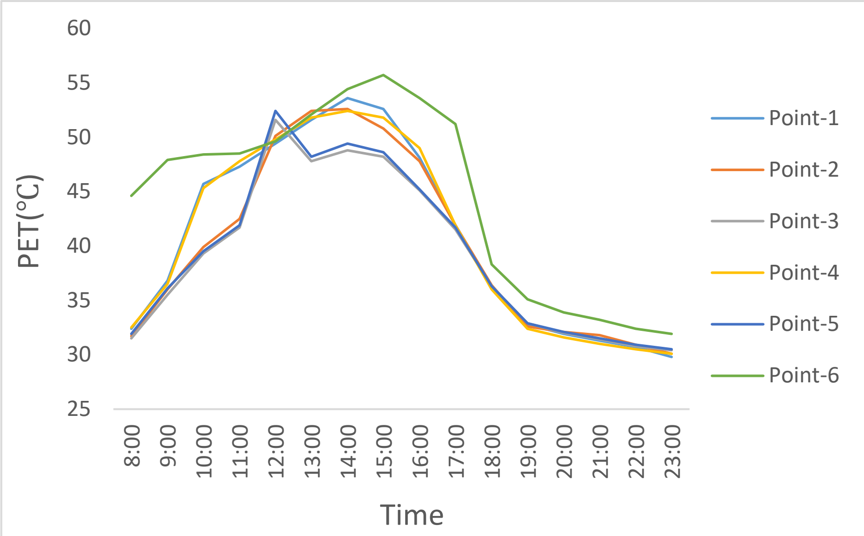

Figure.7-2 The thermal sensation under case-1

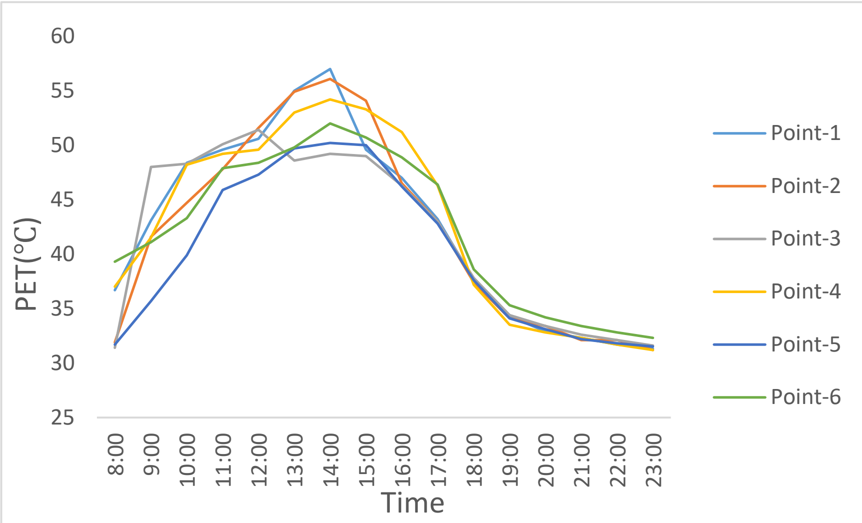

Figure.7-3 The thermal sensation under case-2

Different from case-1 and case-2, the cooling effect of case-3 is limited. According to the final result of case-3, the cooling effect of grass is very small. Compared to the existing scenario, the extent can't be changed too much (Figure. 7-4).

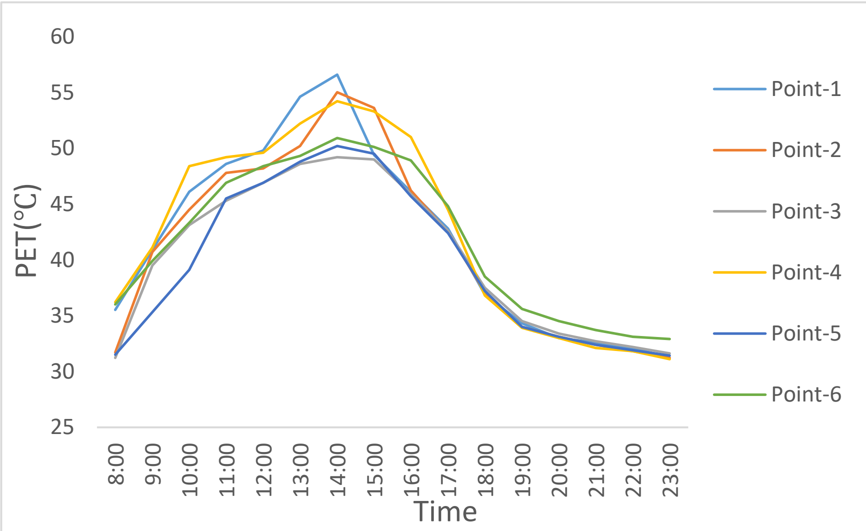

Figure.7-4 The thermal sensation under case-3

The last case (case-4) is through changing paving material with higher albedo to improve humans' thermal sensation at daytime. Like case-3, the effect of changing paving material is not obvious.

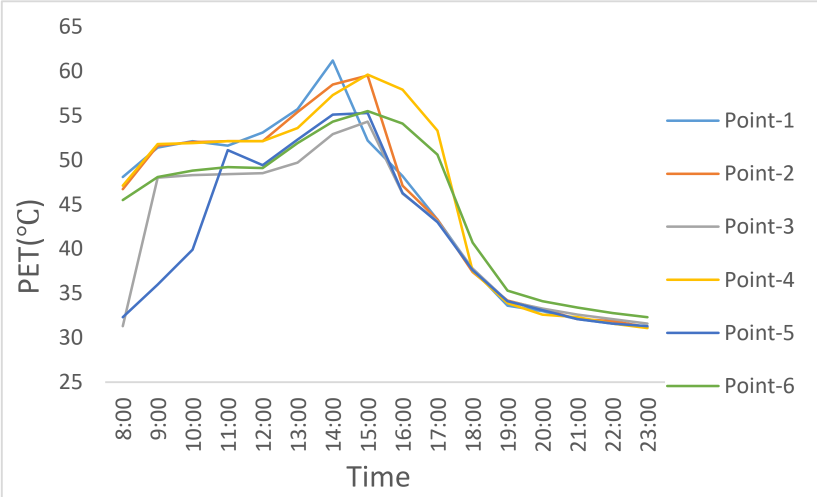

Figure.7-5 The thermal sensation under case-4

7.2.2. The new cases of Tai Zhou Old block

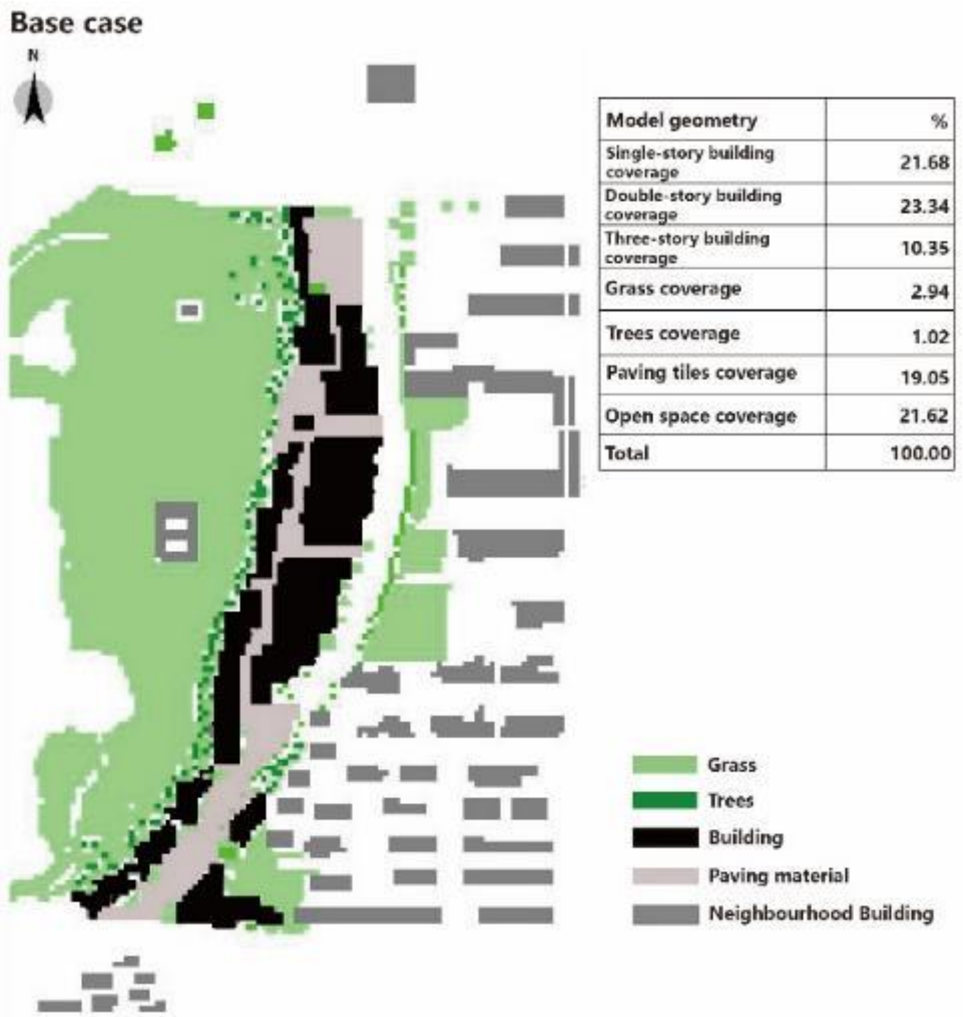

Figure. 7-6 The summary of the basic input configurations

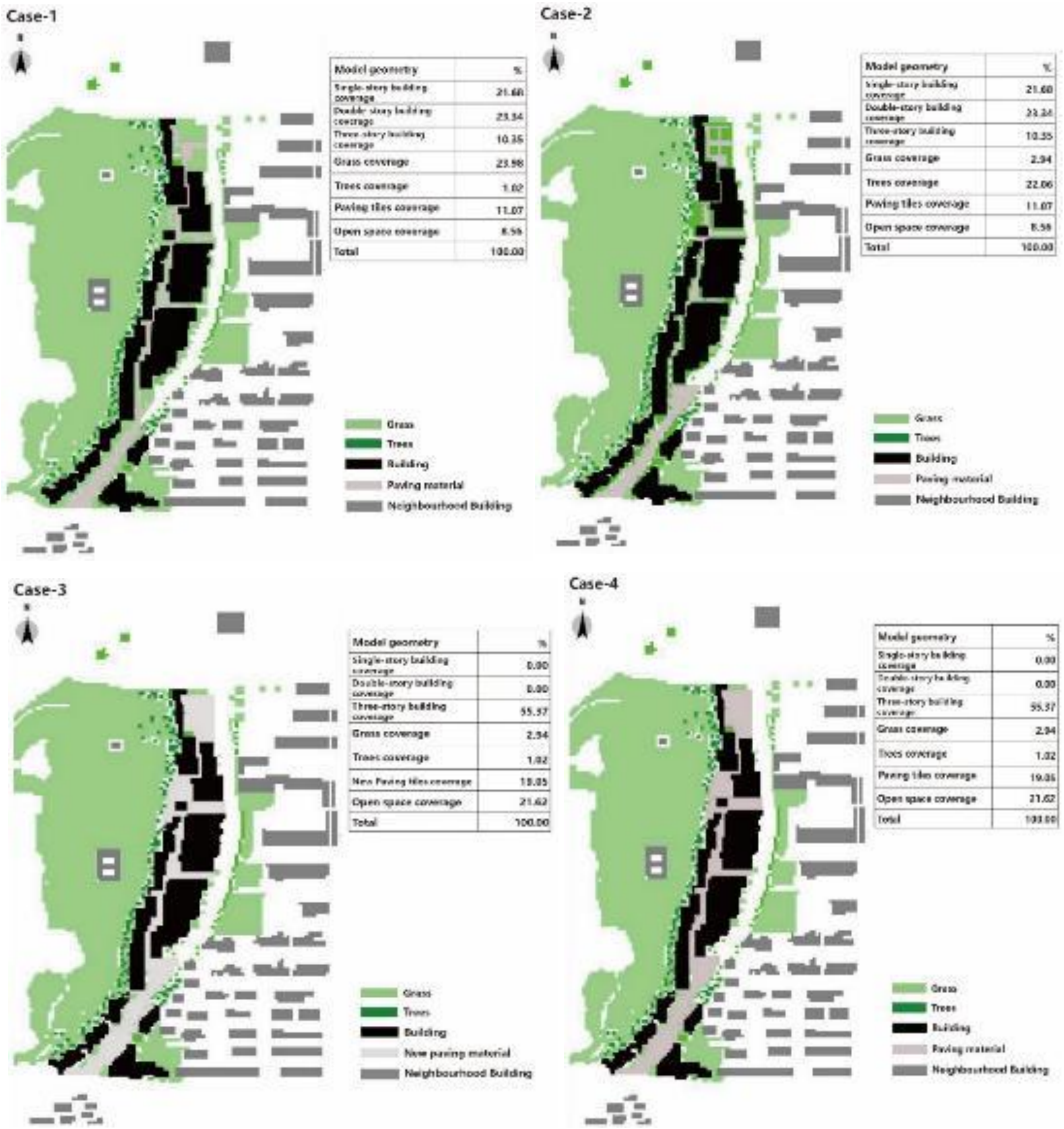

Figure. 7-7 The summary of the new configurations

As we mentioned, based on the current simulated conditions of the model, this existing scenario is defined as a base case, and four new scenarios (Figure. 7-3 and 7-4) were conducted to evaluate and assess the cooling effect of different parameters in this work.

In scenario-1, the grass coverage ratio increased to 23.98% aimed at understanding its influence on cooling effect. As in case-1, in case-2, the tree coverage ratio increased aimed at improving outdoor thermal comfort and evaluated its effect in accordance with the local design specification. Case-3 changed the existing pavement material to evaluate its cooling effect and assess its potential in reducing the outdoor energy consumption. In scenario-4, as mentioned above, the buildings in this region won't exceed three stories. This scenario aimed to increasing average building height to evaluate its cooling effect, where the three-story building coverage ratio was increased to 55.37%. The final of case-1 shows that in canyon space the PET at daytime have improved too much (Figure.7-8).

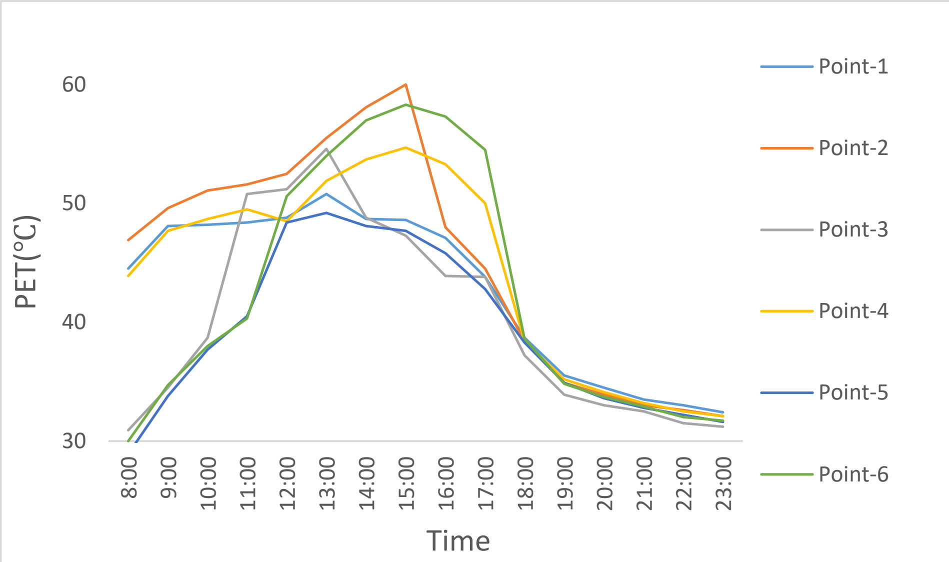

Figure. 7-8 The thermal sensation under case-1

The cooling effect of case-2 is through providing shading area and transpiration for human, the final results also proved that the effect of trees can make a contribution to canyon space and open space.

The thermal environment of all the selected sites can be improved obviously. The cooling effect of case-2 isn't better than case-1 in canyon space (Figure 7-9).

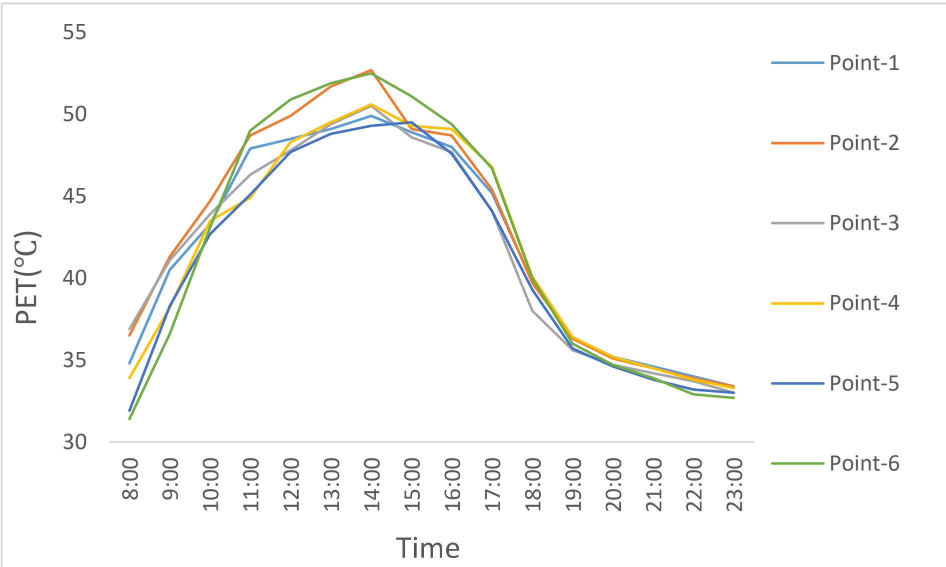

Figure. 7-9 The thermal sensation under case-2

Different from case-1 and case-2, the cooling effect of case-3 is limited. According to the final result of case-3, the cooling effect of grass is very small. Compared to the existing scenario, the extent can't be changed too much (Figure. 7-10).

The last case (case-4) is through changing paving material with higher albedo to improve humans' thermal sensation at daytime. Like case-3, the effect of changing paving material is not obvious.

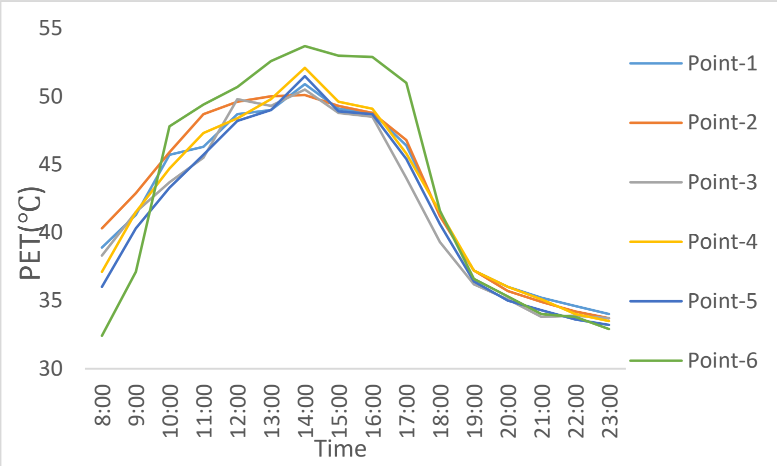

Figure. 7-10 The thermal sensation under case-3

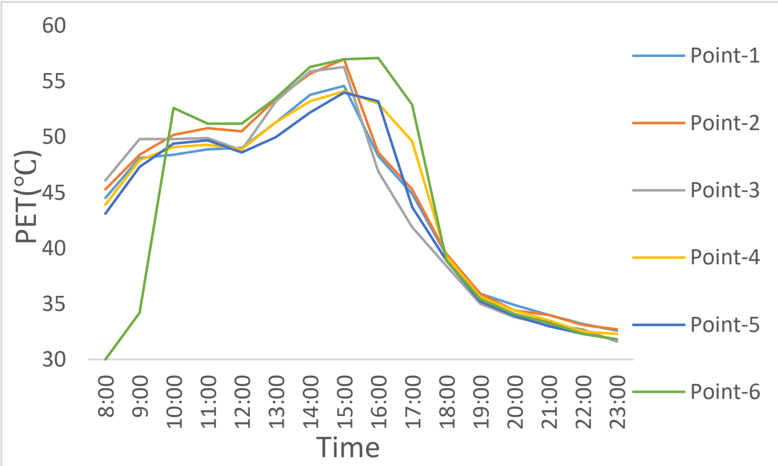

Figure. 7-11 The thermal sensation under case-4

7.2.3. The new cases of Ling Nan Tian Di block

In this study, real renewal process of the realistic pedestrianized-zone is simulated in four cases. The new numerical simulation is carried out with the detailed geometry of buildings, trees, grass and hard paving material to evaluate the effects of different parameter on improvement of urban microclimate. According to the local design specifications, buildings in commercial pedestrianized-zones won’t exceed three-story in order to keep the commercial value [37], therefore, the cooling effect of increasing average building height is determined as case-1. In the case-2, the realization of supplementary trees are added, the local design specification rules that the vegetation coverage ratio isn’t less than 25% of the whole region. The case-3 aims at evaluating the cooling effect of the new paving ground material with higher albedo. The last case (case-4) is various aforementioned cases. Table. 9 shows the detailed information of the new cases. Figure.16 shows that all the cases with different parameter coverage ratio. Here, we discuss the impacts under new cases on humans’ thermal sensation. The hourly diagram of ΔPET values of the selected points are shown in Figure. 7-12. As expected, the magnitude of PET reduces under the new cases, that is to say, all new cases can make contributions to improve outdoor thermal comfort. The final of case-1 shows that

in canyon space the PET at daytime have improved too much (Figure.7-12).

The cooling effect of case-2 is through providing shading area and transpiration

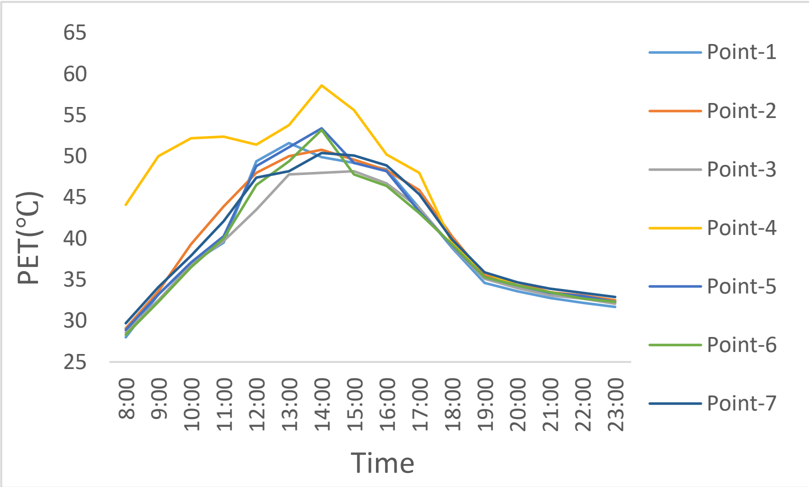

Figure. 7-12 The thermal sensation under case-1

for human, the final results also proved that the effect of trees can make a contribution to canyon space and open space. The thermal environment of all the selected sites can be improved obviously. The cooling effect of case-2 isn't better than case-1 in canyon space (Figure 7-13).

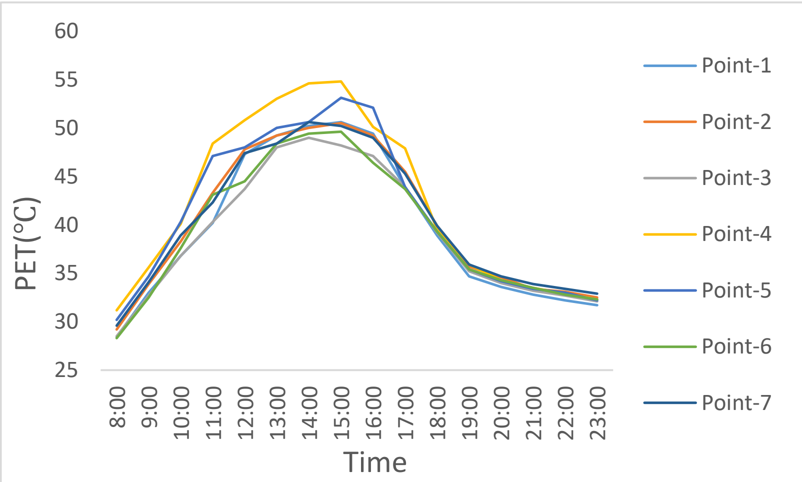

Figure. 7-13 The thermal sensation under case-2

Different from case-1 and case-2, the cooling effect of case-3 is limited. According to the final result of case-3, the cooling effect of grass is very small. Compared to the existing scenario, the extent can't be changed too much (Figure. 7-14).

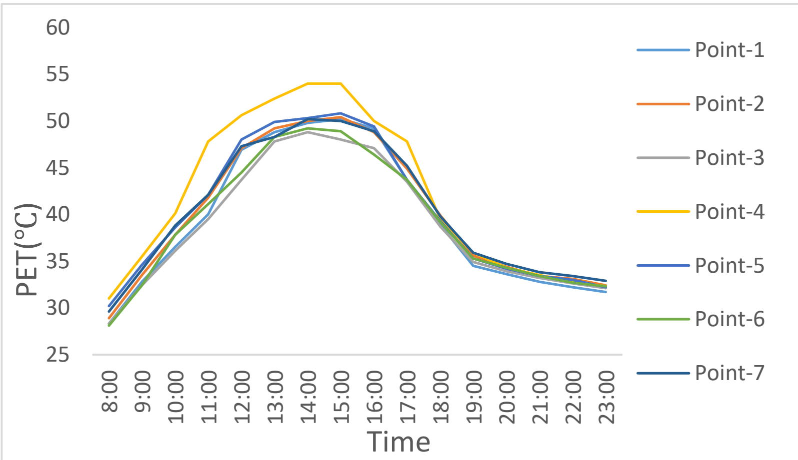

Figure. 7-14 The thermal sensation under case-4

The last case (case-4) is through changing paving material with higher albedo to improve humans' thermal sensation at daytime. Like case-3, the effect of changing paving material is not obvious.

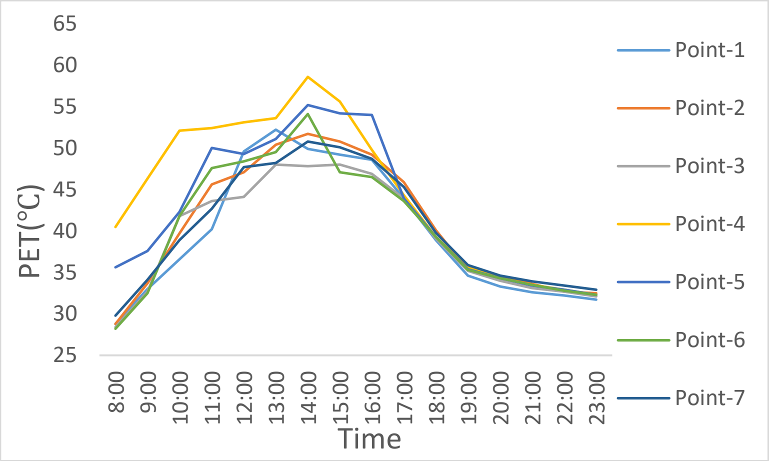

Figure. 7-15 The thermal sensation under case-4

7.3. The cooling effect of different cases

As mentioned above, The required parameters for calculating the index PET in the software ENVI-met includes the air temperature, relative humidity, wind velocity, mean radiant temperature, human's clothing and activity.

The corresponding values of the new strategies (ΔPET) is shown in Equation.7-1.

$$\Delta PET = PET - PET_S \quad (7\text{-}1)$$

Where PET is the existing thermal situation in the pedestrian block; PETS is the new thermal comfort under the new strategies. ΔPET is the discrepancy of PET and PETS. This equation can represent the thermal comfort modification effect of the new strategies.

7.3.1. The cooling effect of different parameters in Dao He Old block

Figure. 7-16 shows that the ΔPET of point-1, it can be concluded that the case-4 has the most effective influence on reducing PET in the daytime, ΔPET ranging from 0.5℃ to 16.3℃, due to the shading of the buildings and vegetation. The effect of case-1 is very similar to the case-4, in addition, the effect of case-2 and case-3 are not as effective as the former two ways. Changing paving material (case-3) is the least effective method.

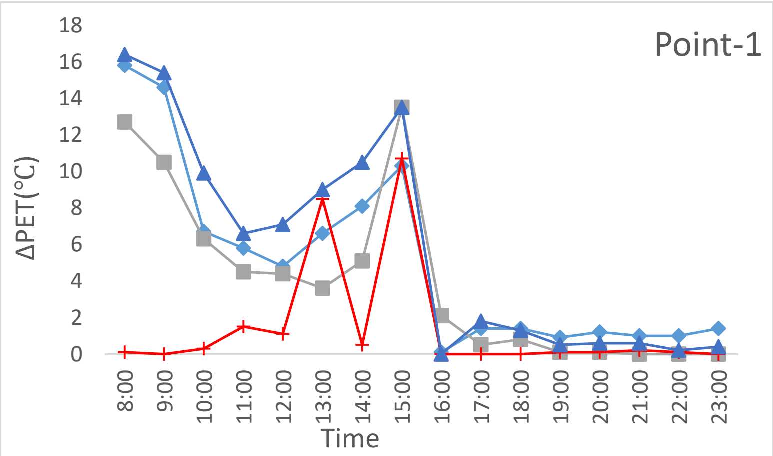

Figure.7-16 The thermal sensation improvement under point-1

It is shown that in Figure. 7-17, the change of the curve is similar to the point-1, case-3 is not effective in reducing PET in the daytime and case-4 is the most effective method, which can alleviate urban heat island and improve thermal comfort 16℃ PET at 8:00am in the morning, in addition, the effect of case-1 is very similar to the case-4. The effect of case-2(50%) is a little better than the 25%-scenario.

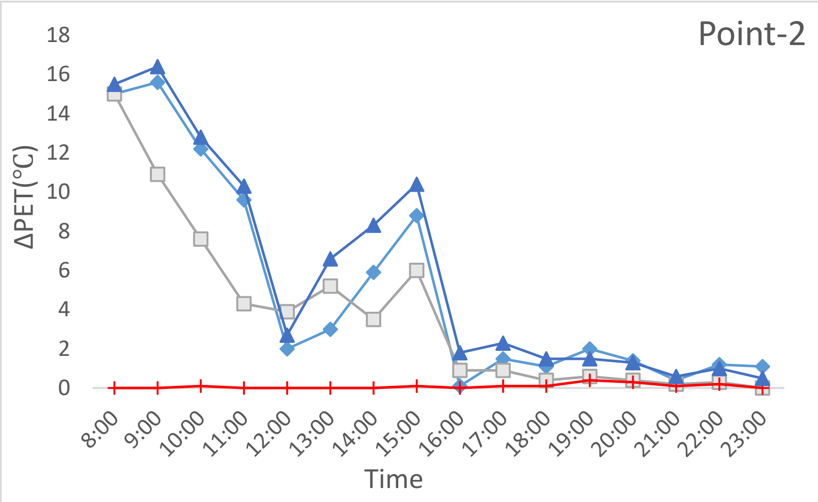

Figure.7-17 The thermal sensation improvement under point-2

According to the result (Figure.7-1), it is found that case-1 and case-4 are most significant in ameliorating heat stress. Like point-1 and point-2, the case-3 has no effect in improving thermal comfort. The maximum of case-1 is 8.5℃ and way-4 is 14.4℃.The difference between way-2 (25%) and way-2 (50%) is not obvious after 4:00pm.

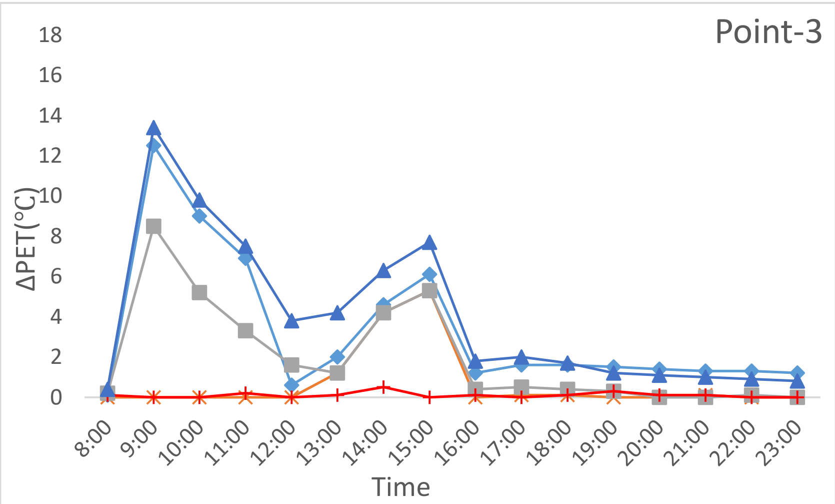

Figure.7-18The thermal sensation improvement under point-3

Because of different spatial morphology, different point will have different microclimate during the daytime. Point-4 is a west-east oriented street which has a worse microclimatic condition than other points. Figure. 7-17 shows the detailed information of thermal comfort modification. Except of case-3, other ways can cool down the environment effectively. The changing trend of point-5 (Fig. 7-18) shows that case-1 and case-4 have an effective influence on reducing PET. The maximum ΔPET can reach 9.9℃ at 11:00am. After 4:00pm, all the new cases have a little difference.

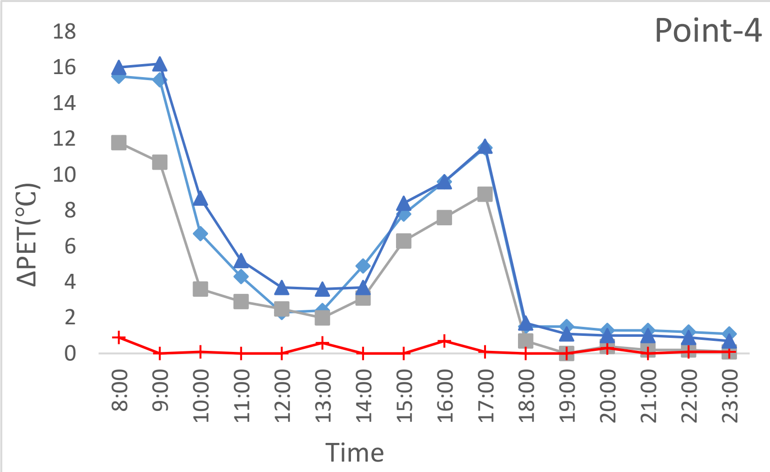

Figure.7-19 The thermal sensation improvement under point-4

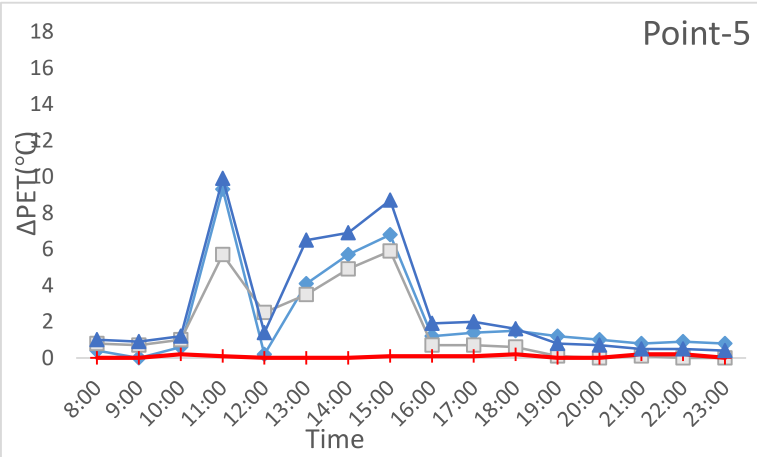

Figure.7-20 The thermal sensation improvement under point-5

Unlike other points, point-6 belongs to an open space, which means the whole area will experience a long period of solar exposure and lead to a worse thermal comfort in the daytime. Comparison of PET evolution of point-6 can be seen in Figure. 7-19. Different from other points, case-1 can’t improve thermal comfort condition effectively. The best way is case-3 and case-4, which means that the only way to improve thermal comfort in open space is increasing vegetation which can reduce maximum 8.7℃ PET at 8:00am in the daytime.

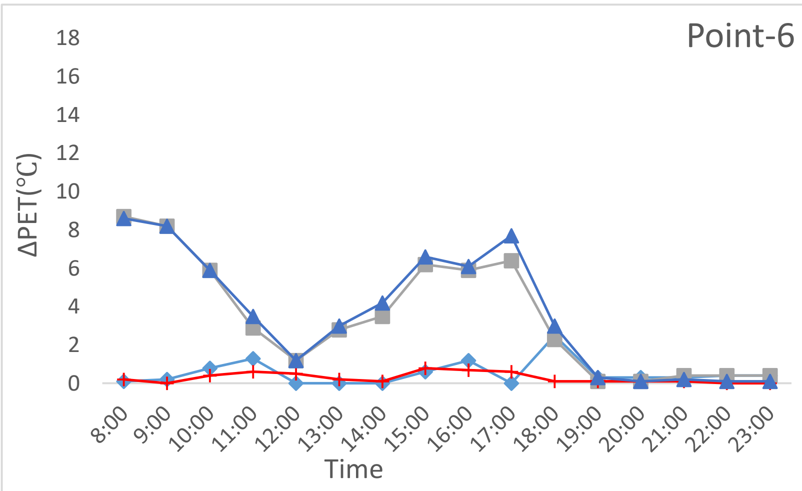

Figure.7-21 The thermal sensation improvement under point-6

According to the previous studies, the hottest time in China always occurs from 14:00 to 16:00, in this study, we found the hottest time in this region occurs at 15:00. Also, the higher air temperature, the cooling effect will be (Figure 7-22 and 7-23).

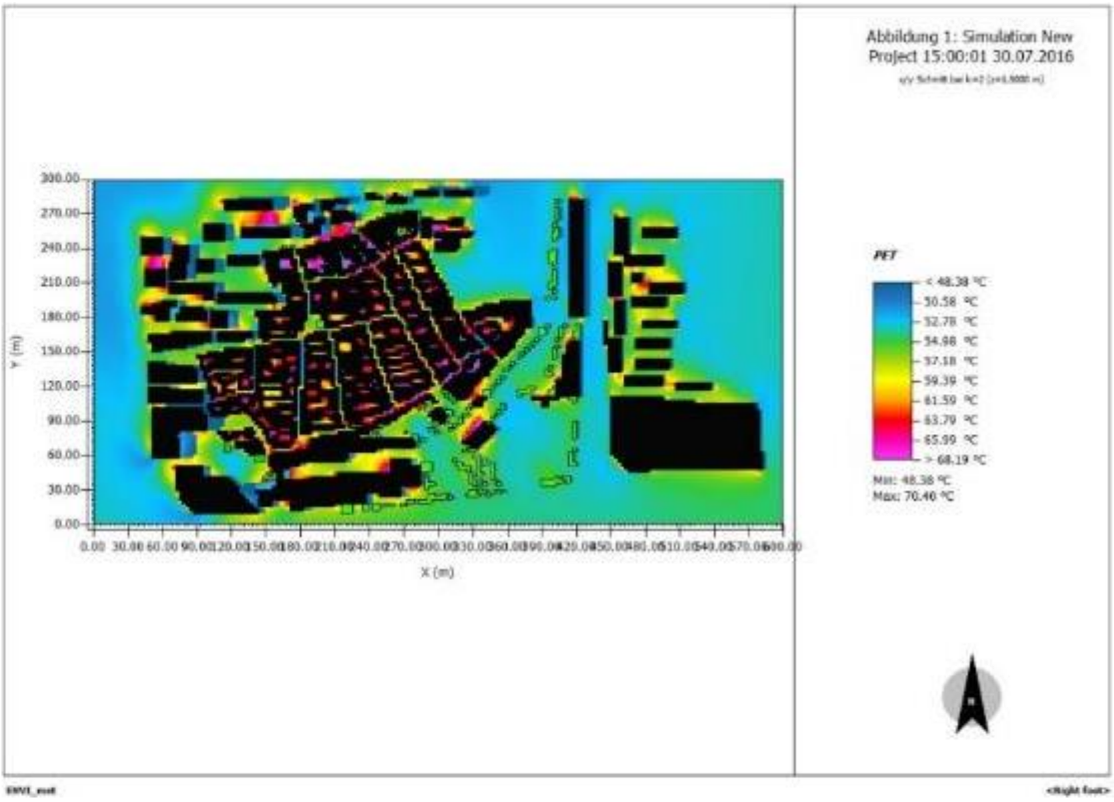

Figure.7-22 The thermal sensation of existing scenario at 15:00 on Jul 30th

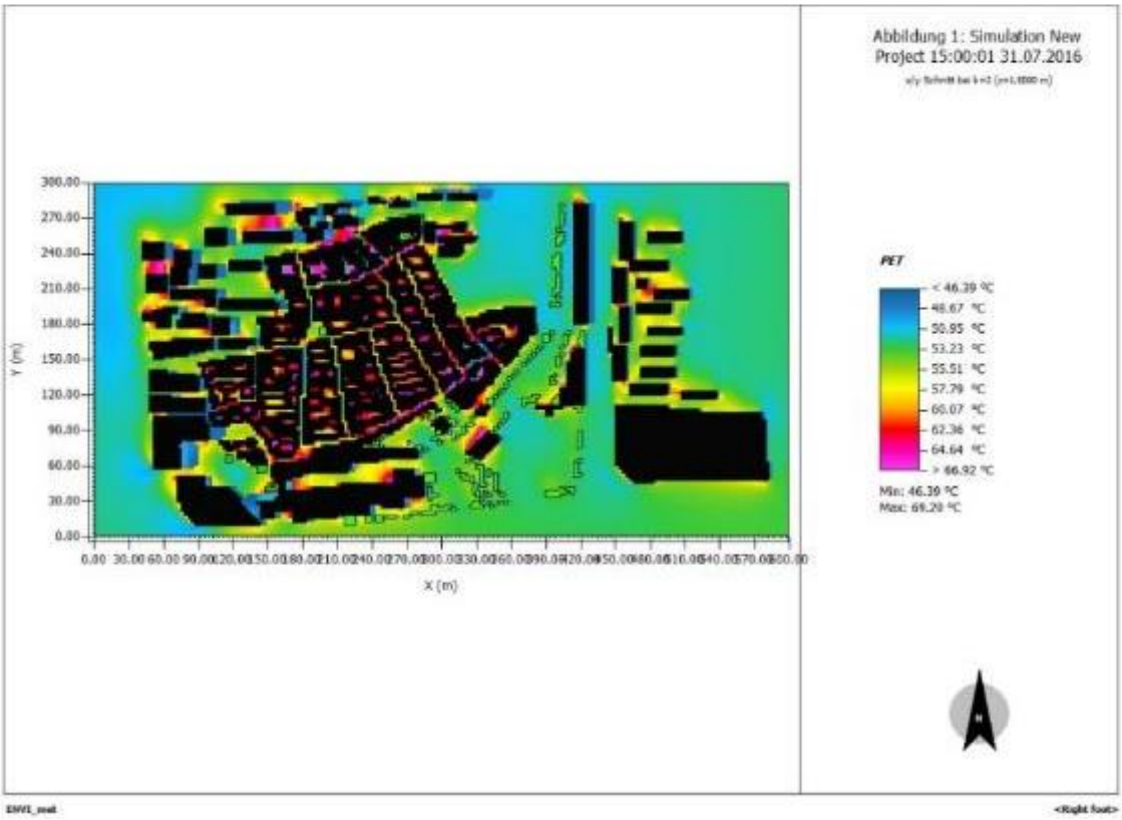

Figure.7-23 The thermal sensation of existing scenario at 15:00 on Jul 31th

The cooling effect of different cases of the two measured days are shown in Figure 7-24. As we can be seen from this figure, the best cooling effect is case-1, which aims at increasing average building height to improve humans' thermal comfort obviously. Also, in case-2, increasing tree coverage ratio also can alleviate heat stress obviously. The extent of case-3 and case-4 are limited.

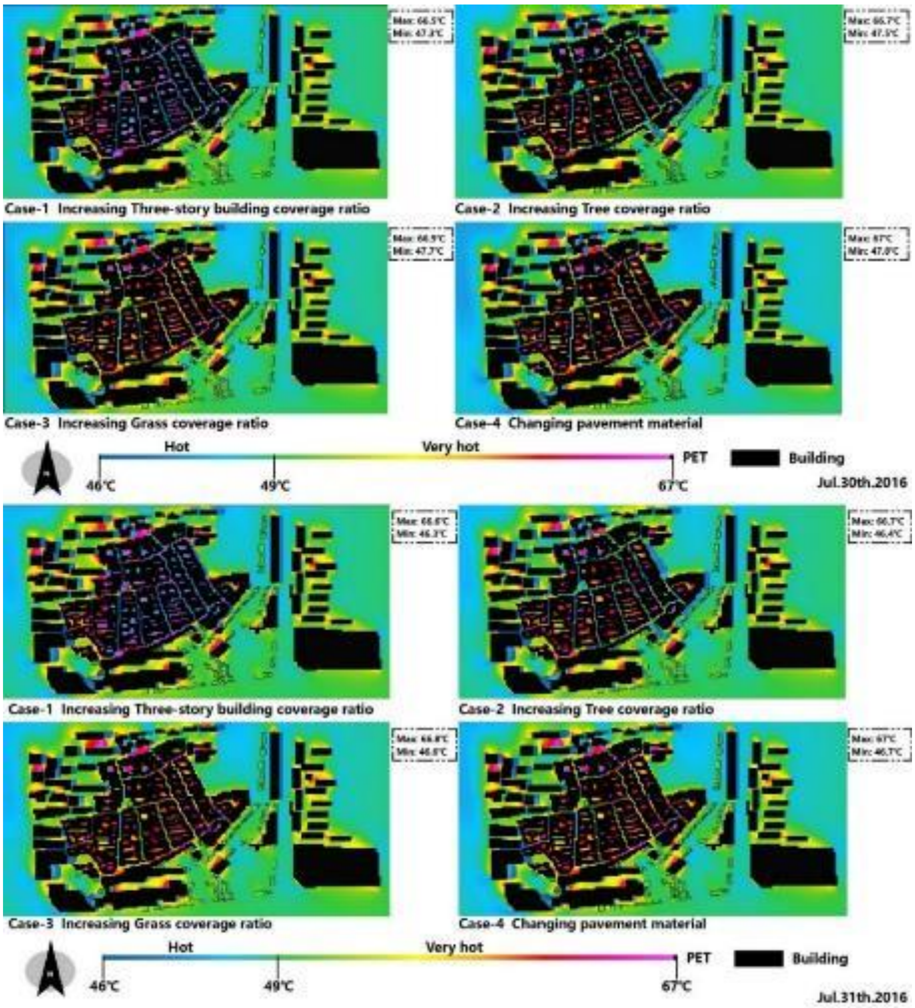

Figure.7-24 The thermal sensation of existing scenario at 15:00 on two measured days

These PET results are processed with the same range and conditions to obtain a fair comparison between the base case and new cases. In the first measured day (30th, 2016), increasing building height can not only supply more shading for human but also impede solar radiation at daytime, the impact of shading on thermal comfort is quantified by calculating the difference of PET between canyon space and open space (Fig. 25-a), in which a positive ΔPET (thermal comfort improvement) from 0.8℃ to 12.6℃ has appeared, meanwhile, an invalid effect has been found in open space during the daytime. Trees' function is through transpiration and providing shading to prevent the solar radiation, thus improving thermal comfort at daytime. It is obvious that the reduction of PET has appeared both in canyon space and open space (Fig. 25-b), in which the ΔPET values ranges from 0.3℃ to 9.2℃. Fig. 19-c shows the effectiveness of the grass, unlike trees, the cooling effect of grass jest depends on the transpiration, which leads to a worse cooling result in a comparison with trees. Compared to other cases, as is shown in Fig. 25-d, changing the pavement material with a high albedo also can improve thermal comfort, but the extent is limited. In the second measured day, all the variation trend of different cases are similar to the first day (Fig. 25-e, f, g, h). In our study, numerical simulation are conducted to evaluate the correlation between different parameters and humans' thermal comfort in extreme summer, the current results show that the spatial distribution of humans' thermal comfort modification through the synergistic effect of the different parameters in general.

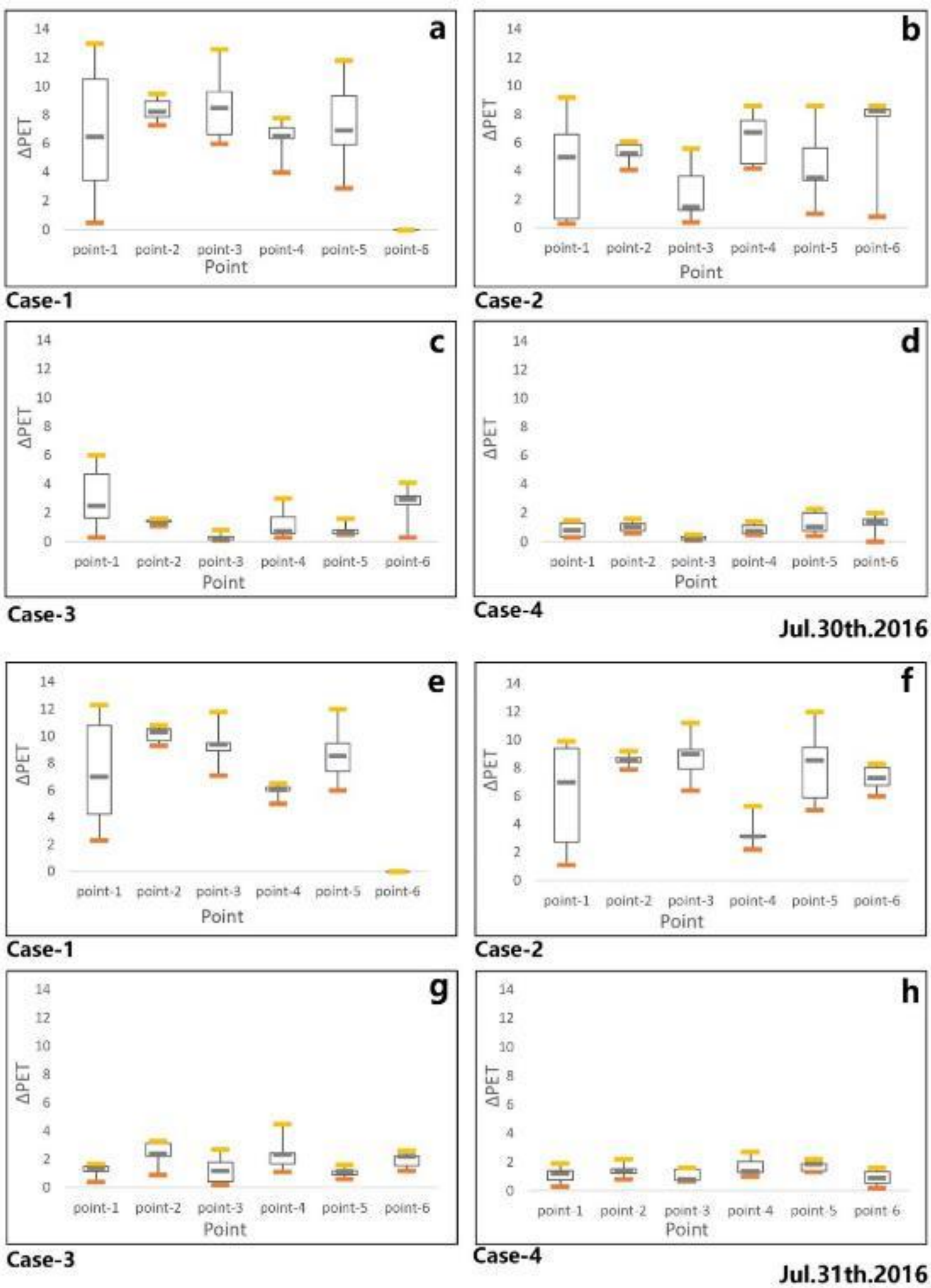

Figure.7-25 Cooling effect of the new cases at 3:00pm

As mentioned above, the whole zone was consist of open space and canyon space, the effectiveness of different parameter in open space are shown in Figure. 7-26. Different parameter has different effect in improving thermal comfort at the hottest time during the measured period. The multiple regression analyses of the different parameter about ΔPET values at 3:00pm are conducted to assess the contribution of these on improving thermal comfort. The correlation coefficient (R2) between PET and different parameter is served to describe the proportion that can be explained by the variables of the regression model. A strong positive correlation is found between the percentage of trees (Case-2) and ΔPET with the correlation coefficient being 0.9713, it can be observed that 3% increase in the coverage ratio of trees can reduce 0.78℃ PET at hottest time during the extreme summer. Meanwhile, an irrelevant relationship between building height and ΔPET can be observed (Case-1), which means that increasing building height can't effectively improve thermal comfort in open space. The impacts of other parameters including grass (Case-3) and pavement material (Case-4) can reduce PET, but the extent is limited.

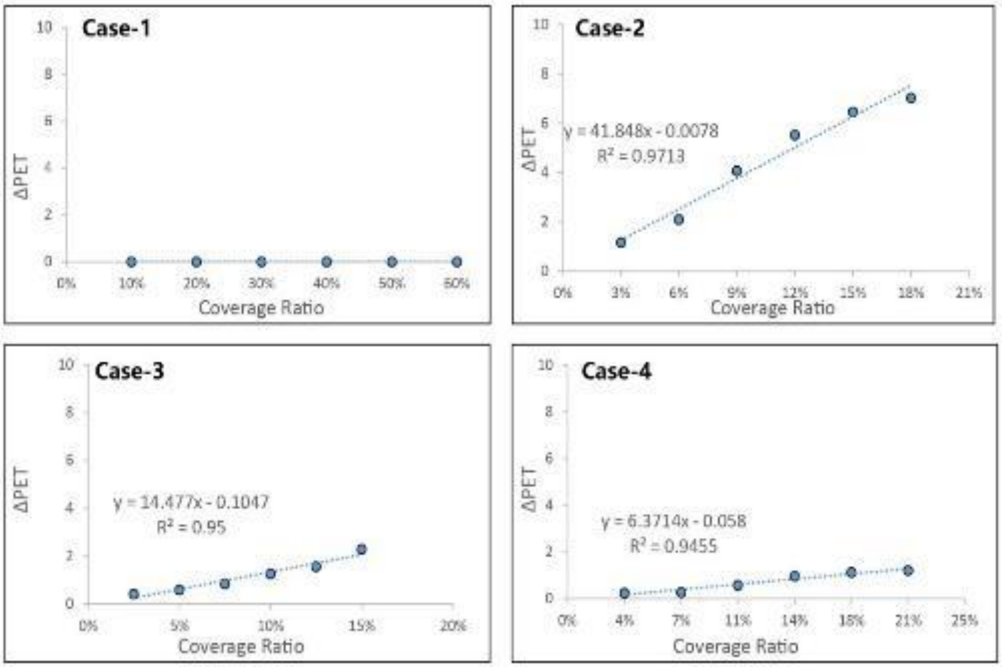

Figure.7-26 Correlation between thermal comfort and coverage ratio of different parameter in open space at 3:00pm

Figure. 7-27 shows the changing situation in canyon space, unlike open space, the heat stress can be alleviated in all the new cases. Increasing building height can effectively reduce PET (Case-1) at daytime, looking at its values, it's easy to find that 10% increase in the coverage ratio of the three-story building can raise 1.3℃ in PET, this effect can be attributed to the shading in street. In addition, increasing trees coverage ratio also can lead to a thermal comfort improvement (Case-2), ascension of 3% in the coverage ratio of trees would result in a decrease of 0.9℃ in PET values. The effect of grass (Case-3) is through reducing reflected radiation to improve thermal comfort, but the result is poor. Like increasing coverage ratio of grass, changing pavement material with a high albedo (Case-4) can decrease diffuse reflection, which can improve thermal comfort, but the simulated result isn't obvious.

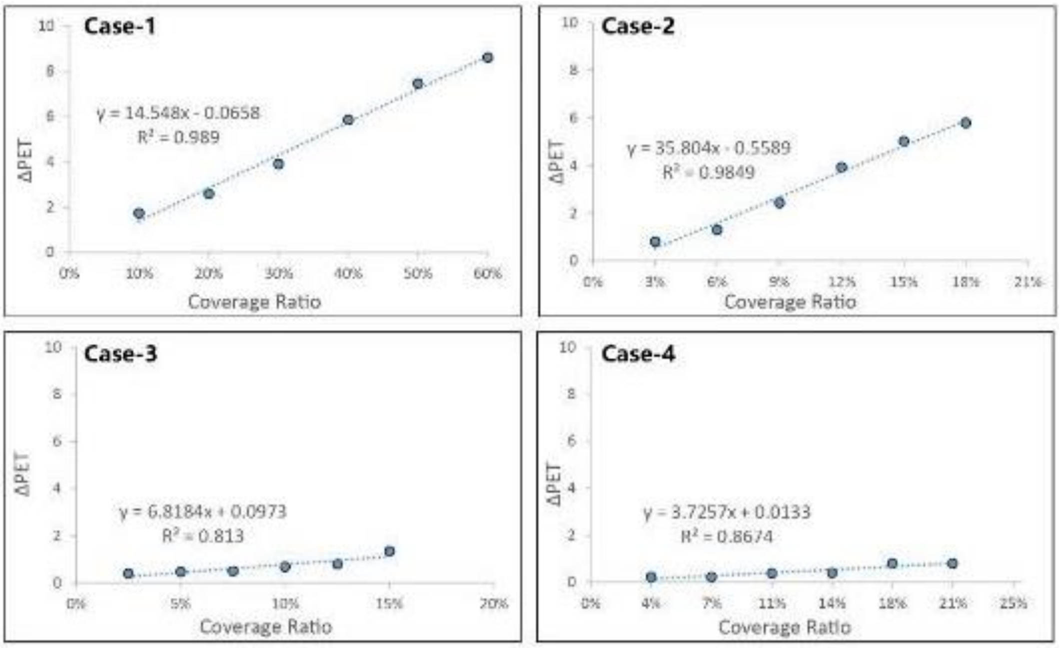

Figure.7-27 Correlation between thermal comfort and coverage ratio of different parameter in canyon space at 3:00pm

According to all the results of the multiple regression, designers and policy makers can choose the best way to redesign this block and improve the outdoor energy efficiency. The final result which indicates the correlation between each parameter and humans' thermal comfort is classified into different level for choosing (Figure.7-28).

Spatial geometry	Building	Tree	Grass	Material
Open space	0	0.9713	0.95	0.9455
Canyon space	0.989	0.9849	0.813	0.8674

R^2scale	Level of effect
0.75-1	Most effective
0.50-0.75	More effective
0.25-0.50	Less effective
0-0.25	Least effective

Figure. 7-28 Correlation between different parameter and thermal comfort

7.3.2. The cooling effect of different parameters in Tai Zhou Old block

The diagram of ΔPET values are shown in Figure 29-34. It can be observed that, the curves of ΔPET values in each selected point are relatively proximate. Most of the reconstructed ways make a contribution to improvement of the thermal comfort (positive ΔPET), but the way-3 may lead to a depravation (negative ΔPET). Figure. 7-29 shows that the ΔPET of point-1, it can be seen that the case-4 has the most effective influence in reducing PET in the daytime, ΔPET ranging from 0.5℃ to 12.3℃, due to the shadows of the buildings and vegetation. The effect of case-2 (vegetation-50％) is very similar to case-4, in addition, the effect of case-1 and case-3 is not so obvious. It is shown that in Figure. 7-30, the change of the curve is similar to the point-1, case-1 and case-3 are not effective in reducing PET and case-4 is the most effective method which can alleviate urban heat island and improve thermal comfort 12.4℃ in the morning. After 18:00pm, the difference of all the reconstructed ways are not obvious. According to the result (Figure. 7-31), it is found that case-1 and case-4 are most significant in ameliorating heat stress. Unlike point-1 and point-2, the reconstructed way-1 also has a better effect in improving thermal comfort. The maximum of case-1 is 16.6℃ and case-4 is 17.2℃.

The difference between case-2 (25%) and case-2 (50%) is not obvious. Case-3 has the lowest effect in reducing PET.

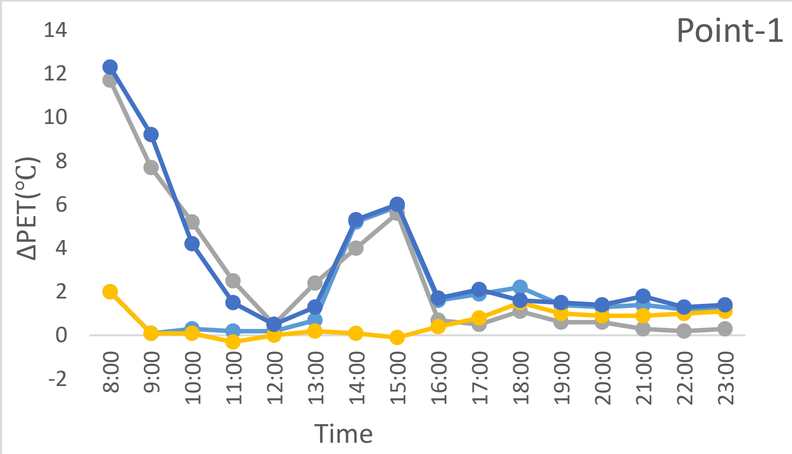

Figure.7-29 The thermal sensation improvement under point-1

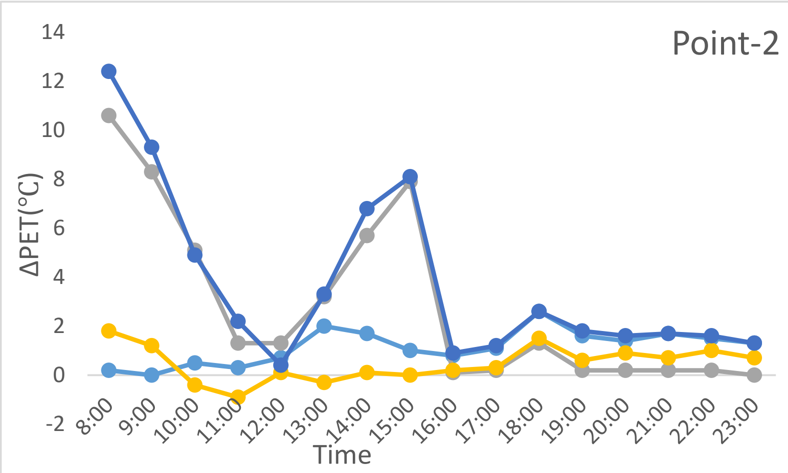

Figure.7-30 The thermal sensation improvement under point-2

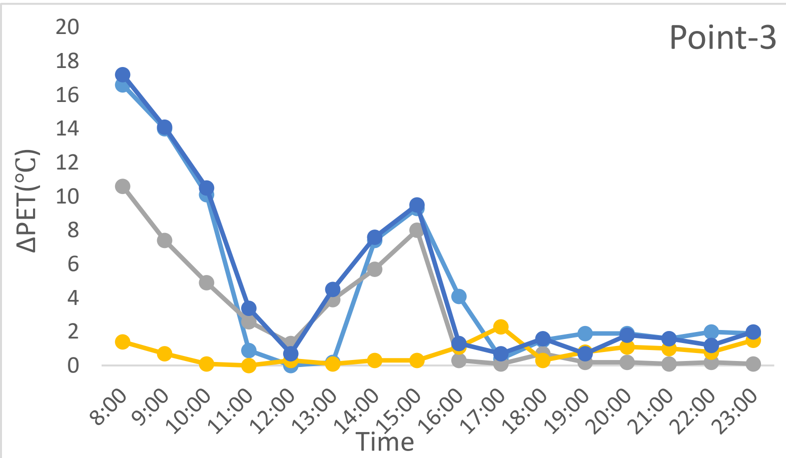

Figure.7-31 The thermal sensation improvement under point-3

Because of different spatial morphology, different point will have different microclimate during the hours of a day. Point-4 is a west-east oriented street which has a worse microclimatic condition. Figure. 7-32 shows the detailed information of thermal comfort modification. Changing buildings height is not a significant factor. In this diagram, it is concluded that way-4, way-2 (25%-vegetation) and way-2 (50%-vegetation) can cool down the area in the daytime effectively. The case-1 and case-3 are not suitable for improving thermal comfort. Because of the same spatial geometry, the changing trend of point-5 curve is similar to point-3 (Figure. 7-32). The maximum ΔPET can reach 16.4℃ at 8:00am, case-3 is not effective in reducing PET. After 16:00pm, all the reconstructed ways have a little difference. Compared to point-3 and point-5, point-6 belongs to a shallow street. That means the whole area will experience a long period of solar exposure which will lead to a bad thermal comfort in the daytime. Comparison of PET evolution of point-6 can be seen in Figure.7-33. Different from other points in the same time, the maximum ΔPET occurs at 11:00am. The way-4 has the most effective influence in improving thermal comfort (Figure. 7-34).

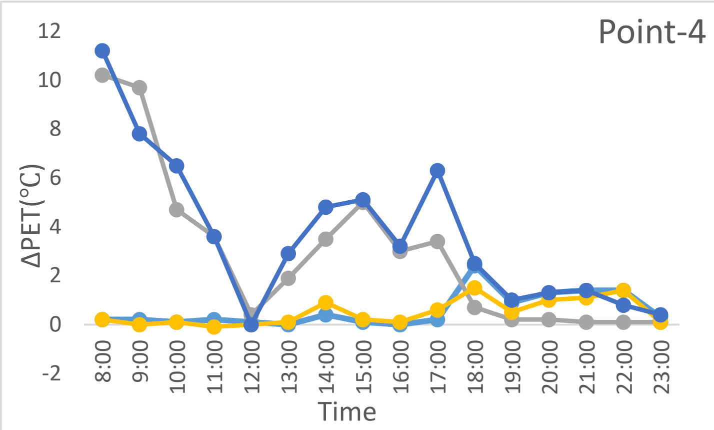

Figure.7-32 The thermal sensation improvement under point-4

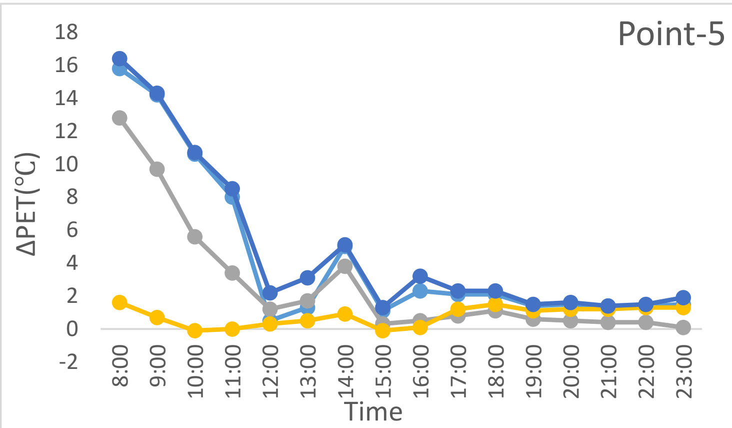

Figure.7-33 The thermal sensation improvement under point-5

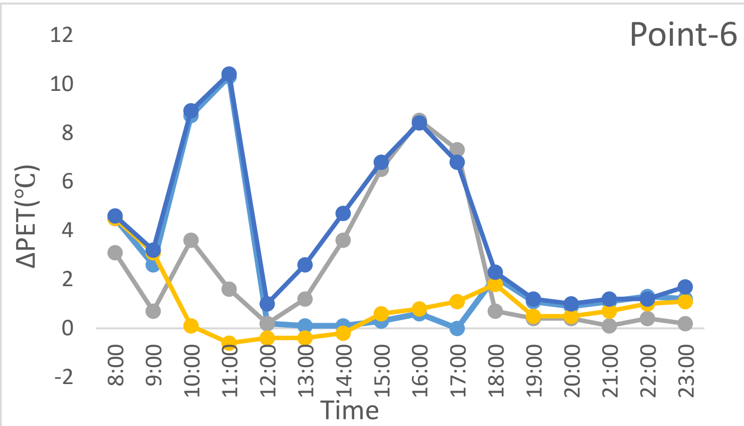

Figure.7-34 The thermal sensation improvement under point-6

From the past study, the worst thermal comfort condition always occurs from 2:00pm to 4:00pm in both the actual measurement and the Envi-met modeling. In this study, the LEONARDO images in Figure.7-35 and 7-36 show that the spatial distribution of PET across the study area for the 28th and 29th scenarios at 3:00pm.

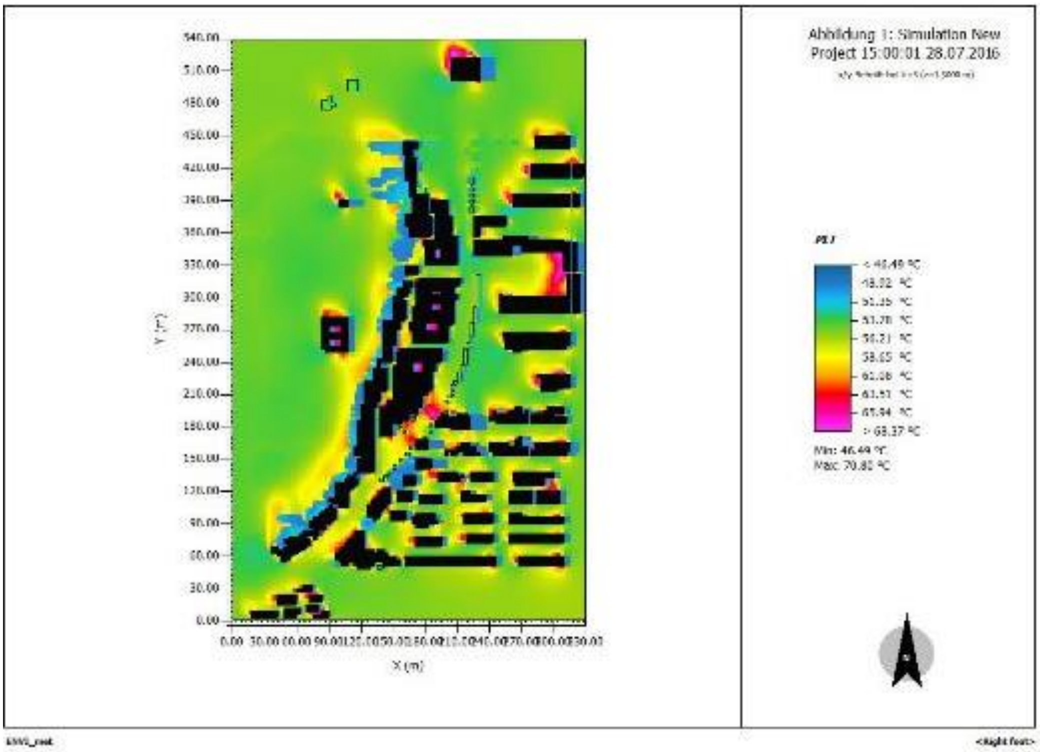

Figure. 7-35 Spatial distribution of PET (3:00pm) at (Z＝1.5m) for the existing scenario on Jul. 28th

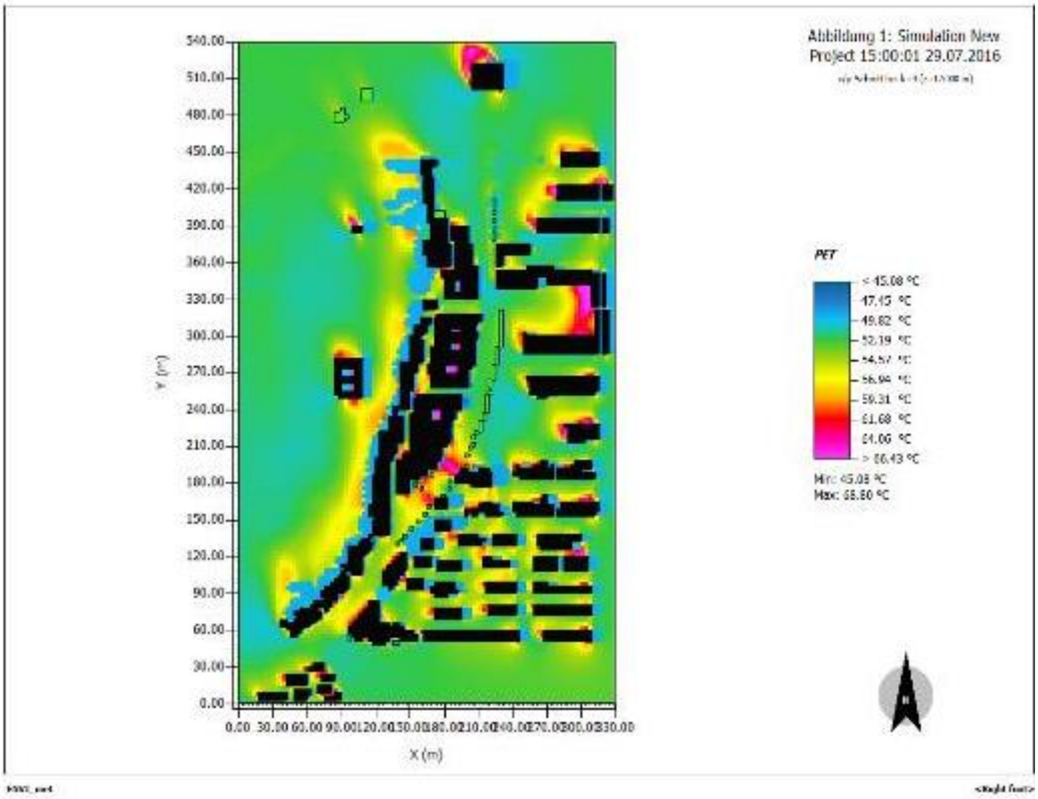

Figure. 7-36 Spatial distribution of PET (3:00pm) at (Z＝1.5m) for the existing scenario on Jul. 29th

Figure. 7-37 shows the distribution of PET based on the new scenarios. The PETs at the peak time (3:00pm) were compared to that of the existing scenario at a pedestrian level (1.5 m) (Figure.7-38).

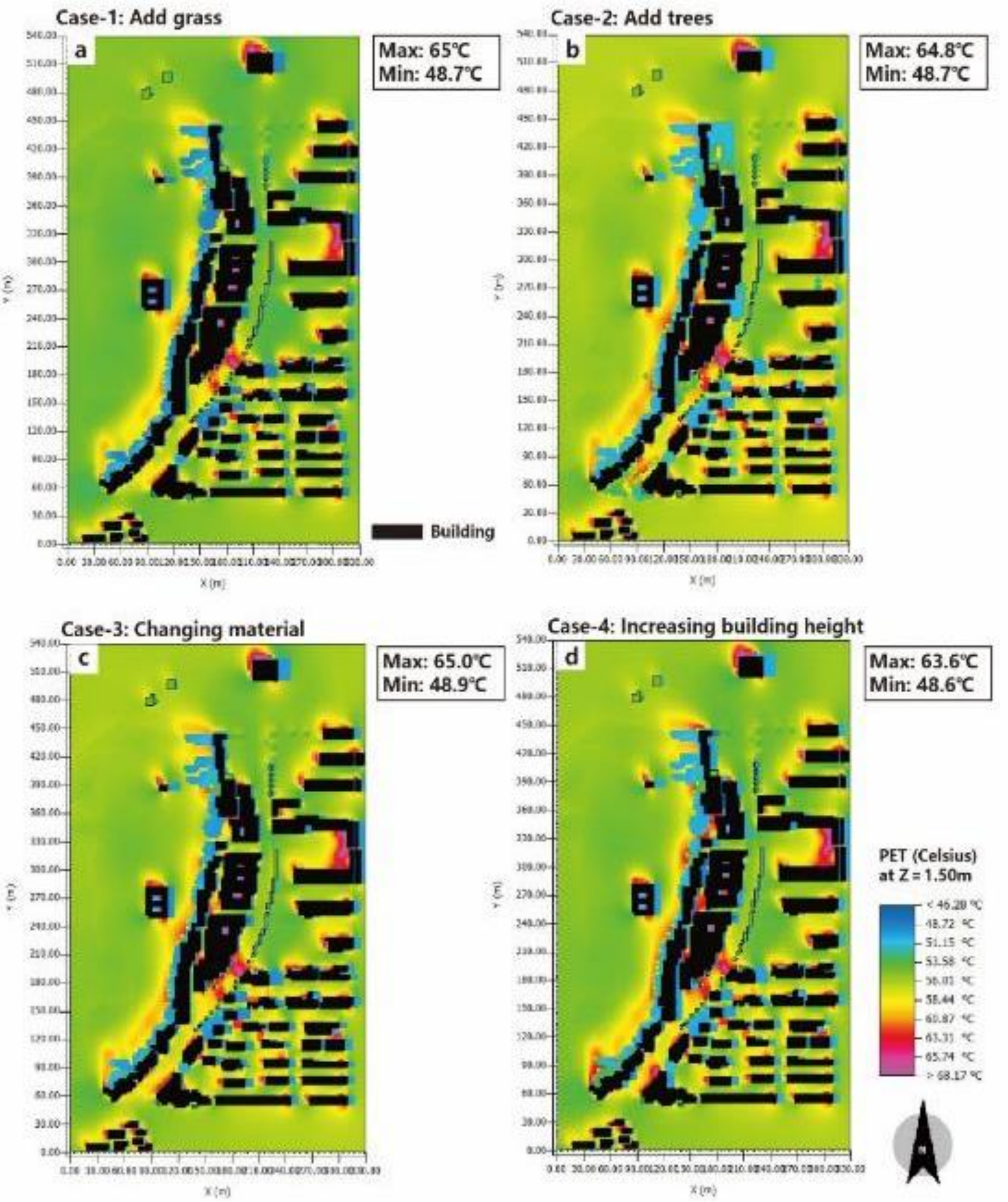

Figure. 7-37 PET in different cases at 3:00pm, (a) adding grass (b) adding trees (c) changing paving material with a high albedo (d) increasing building height at the pedestrian level (1.5m)

In Figure 7-38, the detailed cooling effect in each scenario can be easily observed, where the final PET results were processed with the same condition and range to evaluate a fair comparison between the existing scenario and four new ones. In the final simulated results, increasing tree coverage ratio of scenario-2 can significantly improve humans' thermal comfort, especially in open spaces (point-1), where ΔPET ranges from 1.5 to 3.1 ℃. In addition, trees also can improve thermal comfort in canyon space, which directly reduces PET from 1.2 to 8.1 ℃(point-5).

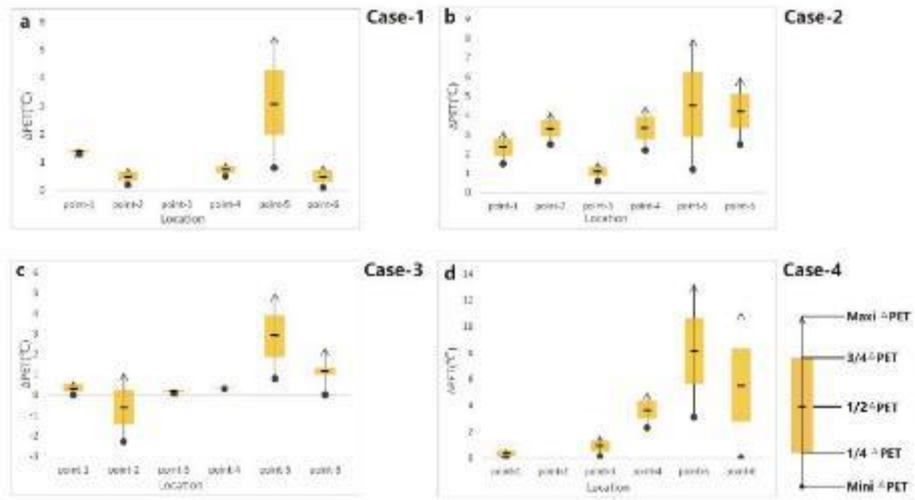

Figure. 7-38 Cooling effect of the new cases at 3:00pm, including (a) adding grass (b) adding trees (c) changing paving material with a high albedo (d) increasing building height at the pedestrian level (1.5m)

This cooling function can be attributed to shading and transpiration at daytime. In addition, in scenario-4, increasing three-story building coverage ratio a and average building height can obviously decrease PET, which ranges from 2.1 to 12.5℃ in canyon space (point-5), moreover, the microclimatic conditions in open space (point-1, point-2) don't change too much. Meanwhile, increasing the grass coverage ratio (scenario-1) and changing paving material with a higher albedo (scenario-3) also reduces PET effectively. But the extent can't reach scenario-2 and scenario-4. In our work, numerical simulations are conducted to assess the correlation between different parameters and modifications of thermal sensation in extreme summer, current results just show the distribution of PET modification through synergistic effect of different parameters in general. In next part, we will supply a more detailed introduction about the effect under four scenarios. According to the field survey, the whole region consist of open space and canyon space. Each different parameter will have different influence on sites. The effectiveness of all parameters in open space are shown in Figure. 7-39. The R2 between a parameter andΔ PET stands for the proportion that can be interpreted by variables of different regression models. As can be seen from this figure, a strong positive correlation was obtained between the ΔPET and tree coverage ratio (scenario-2), where it can be concluded that a 5% increase in tree coverage ratio could reduce PET by 0.4 ℃. Meanwhile, an invalid correlation between ΔPET and the percentage of three-story buildings can be found (scenario-4). The effect of grass (scenario-3) and paving material with a high albedo (scenario-4) were found to reduce PET effectively, but the extent is limited. What's worse, a negative correlation between the coverage ratio of the new paving material and Δ PET can be found, in which an ascension of 5% in the new paving material with high albedo may result in a little increase in PET. Because the paving material can be easily heated-up by solar radiation and enhance diffuse reflection, so it may decrease thermal comfort at daytime. According to the result of regression (Fig. 22-e, Fig. 22-f), it can be concluded that the correlation between Δ PET and H/W is irrelevant, what's worse, a weak negative effect occurs by increasing SVF.

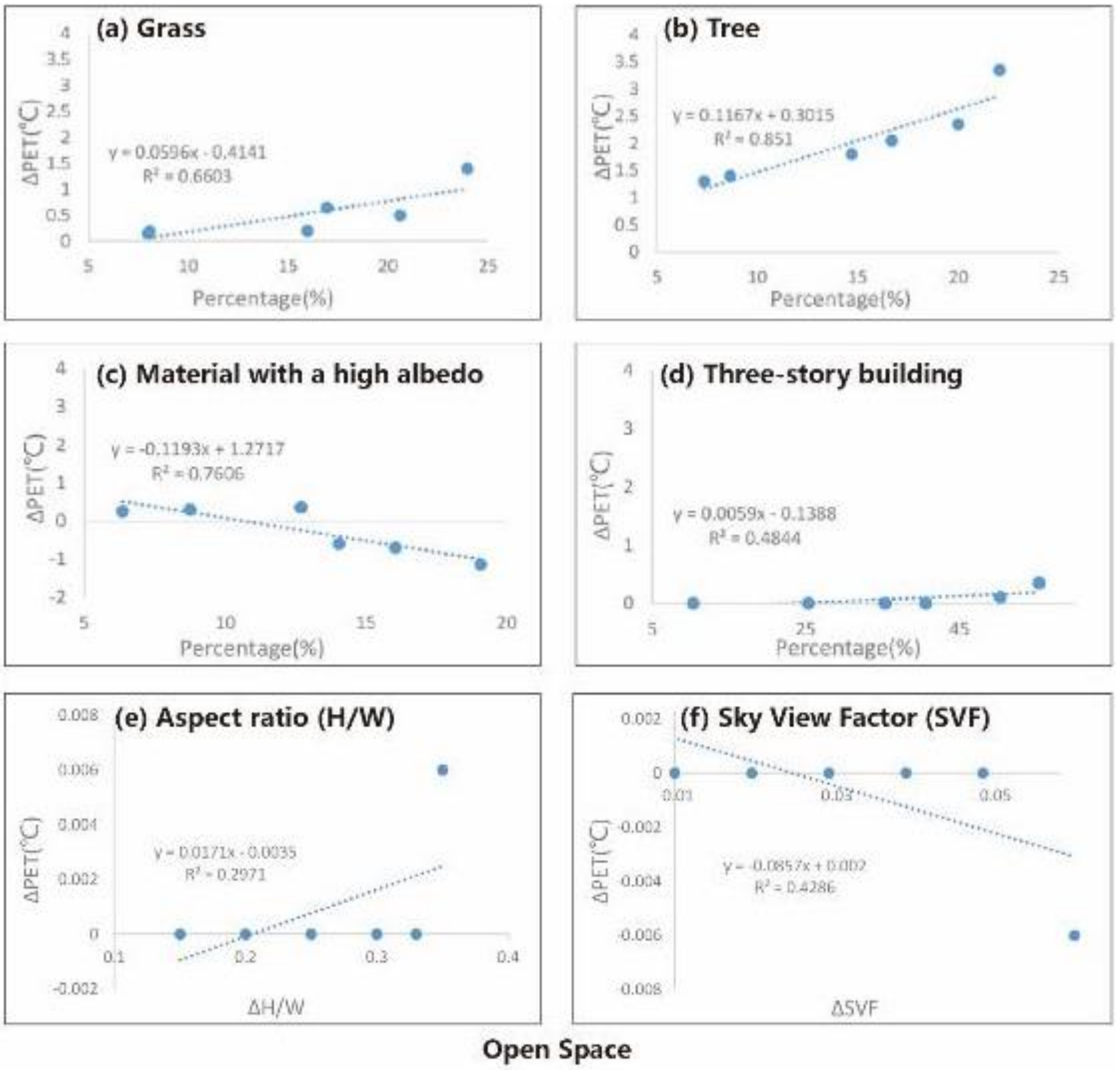

Figure. 7-39 Correlation between parameters and thermal comfort modification in open space at 3:00pm

In canyon space, as in open space, the increase in tree coverage ratio can also reduce PET obviously (case-2), a 5% increase in percentage of trees would contribute a reduction of 0.25 ℃ PET at daytime.

Meanwhile, increasing three-story building coverage ratio (case-4) can largely improve thermal comfort, it can be proved that 10% increase in the percentage of buildings would reduce 0.5℃ ΔPET at daytime, thus this function can be attributed to the canopy-shading, which could impede day-time radiation.

Different from open space, increasing H/W can effectively reduce PET, an ascension of 0.1 in H/W can reduce 0.15℃PET, meanwhile, an 0.1 increase in SVF will lead to increase 0.11℃PET at daytime.

According to the multiple regression analysis of the other two scenarios (scenario-1 and scenario-2), it can be concluded that grass and paving material with a high albedo can also improve thermal environment in canyon space. Grass can improve thermal environment by reducing reflected radiation at daytime. Paving material with lower albedo may be heated-up by radiation, so it is important to reduce the coverage ratio of such materials in canyon space.

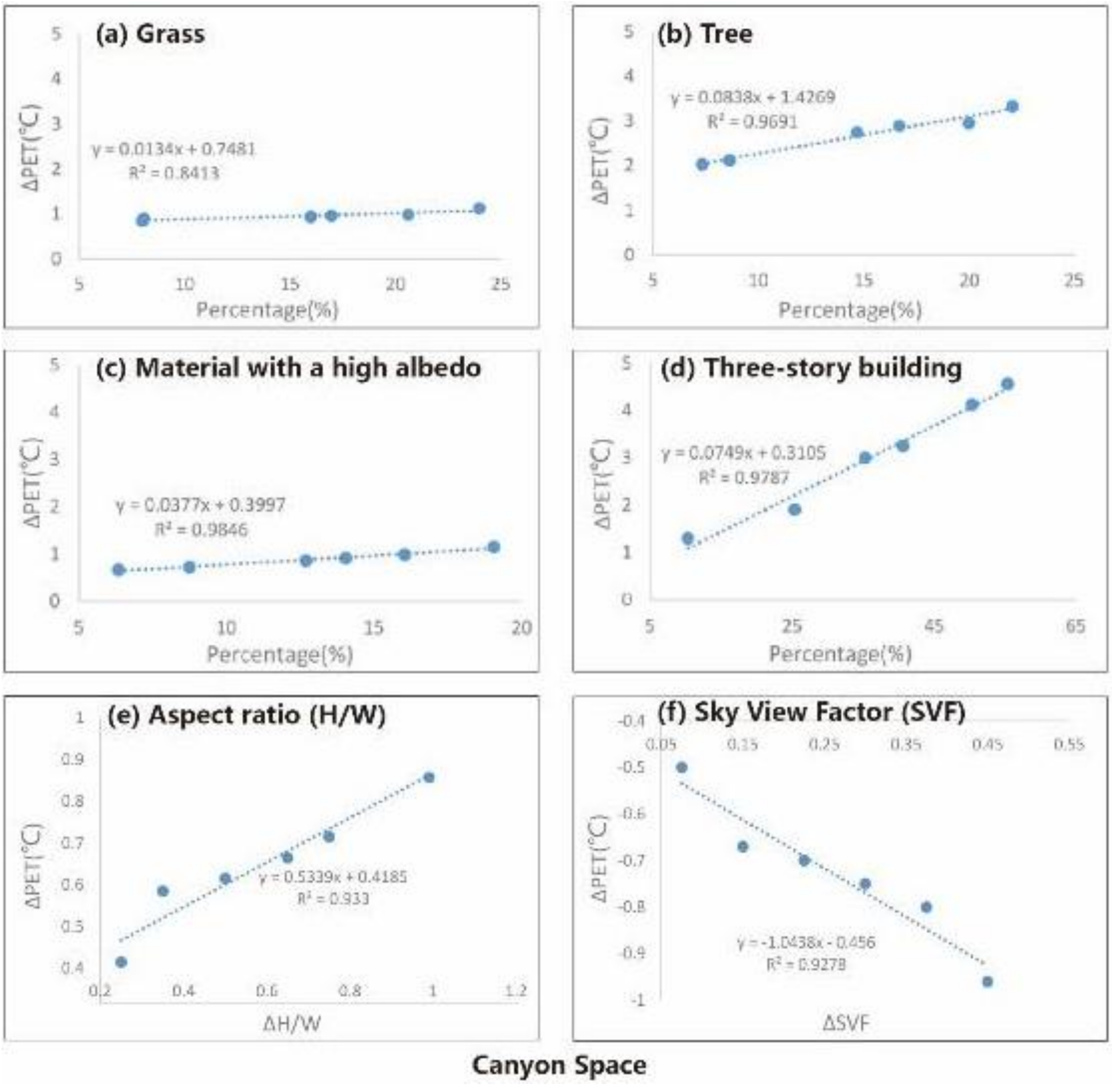

Figure. 7-40 Correlation between parameters and thermal comfort modification in canyon space at 3:00pm

Multiple regression of these different parameters about Δ PET at 3:00pm are assessed to achieve the effect of them on the thermal modification. The final conclusion can help designers and policy makers to improve the outdoor energy efficiency. The final result which indicates the correlation between each parameter and humans' thermal comfort is classified into different level for choosing (Figure. 7-41).

Spatial geometry	Grass	Tree	Material	Building	H/W	SVF
Open space	+0.6603	+0.851	-0.7606	+0.4844	+0.2971	-0.4286
Canyon space	+0.8433	+0.9691	+0.9846	+0.9787	+0.933	-0.9278

R^2 scale	Level of importance
0.75-1	Most important
0.50-0.75	More important
0.25-0.50	Less important
0-0.25	Least important

Figure. 7-41 Relationship between thermal comfort and different parameters

7.3.3. The cooling effect of different parameters in Tai Zhou Old block

As mentioned above, based on the current conditions of the simulated model, this existing case is defined as base and four new cases are developed to compare and evaluate the cooling effect of different parameter. Figure. 7-42 shows that the base case and four new cases with different coverage ratio of different parameter.

Figure. 7-42 The new cases: various types of different coverage ratio

All the new scenarios including the followings: (Case-1) As mentioned above, the buildings in pedestrianized-zone won't exceed three stories, this case aims at increasing building height to understand its cooling effect, in which the three-story building coverage ratio is added to 63.3% of this area. (Case-2) In this case, the coverage ratio of tree is added to 22% in order to make a better understanding of its influence. (Case-3) Like case-2, this scenario is applied by increasing coverage ratio of grass to improve outdoor thermal comfort and evaluate cooling effect in accordance with the local design specification. The last case (Case-4) is through changing the existing pavement material to assess the cooling effect and finding out its potential to increase outdoor energy efficiency. From the new cases, Figure. 17 and Figure. 18 show the improvement of PET has appeared in whole area. The PETs at peak time (2:00pm) are compared to the base case at a pedestrian level (1.5m) (Figure.7-44). In Figure. 7-44, it shows the detailed cooling effect of different cases, in which these PET results are processed with the same range and conditions to obtain a fair comparison between the existing scenario and four new cases. In the simulated result, increasing the coverage ratio of trees (Case-2) can improve humans' thermal comfort obviously, especially in open space (Point-4), where ΔPET ranges from 2.0℃ to 8.2℃. In addition, trees also can affect the thermal comfort in canyon space, which can reduce PET from 0.3℃ to 6.3℃ (Case-6). Its function can be attributed to transpiration and shading at daytime. In case-1, even increasing building height and increasing the coverage ratio of three-story building can also alleviate heat stress, it's not obvious, what's worse, the microclimatic conditions in open space (Point-4, Point-7) don't change too much. Meanwhile, increasing the coverage ratio of grass (Case-3) and replacing pavement material with higher albedo (Case-4) also can reduce PET effectively. But the extent can't reach case-1 and case-2. From the new cases, Figure. 17 and Figure. 18 show the improvement of PET has appeared in whole area. The PETs at peak time (2:00pm) are compared to the base case at a pedestrian level (1.5m) (Fig.18). In Figure. 18, it shows the detailed cooling effect of different cases, in which these PET results are processed with the same range and conditions to obtain a fair comparison between the existing scenario and four new cases. In the simulated result, increasing the coverage ratio of trees (Case-2) can improve humans' thermal comfort obviously, especially in open space (Point-4), where ΔPET ranges from 2.0℃ to 8.2℃. In addition, trees also can affect the thermal comfort in canyon space, which can reduce PET from 0.3℃ to 6.3℃ (Case-6). Its function can be attributed to transpiration and shading at daytime. In case-1, even increasing building height and increasing the coverage ratio of three-story building can also alleviate heat stress, it's not obvious, what's worse, the microclimatic conditions in open space (Point-4, Point-7) don't change too much. Meanwhile, increasing the coverage ratio of grass (Case-3) and replacing pavement material with higher albedo (Case-4) also can reduce PET effectively. But the extent can't reach case-1 and case-2.

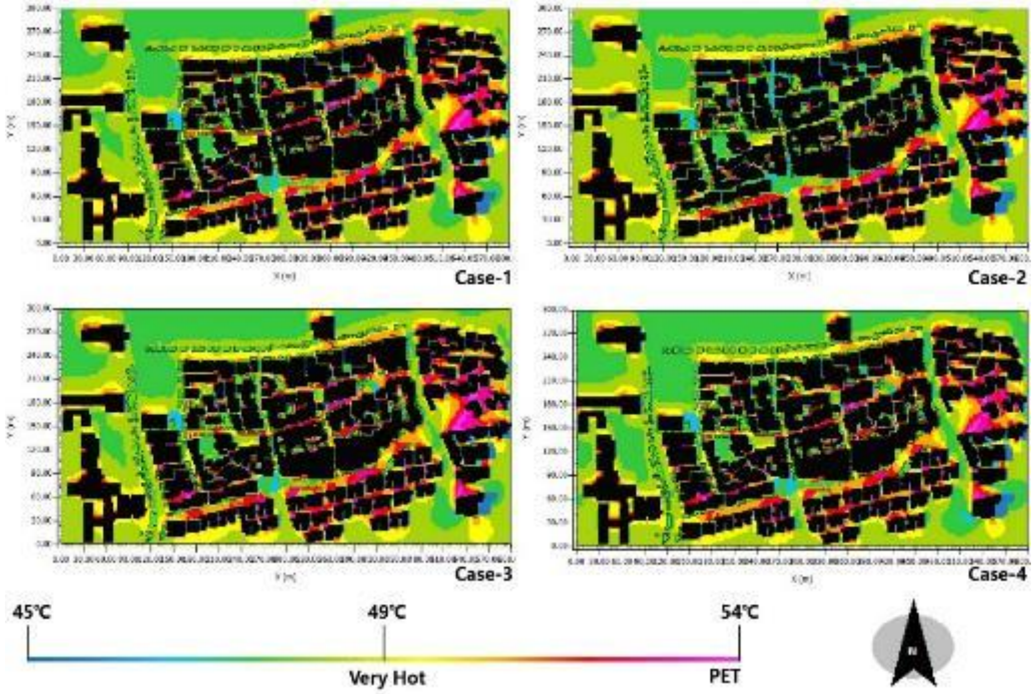

Figure. 7-43 New PET distribution in different cases at 2:00pm during the measured day

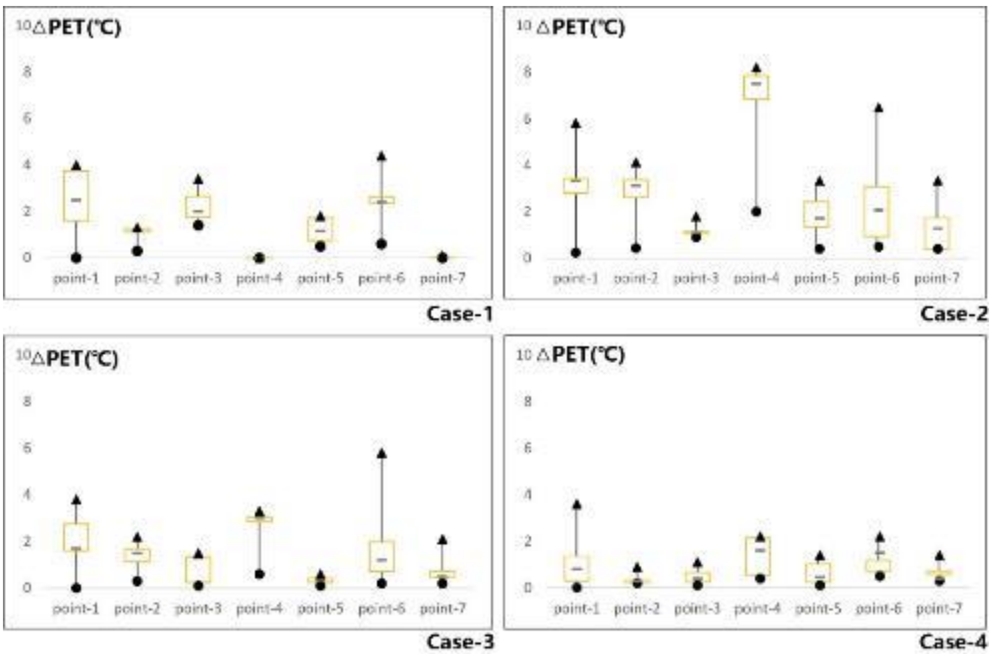

Figure. 7-44 Cooling effect of the new cases at 2:00pm

As mentioned above, the whole area was consist of open space and canyon space. Each parameter will have different influence on different spaces. The effectiveness of different parameters. The correlation coefficient (R2) between PET and different parameter is served to represent the proportion which can be interpreted by the variables of different regression model. In this figure, a strong positive correlation is found between the coverage ratio of trees and ∆PET (Case-2), in which we can conclude that 2% increase of the percentage of trees would reduce 0.8℃ in PET. Meanwhile, an invalid relationship between the percentage of three-story building and ∆PET can be observed (Case-1). The impacts of grass (Case-3) and pavement material with a high albedo (Case-4) are found to reduce PET effectively, but the extent is limited.

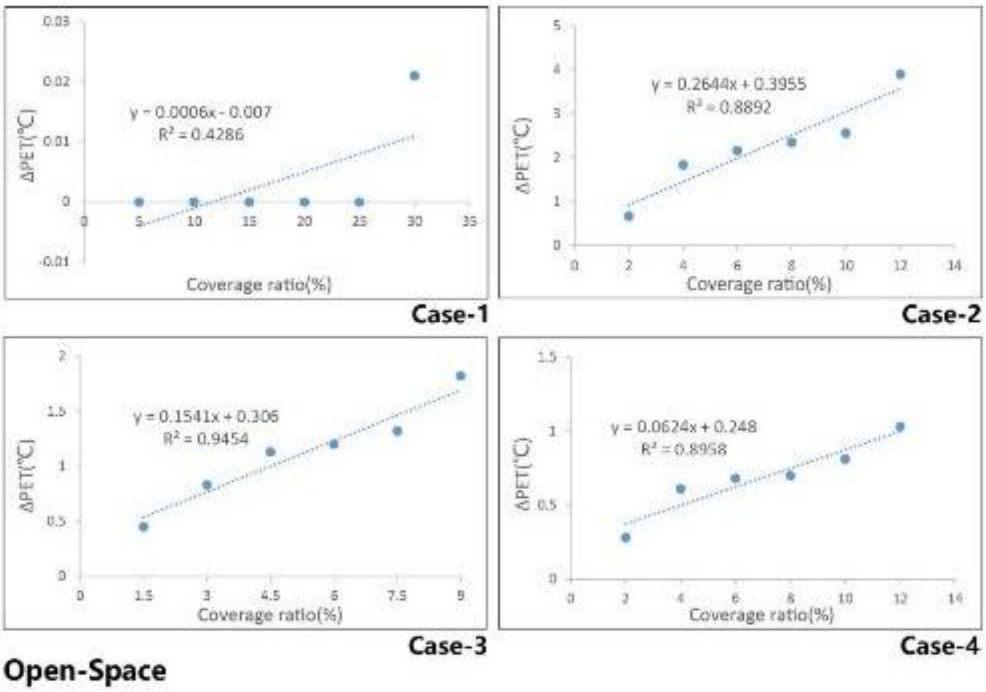

Figure. 7-45 Correlation between thermal comfort and coverage ratio of different parameter in open space at 2:00pm

Like the open space (Figure. 20), increasing the coverage ratio of trees also can reduce PET effectively (Case-2). Ascension of 2% in percentage of trees would lead to a 0.4℃ of PET in canyon space. In addition, increasing percentage of three-story building can make a contribution to thermal comfort improvement (Case-2), thus effect can be attributed to the canopy-shading, which can impede radiation. In accordance with the multiple regression analysis of other two cases (Case-3, 4), it can be concluded that grass land and the pavement material with a high albedo are also deterministic toward the thermal comfort improvement in canyon space. Grass can improve thermal comfort by reducing reflected radiation. The pavement material with lower albedo may be easily heated-up by radiation, so it’s necessary to reduce the coverage ratio of this zone. In order to make a deep understanding of the contribution of each parameter at daytime in different spaces. The result which indicates the correlation coefficient (R2) is presented in Figure. 7-48 and the R2 is classified into different levels of importance. In view of thermal comfort, the index PET in this study is used to calculate the energy balance of human’s body which is directly affected by surrounding factors. The numerical simulation result suggests us that a useful prediction of the effects of a pedestrianized-zone renewal can improve humans' thermal sensation through choosing a best way, thus helping to reduce outdoor energy consumption and improve energy efficiency effectively.

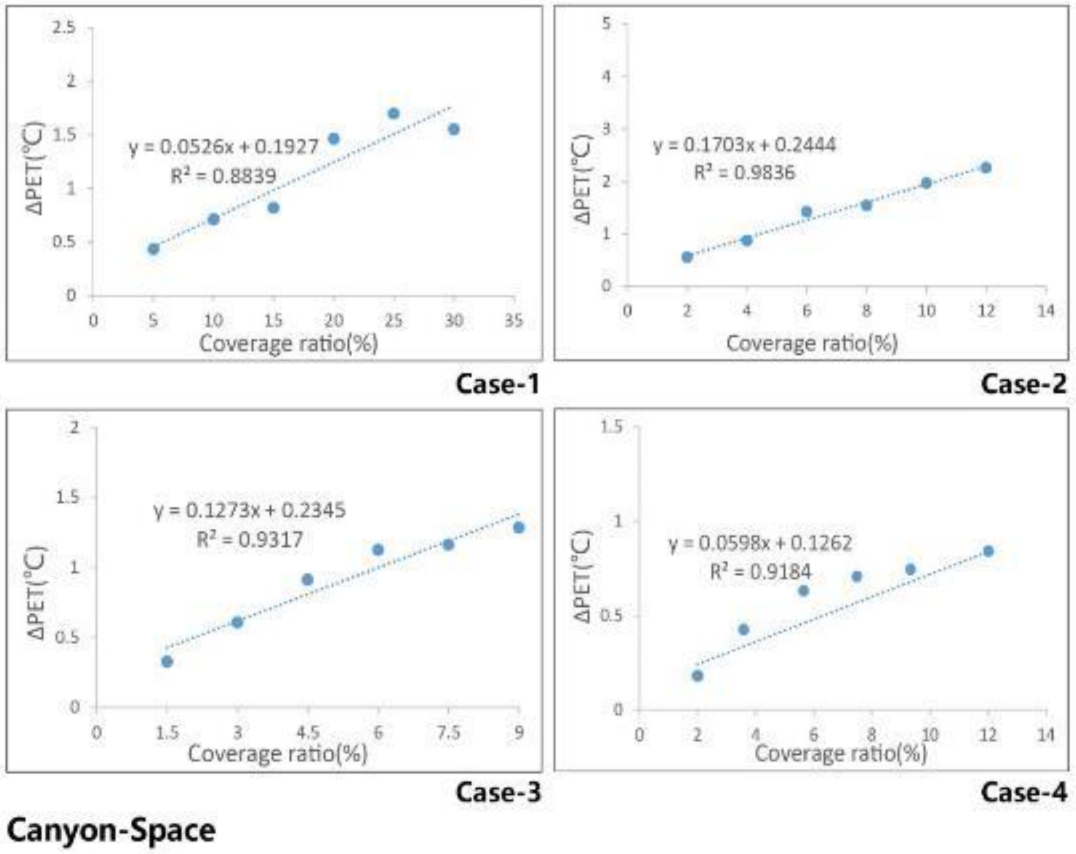

Figure. 7-46 Correlation between thermal comfort and coverage ratio of different parameter in open space at 2:00pm

Spatial geometry	Building	Tree	Grass	Material
Open space	0.4286	0.8892	0.9454	0.8958
Canyon space	0.8839	0.9836	0.9317	0.9184

R^2 scale	Level of effect
0.75-1	Most effective
0.50-0.75	More effective
0.25-0.50	Less effective
0-0.25	Least effective

Figure. 7-47 Correlation between different parameter and thermal comfort

7.4. The thermal calendar under new cases

7.4.1. The thermal calendar of Dao He Old block

Compared to the existing thermal comfort calendar (Figure. 7-49), point-1, 4 also have a cooling time from 8:00am to 10:00am in the daytime, point-2 can be visited from 8:00am to 11:00am and point-3, 5 have a good time for visiting from 8:00am to 12:00am, in addition, vegetation is the second influential factor. After 6:00pm, all the point-s have a good visiting environment. Different from the existing scenario, all the points are in "suitable" stage after 9:00 pm, two hours earlier than the existing scenario. According to the local design specification, the tree canopy coverage is not less than 25% in a built environment, but the existing block is not more than 5%. The thermal comfort calendar of 25%-vegetation is shown in Figure. 7-50. As figure shows that the thermal comfort of point-1and point-3 are better than the existing scenario from 8:00am to 9:00am, point-2, 4, 6 also can be visited from 8:00am to 10:00am and point-5 is at "Suitable"

and “Fairly suitable” stages from 8:00am to 11:00am. All the result means that the effectiveness of the increased trees coverage in reducing PET is more
significant than increased building height in the aspect of the open space. From 10:00am to 6:00pm, even the vegetation can cool down the inner space, all the selected points are not suitable for visiting. Like the existing scenario and case-1, after 6:00pm, all the points are suitable for visiting.

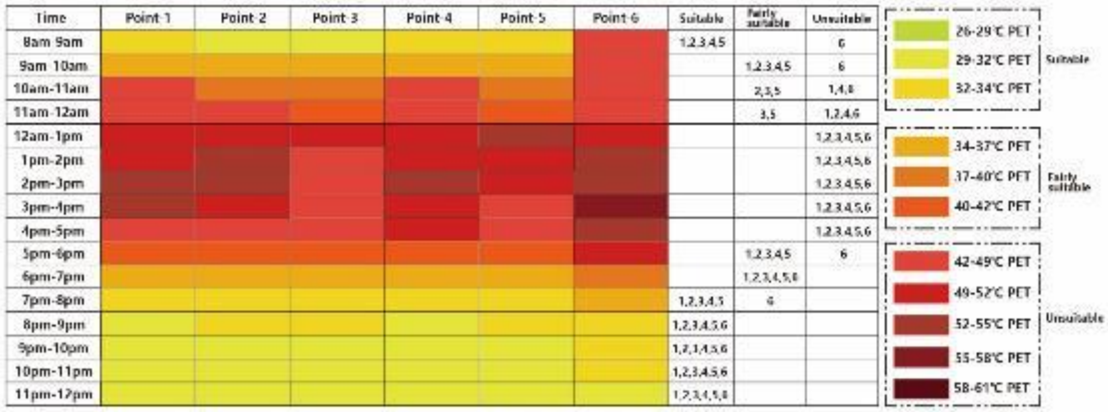

Figure. 7-48 Thermal comfort calendar of case-1

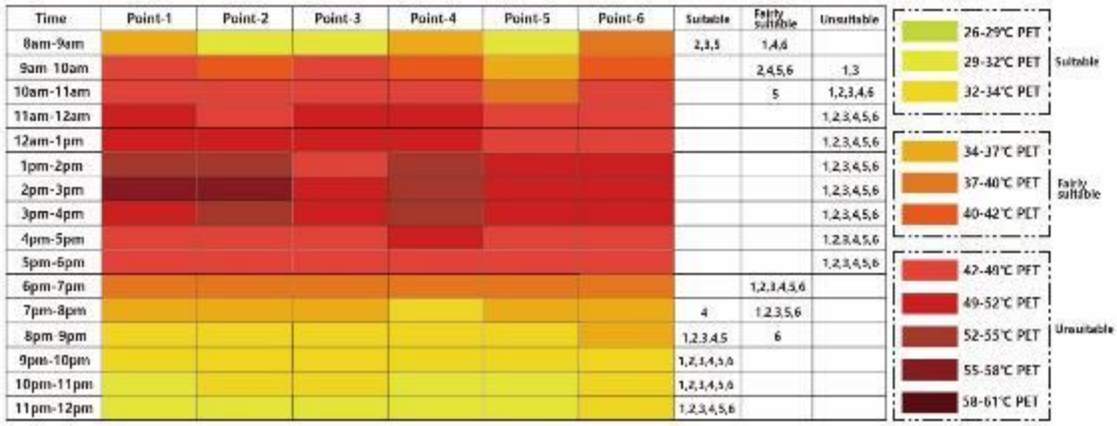

Figure. 7-49 Thermal comfort calendar of case-2

The calendar of case-3 is shown in Figure. 137. It is similar to the 25% -vegetation, tourists can visit the whole block from 8:00am to 10:00am and from 6:00pm to 12:00pm. Through compared the two simulation result, it is shown that the 50%-vegetation has a slightly better cooling effect than 25%- vegetation in the daytime. In the aspect of different oriented streets, increasing vegetation coverage has a better effect in point-2, 3, 5 than point-1, 4, 6. The increased tree coverage in reducing the PET in canyon-space is not as significant as the increased building height. On the contrary, the increased tree coverage is a more effective method to cool down the inner microclimate in the open spaces.

Figure.7-52 shows that the thermal calendar o after changing paving material with a high albedo. As the previous studies show that the pavement surface with a high albedo can keep the ground cooler, this research also finds that the high albedo results in decreased PET. Compared to the existing scenario, the new thermal calendar is not changed too much. The thermal calendar of rcase-4 is shown in Figure. 7-52. Compared to other scenarios, case-4 has the most effective influence on improving thermal comfort conditions in the daytime. After innovation, except the whole region can be visited from 8:00am to 10:00am and from 6:00pm to12:00pm, point-2, 3, 4 also can be visited from 10:00am to 12:00am, which largely broadens cooling time for tourists.

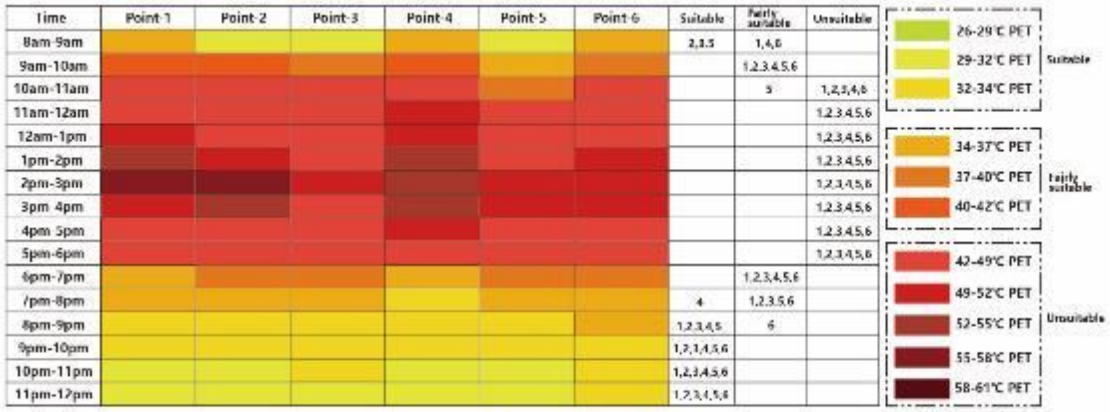

Figure. 7-50 Thermal comfort calendar of case-3

Figure. 7-51 Thermal comfort calendar of case-4

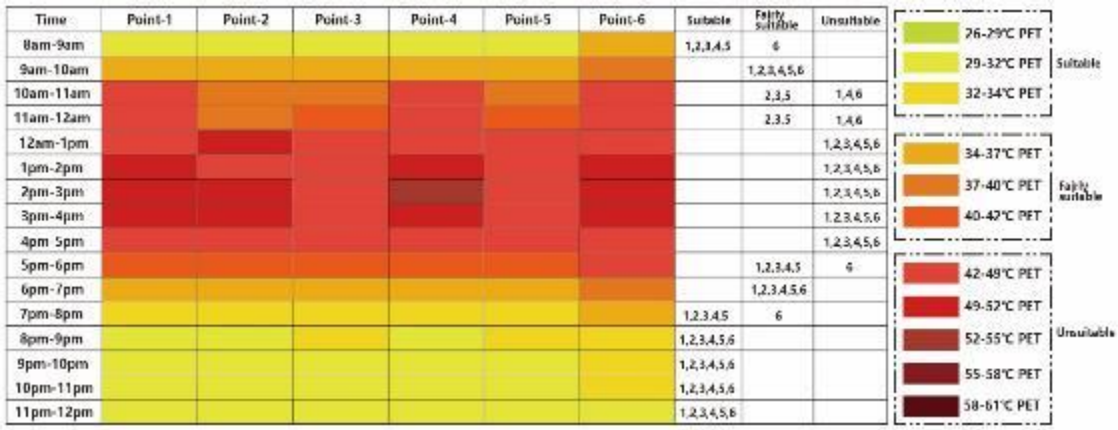

Figure. 7-52 Thermal comfort calendar of case-1, 2 , 3, 4

7.4.2. The thermal calendar of Tai Zhou Old block

According to the simulated results through increasing buildings height, it is obvious that the street with a high aspect ratio can reduce PET in the daytime. From the Figure. 7-54, compared with the existing thermal comfort calendar, point-1, 2, 4 also have a bad thermal comfort in the daytime from 8:00am to 18:00pm which proves that a high aspect ratio has a weak influence on the open space and the east-west oriented street, point-5, 6 have a good visiting time from 8:00am to 11:00am and point-3 is from 8:00am to 10:00am. After 18:00pm all the points have a good visiting surroundings.

Different from the existing scenario, all the points are in “suitable” stage after 21:00 pm, two hours earlier than the existing scenario. The way-1 has a strong influence on reducing the daytime PET and improve the thermal comfort.

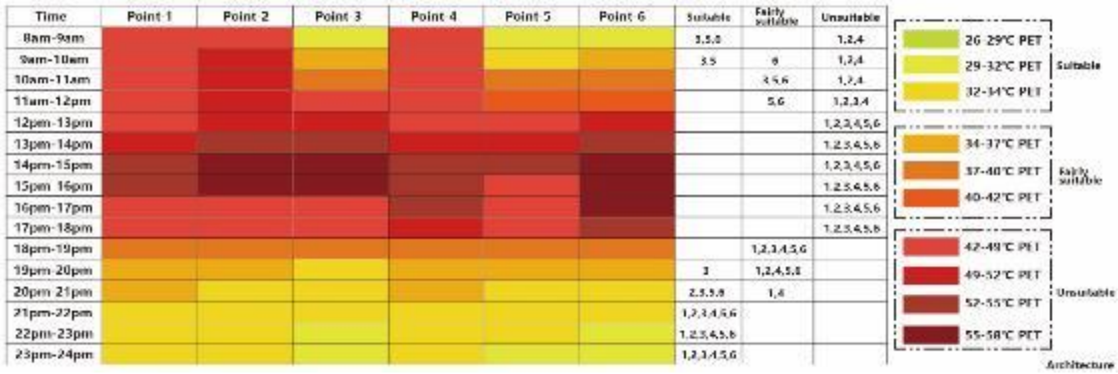

Figure. 7-53 Thermal comfort calendar of case-1

According to the local design specification, the tree canopy coverage is not less than 25% in a built environment, but the existing block is not less than 5%. The thermal comfort calendar of 25%-vegetation is shown in Figure. 7-55. As figure shows that the thermal comfort of point-1, 2 is lower than the existing scenario and way1 from 8:00am to 10:00am which means that the effectiveness of the increased tree coverage in reducing PET is more significant as increased building height in the aspect of open space. From 10:00am to 17:00pm, even the vegetation can cool down the inner space, all the tested points are not suitable for visiting. Like the existing scenario and reconstructed way1, after 18:00pm, all the points are suitable for visiting.

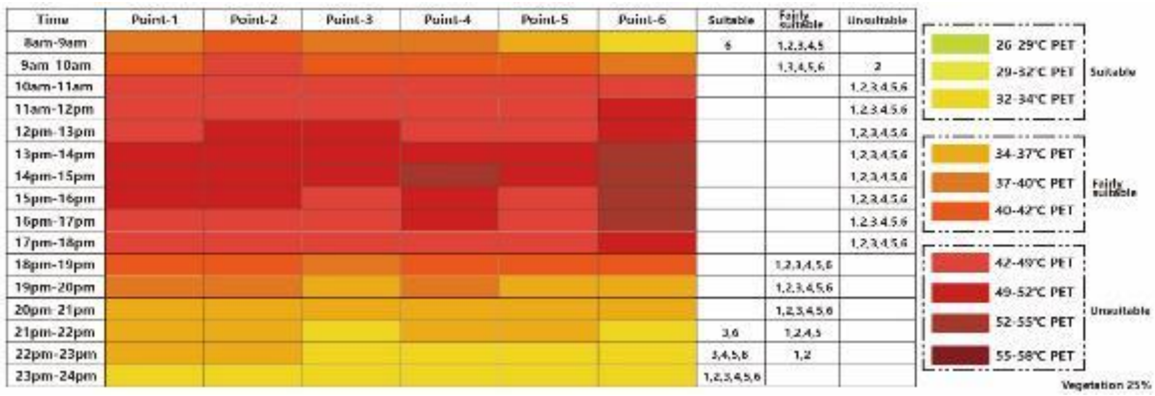

Figure. 7-54 Thermal comfort calendar of case-2

Figure. 7-56 shows that the thermal calendar of the ground surface after changing a material with a lower albedo. As the previous studies show that the pavement surface with a high albedo can keep the ground cooler, this research finds that the high albedo results in increased PET. Compared to the existing scenario, the way3 is not effective in reducing PET in the daytime.

The calendar of 50%-vegetation is shown in Figure. 7-57. It is similar to the 25% - vegetation, tourists can visit the block from 8:00am to 10:00am and from 18:00pm to 24:00pm. Through compared the two simulation result, it is shown that the 50%-vegetation has a more obvious cooling effect in the daytime. The thermal calendar of reconstructed way4 is shown in Fig. 34. Compared with the existing scenario, case-1, case-2, case-3, the reconstructed way has the most effective influence in reducing PET. Different from the aforementioned ways, the tourists also can visit point-3, 4, 5, 6 form

10:00am to 11:00am, what's more, the cooling effect is better than other ways.

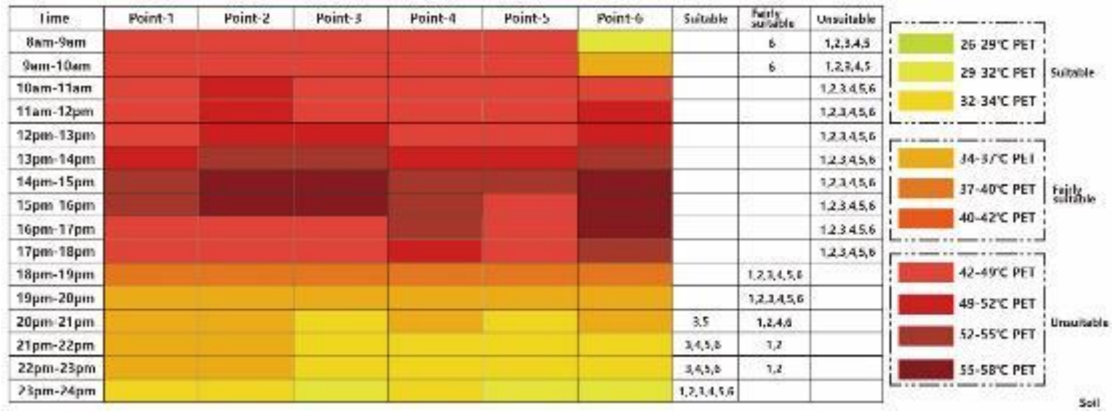

Figure. 7-55 Thermal comfort calendar of case-3

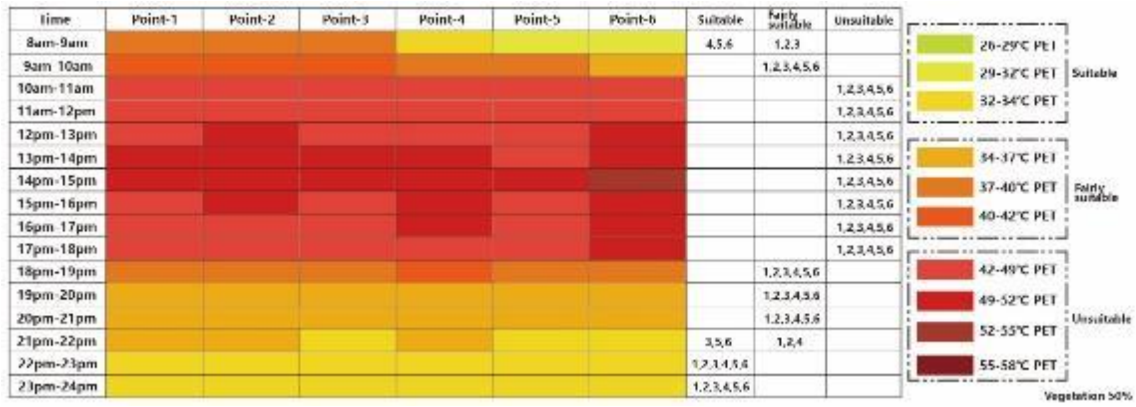

Figure. 7-56 Thermal comfort calendar of case-4

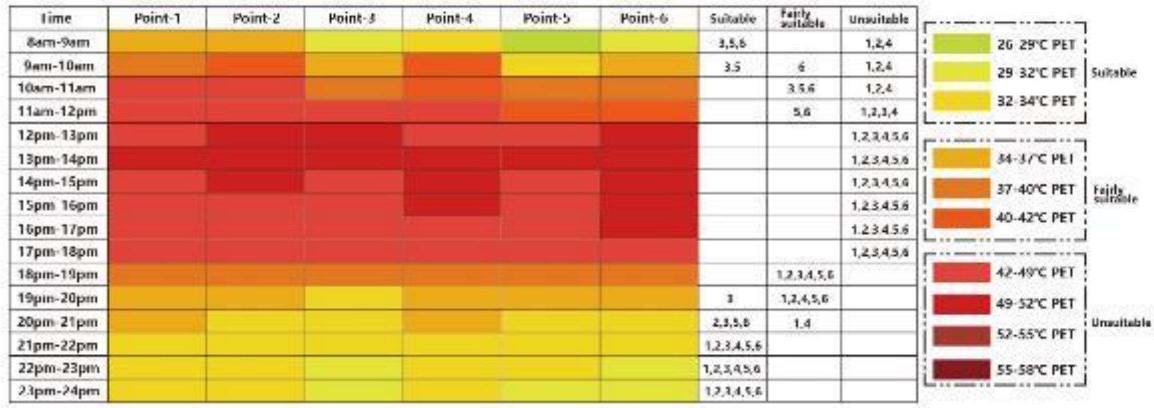

Figure. 7-57 Thermal comfort calendar of case-1, 2 , 3, 4

7.4.3. The thermal calendar of Ling Nan Tian Di block

In accordance with the simulated outcome under increasing building height (case-1), it is essential that the canyon with higher aspect ratio (H/W) (Figure. 7-58) can effectively reduce PET at daytime. Compared to the old thermal comfort calendar (base case) from 8:00am to 9:00am in early morning, except of point-4, other points are all at "suitable" stage. Like existing scenario, after 7:00pm all the points have a good visiting environment. As simulated result shows that different tree species will have different cooling effect at daytime. As Figure. 20 shows that increasing the vegetation coverage ratio of this zone can broaden the visiting times for tourists, compared to the existing scenario, point-4 also can be visited from 8:00am to 10am, moreover, point-1, 2,3 are all at “ Fairly suitable” stage from 10:00am to 11:00am. After 7:00pm, the difference between new thermal calendar and existing scenario isn’t obvious. As mentioned above, trees with higher LAI will have a much cooler effect in reducing PET at daytime. As expected, the cooling effect of *“Bischofia Javanica”* is much better than the *“Ficus Microcarpa”*. As is shown in Figure. 7-58, all the selected points are all at “Suitable” stage from 8:00am to 9:00am. Compared to the *“Ficus Microcarpa”* Compared to existing scenario, changing paving material (Figure. 7-59) can’t effectively expand the cooling time for tourists. scenario, even in the “Unsuitable” period, the *“Bischofia Javanica”* can alleviate heat stress effectively.

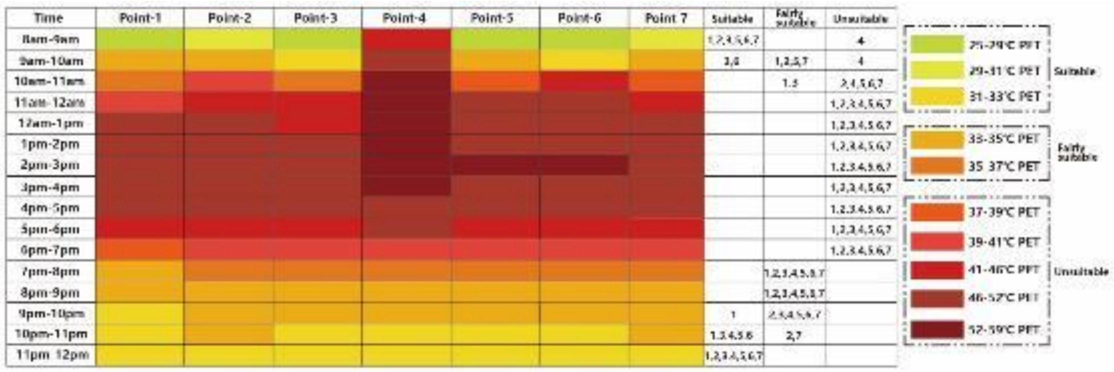

Figure. 7-58 Thermal comfort calendar of case-1

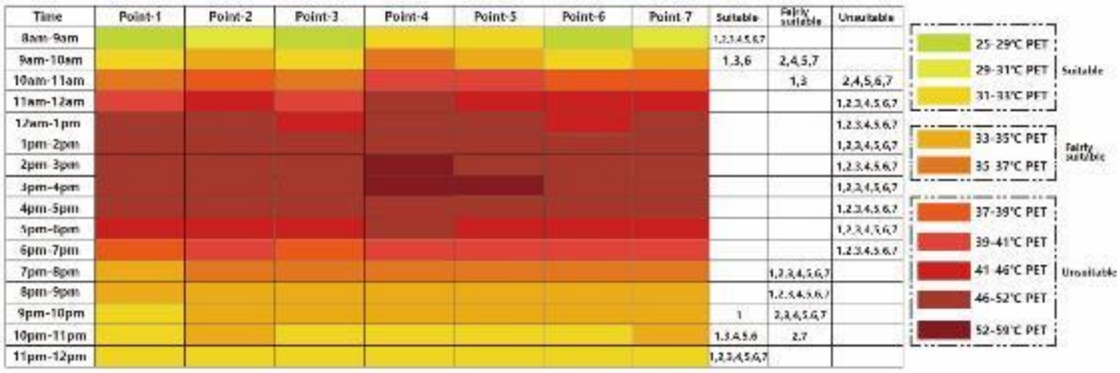

Figure. 7-59 Thermal comfort calendar of case-2

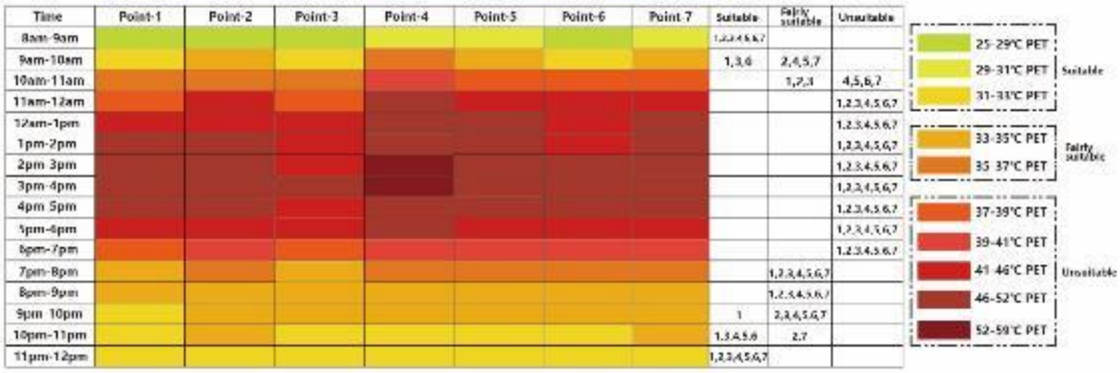

Figure. 7-60 Thermal comfort calendar of case-3

Figure. 7-60 shows the thermal calendar under case-4, compared to all the aforementioned calendars, the last case has the strongest influence on expanding visiting time for tourists. Except of point-4 and point-7, other points can also be visited from 10:00am to 11:00am.

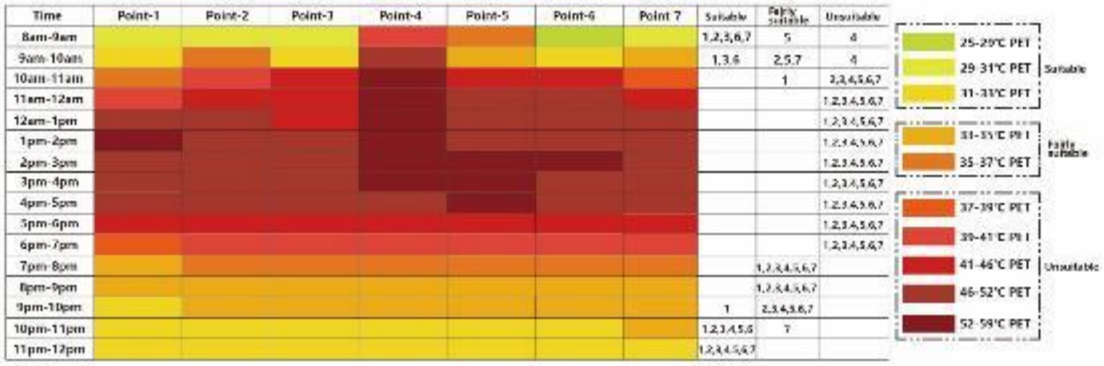

Figure. 7-61 Thermal comfort calendar of case-4

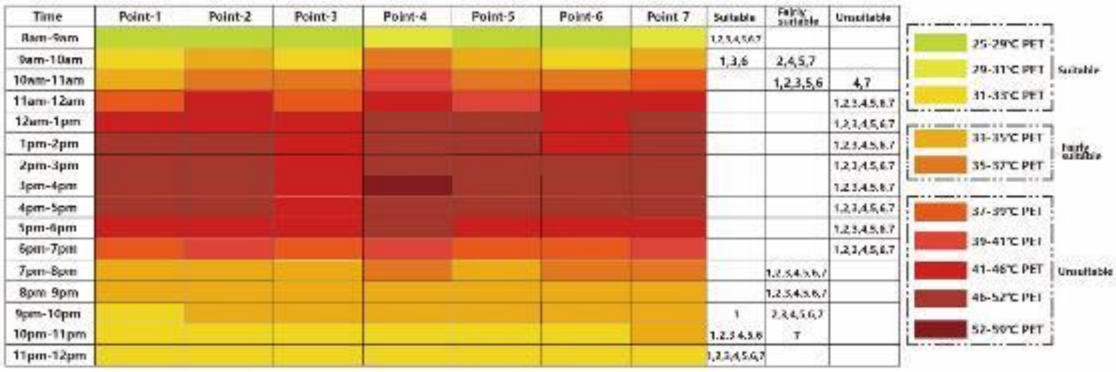

Figure. 7-62 Thermal comfort calendar of case-1, 2, 3 , 4

7.5. The summary

Urban tourism is a significant factor to improve the financial income of a city. Research about the tourism has been conducted by using data provided by meteorological stations and numerical simulation in this study. Also, this study highlights the importance of planning strategies in creating thermally comfortable environment at pedestrian level in a commercial block. Because of the importance in Tai Zhou city, Dao He Old Block and Ling Nan Tian Di attracts many tourists every year.

Numerical simulation and on-site measurement are performed to examine humans' thermal comfort in extreme summer, which will help designers and local managers understand the impact of different thermal comfort. According to the simulation results, almost none parts of this block are within comfortable zone during the day in the existing scenario in the daytime, however, the area of point-3 can be stilled visited from 8:00am to 9:00am and point-5 can be visited from 8:00am to 11:00am, other points are still limited for visiting.

The new cases for redesigning this block is shown in three stages: increasing building height, increasing vegetation coverage ratio, changing paving material. These new strategies are also modelled using ENVI-met to examine their effect on pedestrian thermal comfort in extreme summer. The new results show that deeper canyon (increasing building height) with high aspect ratio (H/W) and lower sky view factor (SVF) contributes to a lower level of PET at daytime, compared to the existing scenario. In open space, increasing tree coverage ratio can cause 0.5℃-8.7℃ reduction on PET at pedestrian level. Incorporating future strategies have caused an overall improvement in outdoor humans' pedestrian thermal comfort in extreme summer. Comparison of

PET level across different strategies shows that increasing aspect ratio (H/W) can ameliorate heat stress in canyon space, which can broaden visiting time for tourists. Because of the lack of shading, open space experiences a worse thermal environment at daytime, increasing tree coverage ratio is the only important strategy in mitigating thermal discomfort at pedestrian level, along with increasing vegetation ratio to 25% can generate a small reduction at PET level, also the visiting time for tourists isn't changed too much. But the simulation results for increasing coverage ratio from 25% to 50% would lead to a more cooling effect, therefore, a more cooling time for tourists is given. Even changing paving material also can alleviate heat stress, but it's still limited. The various strategies (case-4) is the most effective method in improving thermal comfort, compared to existing scenario, the comfortable time for tourists is nearly more than three hours.

The final results of this study could help tourists choose the best time for visiting this region also provide urban panning recommendations for designers and policy makers. Based on the conclusions of the current work, for improving thermal comfort at pedestrian level, it is suggested that:

1. Increasing building height. Shading tends to be an important factor throughout the daytime hours in canyon space. According to the previous studies [5-6], the most effective shading elements are often vertical objects such as building themselves, which can cast deep shadows that impede direct solar radiation, in addition, the heat may dissipate through long-wave radiation and turbulent transport throughout the sky vault above the street.
2. Increasing vegetation coverage ratio. Trees intercept not only solar radiation, but also long-wave radiation from the ground, building surfaces and the sky. Many researchers have reported that trees reduce air temperature in their vicinity, and often this is attributed to evapotranspiration from the leaf canopy.
3. Reducing the percentage of harden ground. The simulation result shows that the paving material with high albedo can contribute to a lower PET at daytime, but it's still limited. Designers can use lawn and trees to replace harden ground to their largest extent.
4. Combining various strategies. It is observed from the simulation result that various strategies can largely reduce PET at daytime, which also provides a better cooling time for tourists.

In addition, this study also has some limitations. Even there is a strong correlation between measured data and simulated data, the software ENVI-met still has some disadvantages. For instance, the walls of the buildings are set up as a single wall, which may not happen in the real world. Furthermore, the simulation only considers air temperature and relative humidity, while wind velocity, direction and cloudiness are ignored.

Chapter-8.

Summary and outlook

8. Summary and outlook

8.1. Main conclusions of this paper

This article revolves around the typical city of hot and humid climate of Tai Zhou and Fo Shan, in the comfort of the thermal environment, researching user activities and the scenery of the pedestrian street on the three levels of design, qualitative and quantitative research on the impact of landscape design on street microclimate and user behavior, the specific research work and main conclusions are as follows:

8.1.1. Hot-summer and Cold-winter climate zone

1. In canyon space, increasing three-story building coverage ratio (TSBCR) can directly change humans' thermal sensation, where it shows that Δ PET= 0.0749 ×TSBCR＋0.3105 with the most important R^2 value of 0.9787. Meanwhile, increasing three-story building coverage ratio can largely improve thermal comfort, it can be proved that 10% increase in the percentage of buildings would reduce 0.5℃ ΔPET at daytime, thus this function can be attributed to the canopy-shading, which could impede day-time radiation. Which could impede day-time radiation. Different from open space, increasing H/W can effectively reduce PET, an ascension of 0.1 in H/W can reduce 0.15℃PET, meanwhile, an 0.1 increase in SVF will lead to increase 0.11℃PET at daytime. The increase in tree coverage ratio can also reduce PET obviously, a 5% increase in percentage of trees would contribute a reduction of 0.25 ℃ PET at daytime.
2. In open space, the most essential factor on alleviating heat stress in open space is adding trees coverage ratio (TCR), where it shows that Δ PET= 0.1167×TCR ＋0.3051 with the most important R2 value of 0.851, as TCR increases from 1.02% to 22.06%, a strong positive correlation was obtained between the ΔPET and tree coverage ratio (scenario-2), where it can be concluded that a 5% increase in tree coverage ratio could reduce PET by 0.4 ℃.

8.1.2. Hot-summer and Warm-winter climate zone

1. In canyon space, it's easy for us to utilize the linear regression for understanding the relationship between coverage ratio of trees (TCR) and thermal comfort in canyon space, which shows that Δ PET= 0.1703×TCR＋ 0.2444 with a most important R2 value of 0.9836, for TCR increases from 12.5% to 22%. Ascension of 2% in percentage of trees would lead to a 0.4℃ of PET in canyon space. In addition, increasing percentage of three-story building can make a contribution to thermal comfort improvement (Case-2), thus effect can be attributed to the canopy-shading, which can impede radiation. In accordance with the multiple regression analysis of other two cases (Case-3, 4), it can be concluded that grass land and the pavement material with a high albedo are also deterministic toward the thermal comfort improvement in canyon space. Grass can improve thermal comfort by reducing reflected

radiation. The pavement material with lower albedo may be easily heated-up by radiation, so it's necessary to reduce the coverage ratio of this zone.

2. In open space, increasing overage ratio of trees (TCR) can effectively improve humans' thermal comfort, which shows that Δ PET= 0.2644×TCR＋0.3955 with a most important R2 value of 0.8892. A strong positive correlation is found between the coverage ratio of trees and ΔPET (Case-2), in which we can conclude that 2% increase of the percentage of trees would reduce 0.8℃ in PET. Meanwhile, an invalid relationship between the percentage of three-story building and ΔPET can be observed (Case-1). The impacts of grass (Case-3) and pavement material with a high albedo (Case-4) are found to reduce PET effectively, but the extent is limited.

8.2. The innovation of this article

The innovation of this article is as following:

1. The theoretical framework of microclimate research in typical urban pedestrian streets in southern China is summarized. Analyzing the summer microclimate conditions and usage of the pedestrian street in the hot and humid area, and analyzing the street orientation, aspect ratio, plant shading, spray impact on microclimate, and the landscape design in the urban pedestrian streets.
2. At the same time, using field measurements to Study the steps under the influence of urban microclimate the street comfort and use conditions, systematically and comprehensively studied the summer microclimate problem in the hot summer and cold winter regions, and use the statistical analysis method to carry out the city in the hot and humid area.
3. Compared the simulated result to measured data, and find out the accuracy of the simulated software. Evaluating different parameters (building height, vegetation, paving material) on decreasing heat stress in hot summer.
4. In this study, the thermal calendar for human is put forward. In addition, the new thermal calendar for human under the effect of different parameter (building height, vegetation, paving material) is also evaluated.

8.3. Prospects for future research work

1. In this study, we only consider a single tree species, it is very important for us to consider more species in our future work.
2. It is important to mention that the building façade material in the software is assumed as the same material, perhaps this isn't existed in the real world.
3. In this study, we don't consider other parameters such as water body and so on.

Reference

[1] Norman J. Rosenberg, Blaine L. Blad, Shashi B. Verma. Microclimate, The Biological Environment [M]. Second Edition. USA:Wiley-Interscience Publication, 1983: 1-5

[2] Wikipedia,UrbanClimate [DB/OL]. http://en.wikipedia.org/wiki/Urban_climate, last modified on 9 December 2009.

[3] United Nations Website, World Urbanization Prospects-The 2007 Revision Population Database [DB/OL], http://esa.un.org/unup, last modified in 2007.

[4] Matthias Roth, Review of urban climate research in (sub)tropical regions[J]. International Journal of Climatology, 2007, 27:1859-1873

[5] United States Environemntal Protection Agency Website, Actions Local Heat Island Effect [DB/OL]. http://yosemite.epa.gov/oar/globalwarming. nsf/content /Actions Local Heat Island Effect. html, cited in 2009

[6] Stéphanie Vandentorren, et al. Mortality in 13 French Cities During the August 2003 Heat Wave [J] American Journal of Public Health, 2004, 94(9)

[7] Kovats S, Wolf T, Menne B, Heatwave of August 2003 in Europe: provisional estimates of the impact on mortality [N]. Eurosurveillance Weekly, 11 March 2004; 8(11).

[8] H. E. Landsberg, The Urban Climate [M]. London: Academic Press, 1981:5-10

[9] T. R. Oke, City size and the urban heat island [J]. Atmos. Environ., 1973,7: 69- 79.

[10] F. Fezer, Wieweit verbessern Griinfl/ichen das Siedlungsklima [J]. Heidelberg Univ. J,1976, 57: 77 - 79.

[11] L. Finke, Zuordnung und Mischung von bebauten und begrunten Flachen [M]. Schriftenr. Stadtebau Forsch. 03.044, BMRBS, Bonn, 1976: 60-90

[12] F. Wilmers, Green for melioration of urban climate [J]. Energy and Buildings, 1988, 11: 289-299

[13] FRITZ WILMERS, Effects of Vegetation on Urban Climate and Buildings[J]. Energy and Buildings, 1990/91: 15-16, 507-514

[14] Diane Relf, Enhancing Our Environment through Landscaping [M]. Virginia Cooperative Extension, 1996: 48-69

[15] Linares, C., & Diaz, J. (2008). Impact of high temperature on hospital admissions: comparative analysis with previous studies about mortality. The European Journal of Public Health, 18, 317–322.

[16] Andrade, H., & Alcoforado, M. J. (2008). Microclimatic variation of thermal comfort in a district of Lisbon (Telheiras) at night. Theoretical and Applied Climatology, 92, 225–237.

[17] Ali-Toudert, F., & Mayer, H. (2007). Thermal comfort in an east–west oriented street canyon in Freiburg (Germany) under hot summer conditions. The oretical land Applied Climatology, 87, 223–237.

[18] Bottillo, S., De Lieto Vollaro, A., Galli, G., & Vallati, A. (2014). Fluid dynamic and heat transfer parameters in an urban canyon. Solar Energy, 99, 1–10. http://dx.doi.org/10.1016/j.solener.2013.10.031

[19] Chen, L., Ng, E., An, X., Ren, C., Lee, M., Wang, U., et al. (2012). Sky view factor analysis of street canyons and its implications for daytime intra-urban air temperature differentials in high-rise, high-density urban areas of Hong Kong: a GIS-based simulation approach. International

Journal of Climatology, 32,121–136. http://dx.doi.org/10.1002/joc.2243
[20] Sharmin, T., & Steemers, K. (2013). Effect of canyon geometry on outdoor thermal comfort: a case study of high-density, warm-humid climate. In Proceedings of the 29th PLEA conference, sustainable architecture for a renewable future.
[21] Shashua-Bar, L., Pearlmutter, D., & Erell, E. (2009). The cooling efficiency of urban landscape strategies in a hot dry climate. Landscape and Urban Planning, 92,179–186. http://dx.doi.org/10.1016/j.landurbplan.2009.04.005
[22] Ca, V. T., Asaeda, T., & Abu, E. M. (1998). Reduction in air conditioning energy caused by a nearby park. Journal of Energy and Buildings, 29, 83–92.
[23] Wong, N. H., & Chen, Y. (2004). The thermal effects of city greens on surroundings under the tropical climate. In Built environments and environmental buildings, proceedings of the 21st international conference of passive and low energy architecture.
[24] Kumakura, E., Nakaohkubo, K., & Hoyano, A. (2013). Solar shading effects by tree species in an urban environment using numerical simulation tool. In Proceedings of the 29th PLEA conference, sustainable architecture for a renewable future.
[25]U.S. Department of Energy, Landscaping [EB/OL]. http://www.energysavers.gov/your_home/ landscaping/index.cfm/mytopic=1195, cited in 2009
[26]V. Olgyay, Design with Climate: Bioclimatic Approach to Architectural Regionalism[M]. USA: Princeton University Press, 1963:
[27] Alan K.Meier, Strategic landscaping and air-conditioning savings-A literature review [J]. Energy and Buildings, 1990/91:15-16, 479-486.
[28] ASHRAE Standard 55-1992, Thermal. Environmental. Conditions for. Human Occupancy [S], USA: Atlanta: American Society of Heating, Refrigerating and Air Conditioning Engineers (ASHRAE), 1992
[29] Matthias Roth, Review of urban climate research in (sub) tropical regions[J]. International Journal of Climatology, 2007, 27:1859-1873
[30] Emmanuel R, Johansson E, Influence of urban morphology and sea breeze on hot humid microclimate: the case of Colombo, Sri Lanka.[J]. Climate Research, 2006(30): 189–200.
[31] Ribeiro H, Heat island in Sao Paolo, Brazil: effects on health [J]. Critical Public Health, 2005(15): 147–156.
[32] Pearlmutter D, Berliner P, Shaviv E, Integrated modeling of pedestrian energy exchange and thermal comfort in urban street canyons [J]. Building and Environment, 2007,42: 2396–2409
[33] Jonsson P., Vegetation as an urban climate control in the subtropical city of Gaborone, Botswana. [J]. International Journal of Climatology, 2004, 24: 1307–1322.
[34] Pearlmutter D, Berliner P, Shaviv E, Urban climatology in arid regions: current research in the Negev desert[J]. International Journal of Climatology , 2007, 27:222-237
[35] Offerle B, Jonsson P, Eliasson I, Grimmond CSB, Urban modification of the surface energy balance in the West African Sahel: Ouagadougou, Burkina Faso[J]. Journal of Climate, 2005, 18: 3983–3995.
[36] Emmanuel R, Assessment of impact of land cover changes on urban bioclimate: the case of Colombo, Sri Lanka[J]. Architectural Science Review, 2003, 46: 151–

158.
[37] Kok, Wing Sze Vince, Design for human comfort outdoors in cold climates, with specific reference to Winnipeg transit stops [D]. Canada: University of Manitoba, 2001.
[38] Lam, K. C., Feng Shui handbook [M]. New York: Henry Hot and Company, 1996: 142-154
[39] Hack, G., Lynch, K., Site planning [M]. Cambridge: MIT Press, 1986.
[40] Howard L, The climate of London, vols. I–III. [M]. London: Harvey and Dorton. 1883.
[41] Oke TR, The energetic basis of the urban heat island [J]. Atmospheric Environment, 1982, 7:769 -779.
[42] Tso CP, A survey of urban heat island study in two tropical cities [J]., Atmospheric environment, 1996, 30(3):507–519.
[43] Shudo H, Sugiyama J, Noriyoshi Y, et al, A study on temperature distribution influenced by various land uses[J]. Energy and Buildings, 1997, 26:199–205.
[44] Voogt JV, Viau AA, Paquet F, Mapping regional air temperature fields using satellite-derived surface skin temperatures[J]. International Journal of Climatology, 1997,17:1559–79.
[45] Voogt JA, Oke TR, Complete urban surface temperatures [J]. Journal of Applied Meteorology 1997, 36(9):1117–1132.
[46] Pauleit S, Ennos R, Golding Y, Modeling the environmental impacts of urban land use and land cover change—a study in Merseyside, UK[J]. Landscape and Urban Planning, 2005, 71:295–310.
[47] Fehrenbach U, Scherer D, Parlow E, Automated classification of planning objectives for the consideration of climate and air quality in urban and regional planning for the example of the region of Basel, Switzerland[J]. Atmospheric Environment, 2001, 35:5605–5615.
[48] Noto K, Dependence of heat island phenomena on stable stratification and heat quantity in a calm environment [J]. Atmospheric Environment, 1996,30:475–485.
[49] Klysik K, Spatial and seasonal distribution of anthropogenic heat emissions in Lodz, Poland [J]. Atmospheric Environment, 1996, 30(20):3397–3404.
[50] Giridharan R, Ganesan S, Lau SSY, Daytime urban heat island effect in high-rise and high-density residential developments in Hong Kong [J]. Energy and Buildings, 2004, 36:525–534.
[51] Ryozo Ooka, Recent development of assessment tools for urban climate and heat-island investigation especially based on experiences in Japan [J]. International Journal of Climatology, 2007, 27: 1919–1930
[52] A.John.Arnfield, Two decades of urban climate research: A review of turbulence, exchanges of energy and water, and the urban heat island [J]. International Journal of Climatology, 2003, 23: 1-26
[53] Lowry WP, Empirical estimation of urban effects on climate: a problem analysis[J]. Journal of Applied Meteorology, 1977, 16: 129-135
[54] Lowry WP, Urban effects on precipitation amount [J]. Progress in Physical Geography, 1998, 22: 477-520
[55] Montavez JP, Rodriguez A, Jimenez JI, A study of the urban heat island of Granada[J].

International Journal of Climatology 2000, 20: 899-911
[56] Tereshchenko IE, Filonov AE, Air temperature fluctuations in Guadalajara, Mexico, from 1926 to 1994 in relation to urban growth[J]. International Journal of Climatology, 2001, 21: 483–494.
[57] Magee N, Curtis J, Wendler G, The urban heat island effect at Fairbanks, Alaska[J]. Theoretical and Applied Climatology, 1999, 64: 39–47.
[58] Nasrallah HA, Brazel AJ, Balling RC, Analysis of the Kuwait City urban heat island [J]. International Journal of Climatology, 1990, 10 :401–405
[59] Moreno-Garcia MC, Intensity and form of the urban heat island in Barcelona[J]. International Journal of Climatology, 1994, 14: 705–710.
[60] Morris CJG, Simmonds I, Plummer N, Quantification of the influences of wind and cloud on the nocturnal urban heat island of a large city[J]. Journal of Applied Meteorology , 2001, 40 :169–182.
[61] Kuttler W, Barlag A-B, Roßmann F, Study of the thermal structure of a town in a narrow valley[J]. Atmospheric Environment, 1996, 30:365–378.
[62] Kumar S, Prasad T, Sashidharan NV, Heat island intensities over Brihan Mumbai on a cold winter and hot summer night[J]. Mausam, 2001, 52 : 703–708.
[63] Unger J, Sümeghy Z, Zoboki J, Temperature cross-section features in an urban area[J]. Atmospheric Research , 2001, 58: 117–127.
[64] Figuerola PI, Mazzeo NA, Urban–rural temperature differences in Buenos Aires [J]. International Journal of Climatology , 1998, 18:1709–1723.
[65] Winkler JA, Skaggs RH, Baker DG, Effects of temperature adjustments on the Minneapolis–St. Paul urban heat island[J]. Journal of Applied Meteorology, 1981, 20: 1295–1300.
[66] Tarleton LF, Katz RW, Statistical explanation for trends in extreme summer temperatures at Phoenix, Arizona [J]. Journal of Climate , 1995, 8: 1704–1708.
[67] Goldreich Y, Urban climate studies in Johannesburg, a sub-tropical city located on a ridge — a review [J]. Atmospheric Environment , 1992, 26: 407–420.
[68] Kuttler W, Barlag A-B, Roßmann F, Study of the thermal structure of a town in a narrow valley[J]. Atmospheric Environment, 1996,30:365–378.
[69] Holmer B, Eliasson I, Urban–rural vapour pressure differences and their role in the development of urban heat islands [J]. International Journal of Climatology , 1999, 19:
989–1009.
[70] TOSHIO OJIMA, Changing Tokyo Metropolitan Area and its Heat Island Model [J]. Energy and Buildings, 1990/91, 15. 16: 191 - 203
[71] TOSHIO OJIMA, Earth Surface Heat Balance Changes Caused by Urbanization [J]. Energy and Buildings, 1982, 4: 99 – 114.
[72] HIRONORI WATANABE, et al., Urban Environmental Design of Land Use in Tokyo Metropolitan Area [J]. Energy and Buildings, 1990/91, 15/16 :133 – 137.
[73] Akashi Mochida, et al., CFD analysis of mesoscale climate in the Greater Tokyo area [J]. Journal of Wind Engineering and Industrial Aerodynamics, 1997, 67& 68: 459-477.
[74] Tran Hung, Daisuke Uchihama, Shiro Ochi, et al., Assessment with satellite data of the urban heat island effects in Asian mega cities [J]. International Journal of Applied

Earth Observation and Geoinformation, 2006, 8: 34–48.
[75] Liangmei Huang, Jianlong Li, Dehua Zhao, et al., A fieldwork study on the diurnal changes of urban microclimate in four types of ground cover and urban heat island of Nanjing, China [J]. Building and Environment , 2008, 43: 7–17.
[76] Hong Chen, Ryozo Ooka, Kazuya Harayama, et al., Study on outdoor thermal environment of apartment block in Shenzhen, China with coupled simulation of convection, radiation and conduction [J]. Energy and Buildings, 2004, 36: 1247–1258.
[77] Kitchai Jitkhajornwanich, Adrian C. Pitts, Interpretation of thermal responses of four subject groups in transitional spaces of buildings in Bangkok [J]. Building and Environment, 2002, 37 : 1193-1204.
[78] Bingfeng Yu, Zhi Chen, Pingjun Shang, et al., Study on the influence of albedo on building heat environment in a year-round [J]. Energy and Buildings , 2008, 40:945–951
[79] R. Giridharan, S.S.Y. Lau, S. Ganesan, et al., Lowering the outdoor temperature in high-rise high-density residential developments of coastal Hong Kong: The vegetation influence [J]. Building and Environment, 2007,
[80] John M. M. Asey Cuddihy, Toward sustainable urban design: The impact of urban geometry on the energy consumption of buildings [D]. Canada: University of Toronto, 2005.
[81] Baruch Givoni, Climate Considerations in Building and Urban Design [M]. USA: International Thomson Publishing Inc., 1997: 234-245
[82] Chen Yu, Wong Nyuk Hien, Thermal benefits of city parks[J]. Energy and Buildings, 2006, 38: 105–120
[83] Ca VT, Asaeda T, Abu EM, Reductions in air conditioning energy caused by a nearby park[J]. Energy and Buildings, 1998, 29:83-92.
[84] Baruch Givoni, Comparison of temperature and humidity conditions in an urban park and in the built-up area around it [R]. Haifa, Israel: Research report of building research station, Israel Institute of Technology, 1972
[85] Chi-Ru Chang, Ming-Huang Li, Shyh-Dean Chang, A preliminary study on the local cool-island intensity of Taipei city parks[J]. Landscape and Urban Planning, 2007, 80: 386–395.
[86] J.H. Parker, The effectiveness of vegetation on residential cooling[J]. Passive solar journal, 1983, 2: 123-132.
[87] J.H. Parker, The use of shrubs in energy conservation plantings[J]. Landscape Journal, 1987, 6: 132-139.
[88] N. Al Hemiddi, Measurement of surface and air temperature over sites with different land treatments [A]. Proceeding of Passive and Low Energy Conference [C], Spain. 1991.
[89] N.H. Wong, Steve Kardinal Jusuf, Aung Aung La Win, Htun, et al., Environmental study of the impact of greenery in an institutional campus in the tropics [J]. Building and Environment, 2007, 42: 2949-2970.
[90] Evans.J.M., Schiller.S.D., Application of microclimate studies in town planning: A new capital city, an existing urban district and urban river front development[J]. Atmospheric Environment, 1996, 30(3): 361-364.
[91] Tadahisa Katayama, Tetsuo Hayashi, Yoshitaka Shiotsuki, et al., Cooling effects of a river and

sea breeze on the thermal environment in a built-up area [J]. Energy and Buildings, 1990/91, 15 – 16: 973 - 978

[92] Saburo Murakawa, Takeshi Sekine and Ken-Ichi Narita, Study of the effects of a river on the thermal environment in an urban area [J]. Energy and Buildings, 1990/91, 15 – 16: 993 - 1001

[93] Wong N.H., Yong A., Tan K., et al., Thermal evaluation of vertical greenery systems for building walls[J]. Building and Environment, 2010, 45: 663-672.

[94] B.Bass, B.Baskaran, Evaluating rooftop and vertical gardens as an adaptation strategy for urban areas[M]. Canada: Institute for Research and Construction, National Research Council, 2003.

[95] Introduction to green walls technology, benefits and design[R]. USA: Green roofs for healthy cities. 2008.

[96] Van Bohemen HD, Fraaij ALA, Ottele M, Ecological engineering, green roofs and the greening of vertical walls of buildings in urban areas[R]. USA: Ecocity World Summit. 2008.

[97] S.W.Peck, C. Callaghan, B. Bass, Greenbacks from green roofs: forging a new industry in Canada[R]. Canada: Mortgage and Housing Corporation, 1999.

[98] E. Alexandri, P. Jones, Temperature decreases in an urban canyon due to green walls and green roofs in diverse climates[J]. Building and Environment, 2008, 43: 480-493.

[99] Nyuk Hien Wong, Yu Chen, Investigation of thermal benefits of rooftop garden in the tropical environment[J]. Building and Environment, 2003, 38: 261 – 270.

[100] Wong N.H. etc, The thermal effects of plants on buildings[J]. Architectural Science Review, 2008, 45, 337-348.

[101] Eleftheria Alexandri, Phil Jones, Developing a one-dimensional heat and mass transfer algorithm for describing the effect of green roofs on the built environment Comparison with experimental results[J]. Building and Environment , 2007, 42:2835–2849.

[102] Otavio C. Acevedo, Osvaldo L. L. Moraes, Rodrigo Da Silva, et al., Surface-to-Atmosphere Exchange in a River Valley Environment[J]. Journal of Applied Meteorology and Climatology, 2007, 46.

[103] Yoshida S., Ooka R., Mochida A., et al., Study on effect of greening on outdoor thermal environment using three dimensional plant canopy model[J]. Journal of Architecture Planning and Environmental Engineering, 2000, 536: 87-94.

[104] Akashi Mochida, Hiroshi Yoshino, Satoshi Miyauchi, et al., Total analysis of cooling effects of cross-ventilation affected by microclimate around a building[J]. Solar Energy, 2006, 80: 371-382.

[105] Roger B. Clapp, George M, Hornberger. Empirical quations for some soil hydraulic properties[J]. Water Resource Research , 1978, 14:601-604.

[106] Holtan, H.N., C.B.England, G.P.Lawless, Moisture-tension data for selected soils on experimental watersheds[J]. ARS, 1968,41: 609-612.

[107] Michael Bruse, Heribert Fleer, Simulating surface–plant–air interactions inside urban environments with a three dimensional numerical model [J]. Environmental Modeling & Software , 1998, 13: 373–384.

[108] Gagge,A.P., A.C.Burton, H.d.Bazett, A practical system of units for the description of heat exchange of man with his environment[J]. Science, 1999, 94:428-430.

[109] Gagge,A.P., A.P.Fobelets, L.G.Berglund, A standard predictive index of human response to the thermal environment[J]. ASHRAE Transactions, 1992, 2B:

[110] Parsons, K.C., Havenith, G., Holmér, I., et al., The effects of wind and human movement on the heat and vapour transfer properties of clothing[J]. Ann. Occ. Hyg. 43:347-352.
[111] Havenith, G., Individualized model of human thermoregulation for the simulation of heat stress response[J]. J. Appl. Physiol. 90:1943-1954.
[112] ASHRAE Handbook of Fundamentals[M]. USA:American Society of Heating, Refrigerating and Air-Conditioning Engineers Inc., 2005.
[113] D. Pearlmutter, P. Berliner, E. Shaviv, Integrated modeling of pedestrian energy exchange and thermal comfort in urban street canyons[J]. Building and Environment, 2007, 42: 2396–2409.
[114] Michael Bruse, ITCM – a simple dynamic 2-node model of the human thermoregulatory system and its application in a multi-agent system[J]. Ann. Meteorol. 2005, 41:398-401.
[115] Michael Bruse, Assessing urban microclimate from the user's perspective – Multi-Agent systems as a new tool in urban biometeorology[J]. Ann. Meteorol. 2005, 41:137-140.
[116] P. O. Fanger, Thermal comfort: analysis and applications in environmental engineering[M]. New York :McGraw-Hill, 1972
[117] Rohles, F.H., Jr., R.G. Nevins, The nature of thermal comfort for sedentary man[J]. ASHRAE Transactions, 1971,77(1):239
[118] Website of Environmental Tech. for Urban Architecture Institute of Industrial Science,University of Tokyo, Facilities at Katolab.andOokalab[EB/OL]. http://venus.iis.u-tokyo.ac.jp/english/Facilities/facilities.htm, sited in 2009
[119] Antonio Lopes, Local wind changes with different roughness simulated in a wind tunnel: An example of application to a city district in the north of Lisbon[A]. Fifth International Conference on Urban Climate (ICUC-5)[C]. Poland, 2003.
[120] Michael Schatzmann, Bernd Leitl, Joachim Liedtke, Dispersion in Urban Environments; Comparison of Field Measurements with Wind Tunnel Results[J]. Environmental Monitoring and Assessment, 2000, 65: 249-257.
[121] Wyon D, Use of thermal manikins in environmental ergonomics[J]. Scand J Work Environ Health, 1989, 15 [Suppl 1]:84–94
[122] M. Richards, E. Mc Cullough, Revised Interlaboratory Study of Sweating Thermal Manikins Including Results from the Sweating Agile Thermal Manikin[J]. Journal of ASTM International (JAI), 2005,2:
[123] Burke RA, O'Neill FT, Stricker P , The development of a heat pipe driven manikin with variable flow irrigated skin[A]. Proceedings of the 6th international conference on environmental ergonomics[C]. Canada: Defense and Civil Institute of Envrionmental, 1994: 196–197.
[124] Dozen Y, Adachi K, Ohthuki S, et al., Studies of the heat and moisture transfer through clothing using a sweating thermal manikin[J]. Mercer JB (ed) Thermal physiology, 1989: 519–524.
[125] Meinander H, Coppelius-a sweating thermal manikin for the assessment of functional clothing[A]. Proceedings of NOKOBETEF IV: quality and usage of protective clothing[C]. Kittilii, Finland, 1992: 157–161.
[126]Y.S. Chen, J. Fan, W. Zhang, Clothing Thermal Insulation During Sweating[J]. Textile Research Journal, 2003,73: 152-157.
[127] Anttonen H, Interlaboratory trial of thermal manikin based on thermal

insulation of cold protective clothing in accordance with ENV342[A]. Proceedings of the 3rd international meeting on thermal manikin testing[C]. National Institute for Working Life, Sweden, 1999: 8–11.
[128] Mc Cullough E, Interlaboratory study of sweating manikins[A]. Proceedings of the 5th European conference on protective clothing and NOKOBETEF 7 [C]. Montreux, Switzer- land, 2003.
[129] ISO 9920:2007, Ergonomics Estimation of the Thermal Characteristics of a Clothing Ensemble[S]. USA: ISO - International Organization for Standardization, 2007
[130] ASTM F1291:2003. Standard method for measuring the thermal insulation of clothing using a heated thermal manikin[S]. American Society for Testing and Materials, 2003.
[131] EN-ISO 15831:2004. Clothing physiological effects measurement of thermal insulation by means of a thermal manikin[S]. International Organization for Standardization, 2004.
[132] Robert Farrington, John Rugh, Desikan Bharathan, Using a Sweating Manikin, Controlled by a Human Physiological Model, to Evaluate Liquid Cooling Garments[R]. SAE International, 2005.
[133] Richards M, Mattle M, Development of a sweating agile thermal manikin—SAM[A]. Proceedings of the 4th international meeting on thermal manikins[C]. Switzerland, 2001.
[134] de Freitas CR, Beach climate and recreation: thermo physiological variation, preference and behaviour. Department of Geographical Sciences and Planning[D]. St Lucia: University of Queensland, 1979.
[135] Fanger PO, Thermal comfort[M]. Copenhagen: Danish Technical Press, 1970
[136] VDI, VDI-3787, Part 2: Environmental Meteorology. Methods for the human biometeorological evaluation of climate and air quality for urban and regional planning at regional level [S]. VDI-Handbuch Reinhaltung der Luft, Bd. 1 b., 1998.
[137] Jennifer Spagnolo, Richard de Dear, A field study of thermal comfort in outdoor and semi-outdoor environments in subtropical Sydney Australia[J]. Building and Environment, 2003, 38 :721-738.
[138] Busch, J.F, A tale of two populations: Thermal comfort in air-conditioned and naturally ventilated offices in Thailand[J]. Energy and buildings, 1992,18:235-249.
[139] de Dear, R.J., K.Leow, A.Ameen, Thermal comfort in the humid tropics- Part 1[J]. ASHRAE Transactions ,97(1): 874-879.
[140] Website of Occupational Safety & Health Adminstration, www.osha.gov, Sited in 2009
[141] Threshold Limit Values for Chemical Substances and Physical Agents and Biological Exposure Indices[A]. American Conference of Governmental Industrial Hygienists[C]. Cincinnati, 1992.
[142] ISO 7243: Hot environments-Estimation of the heat stress on working man, based on the WBGT-index[S]. International Standard Orgnization, 1999.
[143] Website of Australian Government, Bureau of Meteorology[DB/OL],, www.bom.gov.au, sited in 2009
[144]Website of English Health and Safety Executive[DB/OL],, http://www.hse.gov.uk/, sited in 2009
[145] D. Minard, Effective temperature scale and its modifications[R]. Naval Medical Research Institute, 1964.

[146] R.K. Macpherson, Physiological responses to hot environments[R]. London: Royal Naval Tropical Research Unit, 1960
[147] C.S. Leithead, A.R. Lind, Heat stress and heat disorders[M]. London: Occupational and Enviornmental Medicine, 1964.
[148] N. Ramanathan, H. Belding, Physiological evaluation of WBGT index for occupational heat stress[J]. Journal of American Industrial Hygiene Association. 1973,34: 375-383.
[149] Website of Juniata College [DB/OL], http://www.juniata.edu/, sited in 2009
[150] Website of Office of climate, Water and Weather Services [DB/OL], http://www.weather.gov/os/windchill/index.shtml, Sited in 2009
[151] R. G. Steadman, The Assessment of Sultriness. Part I: A Temperature-Humidity Index Based on Human Physiology and Clothing Science[J]. Journal of Applied Meteorology, 1979,18:861-873.
[152] R. G. Steadman, The Assessment of Sultriness. Part II: Effects of Wind, ExtrRadiation and Barometric Pressure on Apparent Temperature[J]. Journal of Applied Meteorology, 1979, 18: 874-885
[153] R. G. Steadman, A Universal Scale of Apparent Temperature[J]. Journal of Applied Meteorology, 1984, 23:1674-1678.
[154] Website of national Oceanic and Atmospheric Administration, United Stateds Department of Commerce[DB/OL], www.noaa.gov, sited in 2009
[155] T.V. Lawson, The wind content of the built environment[J]. Journal of Industrial Aerodynamics, 1978,3: 93-105.
[156] T.V. Lawson, A.D. Penwarden, The effects of wind on people in the vicinity of buildings[A]. Proceedings of 4th International Conference on Wind Effects on Buildings.
and Structures[C]. Cambridge University Press, 1975: 605-622.
[157] N.Isyumov, M.Mikitiuk, D.Garnham, A study of the pedestrian-level wind environment for Jubilee Park, Canary Wharf[R]. Report of University of Western Ontario. 2001.
[158] S. Murakami, K. Deguchi, New criteria for wind effects on pedestrians[J]. Journal of Wind Engineering and Industrial Aerodynamics, 1981,7: 289-309.
[159] Igor Knez, Sofia Thorsson, Ingegard Eliasson, et al., Psychological mechanisms in outdoor place and weather assessment: towards a conceptual model[J]. International Journal of Biometeorology, 2009, 53:101-111.
[160] N.B. Hucheon, Thermal environment and human comfort. [J]. Canadian Building Digest: CBD-102, 2000.
[161] Peter Höppe. Different aspects of assessing indoor and outdoor thermal comfort[J]. Energy and Buildings, 2002, 34(6):661-665.
[162] Fiala D., Lomas K.J., and Stohrer M, Computer prediction of human thermoregulatory and temperature responses to a wide range of environmental conditions[J]. Int. J. Biometeorol., 2001,45:143-159.
[163] Gerd Jendritzky, Abdel Maarouf, Dusan Fiala, et al, An update on the development of a universal thermal climate index[A], Proceedings of the 15th Conference on Biometeorology and Aerobiology [C], 2006
[164] Gerd Jendritzky, Abdel Maarouf, Henning Staiger, Looking for a Universal

Thermal Climate Index UTCI for Outdoor Applications[A]. Windsor-Conference on Thermal Standards[C], Windsor, UK, April 5-8, 2001,
[165] Gerd Jendritzky, George Havenith, The Thermal Environment of the Human Being: A subjective retrospection on methodologies[A]. Proceedings 17th Int. Congress Biometeorology [C], 2005
[166] Mark Richards, George Havenith. Progress towards the final UTCI model [A]. Proceedings of the 12th International Conference on Environmental Ergonomics [C], 2007
[167] Feduniw, L, Human thermal comfort for interior designers and architects. Master Degree Thesis[D]. Canada: University of Manitoba, 1998.
[168] B.W. Olesen, Local thermal discomfort in Bruel and Kjaer[R]. Technical Review No. 1, Copenhagen, 1985.
[169] EN-ISO7730-2005, Ergonomics of the thermal environment - Analytical determination and interpretation of thermal comfort using calculation of the PMV and PPD indices and local thermal comfort criteria[S]. International Standard Organization, 2005.
[170]ANSI/ASHRAE 55-2004, Thermal Environmental Conditions for Human Occupancy. American Society of Heating[S]. Refrigerating and Air-conditioning engineers Inc., 2004.
[171] SAE J2234, Equivalent temperature – Truck and Bus[S]. Society of Automotive Engineers, 2007.
[172] T. Han, L. Huang, S. Kelly, C. Huizenga, Z. Hui. Virtual Thermal Comfort Engineering[J]. SAE technical paper 2001-01-0588, 2001
[173] D. P. Wyon, S. Larsson, B. Forsgren, and I. Lundgren, Standard Procedures for Assessing Vehicle Climate with a Thermal Manikin[J]. SAE Technical Paper Series 890049, 1989:1-11.
[174] M. Bohm M., Browen, I. Holmer, H, Nilsson, and O.Noren, Evaluation of Vehicle Climate with a Thermal Manikin - The Relationship between Human Temperature Experience and Local Heat Loss[R]. Swedish Institute of Agricultural Engineering, JTI Report 123, 1990.
[175] Taeyoung Han, Linjie Huang, A Model for Relating a Thermal Comfort Scale to EHT Comfort Index[J]. SAE technical paper series 2004-01-0919, 2004
[176] Taeyoung Han, Linjie Huang, A Sensitivity Study of Occupant Thermal Comfort in a Cabin Using Virtual Thermal Comfort Engineering[J]. SAE technical paper series ,2005-01-1509, 2005.
[177] Ned Wolfe, Xiaoxia Mu, Linjie Huan, et.al, Cooling with Augmented Heated and Cooled Seats[J]. SAE technical paper series 2007-01-1993, 2007
[178] Glenn R. Mc Gregor, Ian Burton, Kristie Ebi, Biometeorology for Adaptation to Climate Variability and Change[J]. Springer, London, 2009.
[179] Driscoll D, Thermal comfort indexes: current uses and abuses [J]. National Weather Digest, 1992 17.4:33-38.
[180] Parsons KC, Human thermal environments: the effects of hot, moderate and cold environments on human health, comfort and performance[J]. Taylor & Francis, London, 2003.
[181] Hanna Swaid, ME. Hoffman, The prediction of impervious ground surface

temperature by the surface thermal time constant (STTC) model[J]. Energy and Buildings, 1989,13: 149-157.
[182] Hanna Swaid, Milo E. Hoffman, Prediction of urban air temperature variations using the analytical CTTC model[J]. Energy and Buildings, 1990, 14:313-324
[183] Hanna Swaid, Milo E. Hoffman, Thermal effects of artificial heat sources and shaded ground areas in the urban canopy layer[J]. Energy and Buildings, 1990/91,15-16:253-261.
[184] Limor Shashua-Bar, Milo E. Hoffman, The Green CTTC model for predicting the air temperature in small urban wooded sites[J]. Building and Environment 2002, 37:1279-1288
[185] H.Swaid, ME.Hoffman, Climatic impacts of urban design features for high- and mid-latitude cities[J]. Energy and Buildings 1990,14:325-336
[186] Limor Shashua-Bar, Milo E. Hoffman, Quantitative evaluation of passive cooling of the UCL microclimate in hot regions in summer[J]. Buildings and Environment , 2004, 39:1087-1099
[187] MM. Elnahas, TJ. Williamson, An improvement of the CTTC model for predicting urban air temperatures[J]. Energy and Buildings, 1997, 25:41-49.
[188] R. Kunz, N. Moussiopoulos, Simulation of the wind field in Athens using refined boundary conditions[J]. Atmospheric Environment, 1995, 29: 3375-3591
[189] R. Martinuzzi, C. Tropea, The ow around surface-mounted, prismatic obstacles
placed in a developed channel flow[J]. J. Fluids Eng. 1993,115: 85-92.
[190] R. Kunz, I. Khatib, N. Moussiopoulos., Coupling of mesoscale and microscale models—an approach to simulate scale interaction[J].Environmental Modelling & Software, 2000,15: 597–602
[191] Gerd Jendritzky, Angelika Gräz, Christina Koppe, et al, How to deal with the urban development, urban climate, human health effect relationship - A Contributiontomethodology[J/OL].http://www.cleanairpartnership.org/pdf/finalpaper_jendritsky.pdf, sited in 2009
[192] Matthias Friedrich, Angelika Gratz, Gerd Jendritzky, Further development of the urban bioclimate model UBIKLIM, taking local wind system into account[J]. Meteorologische Zeitschrift. 2001,10: 267-272.
[193] Alexandri, E., & Jones, P. (2008). Temperature decreases in an urban canyon due to green walls and green roofs in diverse climates. Building and Environment, 43,480–493.
[194] Emmanuel, R., Rosenlund, H., & Johansson, E. (2007). Urban shading—a design option for the tropics? A study in Colombo, Sri Lanka. International Journal of Climatology, 27, 1995–2004.
[195] Shashua-Bar, L., Tsiros, I. X., & Hoffman, M. (2012). Passive cooling design options to ameliorate thermal comfort in urban streets of a Mediterranean climate (Athens) under hot summer conditions. Building and Environment, 57 (November), 110–119.
[196] Emmanuel, R., Rosenlund, H., & Johansson, E. (2007). Urban shading—a design option for the tropics. A study in Colombo, Sri Lanka. International Journal of Climatology, 27, 1995–2004.
[197] http: // www.baidu.com/. (Accessed June 2018)
[198] http://tianqi.2345.com/wea_history/. (Accessed June 2018)
[199] http: // www.envi-met.info/. (Accessed June 2018)
[200] V.P. López-Cabeza, C. Galán-Marín, C. Rivera-Gómez, J. Roa-Fernández, Courtyard microclimate ENVI-met outputs deviation from the experimental data, Building and Environment,

144, 2018, Pages 129-141
[201] Katia Perini, Ata Chokhachian, Sen Dong, Thomas Auer, Modeling and simulating urban outdoor comfort: Coupling ENVI-Met and TRNSYS by grasshopper, Energy and Buildings, 152, 2017, 373-384.
[202] S. Tsoka, A. Tsikaloudaki, T. Theodosiou, Analyzing the ENVI-met microclimate model's performance and assessing cool materials and urban vegetation applications–A review, Sustainable Cities and Society, 43, 2018, 55-76.
[203] Helge Simon, Jenny Lindén, David Hoffmann, Peter Braun, Michael Bruse, Jan Esper, Modeling transpiration and leaf temperature of urban trees – A case study evaluating the microclimate model ENVI-met against measurement data, Landscape and Urban Planning, 174, 2018, 33-40.
[204] Ariane Middel, Kathrin Häb, Anthony J. Brazel, Chris A. Martin, Subhrajit Guhathakurta, Impact of urban form and design on mid-afternoon microclimate in Phoenix Local Climate Zones, Landscape and Urban Planning, Volume 122, 2014, Pages 16-28.
[205] Michael Bruse, Heribert Fleer. Simulating surface–plant–air interactions inside urban environments with a three dimensional numerical model, Environmental Modelling & Software, Volume 13, Issues 3–4, 1998, Pages 373-384.
[206] de Dear R, Pickup J. An outdoor thermal environment index (OUT_SET*) -applications. In: de Dear RJ, Kalma JD, Oke TR, Auliciems A, editors. Biometeorology and urban climatology at the Turn of the Millenium. Selected papers from the ICB-ICUC'99 conference, Sydney, WCASP-50, WMO/TD No. 1026.Geneva: World Meteorological Organization; 2000.
[207] Fanger Po. Thermal comfort. New York: McGraw Hill; 1972
[208] Gagge AP, Fobelets AP, Berglund LG. A standard predictive index of human responds to the thermal environment. ASHARE Transaction 1986; 92: 709-31.
[209] Spagnolo J, de Dear RJ. A field study of thermal comfort in outdoor and semi outdoor environments in subtropical Sydney Australia. Building and Environment 2003; 38: 721-38.
[210] Linares, C., & Diaz, J. (2008). Impact of high temperature on hospital admissions: comparative analysis with previous studies about mortality. The European Journal of Public Health, 18, 317–322.
[211] Andrade, H., & Alcoforado, M. J. (2008). Microclimatic variation of thermal comfort in a district of Lisbon (Telheiras) at night. Theoretical and Applied Climatology, 92, 225–237.
[212] Ali-Toudert, F., & Mayer, H. (2007). Thermal comfort in an east–west oriented street canyon in Freiburg (Germany) under hot summer conditions. The oretical land Applied Climatology, 87, 223–237.
[213] Bottillo, S., De Lieto Vollaro, A., Galli, G., & Vallati, A. (2014). Fluid dynamic and heat transfer parameters in an urban canyon. Solar Energy, 99, 1–10. http://dx.doi.org/10.1016/j.solener.2013.10.031
[214] Chen, L., Ng, E., An, X., Ren, C., Lee, M., Wang, U., et al. (2012). Sky view factor analysis of street canyons and its implications for daytime intra-urban air temperature differentials in high-rise, high-density urban areas of Hong Kong: a GIS-based simulation approach. International Journal of Climatology, 32,121–136. http://dx.doi.org/10.1002/joc.2243
[215] harmin, T., & Steemers, K. (2013). Effect of canyon geometry on outdoor thermal comfort: a case study of high-density, warm-humid climate. In Proceedings of the 29th PLEA conference, sustainable architecture for a renewable future.

[216] Shashua-Bar, L., Pearlmutter, D., & Erell, E. (2009). The cooling efficiency of urban landscape strategies in a hot dry climate. Landscape and Urban Planning, 92,179–186. http://dx.doi.org/10.1016/j.landurbplan.2009.04.005
[217] Ca, V. T., Asaeda, T., & Abu, E. M. (1998). Reduction in air conditioning energy caused by a nearby park. Journal of Energy and Buildings, 29, 83–92.
[218] Wong, N. H., & Chen, Y. (2004). The thermal effects of city greens on surroundings under the tropical climate. In Built environments and environmental buildings, proceedings of the 21st international conference of passive and low energy architecture.
[219] Kumakura, E., Nakaohkubo, K., & Hoyano, A. (2013). Solar shading effects by tree species in an urban environment using numerical simulation tool. In Proceedings of the 29th PLEA conference, sustainable architecture for a renewable future.
[220] Jelena Djekic, Aleksandra Djukic, Milena Vukmirovic, Petar Djekic, Milena Dinic Brankovic, Thermal comfort of pedestrian spaces and the influence of pavement materials on warming up during summer, Energy and Buildings, 159, 2018, 474-485.
[221] Federica Rosso, Iacopo Golasi, Veronica Lucia Castaldo, Cristina Piselli, Anna Laura Pisello, Ferdinando Salata, Marco Ferrero, Franco Cotana, Andrea de Lieto Vollaro, On the impact of innovative materials on outdoor thermal comfort of pedestrians in historical urban canyons, Renewable Energy, 118, 2018, 825-839.
[222] Yujun Yang, Dian Zhou, Weijun Gao, Zihan Zhang, Wei Chen, Wangchongyu Peng, Simulation on the impacts of the street tree pattern on built summer thermal comfort in cold region of China, Sustainable Cities and Society, 2018, 563-580.
[223] P. Höppe. The physiological equivalent temperature – a universal index for the biometeorological assessment of the thermal environment [J]. International Journal of Biometeorology, 1999, 43(2):71.
[224] Tobi Eniolu Morakinyo, Kevin Ka-Lun Lau, Chao Ren, Edward Ng, Performance of Hong Kong's common trees species for outdoor temperature regulation, thermal comfort and energy saving, Building and Environment, 2018, 157-170.
[225] Giuseppe Maggiotto, Riccardo Buccolieri, Marco Antonio Santo, Laura Sandra Leo, Silvana Di Sabatino. Validation of temperature-perturbation and CFD-based modelling for the prediction of the thermal urban environment: the Lecce (IT) case study, Environmental Modelling & Software, 2014, 157-170.
[226] Pui Kwan Cheung, C.Y. Jim. Comparing the cooling effects of a tree and a concrete shelter using PET and UTCI, Building and Environment, 2018, 49-61.
[227] J. Paetzold, S. Cochard, A. Vassallo, D.F. Fletcher. Wind engineering analysis of parabolic trough solar collectors: The effects of varying the trough depth, Journal of Wind Engineering and Industrial Aerodynamics, 2014, 118-128.
[228] Chao Yuan, Leslie Norford, Edward Ng. A semi-empirical model for the effect of trees on the urban wind environment, Landscape and Urban Planning, 2017, 84-93.
[229] Fangying Gong, Zhao-Cheng Zheng, Edward Ng, Modeling Elderly Accessibility to Urban Green Space in High Density Cities: A Case Study of Hong Kong, Procedia Environmental Sciences, 2016, 90-97.
[230] Liang Chen, Edward Ng, Outdoor thermal comfort and outdoor activities: A review of research in the past decade, Cities, 2012,118-125.
[231] Tobi Eniolu Morakinyo, Yun Fat Lam, Simulation study on the impact of tree-configuration,

planting pattern and wind condition on street-canyon's micro-climate and thermal comfort, Building and Environment, 2016, 262-275.
[232] Xiyan Xu, Shibo Sun, Wei Liu, Ester Higueras García, Li He, Qi Cai, Sijing Xu, Jingjing Wang, Jianning Zhu, The cooling and energy saving effect of landscape design parameters of urban park in summer: A case of Beijing, China, Energy and Buildings, 2017, 91-100.
[233] CSADI. The commercial building design specification. Available on line at: https://wenku.baidu.com/view/4c4a9df76529647d272852bb.html; 2018.
[234] Ruzana Sanusi, Denise Johnstone, Peter May, Stephen J. Livesley, Microclimate benefits that different street tree species provide to sidewalk pedestrians relate to differences in Plant Area Index, Landscape and Urban Planning, 2017, 502-511.
[235] F. Ali-Toudert, M. Djenane, R. Bensalem, H.Mayer, Outdoor thermal comfort in the old desert city of Beni-Isguen, Algeria, Clim. Res. 28 (2005) 243-256, http://dx.doi.org/10.3354/cr028243.
[236] R. Emmanuel, E. Johansson, Influence of urban morphology and sea breeze on hot humid microclimate: the case of Colombo, Sri Lanka, Clim. Res. 30 (2006) 189-200, http://dx.doi.org/10.3354/cr030189.
[237] K.C. Goh, C.H. Chang, The Relationship between Height to Width Ratios and the Heat Island Intensity at 22 : 00 h for Singapore Royal Meteorological Society This Document May be Used for Private Study or Research Purpose Only. This Document or Any Part of it May Not be Duplicate, vol. 19, 1999, 1011-1023.
[238] E. Johansson, Influence of urban geometry on outdoor thermal comfort in a hot dry climate: a study in Fez, Morocco, Build. Environ. 41 (2006) 1326-1338, http://dx.doi.org/10.1016/j.buildenv.2005.05.022.
[239] E. Andreou, K. Axarli, Investigation of urban canyon microclimate in traditional and contemporary environment. Experimental investigation and parametric analysis, Renew. Energy 43 (2012) 354-363, http://dx.doi.org/ 10.1016/j.renene.2011.11.038.
[240] Federica Rosso, Iacopo Golasi, Veronica Lucia Castaldo, Cristina Piselli, Anna Laura Pisello, Ferdinando Salata, Marco Ferrero, Franco Cotana, Andrea de Lieto Vollaro, On the impact of innovative materials on outdoor thermal comfort of pedestrians in historical urban canyons, Renewable Energy, 118, 2018, 825-839.

Appendix-1

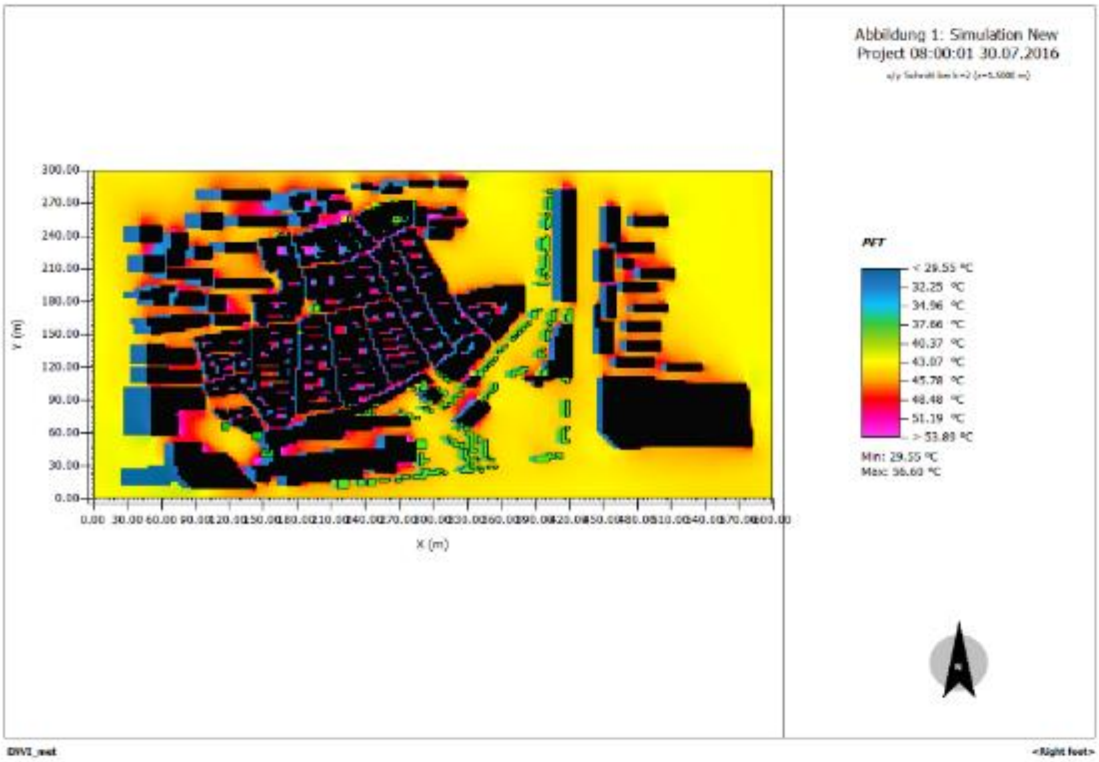
Abbildung 1: Simulation New Project 08:00:01 30.07.2016
PET
< 29.55 °C
32.25 °C
34.96 °C
37.66 °C
40.37 °C
43.07 °C
45.78 °C
48.48 °C
51.19 °C
> 53.89 °C
Min: 29.55 °C
Max: 56.60 °C
Y (m)
X (m)

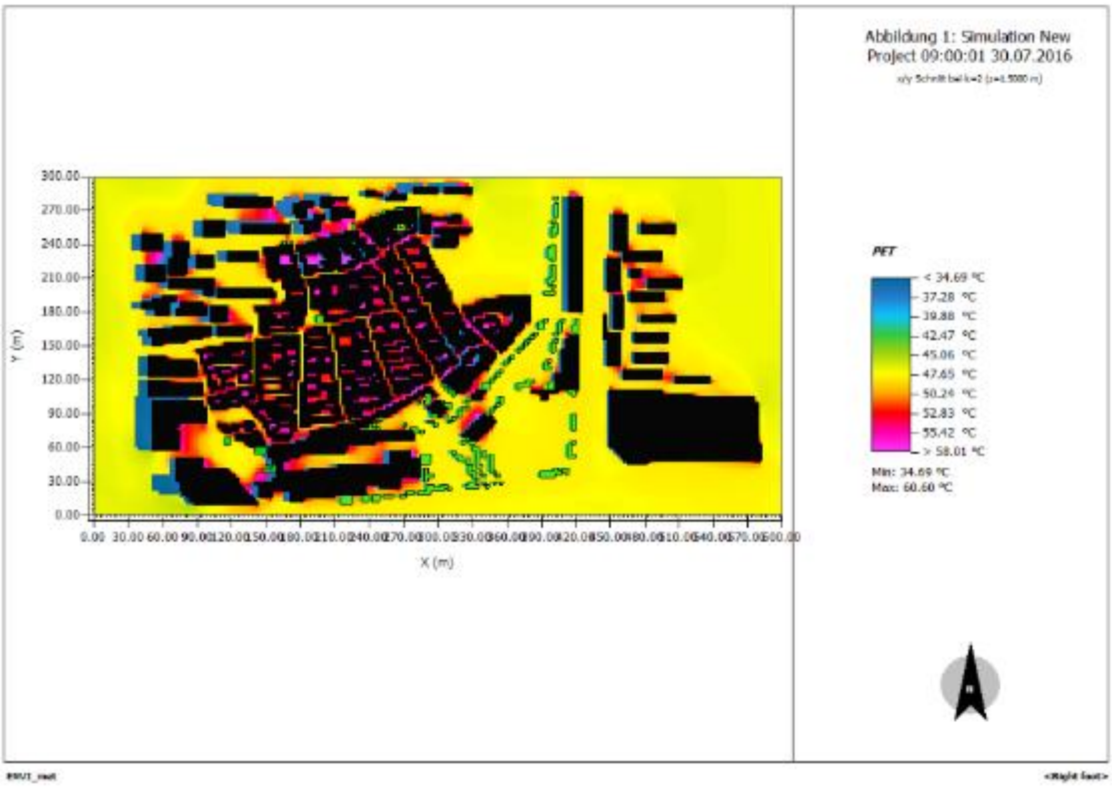
Abbildung 1: Simulation New Project 09:00:01 30.07.2016
PET
< 34.69 °C
37.28 °C
39.88 °C
42.47 °C
45.06 °C
47.65 °C
50.24 °C
52.83 °C
55.42 °C
> 58.01 °C
Min: 34.69 °C
Max: 60.60 °C
Y (m)
X (m)

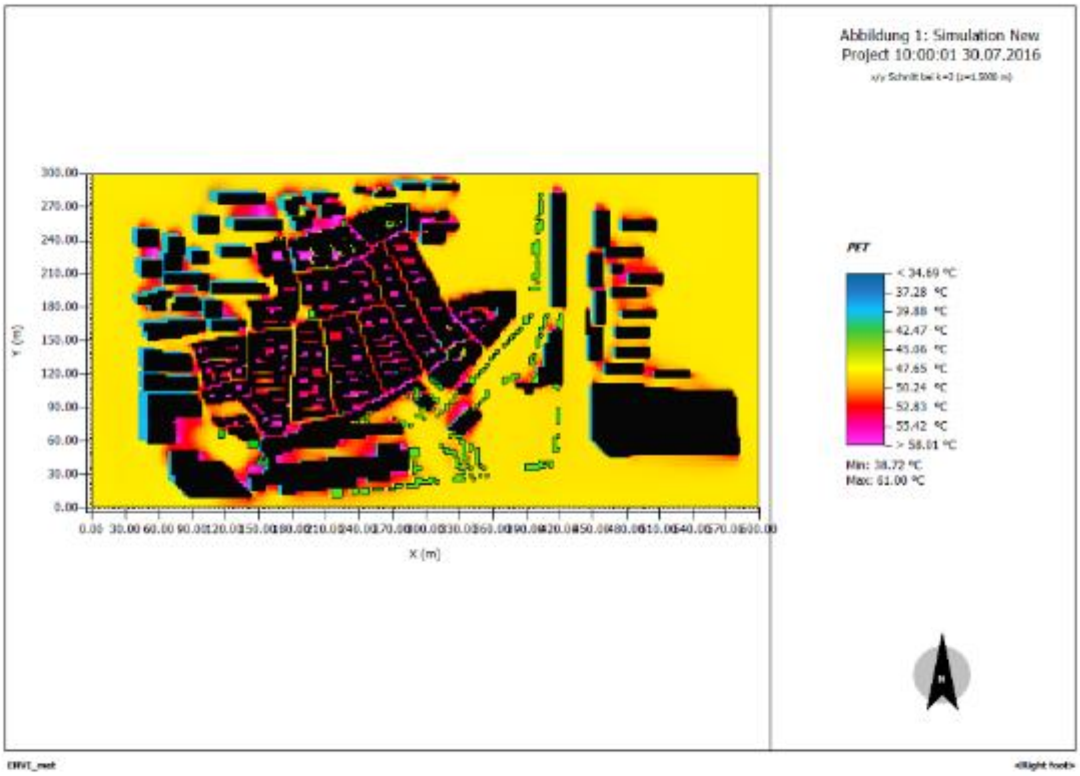
Abbildung 1: Simulation New Project 10:00:01 30.07.2016
PET
< 34.69 °C
37.28 °C
39.88 °C
42.47 °C
45.06 °C
47.65 °C
50.24 °C
52.83 °C
55.42 °C
> 58.01 °C
Min: 38.72 °C
Max: 61.00 °C
Y (m)
X (m)
ENVI_met
<Right foot>

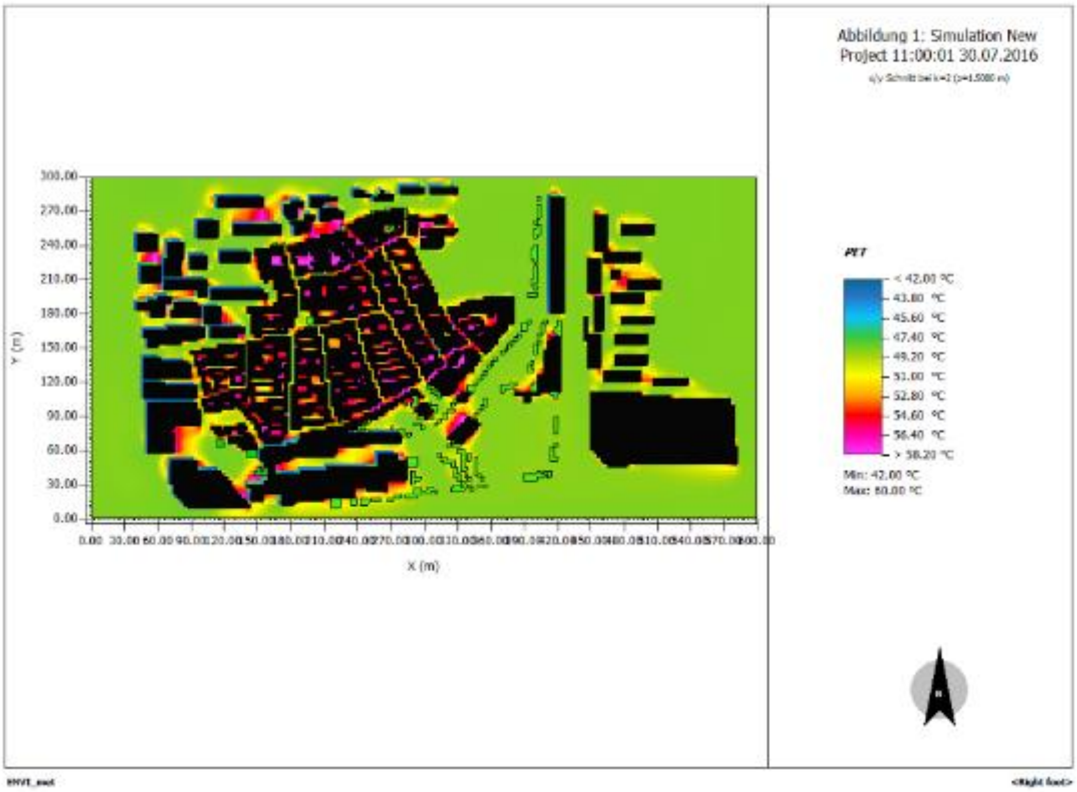
Abbildung 1: Simulation New Project 11:00:01 30.07.2016
PET
< 42.00 °C
43.80 °C
45.60 °C
47.40 °C
49.20 °C
51.00 °C
52.80 °C
54.60 °C
56.40 °C
> 58.20 °C
Min: 42.00 °C
Max: 60.00 °C
Y (m)
X (m)
ENVI_met
<Right foot>

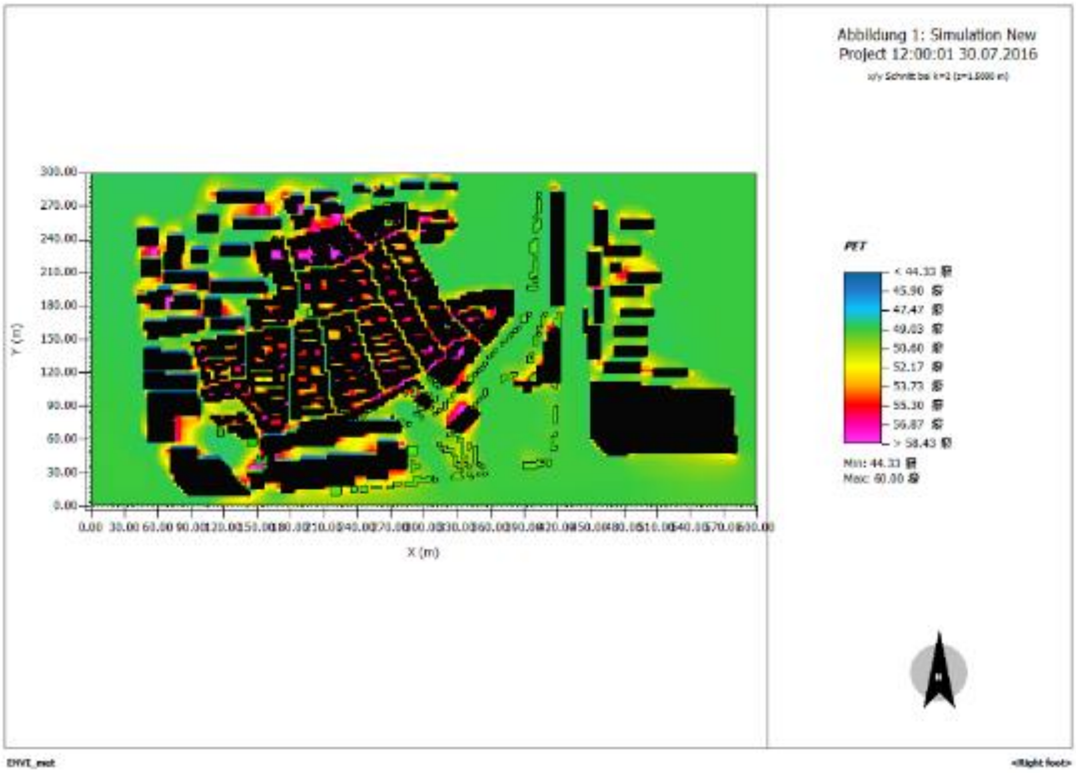
Abbildung 1: Simulation New Project 12:00:01 30.07.2016
PET
< 44.33
45.90
47.47
49.03
50.60
52.17
53.73
55.30
56.87
> 58.43
Min: 44.33
Max: 60.00
Y (m)
X (m)
ENVI_met
<Right foot>

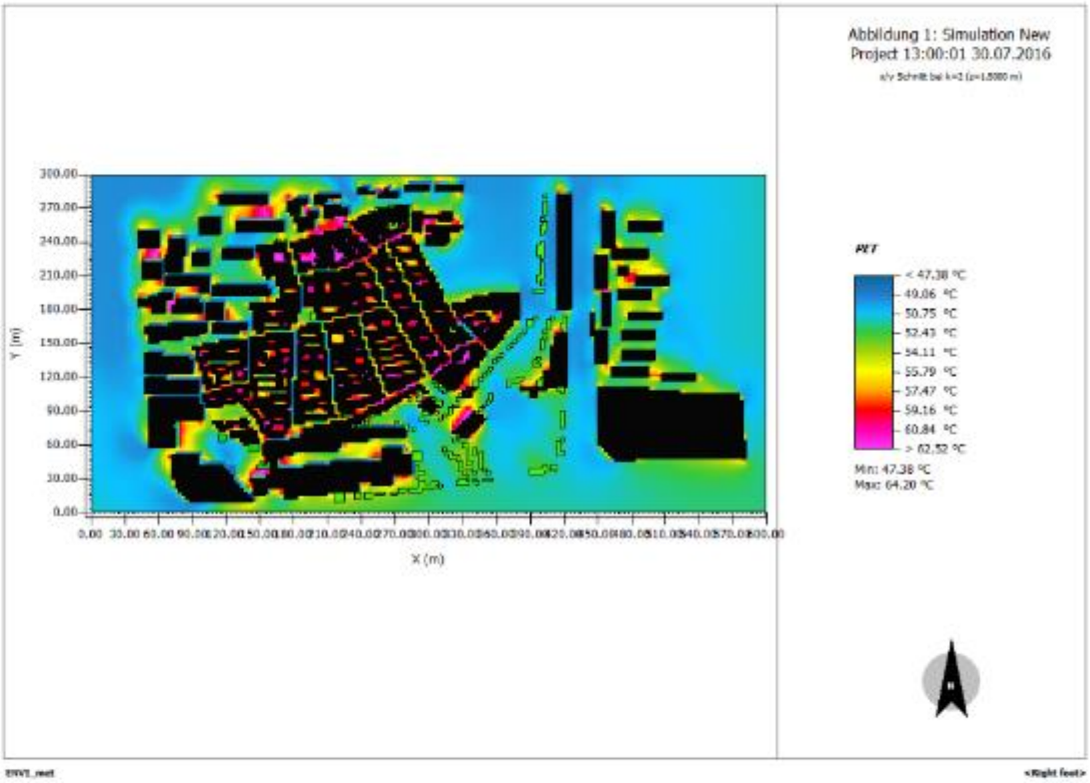
Abbildung 1: Simulation New Project 13:00:01 30.07.2016
PET
< 47.38 °C
49.06 °C
50.75 °C
52.43 °C
54.11 °C
55.79 °C
57.47 °C
59.16 °C
60.84 °C
> 62.52 °C
Min: 47.38 °C
Max: 64.20 °C
Y (m)
X (m)
ENVI_met
<Right foot>

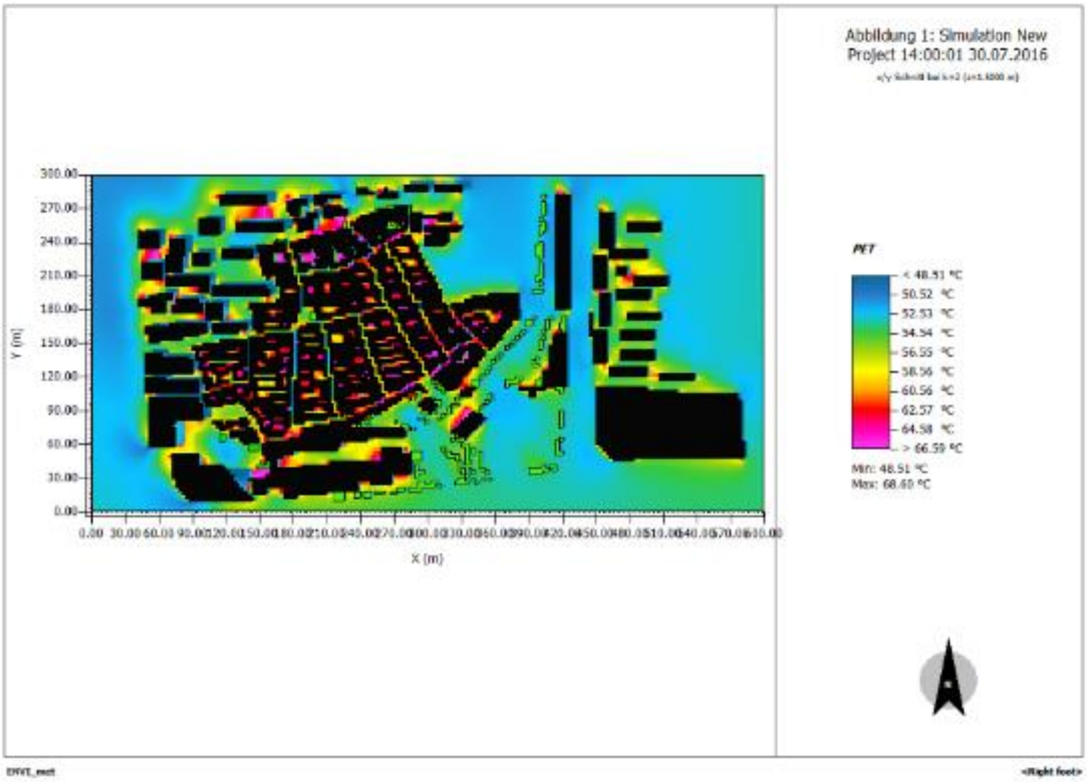
Abbildung 1: Simulation New Project 14:00:01 30.07.2016
PET
< 48.51 °C
50.52 °C
52.53 °C
54.54 °C
56.55 °C
58.56 °C
60.56 °C
62.57 °C
64.58 °C
> 66.59 °C
Min: 48.51 °C
Max: 68.60 °C
Y (m)
X (m)

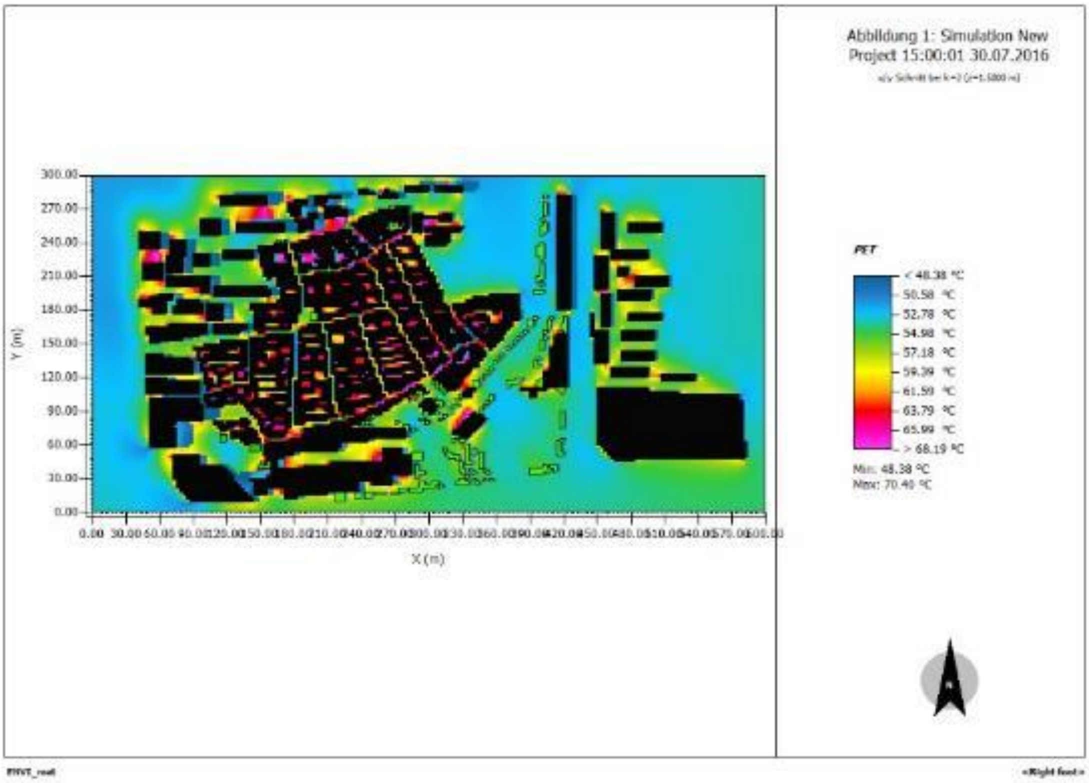
Abbildung 1: Simulation New Project 15:00:01 30.07.2016
PET
< 48.38 °C
50.58 °C
52.78 °C
54.98 °C
57.18 °C
59.39 °C
61.59 °C
63.79 °C
65.99 °C
> 68.19 °C
Min: 48.38 °C
Max: 70.40 °C
Y (m)
X (m)

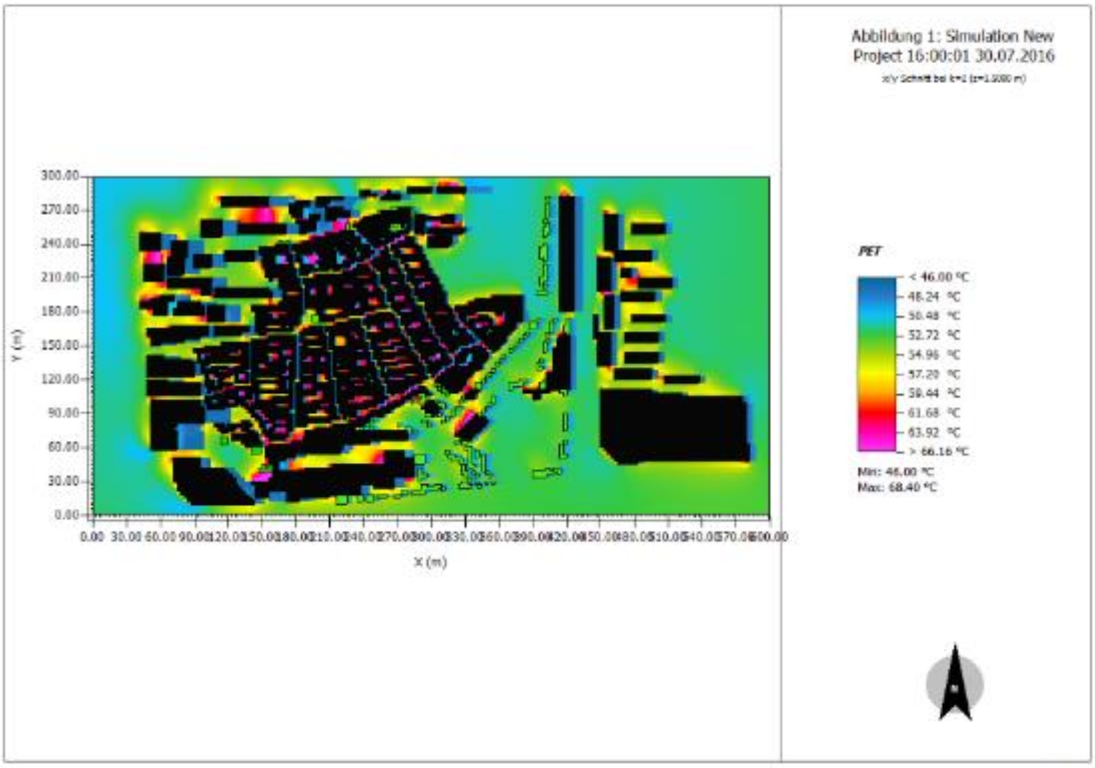
Abbildung 1: Simulation New Project 16:00:01 30.07.2016
x/y Schnitt bei k=1 (z=1.5000 m)
PET
< 46.00 °C
48.24 °C
50.48 °C
52.72 °C
54.96 °C
57.20 °C
59.44 °C
61.68 °C
63.92 °C
> 66.16 °C
Min: 46.00 °C
Max: 68.40 °C
Y (m)
X (m)

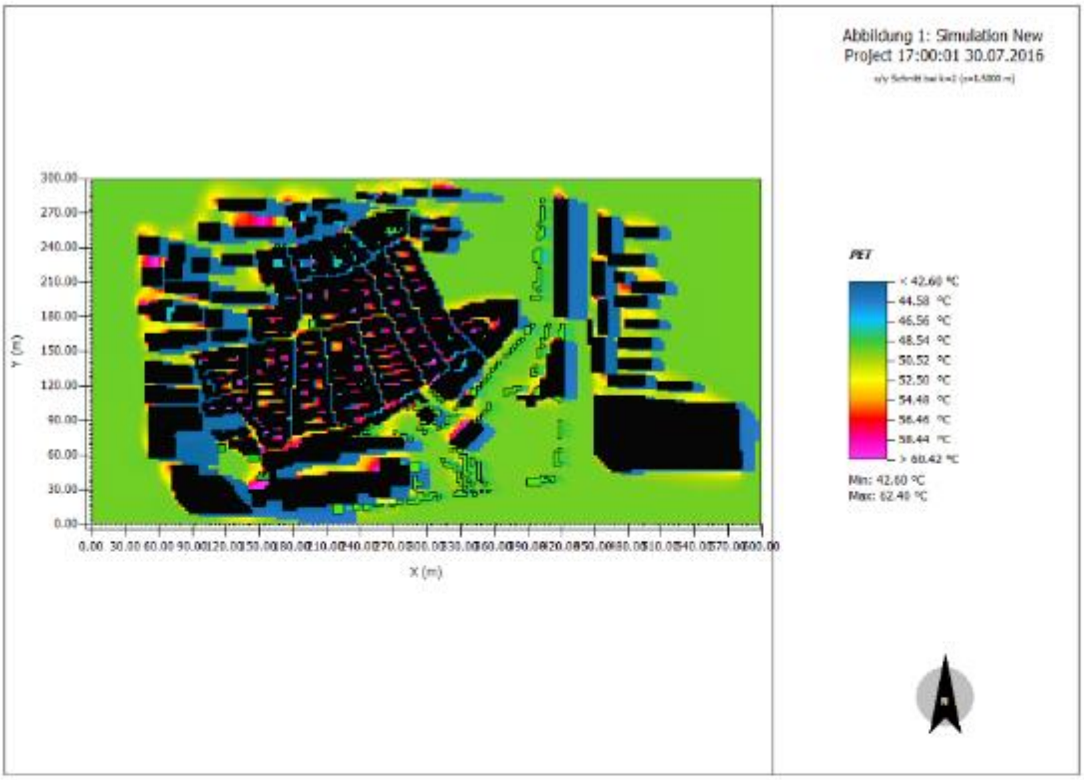
Abbildung 1: Simulation New Project 17:00:01 30.07.2016
PET
< 42.60 °C
44.58 °C
46.56 °C
48.54 °C
50.52 °C
52.50 °C
54.48 °C
56.46 °C
58.44 °C
> 60.42 °C
Min: 42.60 °C
Max: 62.40 °C
Y (m)
X (m)

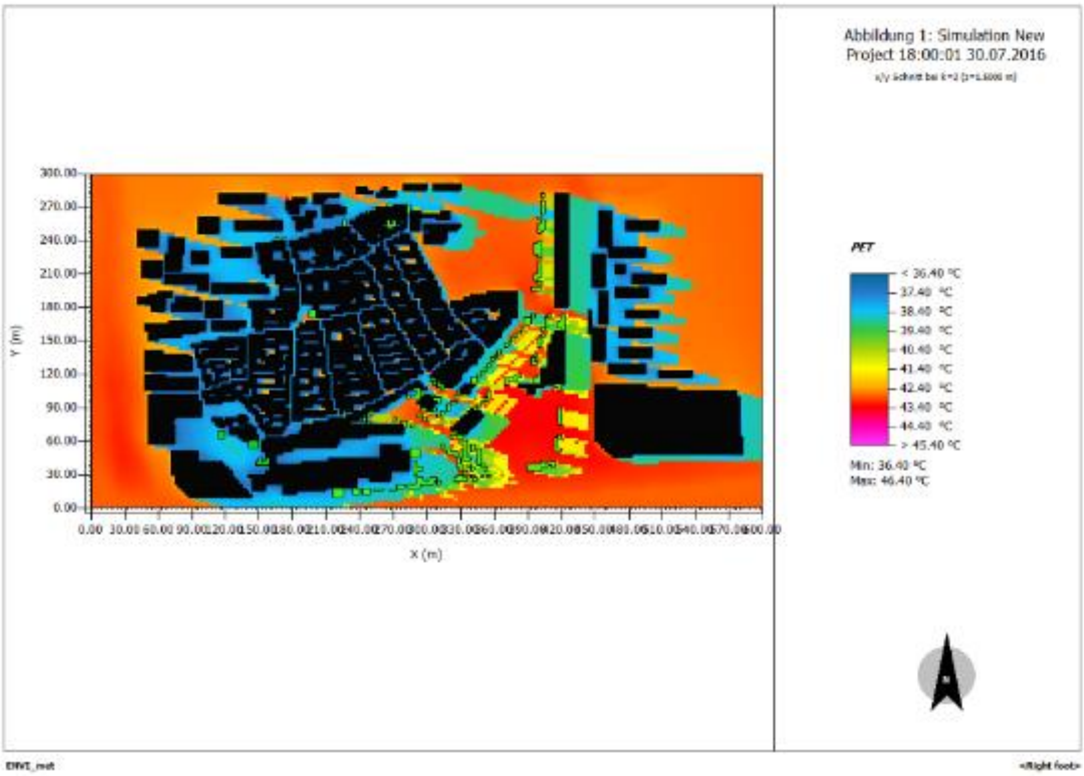
Abbildung 1: Simulation New
Project 18:00:01 30.07.2016
PET
< 36.40 °C
37.40 °C
38.40 °C
39.40 °C
40.40 °C
41.40 °C
42.40 °C
43.40 °C
44.40 °C
> 45.40 °C
Min: 36.40 °C
Max: 46.40 °C
Y (m)
X (m)
ENVI_met
<Right foot>

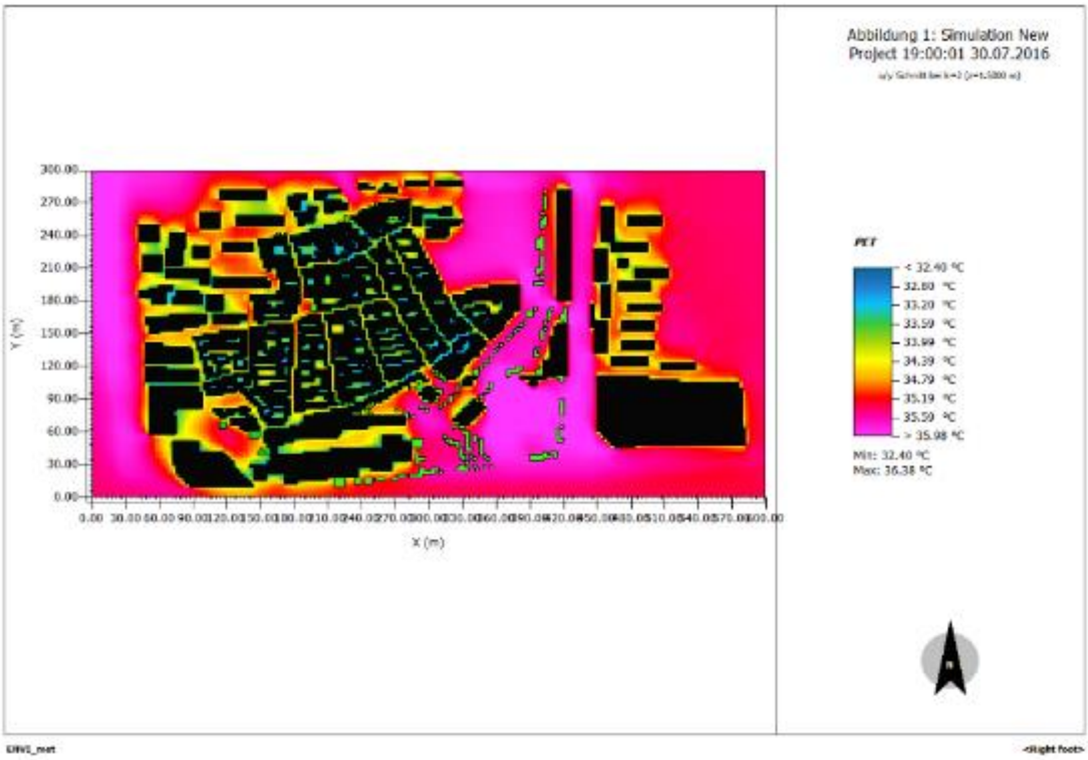
Abbildung 1: Simulation New
Project 19:00:01 30.07.2016
PET
< 32.40 °C
32.80 °C
33.20 °C
33.59 °C
33.99 °C
34.39 °C
34.79 °C
35.19 °C
35.59 °C
> 35.98 °C
Min: 32.40 °C
Max: 36.38 °C
Y (m)
X (m)
ENVI_met
<Right foot>

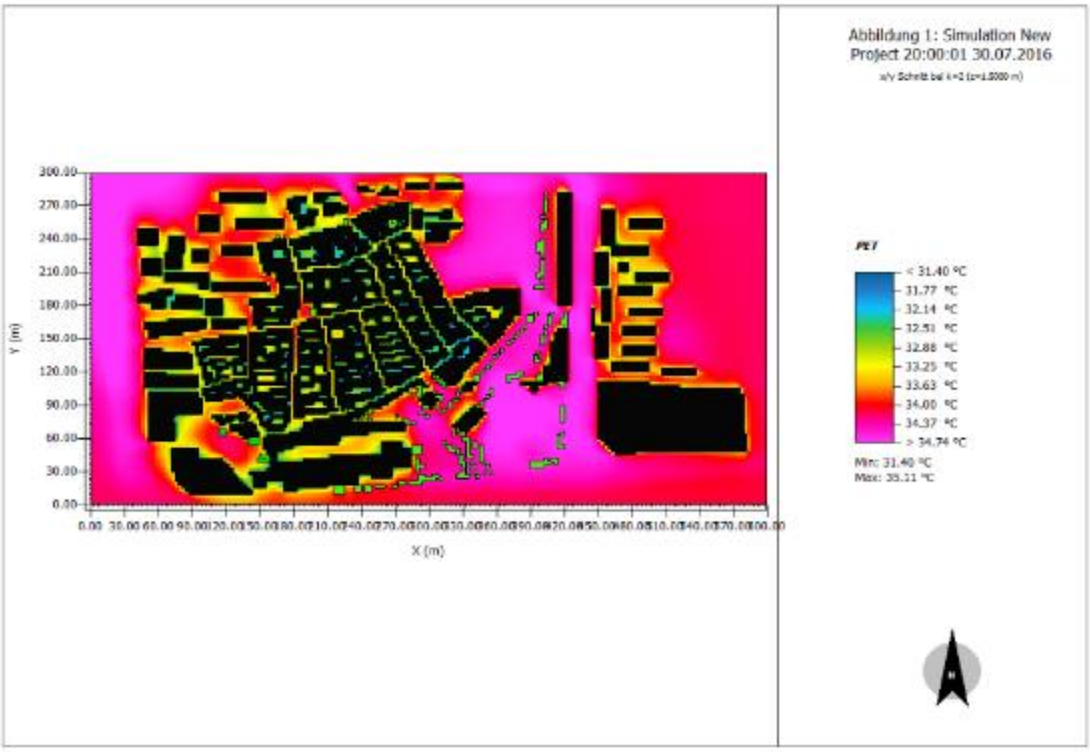
Abbildung 1: Simulation New Project 20:00:01 30.07.2016
PET
< 31.40 °C
31.77 °C
32.14 °C
32.51 °C
32.88 °C
33.25 °C
33.63 °C
34.00 °C
34.37 °C
> 34.74 °C
Min: 31.40 °C
Max: 35.11 °C
Y (m)
X (m)

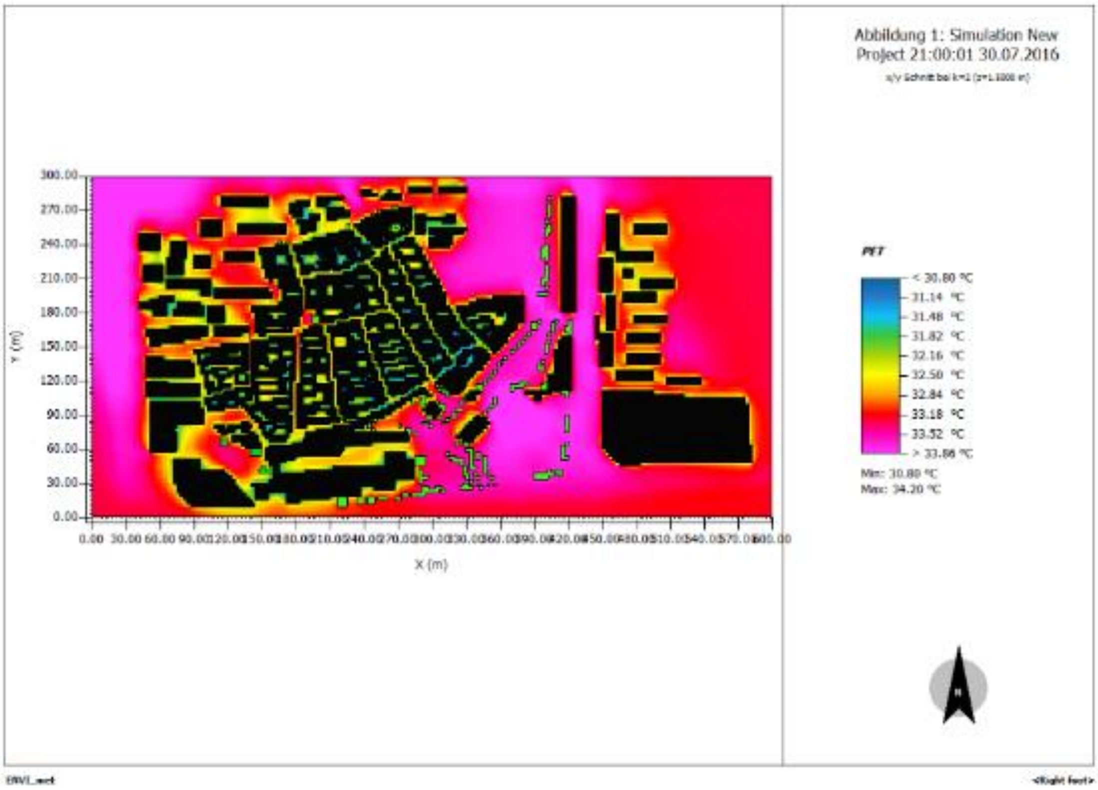
Abbildung 1: Simulation New Project 21:00:01 30.07.2016
PET
< 30.80 °C
31.14 °C
31.48 °C
31.82 °C
32.16 °C
32.50 °C
32.84 °C
33.18 °C
33.52 °C
> 33.86 °C
Min: 30.80 °C
Max: 34.20 °C
Y (m)
X (m)

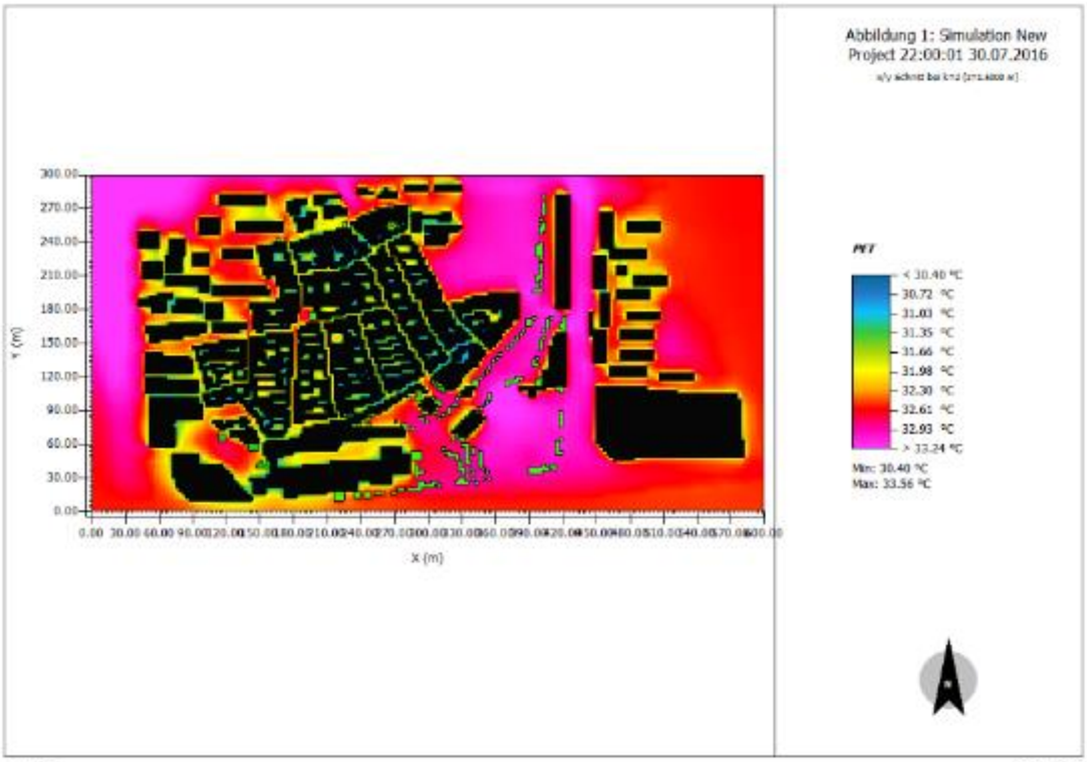

ENVI_met <Right foot>

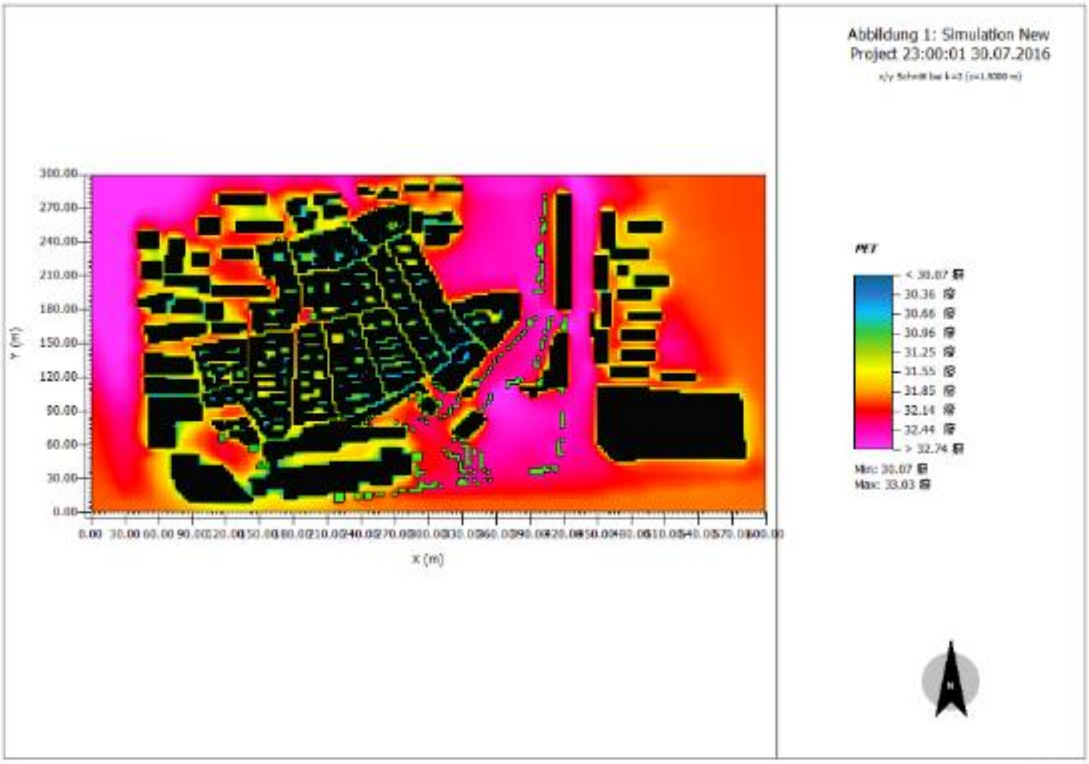

ENVI_met <Right foot>

Appendix-2

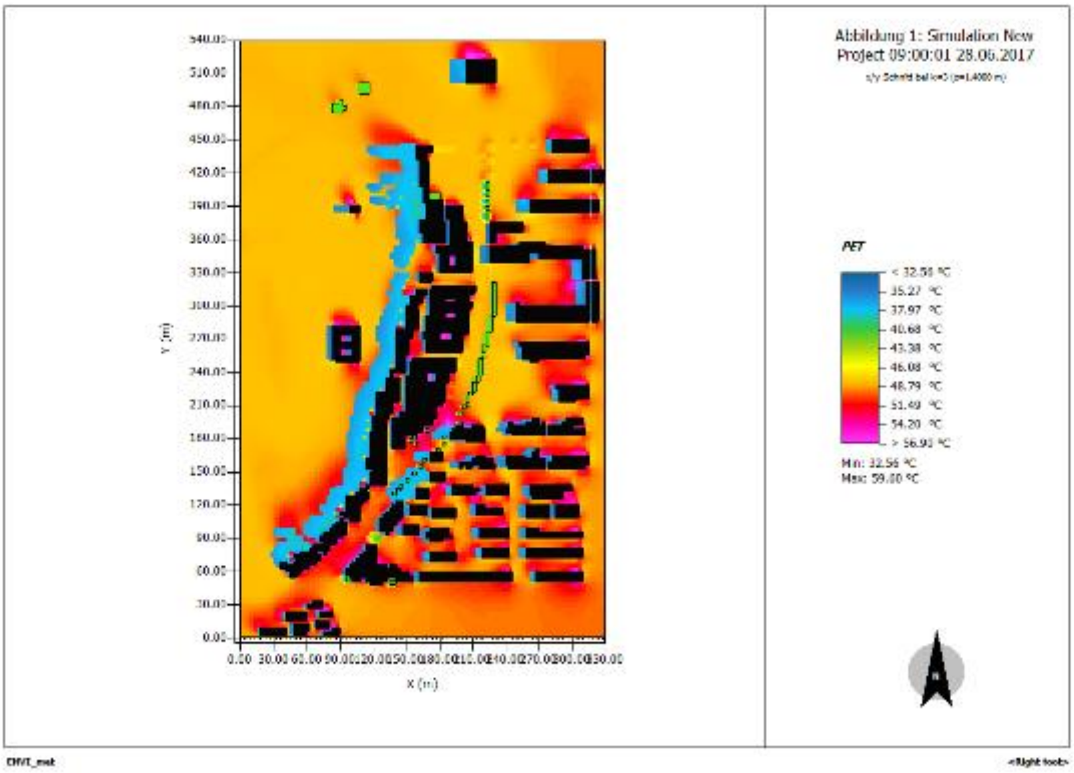
Abbildung 1: Simulation New Project 09:00:01 28.06.2017
PET
< 32.56 °C
35.27 °C
37.97 °C
40.68 °C
43.38 °C
46.08 °C
48.79 °C
51.49 °C
54.20 °C
> 56.90 °C
Min: 32.56 °C
Max: 59.60 °C
Y (m)
X (m)
ENVI_met
<Right foot>

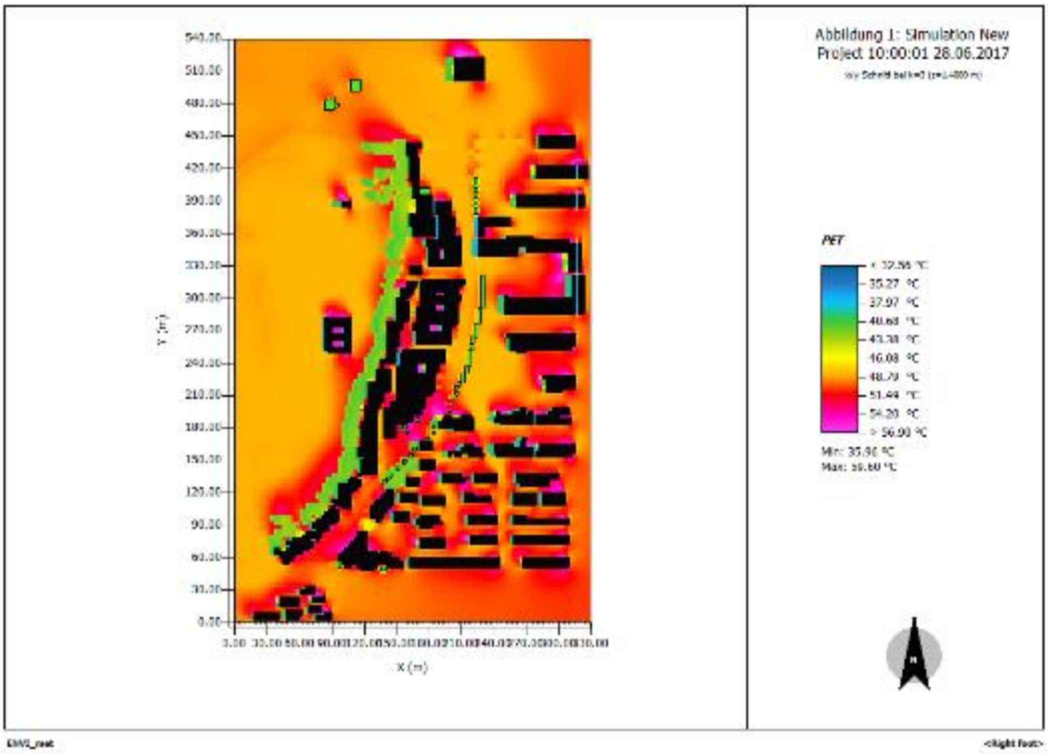
Abbildung 1: Simulation New Project 10:00:01 28.06.2017
PET
< 32.56 °C
35.27 °C
37.97 °C
40.68 °C
43.38 °C
46.08 °C
48.79 °C
51.49 °C
54.20 °C
> 56.90 °C
Y (m)
X (m)
ENVI_met
<Right foot>

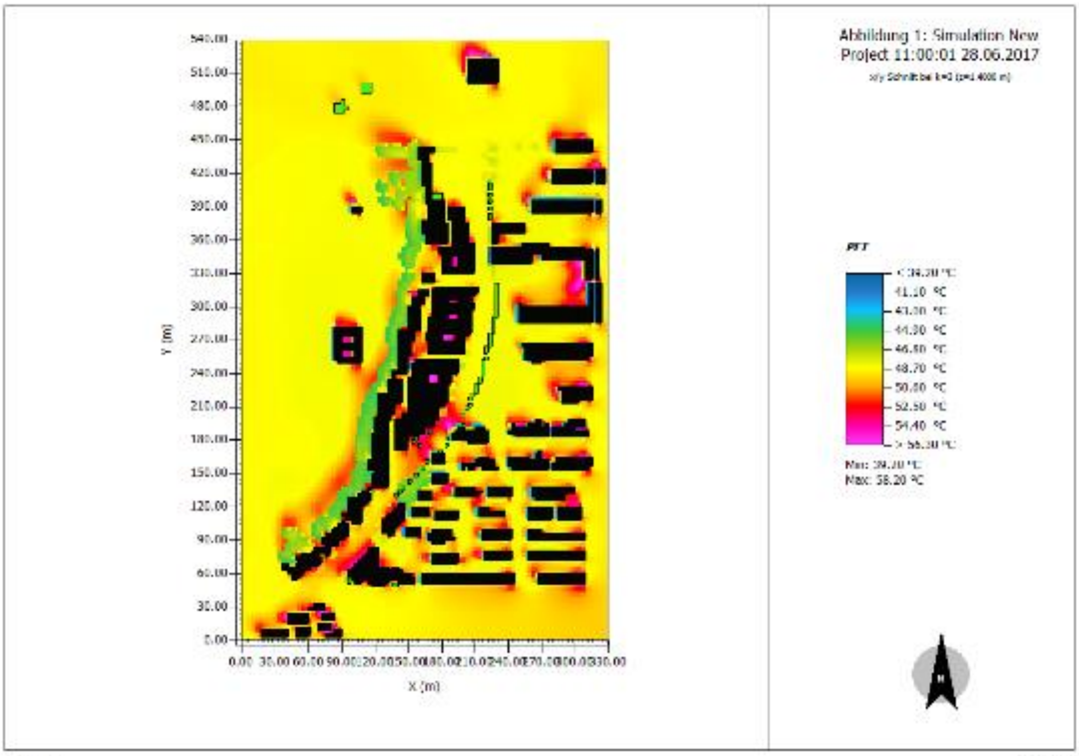

ENVI_met

<Right foot>

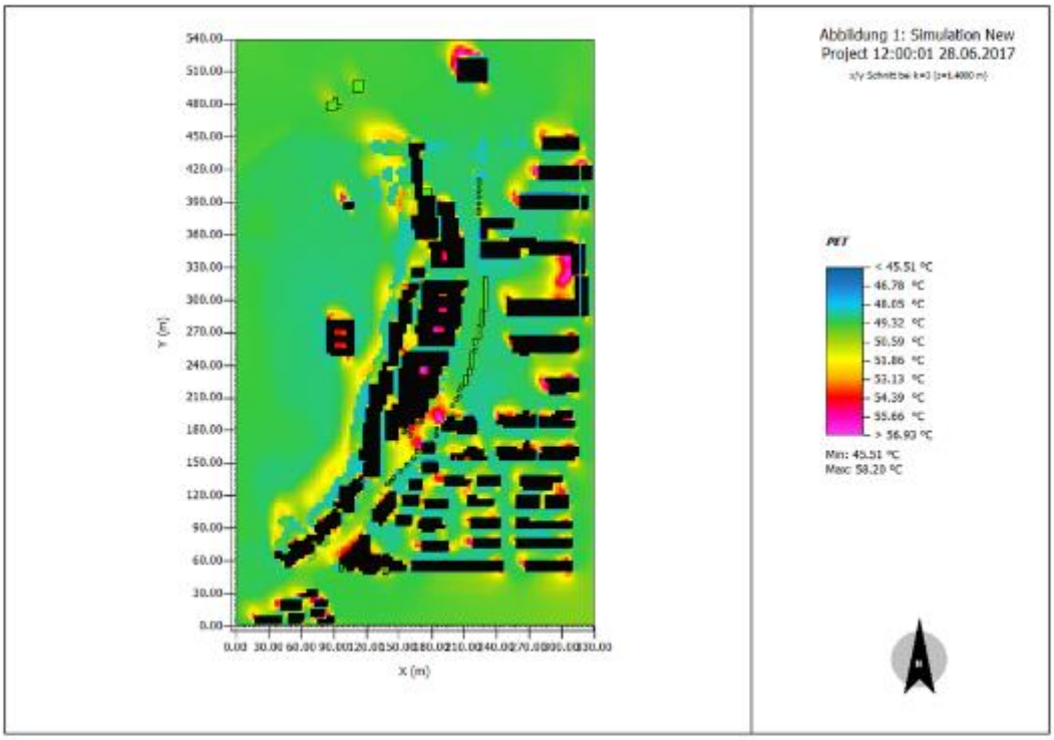

ENVI_met

<Right foot>

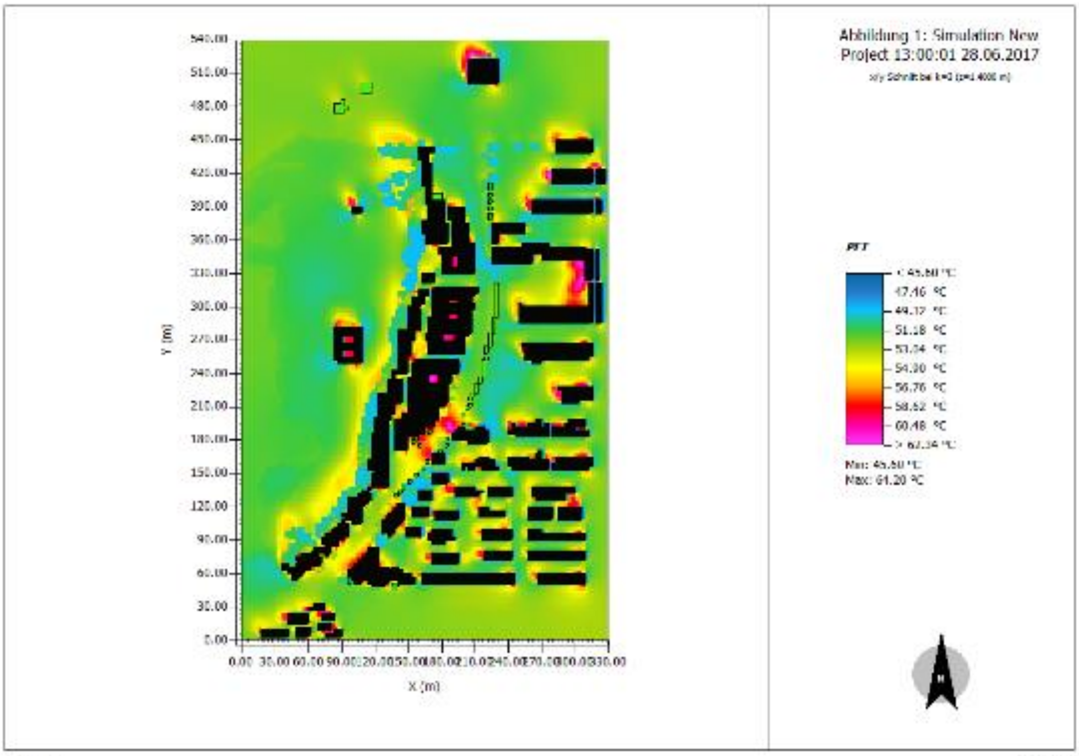

ENVI_met <Right foot>

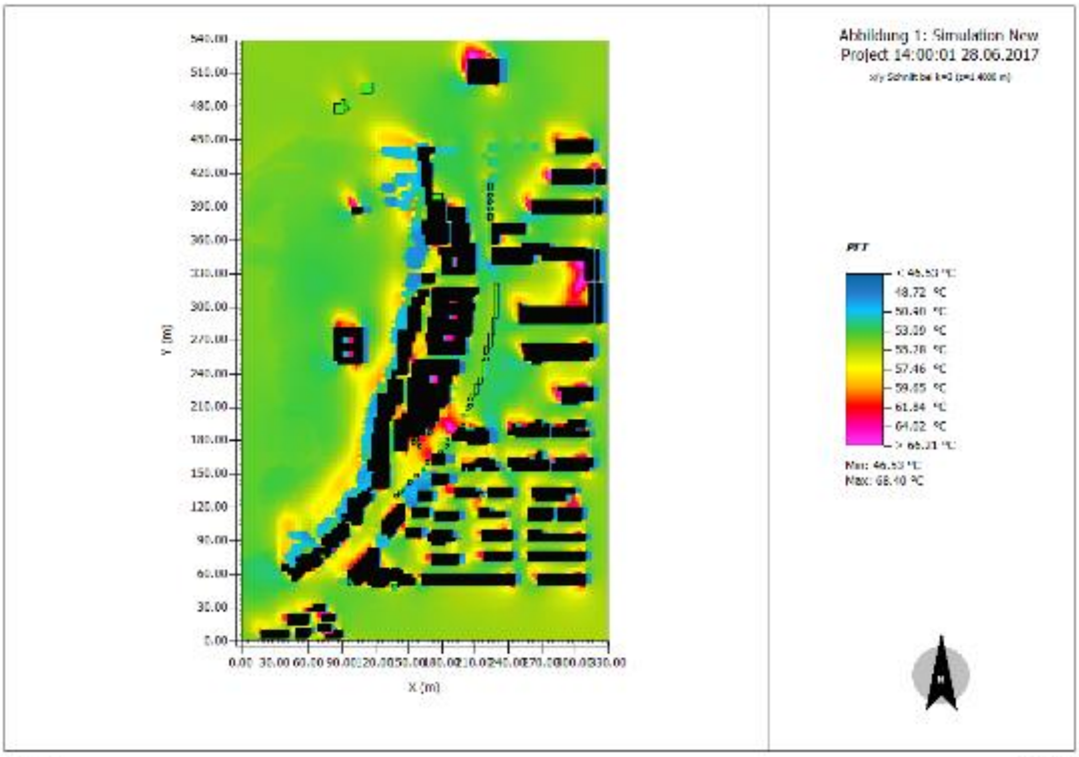

ENVI_met <Right foot>

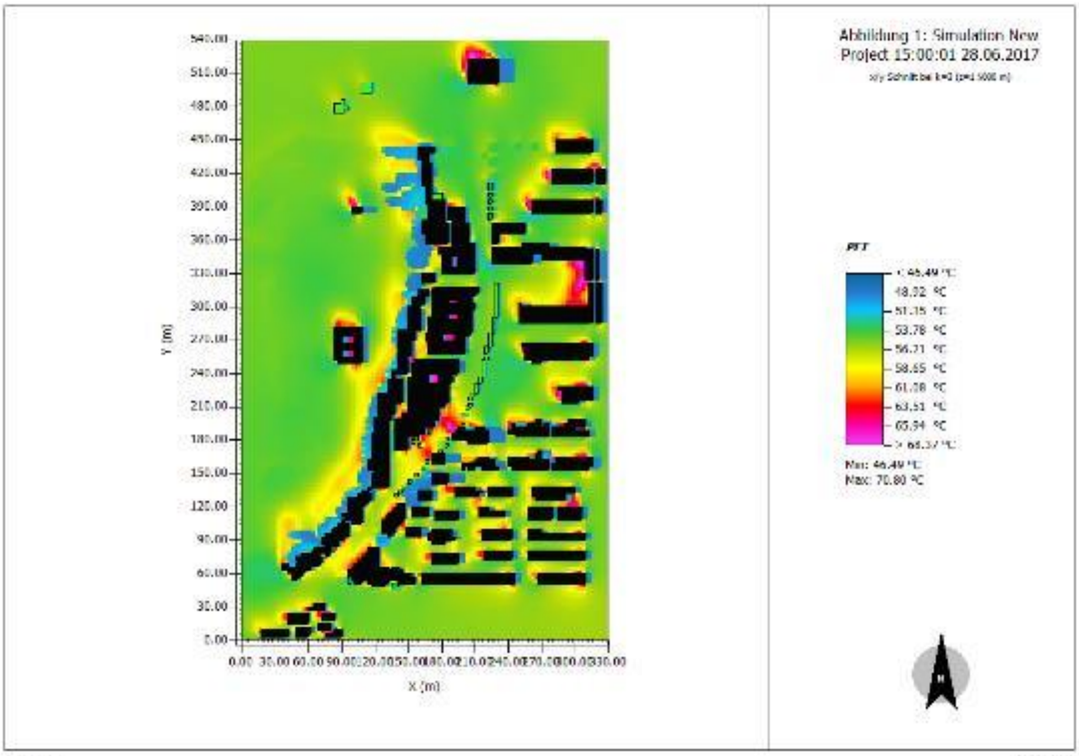

ENVI_met

<Right foot>

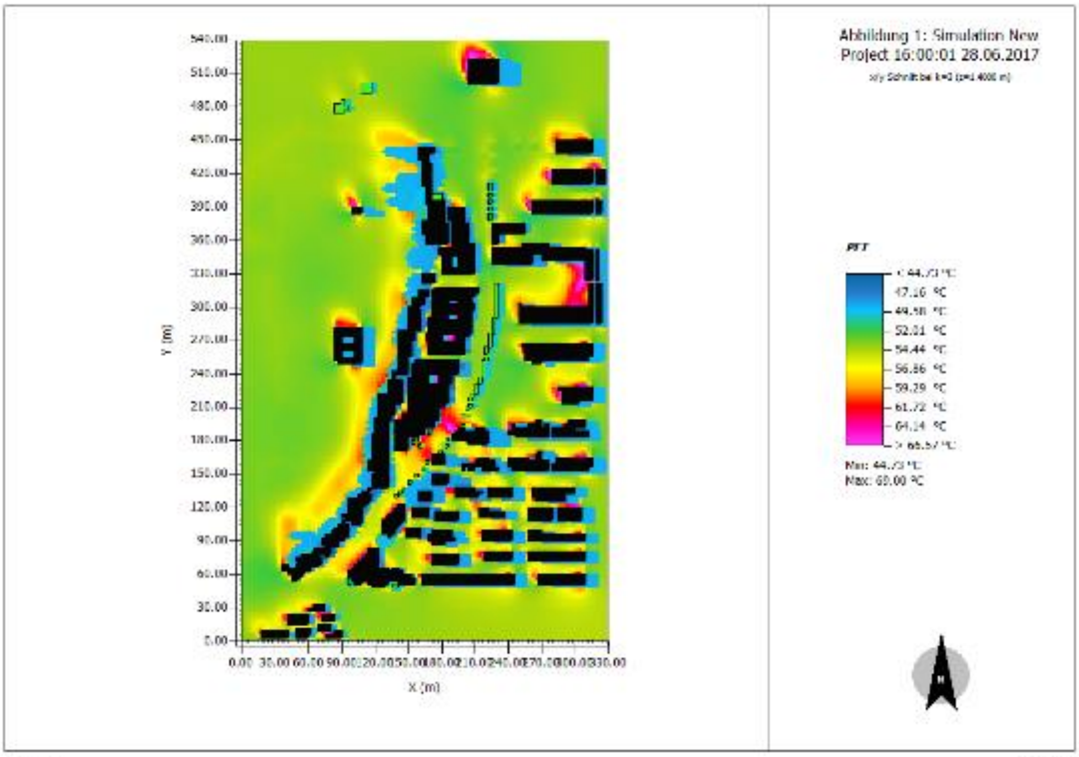

ENVI_met

<Right foot>

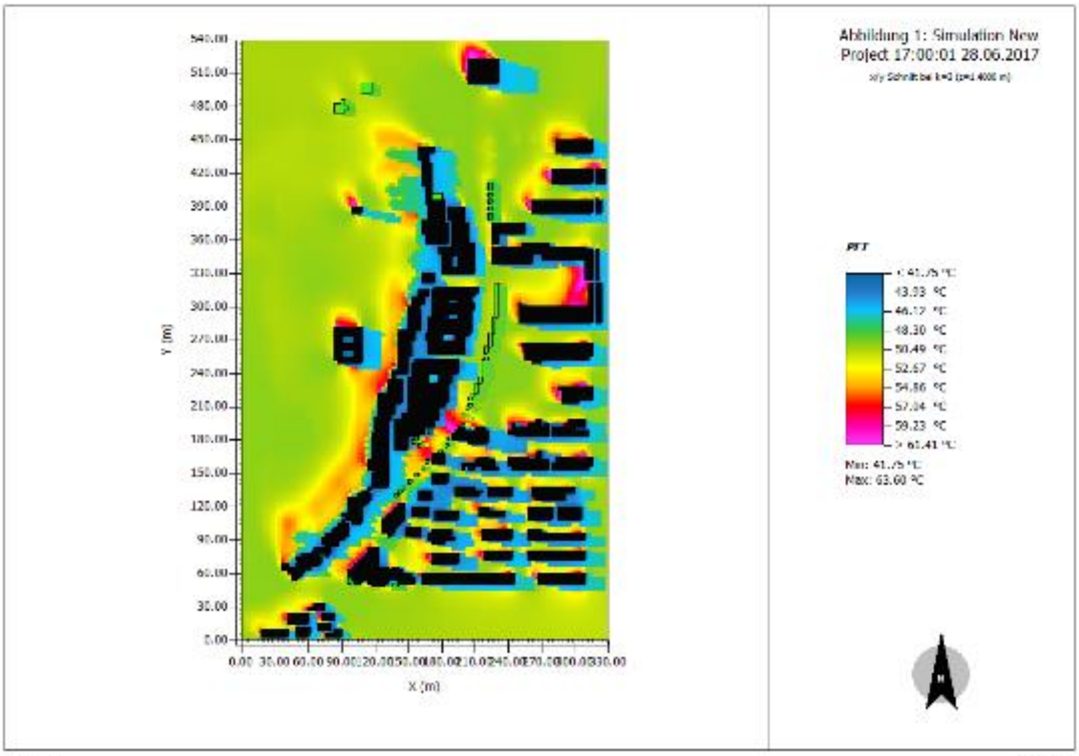
Abbildung 1: Simulation New Project 17:00:01 28.06.2017
PET
< 41.75 °C
43.93 °C
46.12 °C
48.30 °C
50.49 °C
52.67 °C
54.86 °C
57.04 °C
59.23 °C
> 61.41 °C
Min: 41.75 °C
Max: 63.60 °C
X (m)
Y (m)

Appendix-3

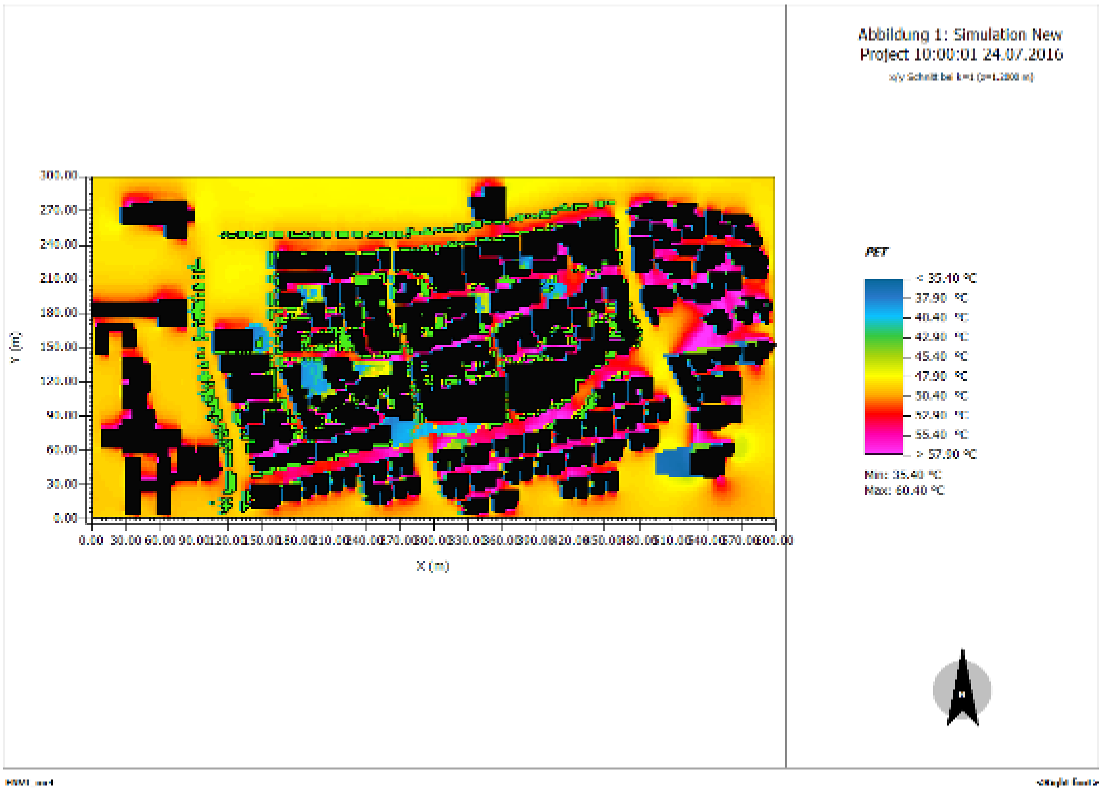
Abbildung 1: Simulation New Project 10:00:01 24.07.2016
PET
< 35.40 °C
37.90 °C
40.40 °C
42.90 °C
45.40 °C
47.90 °C
50.40 °C
52.90 °C
55.40 °C
> 57.90 °C
Min: 35.40 °C
Max: 60.40 °C
Y (m)
X (m)

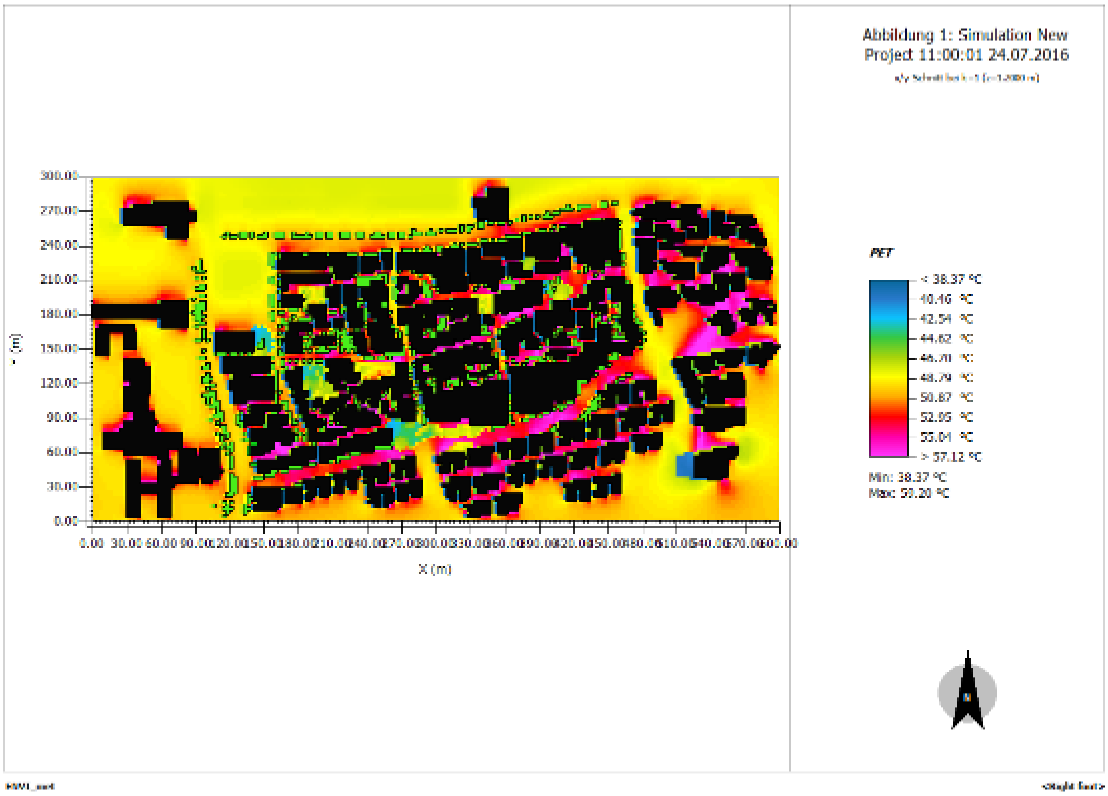
Abbildung 1: Simulation New Project 11:00:01 24.07.2016
PET
< 38.37 °C
40.46 °C
42.54 °C
44.62 °C
46.70 °C
48.79 °C
50.87 °C
52.95 °C
55.04 °C
> 57.12 °C
Min: 38.37 °C
Max: 59.20 °C
X (m)

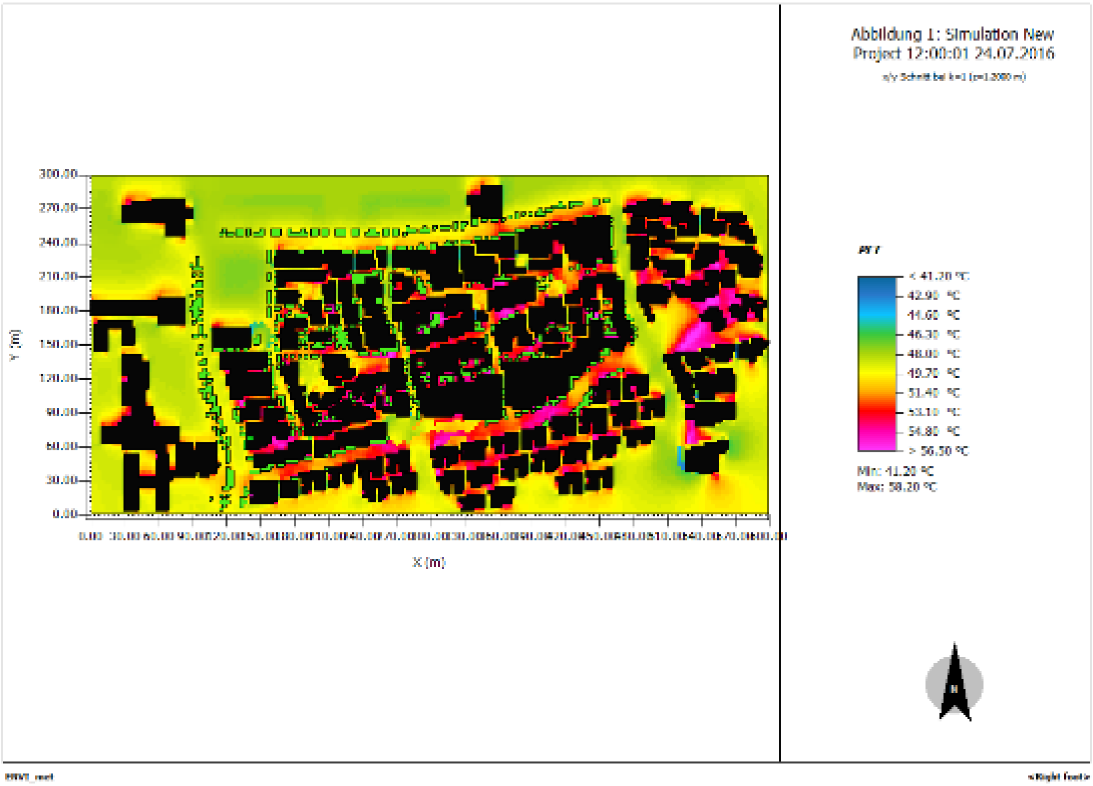
Abbildung 1: Simulation New
Project 12:00:01 24.07.2016
PET
< 41.20 °C
42.90 °C
44.60 °C
46.30 °C
48.00 °C
49.70 °C
51.40 °C
53.10 °C
54.80 °C
> 56.50 °C
Min: 41.20 °C
Max: 58.20 °C
Y (m)
X (m)

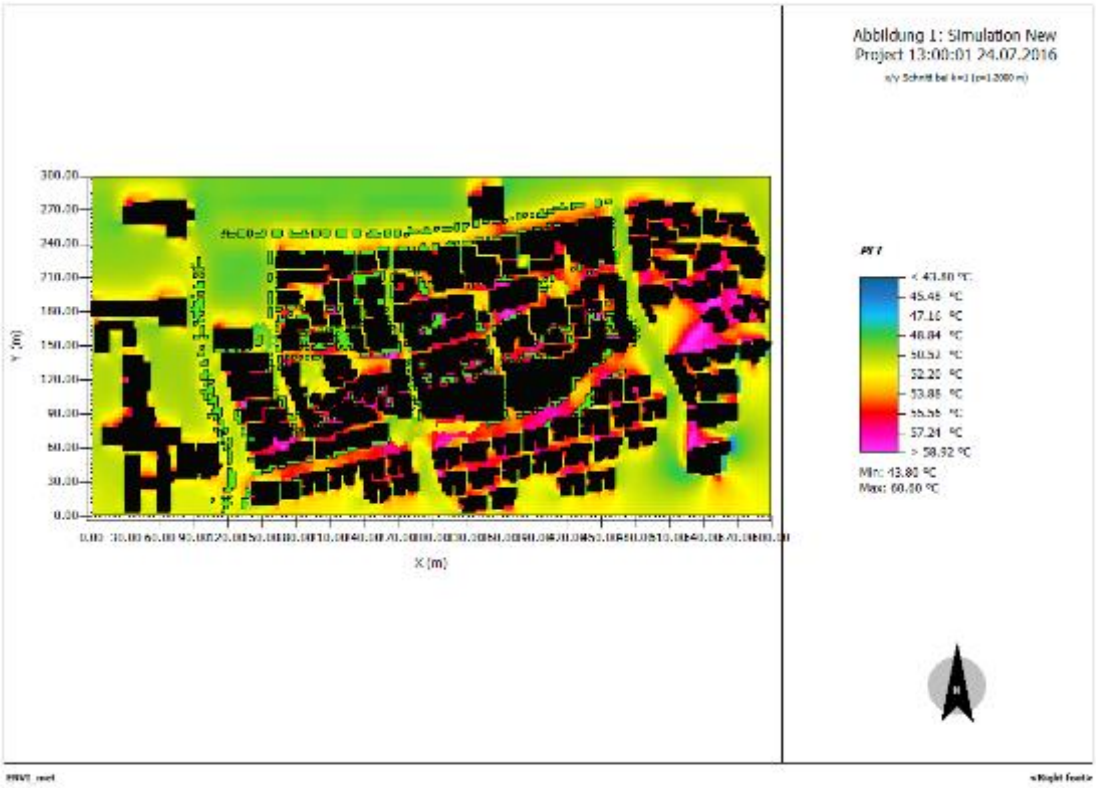
Abbildung 1: Simulation New
Project 13:00:01 24.07.2016
PET
< 43.80 °C
45.48 °C
47.16 °C
48.84 °C
50.52 °C
52.20 °C
53.88 °C
55.56 °C
57.24 °C
> 58.92 °C
Min: 43.80 °C
Max: 60.60 °C
Y (m)
X (m)

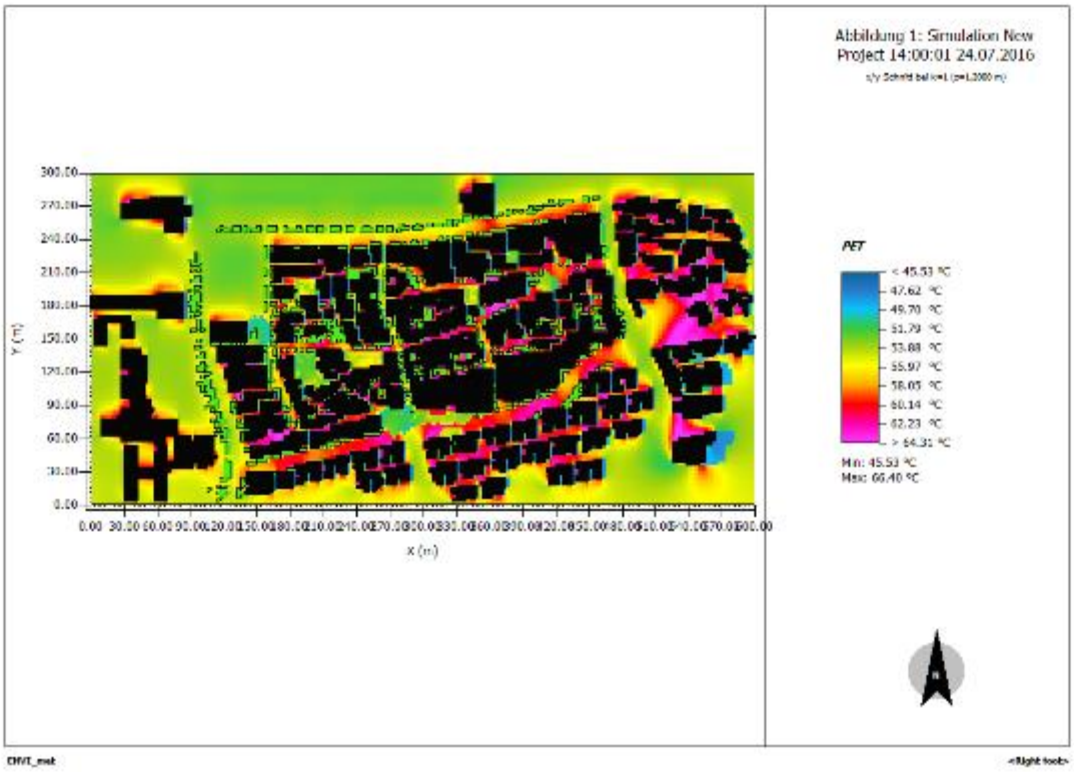
Abbildung 1: Simulation New
Project 14:00:01 24.07.2016
PET
< 45.53 °C
47.62 °C
49.70 °C
51.79 °C
53.88 °C
55.97 °C
58.05 °C
60.14 °C
62.23 °C
> 64.31 °C
Min: 45.53 °C
Max: 66.40 °C
Y (m)
X (m)
ENVI_met
<Right foot>

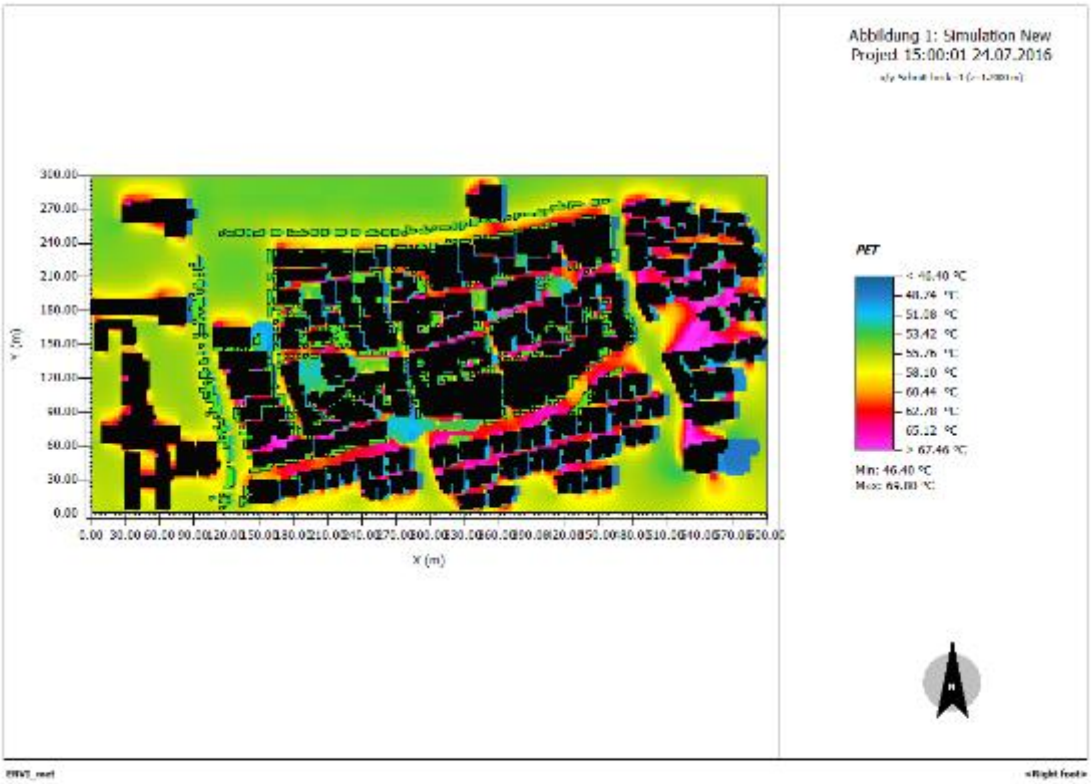
Abbildung 1: Simulation New
Project 15:00:01 24.07.2016
PET
51.08 °C
53.42 °C
58.10 °C
60.44 °C
65.12 °C
> 67.46 °C
Min: 46.40 °C
Y (m)
X (m)

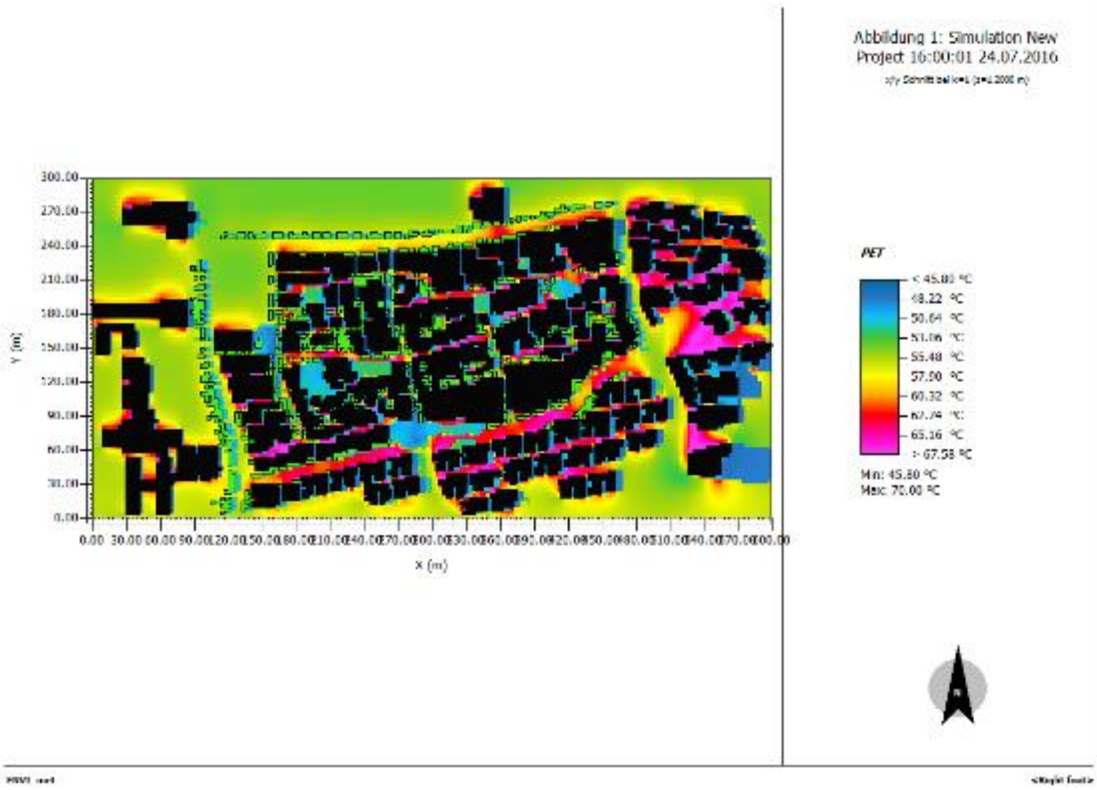
Abbildung 1: Simulation New
Project 16:00:01 24.07.2016
PET
< 45.80 °C
48.22 °C
50.64 °C
55.48 °C
57.90 °C
60.32 °C
65.16 °C
> 67.58 °C
Min: 45.80 °C
Max: 70.00 °C
Y (m)
X (m)

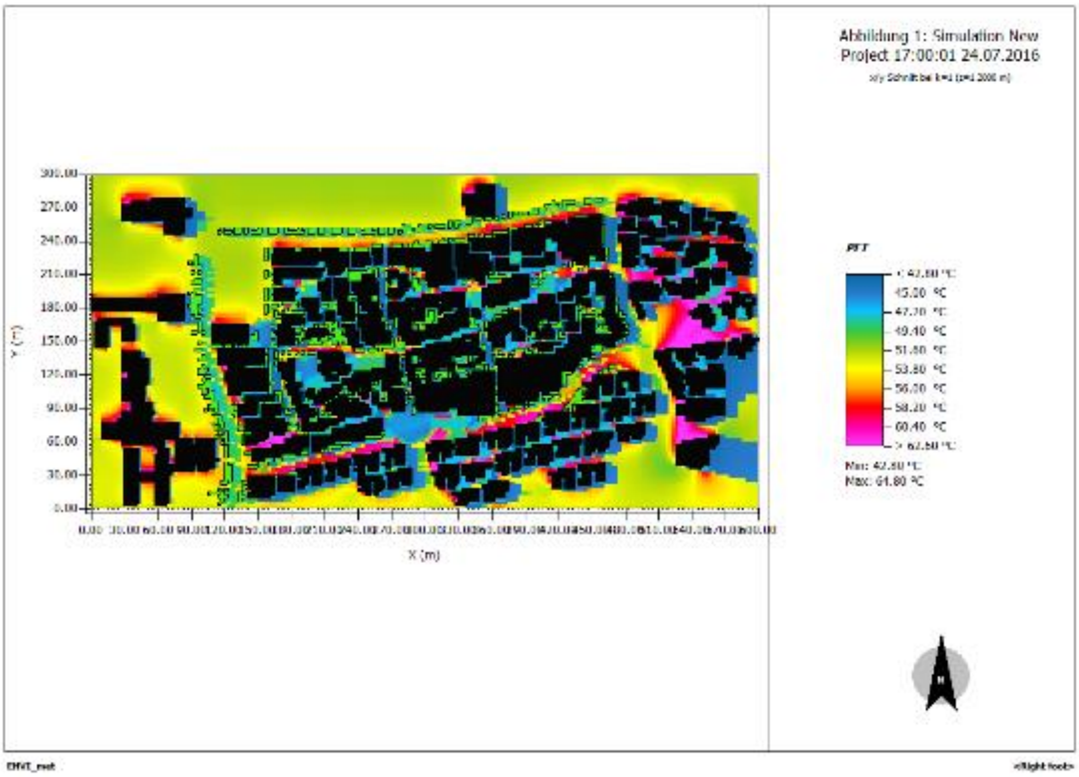
Abbildung 1: Simulation New
Project 17:00:01 24.07.2016
PET
Max: 61.80 °C
Y (m)
X (m)

Research results obtained during the doctoral degree

SCI article:

Xuan Ma, Hiroatsu Fukuda, Dian Zhou, Weijun Gao, Mengying Wang, The study on outdoor pedestrian thermal comfort in blocks: A case study of the Dao He Old Block in hot-summer and cold-winter area of southern China Solar energy, volume 179, 2019, 210-225. Impact factor: 4.674

Ma, X.; Fukuda, H.; Zhou, D.; Wang, M. The Evaluation of Outdoor Thermal Sensation and Outdoor Energy Efficiency of a Commercial Pedestrianized Zone. Energies, volume 12(7), 2019, 1324, Impact factor: 2.702

Ma, X.; Fukuda, H.; Zhou, D.; Wang, M. The study on the pedestrianized-zone for tourists: urban design effects on humans' thermal comfort in hot-summer and warm-winter climate zone of southern China Sustainability, volume 11(10), 2019, 2774, Impact factor: 2.575

SSCI article:

Ma, X.; Fukuda, H.; Zhou, D.; Wang, M. Study on outdoor thermal comfort of the commercial pedestrian block in hot-summer and cold-winter region of southern China-A case study of The Tai zhou Old Block. Tourism Management. Tourism management, volume 79, 2019, 186-205, Impact factor: 6.012